Methionine biosynthesis, transport and metabolism in *Salmonella* Typhimurium

Asma Ul Husna

Submitted in total fulfilment of the requirements
of the degree of Doctor of Philosophy

May 2017

The Department of Microbiology and Immunology

The University of Melbourne

ABSTRACT

Salmonella enterica serovar Typhimurium (*S.* Typhimurium) is a common cause of, gastroenteritis, contributing to significant morbidity and mortality worldwide. In recent years, the prevalence of antibiotic resistance in *S.* Typhimurium has, like many other pathogens, increased, highlighting the need for new drug targets. *Salmonella*, like most other prokaryotes, is capable of *de novo* methionine biosynthesis, a process which is absent from higher eukaryotes. The general aim of this study is to investigate the role of methionine biosynthesis, transport, recycling and salvage in the virulence of *S.* Typhimurium strain SL1344 to identify novel, potential antibiotic targets. A collection of single knockouts was generated in: i) the *de novo* methionine biosynthesis pathway; ii) the high-affinity transporter for methionine; and iii) downstream pathways that use methionine, including the activated methyl cycle and the incomplete methionine salvage pathway in *Salmonella*.

A series of systematic analyses was carried out for each mutant to assess the biochemical requirement for methionine and its downstream utilisation in the growth and virulence of *Salmonella* under conditions that mimic different nutritional environments. Firstly, the mutants were constructed by site-directed mutagenesis and confirmed by PCR and whole genome sequencing. Secondly, the mutants were tested for their ability to grow in M9 minimal media and were validated. Thirdly, the mutants were examined to determine their capacity to grow intracellularly in HeLa cells which provided the indication on whether a pathway/biochemical step is required for growth within the host cell. Finally, the mutants were tested for virulence during either local and/or systemic *Salmonella* infection, hence establishing the role of the pathway/biochemical step in pathogenesis.

All the *de novo* methionine biosynthetic mutants were not able to grow in M9 minimal media without methionine. However, none of the mutants unable to synthesise methionine, were attenuated for intracellular replication in HeLa cells, or in mice. These results indicate that *de novo* methionine biosynthesis is not required for the pathogenesis of *S.* Typhimurium; hence the enzymes in the methionine biosynthesis pathway are unlikely to make suitable targets for antimicrobial therapy against *S.* Typhimurium infection. An alternative to methionine biosynthesis in *S.* Typhimurium is the import of methionine from the environment via at least two mechanisms, the high-affinity transporter encoded by *metNIQ*, and a cryptic low-affinity transporter. The high-affinity transporter mutant was also found not be attenuated in HeLa

cells, nor in mice. Only mutants that were deficient in both *de novo* methionine biosynthesis and high-affinity transporter were attenuated, indicating a functional redundancy between biosynthesis and transport as the source of methionine for the growth and virulence of *S.* Typhimurium *in vitro* and *in vivo*.

The importance of methionine metabolism to *S.* Typhimurium virulence was also investigated. In this study, *S.* Typhimurium mutants blocked in enzymatic functions in the downstream of methionine, including activated methyl cycle, spermidine biosynthesis and incomplete salvage pathway, were analysed for their role in the growth and virulence of *Salmonella* in M9 minimal media, HeLa cells and mice. With the exception of the Δ*pfs* mutant, all the mutants were capable of growing in M9 minimal media and HeLa cells, and were virulent in mice. This indicates that the methionine recycling through the activated methyl cycle, and spermidine synthesis, are not required for *S.* Typhimurium virulence. However, the deletion in the multi-substrate enzyme Pfs led to severely attenuated *S*. Typhimurium for intracellular replication in HeLa cells. The Δ*pfs* mutant was also found to be significantly attenuated in wild-type BL/6 mice. It was hypothesised that the accumulation of S-adenosylhomocysteine is inhibitory to SAM-dependent methyltransferases. The heterologous expression of SahH from *Legionella pneumophila* in *S*. Typhimurium Δ*pfs* mutant led to the removal of S-adenosylhomocysteine and restored growth and virulence both *in vitro* and *in vivo*. These results demonstrate that Pfs is essential for *S*. Typhimurium growth and virulence. In IFN-$\gamma^{-/-}$ mice that are highly susceptible to *Salmonella*, infection with the Δ*pfs* mutant led to accelerated lethality compared to the *aro*$^{-}$ vaccine strain, indicating the requirement of Pfs during *in vivo* infection largely depends on the efficacy of host immunity. Further investigation of host responses to infection with the Δ*pfs* mutant may reveal the specific conditions under which Pfs can be used as a potential target for antibiotic treatment against *S*. Typhimurium.

DECLARATON

This is to certify that

- the thesis comprises only my original work towards the PhD except where indicated the text
- due acknowledgement has been made in the text to all other materials used
- the thesis is fewer than 100,000 words in length, exclusive of tables, figures, bibliographies and appendices

……

Asma Ul Husna
Department of Microbiology and Immunology
The University of Melbourne

PREFACE

Manuscripts in preparation:

- Husna A. U., Wang N, Newton H. J., Wilksch J. J., Strugnell R. A. The role of methionine biosynthesis and transport in the virulence of *Salmonella* Typhimurium.
- Husna A. U., Wang N., Newton H. J., Wilksch J. J., Strugnell R. A. The role of S-adenosylhomocysteine/ Methylthioadenosine nucleosidase (Pfs) in the virulence of *Salmonella* Typhimurium.

ACKNOWLEDGEMENTS

First and foremost, I would like to express my sincere gratitude and thanks to my supervisor Dr. Richard A. Strugnell for allowing me in his laboratory. I appreciate all his continuous support, guidance, encouragement and patience which helped me to grow as a research scientist. His motivation and enthusiasm towards science have been priceless. His ideas, insights and advice helped me to successfully complete the PhD. My sincere gratitude is also reserved for my co-supervisor Dr. Nancy Wang for her tremendous support and invaluable insights throughout my journey. I really appreciate her friendship and willingness to help me whenever I need. I am very grateful to Nancy for her immense contribution specially in my animal experiments. I am deeply indebted to my other co-supervisor Dr. Hayley J Newton for being extremely helpful throughout my candidature. Her joy and enthusiasm for research was contagious and motivational for me. Her valuable help and insightful feedbacks to my project are very much appreciated. My sincere thanks also go to the rest of my PhD committee: Dr. Timothy Stinear and Dr. Malcolm McConville for their insightful comments and brilliant suggestions.

I would like to express my heartfelt gratitude to Dr. Jonathan Wilksch from the Strugnell lab who taught me the techniques of molecular biology and how to make mutant strains. I am grateful to Dr. Mark Davies and Liam Mcintyre for being so generous to analyse the whole genome sequencing data for my mutant strains. They helped me a lot with bioinformatics as well and I am very thankful to them. Endless thanks also go to Sarah Baines from the Stinear Lab who also helped with the whole genome sequencing data analysis. I sincerely thank Dr. Simon Allister Cobbold from the McConville Lab who made significant contributions to this dissertation by doing the Mass Spectrometry analysis.

All members and friends from the Strugnell lab have contributed immensely to my personal and professional time during my PhD candidature. I would like to specially thank them for their friendship and support: Jason, Newton, Monica, Karthik, Leila, Jeanine, Dianna, Hanwei, Matthew, Jessica, Shruti, Anna, Andre, Kasidis, Huimeng, Tim and Hasan. I need to acknowledge the people from several labs: Hartland, Robins-Browne and Newton, for allowing me to use their equipment and reagents. Thanks to all the staff of Bioresource facility, Media Preparation Unit and the graduate student coordinator Rebecca Whitsed. Thanks to GTAC for giving me the opportunity to do some teaching.

Lastly and most importantly, I would like to take this opportunity to thank my family and well-wishers: specially Amma, Abba, Sumin, Bulbul, Moon, Mahir and Faria for their endless love, inspiration, sacrifice, understanding and emotional support. Thank you so much for being a constant source of strength which kept me determined to finish my PhD successfully!

Asma Ul Husna

May 2017

TABLE OF CONTENTS

LIST OF FIGURES

LIST OF TABLES

LIST OF ABBREVIATIONS

The following abbreviations have been used throughout this thesis:

ºC	Degree Celsius
Δ	Delta
Ω	Ohm
ADP	Adenosine diphosphate
Amp	Ampicillin
Amp^R	Ampicillin resistance
AMC	Activated methyl cycle
aro$^-$	*aro*-negative
ATP	Adenosine triphosphate
BLAST	Basic local alignment search tool
bp	Base pair(s)
cfu	Colony forming unit
Chl	Chloramphenicol
Chl^R	Chloramphenicol resistance
CI	Confidence interval
CO_2	Carbon dioxide
CoA	CoenzymeA
dH_2O	Distilled water
DMEM	Dulbecco's Modified Eagle Medium
DNA	Deoxyribonucleic acid

gDNA	Genomic DNA
E.	*Escherichia*
EGTA	Ethylene glycol-bis(oxyethylenenitrilo)tetraacetic acid
EBU	Eosin Blue Uranine
FCS	Fetal Calf Serum
Flp	Flippase
FRT	Flippase recognition target
g	Gram
g	Gravitational force
HIV	Human Immunodeficiency Virus
HRP	Horseradish Peroxidase
IFN-γ	Interferon Gamma
iNTS	Invasive non-typhoidal *Salmonella*
i.v.	Intravenous
Kan	Kanamycin
Kan^R	Kanamycin resistance
Kb	Kilobase pair(s)
LPS	Lipopolysaccharide
µF	Microfarad
µl	Microlitre
µM	Micromolar
M cells	Microfold cells
min	Minute(s)
Met	Methionine
MDR	Multi-drug resistance

ml	Mililitre
MLN	Mesenteric Lymph node
MLST	Multi Locus Sequence Typing
mM	Milmolar
NADH	Nicotinamide Adenine Dinucleotide
NK cells	Natural Killer Cell
Nramp1	Natural resistance-associated macrophage protein 1
NTS	Non-typhoidal *Salmonella*
OD	Optical density
p	Probability
PBS	Phosphate-buffered saline
PCR	Polymerase Chain Reaction
Phe	Phenylalanine
RNA	Ribonucleic acid
ROS	Reactive oxygen species
rpm	Revolutions per minute
RT	Room temperature
S.	*Salmonella*
SAM	S-adenosyl L-methionine
SCV	*Salmonella*-containing vacuole
SDS-PAGE	Sodium dodecyl sulphate- polyacrylamide gel electrophoresis
SIV	Simian immunodeficiency virus
SPI	*Salmonella* pathogenicity island
SNP	Single nucleotide polymorphism
Str	Streptomycin

T3SS	Type 3 secretion system
T_m	Melting temperature
TCA	Tricarboxylic acid cycle
Tet	Tetracycline
Trp	Tryptophan
TSS	Transformation and Storage Solution
Tyr	Tyrosine
UV	Ultraviolet
Vol	Volume(s)
V	Volt
WT	Wild-type
WHO	World Health Organisation
X	times

Chapter 1

Introduction and Literature Review

1.1 Introduction

Salmonella enterica is a Gram-negative bacterial pathogen that causes gastrointestinal and systemic diseases in animals and humans (1, 2). There are about 2500 different serovars in this single species (1, 2). The *S. enterica* serovars Typhi and Paratyphi A, B and C are human-restricted and cause systemic illness (enteric fever) (3); the annual disease burden from enteric fever is estimated to be approximately 220,000 deaths from 21 million cases (4-6). The term "non-typhoidal *Salmonella* (NTS)" is used to describe other disease-causing serovars, which are a leading cause of acute gastroenteritis (7). An invasive form of non-typhoidal *Salmonella* has emerged as a major cause of bloodstream infection with a high mortality rate in sub-Saharan African adults and children (8-10). *Salmonella* also poses a significant threat to the agricultural industry including poultry, cattle and pigs, which are considered as a zoonotic reservoir for the transmission of *Salmonella* to humans (7, 11-16). Due to the increased prevalence of antibiotic resistance in recent years, there is a pressing need for the identification of new targets for antimicrobial drugs and vaccines that will protect against infections caused by *S. enterica* (17).

1.2 The discovery of *Salmonella*

Typhoid fever was first described in Paris in 1829 by P. Ch. A. Luis from Paris who distinguished it from other fevers and found a relationship of the infection with intestines, mesenteric lymph nodes and spleen (18). Karl Ebarth visualised the causative bacillus in the spleen and Peyer's Patches of infected patients in 1880 (1). However, the organism did not get the name *Salmonella* until the year 1900, when French scientist Joseph Leon Lignieres suggested naming the entire genus *Salmonella* after Daniel Elmer Salmon, an American veterinary surgeon (1, 18).

1.3 Classification and nomenclature

The classification and nomenclature of *Salmonella* spp. has been contested for many years and they are complex. Nomenclature has evolved from the "one serotype, one species" concept proposed by the Kauffmann-White classification scheme (19), the basis of which was the serologic identification of O (somatic) and H (flagellar) antigens. According to this scheme, leading to the classification of many different species of *Salmonella* such as *Salmonella paratyphi*, *Salmonella enteritidis* etc. (19, 20). In the 1950s, Kauffmann divided the genus *Salmonella* into four sub-genera (I to IV) based on biochemical characteristics and continued

to retain the "one serovar, one species" concept. Kauffman's sub-genera was considered to be species which were: *S. kaufmannii* (subgenus I), *S. salamae* (subgenus II), *S. arizonae* (subgenus III) and *S. houtenae* (subgenus IV) (20). Later, the Approved Lists of bacterial names by Judicial Commission was published in the Internal Journal of Systems Biology (IJSB) in 1980 and that included five *Salmonella* species: *S. arizonae, S. choleraesuis, S. enteritidis, S. typhi, and S. typhimurium* (20, 21). But, it was demonstrated by Crosa *et al.* that through DNA-DNA hybridization *Salmonella* organisms may be considered as a single species (22). Later, it was shown that *Salmonella bongori* is the only exception (23), which is now considered as a distinct species (24). So, according to Centre for Disease Control and Prevention (CDC), the genus *Salmonella* currently contains two species *Salmonella enterica* (2443 serovars) and *Salmonella bongori* (20 serovars) (24). The former one is the type species which replaced *Salmonella choleraesuis* because *choleraesuis* was confusing as there is also a *Salmonella* serotype Choleraesuis. Serological variants, known as serovars, are determined based on specific antibody recognition against bacterial antigens, such as lipopolysaccharide (O-antigen) or flagella (H-antigen) (25). All pathogenic serovars of *Salmonella* fall into *S. enterica* spp (26). Now *S. enterica* is divided into six subspecies, which are *enterica, salamae, arizonae, diarizonae, houtenae* and *indica.* A new species, "*Salmonella subterranea*" was approved by the Judicial Commission in 2005 (27, 28), but later it was found that this species does not belong to the genus *Salmonella* (29). To reduce the complexities of this subspecies distribution, the CDC designated that, for *Salmonella* nomenclature, the genus name would be followed by the serovar name (not to be italicized and the first letter to be capitalized) (24, 27). For instance, *Salmonella enterica* subs. *enterica* serovar Typhimurium is described as such in the initial citation but can then be referred to as *Salmonella* Typhimurium or *S.* Typhimurium (24, 27).

1.4 Typhoid and paratyphoid fever

Typhoid fever is an acute systemic infection, and the causative agent is the highly-adapted human-restricted *Salmonella enterica* subs. *enterica* serovar Typhi (4, 6). Infection, caused by *Salmonella enterica* subs. *enterica* serovars Paratyphi A, B and C, known as paratyphoid fever, shares similar clinical presentations with typhoid fever can lead to serious complications (6). Both typhoid and paratyphoid fever are endemic in African and Asian countries (30). *S.* Typhi causes typhoid and accounts for 21 million cases of disease every year and about 200,000 deaths (6, 31, 32). According to most recent reports, new models suggest 26.9 million disease episodes occurred in 2010 (33, 34). *S.* Paratyphi A, B and C account for 5 million cases of

disease every year (5, 35). Throughout endemic areas, the incidence of typhoid is high for young adults whereas the incidence rate is quite low for infants and middle aged individuals (36). The infectious dose for typhoid fever is estimated to be between 10^3-10^9 cfu and the incubation period is 1-2 weeks (1). Fever, influenza-like symptoms with chills, headache, abdominal discomfort, malaise, anorexia, dry cough and myalgia are the common symptoms (6). If antibiotic therapy is not provided, fever can persist for several weeks. Myalgia and lethargy may last for 3-4 months (6, 37). The condition of a small percentage (2-4%) of infected children can deteriorate after an initial clinical response, even they were given appropriate treatment (38). Without effective treatment, the case-mortality rate of typhoid fever can be as high as 10-30% (5); when treated appropriately the number reduces to 1-4% (5).

The definitive diagnosis of typhoid fever requires laboratory support because many of its clinical presentations resemble that of other common diseases in endemic regions such as malaria, brucellosis, dengue and typhus (37, 38). Blood culture is widely used and shows positive results in 60-80% of suspected early cases (37, 39). Culture of bone marrow has improved sensitivity irrespective of the duration of the disease and shows 80-95% positivity but is invasive and impractical in most clinical settings (39). Since the late 19th century, a classic serological test named Widal test has been used to diagnose typhoid fever. The Widal test identifies the antibodies against the O (somatic) and H (flagellar) antigens of *S.* Typhi, which appear within 7-10 days after disease onset (39, 40). This test has decreased sensitivity and specificity because it gives mixed results in endemic areas (39, 40). In recent years, there have been a number of more rapid diagnostic tests introduced such as Enzyme Linked Immunosorbent Assay (ELISA), DOT Enzyme Immunoassay (DOT EIA) and DNA testing, however their sensitivity and specificity vary (39). It is widely accepted that the development of an effective rapid diagnosis test would assist in the effective control of typhoid in endemic areas.

1.5 Antibiotic resistance of *S*. Typhi

The control of typhoid fever is ultimately achieved through improvements in sanitation and hygiene (41). Where this is difficult because of infrastructure constraints, antibiotics and vaccines are used to help control the disease. Vaccines against typhoid fever are of limited efficacy (42). Several vaccines have already gone through clinical trials but are not accepted because of the poor efficacy. In particular, there is still a great need for vaccines which are efficient in children under 2 years of age and provide strong humoral and cell-mediated

immunity (42). Besides vaccine generation is costly, so generally they are not affordable in poor countries (43).

Antibiotic therapy is usually an effective treatment for typhoid fever. In 1948, chloramphenicol was discovered, and this was the drug of choice until 1972 when outbreaks of chloramphenicol-resistant *S*. Typhi were reported in Mexico, Vietnam and Korea and India. These resistant strains often also showed resistance to ampicillin (44-47). Later, trimethoprim-sulfamethoxazole (co-trimoxazole) were used as an effective antibiotic drug until late 1980s (48). The first multi-drug resistant *S*. Typhi were described in the late 1980s and were found to be resistant to all the commonly-used drugs: chloramphenicol, ampicillin and co-trimethoxazole (49, 50). Later, fluroquinolones and cephalosporins were used to treat the MDR *S.* Typhi (51, 52) although isolates that showed resistance to fluroquinolones and cephalosporins increased in numbers (53-56). Currently, a combination therapy of fluroquinolones (ofoxacin and ciprofloxacin) and a third-generation cephalosporin is used for the treatment of typhoid fever (57, 58). Interestingly, a decline in resistance to the three first-line drugs has been observed, possibly because of the removal of selective pressure due to treatment with single antibiotics (6, 59, 60). The emergence of multi-drug resistant *S*. Typhi is a serious threat today (61) and there is an urgent need to identify novel antibiotics that are effective against *S*. Typhi, that would be supported by the identification of novel antibiotic targets.

1.6 Non-typhoidal *Salmonella* (NTS)

Infection with non-typhoidal *Salmonella* (NTS) serovars (except human-restricted serovars Typhi and Paratyphi A, B and C) usually cause self-limiting gastroenteritis (7). It is mostly transmitted by the fecal-oral route, similar to typhoid fever, through food products that are obtained from animal sources such as poultry, eggs, and dairy products. Rarely, transmission can also occur through contact with an infected human. Additionally, pets like cats, dogs and reptiles can act as reservoirs of NTS (7, 12, 13). Some recent outbreaks of NTS were related to contaminated vegetables and fruits (62-64). The NTS isolates associated with gastroenteritis in developed countries are generally not able to produce systemic disease in healthy human, though the systemic disease is not uncommon in the elderly in e.g. nursing homes (65). NTS serovars such as Enteritidis and Typhimurium with wide host range, are the two major serovars that frequently cause diseases in human, accounting for 50% of isolates from patients in the United States (12). NTS infections are characterised by gastroenteritis, diarrhoea, abdominal

pain, nausea, fever and muscle pain (66). The incubation period of nontyphoidal salmonellosis is 6-72 hours, most commonly 12-36 hours, but other factors can change the incubation period (1). The global burden of NTS is estimated to be 93.8 million cases of gastroenteritis each year, with approximately 155,000 deaths (67).

1.7 Antibiotic resistance of Non-typhoidal *Salmonella* (NTS)

Although NTS infections are usually self-limiting in healthy individuals, they can be life threatening in the immunocompromised (12, 68, 69). While generally self-limiting, the very high global burden of morbidity caused by these infections indicates NTS infections are still a serious threat to human health. Gastrointestinal NTS infections are usually not treated with antibiotics, although systemic disease, in especially the immunocompromised, does require antibiotic therapy (70).

As NTS serovars are zoonotic, antibiotic misuse in animals can exacerbate the problem if the isolates are subsequently transmitted to humans (71-74). Initial emergence of multi-drug resistance in NTS serovars occurred in Typhimurium DT29 (a phage type mostly restricted to cattle), which caused epidemics in the 1960s (71). Later, new resistant NTS serovars emerged, including Typhimurium DT104, developed a multi-drug resistant phenotype including ampicillin, chloramphenicol, streptomycin, sulphonamides and tetracycline (75, 76). DT104 was largely found in cattle, pigs, poultry and humans (74-76). DT104 was responsible for epidemics in the 1990s in the UK, caused by eating animal-derived food products (74-76). In summary, previous reports revealed that the serovar Typhimurium shows an increased level of antibiotic resistance than other more commonly isolated serovars (>55%) (77, 78).

1.8 Invasive non-typhoidal *Salmonella* (iNTS)

In Africa particularly, NTS been increasingly isolated from invasive bloodstream infections among young children with malaria, immunocompromised adults and HIV patients, and these infections have a high mortality rate (22-25%) (79). In the developing world, especially in sub-Saharan Africa, HIV is a major risk factor (80) for these invasive NTS infections, termed iNTS. It appears that the natural restriction of gastrointestinal serovars to the gastrointestinal tract breaks down in HIV or malarial co-infection, leading to a more extensive dissemination in co-infected patients (81). The annual disease prevalence for iNTS is 175-388 cases per 100,000 in children (below 5 years) and 1800-9000 cases per 100,000 HIV patients in Africa (8-10). NTS serovars Typhimurium and Enteritidis are the commonest cause of iNTS disease in sub-

Saharan Africa (81, 82). Whereas NTS serovars are mostly zoonotic, humans are thought to act as a reservoir for transmission of iNTS (83). iNTS are now considered as a predominant cause of community-acquired blood stream infection in some areas of Africa (84). A new host-adapted serovar of *S.* Typhimurium, ST313 (the MLST type ST313), has been recently reported. This strain is closely associated with iNTS and has caused numerous outbreaks in humans in Africa (81, 84).

Why the HIV positive humans are so highly susceptible to iNTS infection has yet to be well-defined. Previously it has been reported that mucosal CD4+ T cell depletion impairs innate immune responses in the gut associated lymphoid tissues (GALTs) in cases of Simian Immunodeficiency Virus (SIV) infection (85). This may also occur with iNTS-infected HIV patients. Moreover, HIV co-infection causes extensive changes to the development of humoral immunity, which prevents the clearance of iNTS pathogen (86).

Antibiotic resistance in iNTS serovars is a serious concern because of a large number of HIV-positive patients in sub-Saharan Africa. The emergence of new isolate, D23580 (a representative of ST313) associated with multidrug resistance, has been reported in Africa (87).

1.9 Typhoid fever vaccination

There are three licensed vaccines available against typhoid fever. During the 1890s the first human typhoid vaccine was developed independently by Almroth Wright and Richard Pfeiffer, and the vaccine was consisted of killed, whole bacteria that was inoculated parenterally (88). This whole-cell vaccine was acetone-killed, but the presence of toxins including LPS meant that the vaccine was associated with a headache and fever. In some trials, the efficacy of this killed vaccine was poor (89-92). The reactogenicity and, in some cases poor efficacy, led to the two other, now licensed vaccines, Vi and Ty21a (93), and avariant of Vi known as conjugated Vi vaccine (93).

Vi is a subunit vaccine that was generated by the non-denaturing purification of Vi capsular polysaccharides. Vi antigen is made of repeating units of (1-4)-2-deoxy-2-N-acetyl galacturonic acid and is encoded within the *viaB* locus from *S.* Typhi (94, 95). The antigen purification process helps retaining the original structure of the polysaccharides (96). Two main disadvantages of the Vi polysaccharide vaccine are: i) it does not efficiently elicit antibodies in the young, and ii) because Vi is presented as a T-cell independent antigen, there is the little induction of immunological memory and efficacy wains after a short period. Thus, the Vi

antigen is not protective for children under two years with whom there is a large disease burden, and a booster immunisation is recommended every two years (95-97).

Another licensed vaccine is Ty21a, which is an attenuated strain of *S.* Typhi and is used as a live oral vaccine. This vaccine was produced by random mutagenesis of *S.* Typhi Ty2 using a chemical, nitrosoguanidine (98, 99). This strain was developed in 1975 and is a *galE* mutant which leads to a deficiency of uridine diphosphate (UDP)-galactose-4-epimerase, which catalyses the conversion of UDP-glucose to UDP-galactose (98, 99). The loss of this enzyme results in defective synthesis of polysaccharides in the LPS. Chemical mutagenesis resulted in further point mutations such as those which resulted in a loss of the Vi capsular polysaccharide and auxotrophy for isoleucine and valine (98, 99). This vaccine is recommended for adults and children over 6 years of age with a booster required every 5 years (100-102).

To address issues relating to the poor longer term immunogenicity associated with purified Vi, Vi-rEPA, a Vi-conjugate vaccine was developed (103). The approach was to covalently conjugate the recombinant, non-toxic *Pseudomonas aeruginosa* exotoxin A with Vi-capsular polysaccharide. The exotoxin acts as a protein carrier which converts the T-independent immune response against Vi into a T cell-dependent response, which improves immunological memory, increases antibody responses against the Vi polysaccharide, and induces protection in infants of 2-5 years of age, and with a high efficacy of 90% (104-106).

1.10 *Salmonella* pathogenesis: a general picture

S. enterica can survive outside the animal host in contaminated food and water. After ingestion, *S. enterica* can colonise the intestinal lumen and penetrate the epithelial lining of the gut. After penetration into the intestinal mucosa, the bacteria are translocated into the Peyer's Patches (107-110). From the Peyer's Patches, *Salmonella* spp. can disseminate systemically and can survive within intracellular niches of tissues such as the spleen, liver and bone marrows – the degree and type of dissemination depends on properties of both the *Salmonella* species, subspecies and serovar; and the host. In those hosts where a systemic infection occurs, *S. enterica* of various subspecies can persist in the lymph node, gall bladder, liver, spleen and bone marrow (111, 112). From the liver and gallbladder, bacteria can potentially be reseeded into the gut, a cyclic process that may play a role in persistence and transmission to a new host (113). When the bacteria remain confined in the gut, the infection is characterised by a

gastroenteritis (1). When *S. enterica* spread throughout the system, the infection is typically described as enteric (typhoid) fever (Figure 1-1) (1).

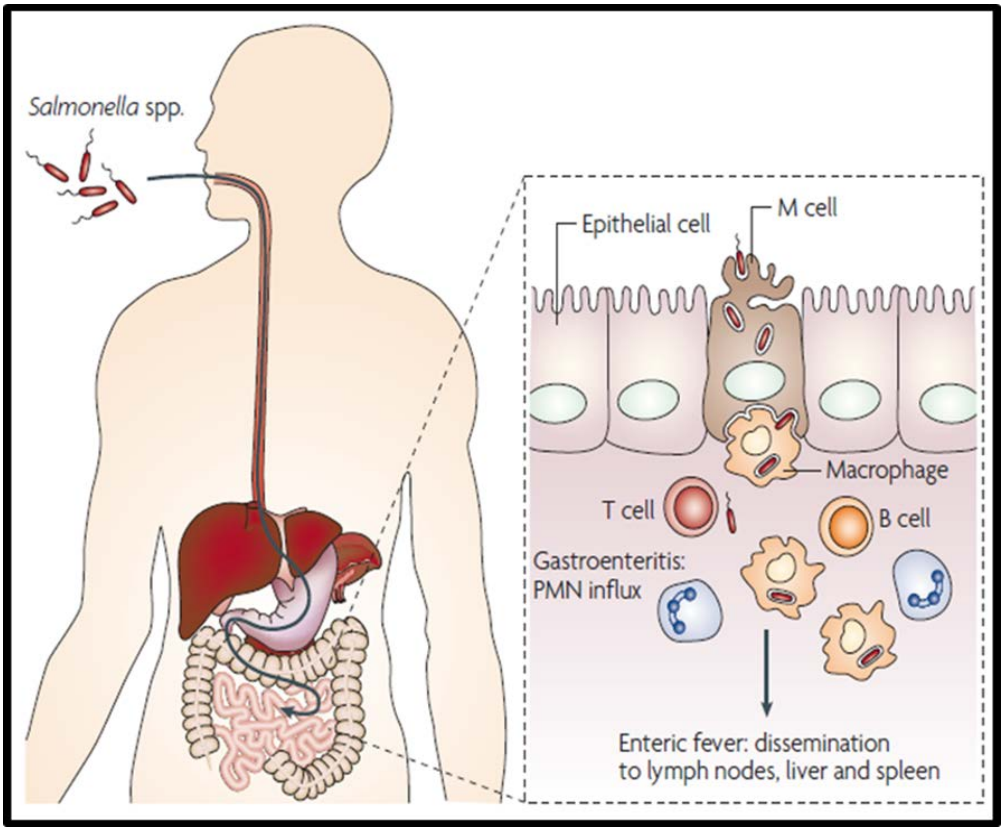

Figure 1-1: *Salmonella* pathogenesis. After ingestion, *S. enterica* can colonise the intestinal lumen and penetrate the epithelial lining of the gut. After penetration into the intestinal mucosa, the bacteria are translocated into the Peyer's Patches. From the Peyer's Patches, *Salmonella* spp. can disseminate systemically and can survive within intracellular niches of tissues such as the spleen, liver and bone marrows. From the liver and gallbladder, bacteria can potentially be reseeded into the gut, a cyclic process that may play a role in persistence and transmission to a new host. Figure is from (114).

1.11 Murine model as a host of *S.* Typhimurium

The pathogen used in this study, *S. enterica* subs. *enterica* var Typhimurium (*S.* Typhimurium), causes diseases in human and animals (see Non-typhoidal *Salmonella*, section 1.6). Due to the strict adaptation of *S.* Typhi and Paratyphi to humans and higher primates, the various aspects of pathogenesis and host immune responses against them are still largely unknown (115). The infection caused by *S.* Typhi in human is similar to the infection in the chimpanzee. But because of the high cost and scarcity of these endangered animals, the use of chimpanzees to study typhoid fever are limited (116). Fortunately, *S.* Typhimurium causes typhoid fever-like systemic infection in mice, including the C57BL/6 and BALB/c mice strains, which is not associated with intestinal inflammation (115). These mouse strains represent well-established

models to study the diseases caused by *S. entrerica* (115). The rationale behind the use of murine host to examine *S. enterica* pathogenesis is largely based on cost-effectiveness and availability and the model infection reflects typical human disease caused by either *S.* Typhi or *S.* Typhimurium (117). Genetically modified mice strains provide further opportunities to study the role of specific host factors in pathogenesis and a diverse array of host immune traits against *S. enterica* (115). Over 5-8 days after oral or intravenous infection genetically susceptible mice show disease signs such as loss of body weight, reduced body temperature control, ruffling of fur and hunching (115). The lesions formed by the initial growth of the bacteria, develop into granulomas with central necrosis and peripheral mononuclear leukocytes (118). These granulomas formed by *S.* Typhimurium in murine host resemble the granulomas formed by *S.* Typhi (119). The lipid A which is an LPS component induces the pro-inflammatory cytokines and inducible nitric oxide synthase (iNOS) which leads to the death of mice (120). Collectively, these observations suggest that the susceptible mice infection with *S.* Typhimurium leads to systemic infection that largely resembles enteric fever Salmonellosis in human, albeit with 100% mortality, which has been reviewed elsewhere (115, 121).

1.12 *S. enterica* replication niches in the host

Salmonella encounters a range of extracellular and intracellular microenvironments that provide specialized niches for *Salmonella* survival and replication. The extracellular replication in the gastrointestinal tract, and the intracellular replication of bacteria inside the membrane-bound vacuoles represent two diversely different microenvironments for the bacterial pathogen (114, 122). *S. enterica* needs to survive and cope with several nutritional and anti-bacterial challenges within these diverse microenvironments.

1.12.1 Intestinal niches and dissemination of *S. enterica*

After infection, mammalian hosts through the oral (natural) route, *S.* Typhimurium survives high acidity in the stomach because of an acid-tolerance response (123). After infection and prior to intestinal epithelial cell invasion, *S. enterica* faces several sub-lethal environmental conditions such as the highly acidic environment of the stomach (123), high levels of bile salts (124, 125), high osmolarity (126), low oxygen tension (126) and high concentrations of the host and bacterial metabolites with anti-*Salmonella* activity such as bactericins (127, 128) in the intestine and short chain fatty acids produced by the dominant gut microorganisms (129). In order to cause disease, *S. enterica* have some defence mechanisms to cope with these stress

conditions (130). *S. enterica* out-compete the gut microbiota and adhere to the intestinal mucosa and then invades the epithelial cells (131). The bacteria preferentially enter the M (Microfold) cells, which are specialised epithelial cells that process the intestinal antigens (108, 132). Junctions that tightly seal the absorptive epithelial cell layer and control the passage of water, ion and some essential metabolites, can be disrupted by *S.* Typhimurium while the bacteria are crossing the barrier, leading to diarrhoea (133). After invasion of the M cells, the bacteria translocate to GALTs, such as Peyer's patches. Later, from the Peyer's patches, *S. enterica* can access the reticuloendothelial system via a variety of cells such as macrophages, neutrophils and dendritic cells and disseminate to other areas of the body (114, 134).

1.12.2 The bacterimic phase of *S. enterica* infection in the host

The bacteria can spread from lymphatic and circulatory system to the secondary infection sites e.g. mesenteric lymph nodes (MLN), bone marrow, gallbladder, spleen and liver (135, 136). Macrophages and dendritic cells are central in the dissemination of *S. enterica* in the infected host and in the initiation of immune reactions (114, 137, 138). It has been suggested that, during the early phase of infection, *S. enterica* can also survive within neutrophils (119). Whereas entry into dendritic cells and macrophages is probably responsible for the movement of the pathogen around the body, neutrophils are thought to be the 'dead end' for *S. enterica* because the cells are short-lived and have strong bacteriocidal activities, such as the production of reactive oxygen species (139).

During chronic infection, the gallbladder acts as a major reservoir of *S. enterica* (140, 141). *S.* Typhimurium can form biofilms on gallstones which result in the chronic carriage and shedding (140, 141). The bacterial presence in the bile can lead to reseeding of the intestines and excretion in faeces, which helps transmission to a new host (140, 141).

In spleen and liver, infected macrophages and dendritic cells are assembled within distinct foci which creates pathological lesions, surrounded by normal tissue in the case of *S.* Typhimurium infection in mice (119, 142). This cellular and tissue organisation to enclose the bacteria into these confined lesions is thought to reduce the uncontrolled spread of the bacteria throughout the tissues. When the infected host fails to form these lesions, then uncontrolled spread occurs throughout the tissues (143).

1.13 Intracellular survival in the *Salmonella*-containing vacuole

Invasion and intracellular survival are dependent on virulence genes, which are clustered together in "pathogenicity islands" on the *Salmonella* chromosome (114, 144-146). The *S. enterica* Type Three Secretion Systems (T3SS) are a classic example of virulence factor that makes invasion and intracellular survival possible. *S. enterica* has two distinct T3SS, which are regulated by different environmental signals and are used to translocate different bacterial effector proteins directly into host cells (114, 144-146). The first *S. enterica* T3SS is invasion-associated and encoded by a pathogenicity island termed *Salmonella* Pathogenicity Island 1 (SPI-1) and the second T3SS mediates the intracellular survival of the bacterium, and the formation of SCV (*Salmonella* containing vacuole) and encoded by *Salmonella* Pathogenicity Island 2 (SPI-2) (114, 144-146).

1.13.1 *Salmonella* pathogenicity Island 1 (SPI-1)

The SPI-1 encoded T3SS becomes activated upon contact with epithelial cells and translocates bacterial effector protein into the eukaryotic cytoplasm (147). When the host effector proteins Rho GTPases are triggered by bacterial SPI-1 proteins SopE, SopE2 and SopB (SigD), it leads to the remodelling of actin cytoskeleton, membrane ruffling and destabilisation of tight junction, and this facilitates bacterial uptake by macropinocytosis (148-151). SopE, SopE2 and SopB are also required for bacterial invasion and for activating the mitogen-activated protein kinase (MAPK) pathways (151). SipA and SipC proteins act to modify the actin cytoskeleton and assist in efficient bacterial uptake in conjunction with the other proteins (152, 153). MAPK directs the activation of host cell transcription factor and the nuclear factors AP-1 and NF-κB respectively, which activate caspases and produce pro-inflammatory cytokines such as IL-8 (154-156). Destabilisation of the tight junction provides for transmigration of the bacteria and PMN (polymorphonuclear leukocytes) from the apical surface to the basolateral surface and results in paracellular fluid leakage (157). SPI-1 is crucial for invading non-phagocytic cells like epithelial cells and M (Microfold) cells in the gut lumen, and the activation of pro-inflammatory cytokines (109, 157).

1.13.2 *Salmonella* pathogenicity Island 2 (SPI-2)

After internalisation, *S. enterica* remains compartmentalised in a vacuole, named spacious phagosome (SP) (158). This phagosome combines with lysosomes, making the internal environment acidic (159-161). The membrane of this compartment shrinks and creates an

adherent membrane around the bacteria. This is called SCV (*Salmonella* containing vacuole) (160, 162, 163). SCV can persist over hours to days supporting the survival of *S.* Typhimurium in the host (164). Pathogens in the phagosome are usually destroyed by a variety of host-protective mechanisms including reactive oxygen species and reactive nitrogen species (165, 166). But *S. enterica* modifies the environment through the secretion of bacterial-protective effector proteins (Chakravortty, Hansen-Wester, & Hensel, 2002; Gallois, Klein, Allen, Jones, & Nauseef, 2001; Haraga et al., 2008; Vazquez-Torres et al., 2000. The ability of *S.* Typhimurium to resist the antimicrobial peptides, nitric oxide and oxidative killing in SCV plays a vital role in its survival in macrophages and this acts as a major virulence trait (114, 167-169). The intracellular acidic environment promotes and coordinates the virulence gene expression in *S.* Typhimurium (170). *S.* Typhimurium is sensitive to the phagosomal environment and induces the expression of the SPI encoded T3SS-2 (171). The intracellular replication of *S. enterica* is associated with the formation of membrane tubules, named *Salmonella*-induced filaments (Sifs) (123, 172). SifA, SseF and SseG are effector proteins, required for maintaining proper positioning of SCV in relation to the Golgi apparatus because *S. enterica* needs nutrients and membrane components which are processed from Golgi (173, 174). It is thought that the main function of the SPI-2 encoded T3SS is to alter host vesicular processing such that useful metabolites, amino acids and lipids are directed to the SCV (147). Some studies that show that the growth of *S. enterica* is restricted in SCV because of the nutritional limitations and egress, the movement to a new cell, may be required to increase the net population of bacteria as the disease progresses (136).

1.14 Bacterial metabolism in the host and its importance

Investigations of *Salmonella* metabolism *in vitro* and *in vivo* is driven by a clear rationale. Metabolism plays a central role in microbial physiology. Previous reports show that the interaction between virulence factors and metabolic pathways allow the pathogen to succeed in host environment (175-178). Control and adjustment in metabolic pathways in host tissues coordinate and regulate the virulence factors in *Staphylococcus aureus* (179). This study has demonstrated that citrate, a component of TCA cycle activates Catabolite control protein E (CcpE) which then controls the expression of virulence genes of *S. aureus* (179). Additionally, genetic disruption of some essential metabolic pathways may lead to growth attenuation of bacterial pathogen in the host, and the attenuated strain can be used as a live-attenuated vaccine (180). The aromatic acid auxotroph strain in *S. enterica* is a good example of this type of

vaccine (180). Moreover, to facilitate new drug development, metabolic pathways can provide targets. Current successful antibiotics only target a small number of features such as DNA replication/synthesis, protein synthesis or cell wall synthesis. A very few number of antibiotics target microbial metabolism such as sulphonamides and trimethoprim which inhibit folic acid biosynthesis (181, 182). Identification of essential metabolic pathways and enzymes which are critical for bacterial virulence may offer novel targets for antimicrobials in the face of increasing resistance of pathogens like *S. enterica*.

Some metabolic pathways are shared between bacteria and their mammalian hosts. Fortunately, and from the perspective of new antimicrobial development, there are some differences which can be exploited (182, 183). Those pathways which are unique to bacteria will need to be analysed to determine whether they are essential for growth and virulence. A careful survey which analysed 700 *S. enterica* enzymes suggested that perhaps 400 enzymes in *S. enterica* metabolism are dispensable (184) and essential pathways are often protected against random mutation by redundancy, reflecting the selective pressure placed on metabolism as a key virulence trait (185). Despite the finding, the authors suggested that some unidentified targets still remain and can be exploited for antimicrobial therapy (185).

1.15 The nutritional profile in the gut during colonisation

In the gut lumen, the predominant nutrient source for *Salmonella* is derived from the diet and host itself including plant polysaccharides and host glycans (186). The epithelium of the host gut is protected by a thick mucus which originally contains a variety of complex proteoglycans and carbohydrates including fucose, mannose, galactose, sialic acid, N-acetylgalactosamine and N-acetylglucosamine (187-189). Pathogenic bacteria including *Salmonella* need to establish a contact with the intestinal epithelia by crossing the mucus layer to effect colonisation (190-192). *S. enterica* is able to exploit the sugars present in the mucus by catalytic degradation to cause disease (193, 194). For instance, *S.* Typhimurium possesses a sialidase and an enzyme to catabolise fucose which degrade the intestinal mucous and helps bacterial attachment (194). A recent study has suggested that the colonisation of *S.* Typhimurium in the intestinal lumen depends on the availability of glycerol, fatty acid, N-acetylglucosamine, glucose, gluconate, arginine and lactate (195). Any of these substrates can provide a carbon source for the bacteria but, in the host, all contribute to pathogenesis (195). Proteomics data revealed *in vivo* expression of some enzymes involved in the metabolism of each of these seven

substrates and suggested that these nutrients can be interconverted and contributed as a sole carbon source (195).

Nutrients can also be provided by enterocytes. Enterocytes are the predominant source of phosphatidylethanolamine, which is a phospholipid in the enterocyte membrane (196). Ethanolamine can act as nitrogen and carbon sources for Enterohaemorrhagic *E. coli* (197). Tetrathionate, derived from H_2S through thiosulfate is produced by *S.* Typhimurium-mediated gut inflammation and tetrathionate respiration where tetrathionate can act as an electron acceptor, enables *Salmonella* to grow anaerobically (198). This respiration provides a colonisation advantage to the bacteria relative to the other competitive and commensal fermentative microbiota in the inflamed gut (198) by supporting the fermentative utilisation of ethanolamine, which is not readily fermented by the pathogen, as a carbon source (199).

Another important component of the gut nutritional profile is the short chain fatty acids (SCFAs). SCFAs are produced through fermentation of indigestible carbohydrates by intestinal microbiota (200). The major SCFAs present in the gut are acetate followed by propionate and butyrate (200). Propionate can act as a carbon source for *Salmonella* at low concentrations (201). At high concentrations, SCFAs are inhibitory for *S. enterica* colonisation (202-204). SCFAs can regulate the expression of the genes contributing to virulence of *S. enterica* (205-208). Acetate induces the SPI-1 encoded T3SS which is involved in invasion whereas, propionate and butyrate exert the opposite effect on the SPI-1 encoded T3SS in *S.* Typhimurium (129). It has also been suggested that the presence of the fatty acids helps *S.* Typhimurium to move to the site of colonisation (129).

1.16 The nutritional profile in the *Salmonella*–containing vacuole

Salmonella virulence is thought to be dependent on the bacterium's ability to enter, survive and replicate within phagocytic and non-phagocytic host cells (209-212). Internalised *S.* Typhimurium resides in the *Salmonella* containing vacuole (SCV) (209-212). It is thought that the SCV in host cells is nutritionally-limited compared with the nutritionally-rich intestinal lumen (195). SCVs are deprived of substrates and amino acids, previous reports have shown that specific *Salmonella* mutants rely on *de novo* biosynthesis of such substrates and amino acids for intracellular survival and replication (180, 213-216). Direct examination of the metabolic environment in SCV is difficult and subject to technical limitations such as conservative purification (195).

Blocking the biosynthesis of chorismate makes *S.* Typhimurium auxotrophic for aromatic amino acids (Tyr, Phe, Trp), dihydroxybenzoate and para-hydroxybenzoate. This auxotrophy is associated with and slows growth rate *in vivo* growth, suggesting that the intracellular environment of SCV is deficient for one or more of these metabolites (180, 216, 217). It is held that, for survival within SCV in murine macrophages, *S.* Typhimurium are not starved of amino acids, iron and potassium, but there is a putative deficiency in phosphate and magnesium in SCV (218). The gene expression profile suggests that when *S.* Typhimurium and *S.* Typhi forms the SCV in epithelial cells, the genes responsible for uptake of magnesium, phosphate and iron are upregulated (218, 219). Further studies revealed an increased induction of biotin synthesis genes of *S.* Typhimurium in infected epithelial cells compared to infected macrophages, which suggests that biotin may be more plentiful in macrophages than epithelial cells (220). The same study also showed that the biotin synthesis was not essential for *S.* Typhimurium survival and replication in epithelial cells (220). A recent report suggested that some amino acids including aspargine, tryptophan and glycine are limited to support the growth of *S.* Typhimurium in host whereas threonine and serine are sufficiently available (221). Based on microarray analysis, *S.* Typhimurium preferentially uses the Entner–Douderoff pathway to metabolise gluconate and similar sugars as a carbon source in macrophages (218). In addition, in human macrophages, *S.* Typhi is known to utilise the glyoxlate bypass pathway for fatty acid synthesis and fatty acids as a carbon source (219).

The growth of *S.* Typhimurium in epithelial cells requires differential expression of genes encoding SPI1 and SPI2; more than 40% of gene expression seen in epithelial cells is modified in macrophages. This differential gene regulation suggests that the metabolic environment of SCV is different based on cell types, and almost certainly different from the external environment (218, 220).

Proteomics has been used to study differential expression of proteins in extracellular and intracellular environments during *S. enterica* infection. One study found that divalent metal-ion transporter proteins are highly expressed in macrophages indicating that *S.* Typhimurium encounters a divalent metal ion-limited condition in the macrophage SCV (222). In addition, there is also evidence of an elevated expression of a putative glutathione-dependent glyoxalase, which is involved in the detoxification of methylglyoxal in *S.* Typhimurium (222). Larger proteomics studies determined the expression level of 477 metabolic enzymes among 1182 in *S.* Typhimurium proteins identified in mice spleen. These included transporters and enzymes

that are involved in metabolism and transport of carbohydrates, lipids, amino acids and nucleosides, although some lowly expressed proteins may not have been detected due to technical limitations (195).

1.17 Met metabolism and transport and its role in bacterial virulence

Methionine (Met) is a sulphur-containing amino acid and an essential component of proteins. Met was first isolated from protein by Mueller in 1922 (223). In 1928, Barger and Coyne identified its structure as a γ-methylthiol derivative of α-amino-*n*-butyric acid (224). Met is obtained through diet in mammals, but most bacteria, fungi and plants synthesise this amino acid from aspartate. Human and animals may also acquire this amino acid from gut flora (225, 226). In 1953, Catoni showed that transmethylation reaction of Met with ATP to form S-adenosylmethionine (SAM) provides the primary and major methyl donor found in all living cells (227). In 1966, Adams and Capecchi, and Clark and Marcker identified the role of formylated Met in the translation of mRNA (228, 229).

Met is a member of aspartate family of amino acids (228, 229). Aspartate is generated from oxaloactetate, which is a α-ketoacid of the TCA cycle (224, 230). In *E. coli* and *Salmonella* spp., the carbon backbone of Met is obtained from aspartate, and cysteine donates the sulphur; further upstream, sulphate provides the sulphur to cysteine via the sulphate assimilation pathway (224, 230). The methyl group of Met is derived from tetrahydrofolate in the one-carbon cycle, and the origin of this methyl group is serine (224, 230).

Met metabolism comprises the anabolism and catabolism of Met. Like many other enteric bacteria, a model pathway for Met biosynthesis in *E. coli* and *Salmonella* spp. has been reported (Figure 1-2). In *E. coli* and *Salmonella* spp. the *de novo* synthesis of Met is initiated from homoserine to form O-succinyl L-homoserine, followed by L-cystathionine, L-homocysteine and subsequently L-Met (224, 230). The predominant methyl donor S-adenosyl methionine (SAM) is formed when Met reacts with ATP (227, 231) and then SAM either goes into the activated methyl cycle to recycle Met and other essential components, or to a functional Met salvage pathway to recycle sulphur through methylthioadenosine (232, 233). In enteric bacteria such as *E. coli* and *Salmonella* spp., the presence of an operational salvage pathway is yet to be demonstrated (234-236).

The reactions of Met biosynthesis pathway are conserved in *E. coli* and *Salmonella* spp. While each reaction of the pathway has alternate reaction processes, in different bacteria and broader

phyla the intermediate metabolites remain conserved. For example, the first reaction can occur in three enzymatic ways: i) Acetylation through homoserine transacetylase which uses acetyl CoA as a substrate and generates O-acetylhomoserine. This enzyme is present in bacteria such as *Leptospira meyeri* (237) and *Corynebacterium glutamicum* (238) and in fungi like *Sachharomyces cerevisiae* (239) and *Neurospora crassa* (240); ii) Succinylation through homoserine trans-succinylase which uses succinyl CoA as a substrate and generates O-succinylhomoserine. This enzyme is present in *E. coli* (241) and *Pseudomonas aeruginosa* (242); iii) Phosphorylation of homoserine by homoserine kinase to form O-phosphohomoserine which occurs in plants (243). Similarly, the synthesis of homocysteine can occur as a result of three enzymatic processes: i) O-acetylhomoserine directly condenses with sulphide to form homocysteine and this reaction is catalysed by O-acetylhomoserine sulfhydrylase. This happens in some bacteria and fungi (244, 245); ii) O-succinylhomoserine condenses directly with sulfide to form homocysteine, which is catalysed by O-succinylhomoserine sulhydrylase. This is found in *Pseudomonas* species (242, 246); iii) Trasnssulfuration where homocysteine synthesis occurs in two enzymatic steps: Cystathionine gamma synthase (CGS) which generates cystathionine, and cystathionine beta lyase which converts cystathionine into homocysteine. Transsulfuration occurs in plants, many bacteria and fungi (247-250). CGS can utilise all three or one or two of O-acetylhomoserine, O-succinylhomoserine and O-phosphohomoserine (251). The last step of the pathway, the conversion of homocysteine to Met happens even in organisms which do not have the capacity to synthesise Met (252). There are two types of Met synthases: i) the Vitamin B12-dependent Met synthase which is present in mammals, protists and most other bacteria (253-255); and ii) Vitamin B12-independent Met synthase which is present in bacteria, plants and fungi (256-258).

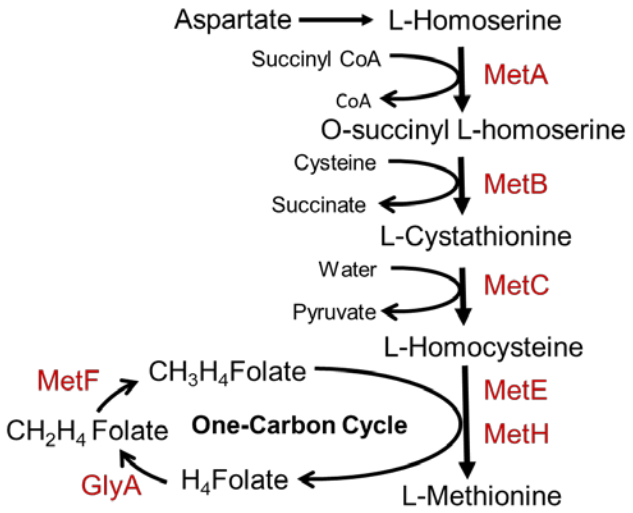

Figure 1-2: Met biosynthesis pathway. In *E. coli* and *Salmonella* spp. the *de novo* synthesis of Met is initiated from homoserine to form O-succinyl L-homoserine, followed by L-cystathionine, L-homocysteine and subsequently L-Met. Enzymes in this pathway are shown in red. Arrows indicate the direction of catalytic reactions. Figure adapted from (259).

Salmonella spp. can import Met though two different systems: either a high-affinity or putatuve low-affinity transporter(s). The high-affinity transporter (K_m~0.1 μM) is composed of three proteins: an ATPase (encoded by *abc*), a permease (encoded by *yaeE*) and a substrate binding protein (encoded by *yaeC*), which are known as MetN, MetI and MetQ, respectively (collectively known as MetD) (260-262). MetNIQ is a member of the Met Uptake Transporter (MUT) family. On the other hand, it is postulated that there is at least one cryptic low-affinity transporter, putatively called MetP (K_m~20 to 40 μM) (263-265) (Figure 1-3).

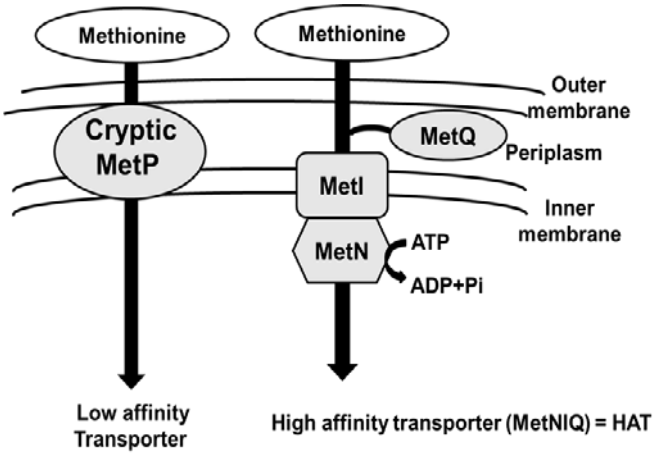

Figure 1-3: Schematic diagram of Met transport in *S.* Typhimurium. Met is transported in *S.* Typhimurium through two types of transporters. The high-affinity transporter is composed of three different proteins, MetN, MetI and MetQ; and low-affinity transporter/s (MetP) is cryptic. Adapted from (259).

The connection between Met metabolism and bacterial virulence has been reported. Previous studies found that amongst transposon mutants, an uncharacterised Met auxotroph of *S.* Typhimurium became defective for intracellular survival in macrophages and epithelial cells, and an approximately 10,000-fold increase in LD50 was demonstrated in mice (209, 215). *Ejim et. al* showed the connection between Met auxotrophy and *S.* Typhimurium virulence (266). They investigated a single mutant Δ*metC* (encoding for cystathionine β-lyase) in *S.* Typhimurium exhibited reduced virulence in mice, as the bacterial burden in the spleen was 100-fold less compared to wild-type control at day 3 post-infection. It was also found that mice orally infected with wild-type *S.* Typhimurium succumbed to infection sooner and more frequently than mice infected with the Δ*metC* mutant strain, indicating that the *metC* gene plays a role in the virulence of *S.* Typhimurium in mice (266). Subsequently, a high throughput screen for inhibitors of *E. coli* MetC revealed several compounds that inhibited MetC function, (267), but the *in vitro* or *in vivo* activity of these compounds was not reported. Moreover, a Δ*metC* mutant of *S.* Gallinarum, a poultry pathogen, was found to be attenuated in 1-day-old chickens (268). It was shown that mutations in the regulation of Met metabolism, affecting MetR and MetJ, attenuated *Vibrio cholerae* in suckling mice (269). MetR plays an important role in colonisation of *V. cholerae* in the mouse intestine (269). *S.* Typhimurium lacking the high-affinity transporter was significantly attenuated in C3H/HeN mice, suggesting that *de novo* Met biosynthesis may not be sufficient for growth in mice (270).

1.18 One carbon cycle

The synthesis of macromolecules such as proteins, nucleic acids and lipids are required for cellular proliferation. The so-called one-carbon cycle is important in the generation of Met and thereby, plays a key role in protein synthesis (271-275). The one-carbon cycle is also known as the folate cycle as folate is reduced through enzymatic steps to generate tetrahydrofolate (THF) (Figure 3-1). Folate is one of the B Vitamins that is essential for humans and is acquired through diet (276, 277). In bacteria, where folate synthesis occurs, THF acts as a platform where carbon atoms are circulated across the different positions of THF moiety (271-275). Methyl-tetrahydrofolate (mTHF) is generated from methylene-tetrahydrofolate (methylene-THF) through Methylenetetrahydrofolate reductase (MetF). The intermediate mTHF donates a carbon unit to homocysteine through methylation, forming Met which is catalysed by Met synthases (271-275). Thus, the activated methyl cycle starts with homocysteine which is coupled to the one-carbon cycle, and this is how the transsulfuration pathway is linked through

homocysteine (Figure 3-1). The carbon unit that is circulated through the one-carbon cycle can be synthesized *de novo* (271-275). Serine transfers the carbon unit from its side chain to folate, converting serine to glycine and THF to methylene-THF which starts the folate cycle. This conversion is mediated by serine hydroxymethyltransferase (GlyA) (213, 278, 279). Serine can be synthesized from the glycolytic intermediate 3-phosphoglycerate (3-PG) or can be imported through amino acid transporters (271, 272). In addition to serine, the carbon unit can also be derived from the cleavage of glycine through the glycine cleavage system (Gcv). Gcv, which is a series of enzymatic reactions, mediates the cleavage of glycine to produce ammonia, CO_2 and a carbon unit for methylation of THF in a reversible reaction (280, 281).

Besides the generation of Met, nucleic acids are also produced from the one-carbon cycle. Methylation of deoxy uridine monophosphate leads to the formation of deoxythymidine monophosphate (282). THF is produced through this concurrent methylation from mTHF (282). Purines are also generated through this one-carbon cycle (283).

GlyA is an essential enzyme for virulence of *S.* Typhimurium in the murine host (221). This study found that *S.* Typhimurium *glyA* mutant had decreased competitive fitness compared to the wild-type, although it was able to grow in minimal media. This indicates that limited availability of glycine during infection and the Gcv system is insufficient in providing glycine during infection (221).

1.19 Activated methyl cycle

The activated methyl cycle is a metabolic cycle which drives methylation of cellular components and the recycling of Met. The methylation of a variety of macromolecules like DNA, RNA, proteins, hormones, lipids and certain metabolites is of fundamental importance for an organism (233, 284, 285). S-adenosylmethionine (SAM), an integral component of this cycle, is synthesised from Met and donates the activated methyl group to macromolecules in prokaryotes and eukaryotes (as reviewed in (232, 285-287)). SAM acts as a propylamine group donor during polyamine biosynthesis (232, 288). SAM is also involved in SAM radical-dependent vitamin synthesis and in the production of N-acylhomoserine lactone (also known as autoinducer-1) (289-292). The methyl group of Met is activated by ATP to form SAM, through the enzyme SAM synthetase (MetK) (293). As enteric bacteria such as *E. coli* and *S.* Typhimurium do not have a transporter for SAM, deletion in SAM synthetase (MetK) is lethal (293-296). Conditional MetK mutants have been generated and were shown to be resistant to

Met analogues like ethionine, α-DL-methymethionines and norleucine at high temperature (294, 297-299). There has been no investigation of MetK phenotype in *E. coli* and *S.* Typhimurium virulence and pathogenesis *in vivo* because the enzyme is essential.

The methyl group of SAM is used for methylation of macromolecules leading to the formation of S-adenosylhomocysteine (SAH). SAH is removed from the cell by either a one- or two-step process (300). The conversion of SAH to homocysteine can occur in one-step by SAH hydrolase (SahH), and SahH is widely distributed in prokaryotes and eukaryotes (300-302). The alternate pathway, which is present in *E. coli* and *Salmonella* spp., uses the enzyme Methylthioadenosine (MTA)/S-adenosylhomocysteine (SAH) nucleosidase (Pfs) to produce S-ribosylhomocysteine (SRH), the sole substrate of SRH lyase (LuxS). LuxS catalyses the cleavage of SRH to produce homocysteine, a process that simultaneously generates the 4,5-dihidroxy-2,3-pentanedione (DPD), a precursor of autoinducer-2 (AI-2) (303, 304). AI-2 is involved in quorum-sensing which acts as a language for intraspecies and interspecies communication (303-309). Studies have shown that cytoplasmic Pfs is present in 51 of the tested 138 bacterial species, SAH hydrolase was present in 60 species, whereas LuxS and SahH are both present in a few species including *Bifidobacterium longum* NCCC2705 and *Escherichia blattae* (303, 310). Neither of the pathways is present in symbionts and intracellular pathogens which cover about 20% of the tested bacterial species (310). Every bacterium which carries LuxS, also possesses a Pfs (303, 310).

MTA/SAH nucleosidase (Pfs) catalyses the deadenylation reaction in bacteria and can mediate at least three reactions. It hydrolyses the glycosidic bond of three substrates SAH, methylthioadenosine (MTA), and 5'-deoxyadenosine (5'-dADO); adenine and sugar are also generated in the process (311-313). The intracellular level of SAH in *E. coli* MG1655 is estimated to be 1.3 μM which is 50 times higher than the wild-type strain (314). This elevated concentration is high enough to inhibit the SAM-dependent methyltransferases *in vitro*, according to previous studies (315-317).

The structure of Pfs has been characterised for many bacteria by X-ray crystallography (318-320). These studies showed that Pfs enzyme is a dimer. The active site of each enzymatic subunit is partly composed of residues from the second subunit and can distinguish between the adenosyl nucleoside substrates. The active site of Pfs is composed of acidic amino acid residues which are conserved across species (321, 322). The transition state structure of Pfs was determined in *E. coli*, *Streptococcus pneumoniae*, *Neisseria meningitides*, *Staphylococcus*

aureus and *S. enterica* (320, 323-326). The role of Pfs inhibitors has been explored in some pathogenic strains by using transition state analogues. The immucillin-based transition state analogues were used as inhibitors and were found to bind with Pfs of *E. coli* O157:H7 and *Vibrio cholerae*, disrupting biofilm formation, and quorum sensing but, without affecting the bacterial planktonic growth possibly because of drug influx (327, 328). Moreover, substrate analogues and transition state analogues that are active against Pfs in *Borrelia burgdorferi* (the causative agent of Lyme disease) have been shown to exert bacteriocidal and bacteriostatic effect (329). Hence, Pfs could be a potential target for broad spectrum antimicrobial drugs but requires more thorough investigation of its 'essentiality' *in vivo*.

1.20 Quorum sensing and LuxS

Other than the recycling of homocysteine to Met and the production of adenine through activated methyl cycle, *E. coli* and *Salmonella* spp. extract an additional benefit from Pfs- and LuxS-mediated reactions; the generation of 4,5-dihrdroxy-2,3-pentanedione (DPD) which is known as AI-2 and plays a role in quorum sensing (330). This low-molecular-weight signalling molecule, produced by LuxS, is the only member of AHL family that is present in Gram-positive and Gram-negative bacteria (331, 332). *E. coli* and *Salmonella* spp. that lack LuxS do not show any growth defect which indicates that Met and SAM recycling through the activated methyl cycle is not essential for growth (308, 333, 334). In contrast, a *luxS* mutant in Enterohemorrhagic *E. coli* (EHEC) had altered flagellation and motility (333) and a *luxS* mutant in Enteropathogenic *E. coli* (EPEC) showed an adhesion defect to epithelial cells, reduced expression of the EPEC T3SS and decreased flagellation and motility (335).

Quorum sensing is a bacterial communication mechanism that helps to initiate a concerted population response. A great variety of Gram-positive and Gram-negative pathogens utilise this mechanism to coordinate expression of genes linked with virulence and growth (305, 309, 336-341). Quorum sensing was discovered in a marine bacterium *Vibrio fischeri*, which utilises a synthase (LuxI) to produce light and form luminescent colonies. The population size determines their ability to produce light through the production of an autoinducer molecule (342, 343). *V. harveyi* is another marine bacterium that uses the autoinducer molecule, AI-2 (described in section 1.19) (344). The best studied quorum-sensing mechanism is mediated by N-acyl-L-homoserine lactones (AHLs) in Gram-negative bacteria (292, 345, 346).

The regulation of other genes by AI-2 and LuxS has been reported. In *E. coli* and *S.* Typhimurium, the *lsr* operon (codes for Lsr ABC transporter) consists of AI-2-regulated genes that promotes the import of AI-2 into the cell (332, 334) and AI-2 production is strongly linked with the transcriptional level of *pfs* in *S.* Typhimurium (347). Higher transcription accounts for the higher detoxification of SAH by Pfs, leading to the high levels of SRH and elevated activity of LuxS (305). Previous studies found that in *S.* Typhimurium *luxS* mutant, *metE* gene expression was increased when compared with the wild-type strain (306).

1.21 The utilisation of SAM in various cellular reactions

A variety of cellular reactions involve SAM as a methyl donor where the methyl group is transferred from SAM to many different targets including DNA, RNA, proteins, lipids and other metabolites (285, 286, 348). SAM can donate the aminopropyl group during polyamine (predominantly spermidine) biosynthesis (233, 349, 350). SAM also participates in the production of N-acylhomoserine lactone (292) and vitamins, including biotin and lipoic acid (351).

1.21.1 SAM-dependent methylations

1.21.1.1 Methylation of DNA and RNA

Methylation of DNA by SAM-dependent methyltransferases is an essential biological reaction. Dam methylase methylates the adenine in GATC (352) and Dcm methylase methylates the second cytosine site in CC(A/T)GG (353). The methylation by Dam methylase is required for basic functions including proof-reading during DNA replication where the endonuclease MutH cleaves the unmethylated daughter DNA strand when it senses a mismatch, and after that DNA Polymerase I repairs the strand (354). The protein DnaA fixes the methylated site (adenine in GATC by Dam methylase) to permit the correct initiation of bacterial DNA replication (355). In addition, many bacteria have protective restriction endonucleases to cleave foreign DNA, which occurs when bacteria are infected by a ‘promiscuous’ bacteriophages). As these endonucleases cleave at sequence-specific sites, methyl groups are added to those sites to protect their own DNA from being cleaved by the endonucleases (356, 357).

Post-transcriptional modifications of RNA are observed in all forms of life. The post-transcriptional modifications of nucleotides in rRNA (ribosomal RNA) and tRNA (transfer RNA) have been reviewed elsewhere (358-361). In general, RNA modifications such as

methylation of the ribose moiety and/or nucleobases in the nucleotides are observed. One important class of enzymes that play a role in the post-transcriptional modification of RNA, is the Rossman-fold methyltransferases. Rossman-fold methyltransferases are the SAM-dependent RNA methyltransferases that first bind with SAM and catalyse the transfer of the methyl group to RNA. Mostly they function to methylate ribosomal RNA (rRNA) (362-364). Most bacterial rRNA methyltransferases are conserved and not found in eukaryotes (365). Certain RNA methylations sites play a critical role in maintaining ribosomal fidelity, maturation, function and alteration of translational rate and there is evidence that an rRNA methyltransferase is essential for growth of bacteria (366). Another important superfamily of RNA methyltransferases is named SPOUT (SpoU-TrmD), and include SpoU tRNA methyltransferases and TrmD tRNA methyltransferases (reviewed in (367)). The SpoU family was characterised in *E. coli*, and *Saccharomyces cerevisiae* (368-370), and TrmD family consists of bacteria-specific tRNA methyltransferases (371).

RNA methyltransferases have been linked with antibiotic resistance (361, 372, 373). Bacterial ribosomes are targeted by some antibiotics. Bacteria have evolved mechanisms to modify the rRNA by adding methyl groups at different nucleotides in 23S rRNA and 16S rRNA, which can lead to antibiotic resistance (361, 372, 373).

1.21.1.2 Methylation of proteins

Bacterial proteins may be methylated through SAM-dependent methyltransferases, such as Protein Methyltransferase A and B (PrmA and PrmB) methylate the N-termini of ribosomal proteins L11 and L3 in *E. coli* (374, 375). Another protein methyltransferase is CheR methyltransferase which methylates the glutamate residues in a chemotaxis receptor Tar. Tar facilitates the detection of chemical stimuli, ultimately leading to the regulation of the direction of flagellar rotation (376, 377).

1.21.1.3 Methylation of other substrates

SAM is also involved in biosynthesis of isoprenoid quinones such as ubiquinone and menaquinone which serve as redox mediators in respiratory electron transport chain in both prokaryotes and most eukaryotes. In *E. coli*, the *ubiE* gene is the putative structural gene for c-methyltransferase that methylates ubiquinone (ie. coenzyme Q) and menaquinone (ie. MK) (378). Moreover, formation of cyclopropane fatty acid, a key component of bacterial membranes (379, 380), requires the methyl group from SAM (379, 380). The enzymatic

cyclopropanation reaction occurs through a transfer of the methyl group from SAM to the unsaturated fatty acid, resulting in the formation of cyclopropane ring in *E. coli* (379, 380). CFA synthase (a *cfa* gene product) is a methyltransferase that catalyses a transmethylation reaction. Many bacteria, when they encounter stress conditions such as starvation and other forms of growth stasis, modify their membrane lipids by converting the unsaturated fatty acid into cyclopropane fatty acids (380, 381). Synthesis of cobalamin (vitamin B12) also relies on methylation through SAM. Mammals require cobalamin but are unable to synthesise it (277). *S.* Typhimurium only synthesises cobalamin under anaerobic conditions (382-384). There are five steps in the Vitamin B12 synthesis process catalysed by the SAM-dependent methyltransferases encoded by five genes (*cbiE*, *cbiT*, *cbiF*, *cbiH*, and *cbiL*) that mediate contraction of the precorrin ring, to generate cobalamin in *S.* Typhimurium (385, 386).

1.21.2 SAM as an aminopropyl group donor in spermidine biosynthesis and role in virulence

Besides methylation, another major SAM-dependent reaction in the cell is polyamine i.e. spermidine and spermine biosynthesis (233, 349, 350). To initiate the synthesis, SAM is decarboxylated by the enzyme SAM decarboxylase (SpeD). The transfer of aminopropyl group from decarboxylated SAM to putrescine leads to synthesis of spermidine and methylthioadenosine (MTA) (349). This reaction is catalysed by spermidine synthase (SpeE) (349, 350)). In bacteria, putrescine is synthesised either from L-arginine by arginine decarboxylase (SpeA) (387, 388) and agmatine ureohydrolase (SpeB) (389-391) or from L-ornithine by constitutive ornithine decarboxylase (SpeC) (392-394) or acid inducible ornithine decarboxylase (SpeF) (395-397).

Polyamines are polycationic amines in all living cells. Polyamines bound to DNA and RNA play a key role in sustaining structural configuration and stability of the nucleic acids (398-400). There are also reports that polyamines are important for protein synthesis (401-403). Spermidine and spermine have a key role in protecting the bacterial DNA from reactive oxygen species (404, 405). Polyamine-deficient *E. coli* strains are more sensitive to oxidative damage than the wild-type bacteria (406). In bacteria, the predominant polyamines are putrescine and spermidine. The intracellular level of spermidine is 1-3 mM compared to putrescine (0.1-0.2 mM), in most bacteria (288). Putrescine is the predominant polyamine in *E. coli*, followed by spermidine (288). In *E. coli*, the genes responsible for spermidine biosynthesis, *speD* and *speE*, are organised in an operon (407) and are located at some distance from *speABC*, the genes

required for putrescine biosynthesis. *S.* Typhimurium is not able to utilise spermidine and putrescine as the sole sources of carbon and nitrogen, whereas *E. coli* can (408) .

E. coli, *S.* Typhimurium and *S.* Gallinarum Δ*speE* or Δ*speD* mutants have minimal growth defects suggesting that spermidine is not essential for growth (409, 410). Although it has been recently shown that polyamines play a vital role in virulence of several intracellular pathogens including *Legionella pneumophila*, *Francisella tularensis*, and in *Shigella* spp. The function of polyamines in *S.* Typhimurium virulence remains under question (411-414). Some studies revealed that the genes responsible for uptake of putrescine and spermidine are upregulated in *S.* Typhimurium during intracellular growth and replication in epithelial cells and macrophages (218, 220). Putrescine and spermidine affect the invasion, intracellular survival and proliferation of *S.* Typhimurium and *S.* Gallinarum and play a role in virulence (410, 415, 416). The basis for this reduced virulence was not well-understood but could be because of reduced expression of genes coding for T3SS structural components and effectors. The exogenous supply of putrescine and spermidine significantly increases the intracellular survival of *S.* Typhimurium and indicates that polyamines might act as environmental signals for *Salmonella* spp. where they drive transcriptional priming (410, 415, 416).

1.21.3 Radical SAM enzymes

Radical SAM enzymes catalyse a range of reactions where reductive cleavage of SAM yields 5'-deoxyadenosine (5'-DOA) and Met. In these reactions, SAM acts as an oxidising agent which participates in sulphur insertion, anerobic oxidation, ring formation and isomerisation (351). Biotin synthase (BioB) is a radical SAM enzyme that catalyses the sulphur insertion into dethiobiotin and converts it into biotin (289). The sequence homology between lipoate synthase (LipA) and BioB suggests that LipA is also a radical SAM enzyme (290). Accumulation of 5'-DOA (which is also a substrate for MTA/SAH nucleosidase) is inhibitory for radical SAM enzymes and therefore, the removal of 5'-DOA from the cell is required (312, 417, 418).

1.21.4 Participation of SAM in the production of N-acetyl homoserine lactone

The production of acyl homoserine lactone Autoinducer-1 (AI-1) by LuxI/LuxR system from SAM is catalysed by LuxI (Acyl homoserine lactone synthase). The fatty acid chain comes from an acyl carrier protein (fatty acyl-ACP), and the homoserine lactone group is derived from SAM. The homoserine lactone is condensed to the acyl side chain and generates AI-1, and a by-product methylthioadenisine (MTA) (291, 292). When AI-1 is excreted from the cell, it

interacts with LuxR which is a transcriptional regulator and in turn controls the transcription of *lux* operon, which produces the luciferase enzyme and this further leads to luminescence (419). This LuxI/LuxR system was first discovered in *Vibrio fisheri* (342, 344, 419).

MTA, which is formed by LuxI catalysed reaction, is toxic and has an inhibitory effect on SAM-dependent methyltransferases and hence must be removed from the cell (347, 420). Pfs catalyses the reaction to remove this toxic MTA from the cell (329, 421-423). *E. coli* and *Salmonella* do not possess LuxI and therefore do not produce AI-1 (424, 425) but they instead express a protein named SdiA which is a LuxR homologue, and detects the AI-1 molecule produced by other bacteria (333, 426).

1.22 Overview of methionine salvage pathway

Recycling of 5'-methylthioadenisine (MTA) to Met is known as the Met salvage pathway or MTA cycle and is present in both prokaryotes and eukaryotes with a few exceptions, and its primary role appears to be the removal of toxic MTA (235, 236). In *Klebsiella pneumoniae*, *Bacillus subtilis* and *Pseudomonas aeruginosa*, this pathway has been fully characterised (234, 427-430)

In a functional Met salvage pathway, MTA is hydrolysed to 5'-methylthioribose 1-phosphate (MTR1P) through two different pathways. The conversion may be a one-step process from MTA to MTR1P, catalysed by an enzyme MTA phosphorylase. In animals, this type of direct conversion occurs whereas, in bacteria, protozoa and plants, the conversion is conducted in two steps. In these organisms, MTA is cleaved to 5'-methylthioribose (MTR) and adenine and this reaction are catalysed by Pfs. MTR is then phosphorylated by MTR kinase and forms 5'MTR1P. MTR1P is further transformed into 5'-methylthioribulose 1-phosphate (MTRu1P) by MTR1P isomerase. MTRu1P is subsequently converted to 4-methylthio-2-oxobutyrate (MTOB) through some enzymatic reactions mediated by a dehydratase, an enolase, a phosphatase and a dioxygenase. Transaminases finally perform the conversion of MTOB to Met (234, 429, 430).

In many enteric bacteria such as *E. coli* and *Salmonella* spp., the fate of MTR is unknown, and MTR is likely to accumulate in the extracellular medium (431, 432). *E. coli* have an efficient exporter of MTR (431-433). Therefore, it has been suggested that they do not have an analogous mechanism of Met salvage. There are some assumptions which suggest that the loss of functional salvage pathway in some organisms seems to be a response to a specific

ecological niche, as these organisms usually live in anaerobic conditions, and in the presence of sulphur (235, 432, 434). The answer to why these organisms would lack this Met salvage pathway is unresolved. Indeed, there are some interesting hypotheses behind the evolution of this pathway. First, sulphur assimilation is energetically costly so retaining the sulphur in the cells would be advantageous for organisms who live in a low sulphur environment. In contrast, *E. coli* and *Salmonella*, which often live in a sulphur-rich and anaerobic environment, do not require an operational salvage pathway (235, 432, 434). The problem posed to *E. coli* and *Salmonella* spp. would be to eliminate excess sulphur rather than its expanded utilisation (235, 432, 434). Secondly, both *E. coli* and *Salmonella* do not possess the MTR kinase which is consistent with the finding that a Met auxotroph (Δ*metE*) is not able to utilise MTA as a source of Met (435). Collectively, these data support the hypothesis that the salvage pathway is not intact in enteric bacteria like *E. coli* and *Salmonella*.

1.23 Summary and aim

S. enterica poses a significant threat to human and animal health around the world, and new antibiotic is urgently needed. Knowledge concerning the pathogen's metabolic requirements in the host could assist the search for novel drug targets. The host-*Salmonella* interactions vary significantly between local (e.g. the gut) and systemic sites (e.g. the spleen and liver), such differences in growth niche is hypothesised to have profound impact on *Salmonella* metabolism. Metabolic enzymes in Met biosynthesis, one carbon cycle, activated methyl cycle and the incomplete Met salvage pathways were reported to play an important role in the virulence of *Salmonella* and in other bacteria. However, these pathways have not been thoroughly and systematically investigated to examine their role in virulence of *S. enterica.*

The major objective of this thesis is to study the role of Met metabolism by *Salmonella enterica* subsp. *enterica* var. Typhimurium SL1344 in pathogenesis and intracellular survival *ex vivo*, in tissue culture cells and in the experimental model system of choice, the inbred mouse. This study was therefore conducted by generating defined deletion mutants of the enzymes of these pathways and the mutants were characterised by testing their ability to grow *in vitro* in M9 minimal media, the ability to grow intracellularly through intracellular survival assays in HeLa cells and their virulence in C57BL/6 mice.

Chapter 2

Materials and Methods

2.1 Manufacturers and suppliers

The name and locations of manufacturers used of all reagents and equipment in this research are listed in Table 2-1

Table 2-1. List of suppliers and manufacturers of all reagents and equipment in this research

Name	Location
Applied Biosystems	California, USA
BD Biosciences	California, USA
Beckman Coulter	California, USA
Bio-Red Laboratories	California, USA
BMG LABTECH	Ortenberg, Germany
eBioscience	California, USA
Eppendorf	Hamburg, Germany
Geneworks	South Australia, Australia
GraphPad Software	California, USA
Greiner Bio-One	Frickenhausen, Germany
Heraeus	Newport, UK
Life Technologies	California, USA
Merck	Darmstadt, Germany
Miltenyi Bioteck	Rheinisch-Bergische Kreis, Germany
Misonix	New York, USA
MP Biomedicals	Ohio, USA
NEB (New England Biolabs)	Maryland, USA
Nunc	Kamstrupp, Denmark
Oxoid	Hampshire, UK
Promega	Wisconsin, USA
Qiagen	Venlo, Netherlands
Roche Molecular Biochemicals	Mannheim, Germany
Sarstedt	South Australia, Australia
Seward Medical	West Sussex, UK
Sigma-Aldrich	Missouri, USA
Syngene	Cambridge, England
Thermo Fisher Scientific	Massachusetts, USA

2.2 Media, buffers and solutions

The composition of all buffers, solutions and media used in this research are described in Table 2-2

Table 2-2. Culture media, buffers and solutions used in this research

Name	Compositions
M9 Minimal media	**Solution 1 (M9 salt):** 15 g KH_2PO_4, 64 g $Na_2HPO_4.7H_2O$, 2.5 g NaCl, 5 g NH_4Cl, in 1000 ml distilled water **Solution 2:** 200 ml M9 salt, 2 ml 1 M $MgSO_4$, 20 ml 2% Glucose and 100 µl 1 M $CaCl_2$ adjusted to 1000 ml distilled water. M9 minimal media was supplemented depending on the growth requirement of auxotrophic *S.* Typhimurium mutant strains. L-histidine was added at a final concentration 100 µM. L-methionine was added at a final concentration 100 µM
DMEM-Complete	Dulbecco's Modified Eagle Medium (Life Technologies) containing 10% (v/v) heat-inactivated Fetal calf serum (FCS) and GlutaMAX (Life Technologies)
DMEM-No Met	Dulbecco's Modified Eagle Medium (Life Technologies) containing 10% (v/v) heat-inactivated FCS and GlutaMAX (Life Technologies). No methionine and cysteine supplemented in the media
Fetal Calf Serum	FCS (Bovogen) was heat-inactivated in a 56°C water bath for 2 hours prior to use
LB-Miller broth	1% (w/v) tryptone (BD Biosciences), 0.5% (w/v) yeast extract (Merck), 1% (w/v) NaC1; prepared in distilled water and autoclaved
LB Agar Miller (Luria Bertani)	4% (w/v) agar (BD Difco™) in LB-Miller broth
LUS	Luria agar with streptomycin (supplemented at a final concentration 50 µg/ml)
PBS	137 mM NaC1, 2.6 mM KCL, 100 mM Na_2HPO_4, 2 mM KH_2PO_4; prepared in distilled water and autoclaved
PBST	PBS containing 0.05% (v/v) Tween 20
Blocking buffer	PBST containing 5% skim milk
TAE buffer	40 mM Tris base, 5.7% (v/v) glacial acetic acid, 1 mM EDTA in distilled water, pH adjusted to 8.0
Triton X-100 1%	1% (v/v) Triton X-100 in distilled water
Trypan blue, 0.4%	Trypan blue powder (Sigma-Aldrich) was dissolved in distilled water at 0.4% (w/v) and filter sterilised
TSS broth	LB-Miller broth containing: 10% (w/v) PEG 3350, 5% (v/v) DMSO, 50 mM and $MgC1_2$ in distilled water
TSS enhanced buffer	100 mM KC1, 30 mM $CaC1_2$, 50 mM $MgC1_2$ in distilled water
Eosin Blue Uranine (EBU)	**Solution 1:** 5g tryptone, 2.5g yeast extract, 2.5g NaC1, 7.5g agar in 500 ml distilled water, autoclaved **Solution 2**: 1.25g K_2HPO_4 in 50 ml distilled water, autoclaved. After mixing solution 1 and 2, 625 µl 1% Evans Blue Dye and 125 µl 10% Sodium fluorescein (all from filter-sterilised solutions) were added
XLD agar	Xylose lysine deoxycholate agar (Oxoid) was prepared according to manufacturer's instructions
XLDS agar	XLD with streptomycin supplemented at a final concentration 50 µg/ml

2.3 Bacterial strains

All bacterial strains used in this research are listed in Table 2-3

Table 2-3. Bacterial strains used in this research

Strains/Genotype	Phenotype and genotype	Source/Ref
***Salmonella enterica* subspecies *enterica* serovar Typhimurium**		
SL1344	Wild-type	Ref
SL1344 Δ*metA*	Met biosynthetic mutant; deletion of *metA*	This study
SL1344 Δ*metB*	Met biosynthetic mutant; deletion of *metB*	This study
SL1344 Δ*metC*	Met biosynthetic mutant; deletion of *metC*	This study
SL1344 Δ*metE*	Met biosynthetic mutant; deletion of *metE*	This study
SL1344 Δ*metF*	Met biosynthetic mutant; deletion of *metF*	This study
SL1344 Δ*metH*	Met biosynthetic mutant; deletion of *metH*	This study
SL1344 Δ*metE*Δ*metH*	Met biosynthetic mutant; deletion of *metE* and *metH*	This study
SL1344 Δ*metNIQ*	High-affinity transporter mutant	This study
SL1344 Δ*metNIQ*Δ*metB*	High-affinity transporter and met biosynthetic mutant; deletion of *metNIQ* and *metB*	This study
SL1344 Δ*metNIQ*Δ*metE*	High-affinity transporter and met biosynthetic mutant; deletion of *metNIQ* and *metE*	This study
SL1344 Δ*metNIQ*Δ*metH*	High-affinity transporter and met biosynthetic mutant; deletion of *metNIQ* and *metH*	This study
SL1344 Δ*metNIQ*Δ*metE*Δ*metH*	High-affinity transporter and met biosynthetic mutant; deletion of *metNIQ*, *metE* and *metH*	This study
SL1344 Δ*speD*	SAM decarboxylase mutant; deletion of *speD*	This study
SL1344 Δ*speE*	Spermidine synthase mutant; deletion of *speE*	This study
SL1344 Δ*luxS*	Activated methyl cycle mutant; deletion of *luxS*	This study
SL1344 Δ*bioB*	Biotin synthesis mutant; deletion of *bioB*	This study
SL1344 Δ*pfs*	Activated methyl cycle mutant; deletion of *pfs*	This study
BRD509	Aromatic amino acid auxotroph	(436)
BRD666	Restriction negative; modification positive (r^-m^+)	(437)
Escherichia coli		
DH5α (F-endA1hsdR17 (r_K^-, m_k^+) *supE*44 *thi*-1 λ-*rec*A1 *gyrA*96 *relA*1 *deo*R Δ(*lacZYA-arg*F)-U169Φ80d *lacZ* ΔM15; Nal^R	Cloning strain	(438)
MC4100 (Δ(*argF*-lac)U169 *rpsL* 150 *relA* *araD139 fib301 deoC1 ptsF25*)	Cloning strain	(439)

2.4 Plasmids

All plasmids used in this research are listed in Table 2.4

Table 2-4. Plasmids used in this study

Plasmids	Relevant phenotype and genotype	Source/Ref
pGEM-Teasy	High-copy-number, cloning vector for PCR products; Amp^R; Ara-inducible I-SceI and λ Red recombinase	Promega
pACBSR	Medium-copy number, mutagenesis plasmid; p15A ori; Chl^R	(440)
pACYC184	Medium-copy number cloning vector, p15A ori; Tet^R, Chl^R	(441)
pCP20	FLP recombinase, temperature-sensitive replicon; Amp^RChl^R	(442)
pKD4	FRT-flanked Kan^R cassette; Amp^R, Kan^R	(443)
pACYC184 *metB*	*S.* Typhimurium *metB* cloned into pACYC184; Chl^R	This study
pACYC184 *pfs*	*S.* Typhimurium *pfs* cloned into pACYC184; Chl^R	This study
pACYC184 *sahH* (Lp)	*Legionella pneumophila sahH* cloned into pACYC184; Chl^R	This study

2.5 Bacterial growth, preparation for infections and storage

2.5.1 Bacterial culture media

All bacterial culture media used in this study are listed in Table 2-2. The Media Preparation Unit (MPU) at the Department of Microbiology and Immunology, The University of Melbourne prepared LB-Miller liquid media, solid media including LUS plates and XLDS plates (For composition see Table 2-2)

2.5.2 Bacterial growth conditions

To obtain single isolated colonies the bacteria were streak diluted onto LB-agar plates and incubated at 37ºC overnight. Single bacterial colonies were selected with a sterile wire loop or needle from solid agar plates and transferred into 10 ml LB-Miller broth and incubated at 37ºC overnight with shaking (180 rpm). When necessary, appropriate antibiotic(s) were supplemented in the solid and liquid media at a final concentration of 50 μg/mL for ampicillin, kanamycin and streptomycin, and 30 μg/mL for chloramphenicol.

2.5.3 Exponential phase bacteria

To obtain bacteria in the exponential growth phase, 100 µl of overnight liquid culture bacteria in LB-Miller broth were transferred to 10 ml sterile LB-Miller broth and grown with shaking (180 rpm) at 37ºC for 3-4 hours to reach the mid-exponential phase, typically at an optical density (OD_{600}) at 0.6-0.8 for *Salmonella* and *E. coli.*

2.5.4 Growth conditions of *S*. Typhimurium for *in vitro* infections

S. Typhimurium strains were grown in Luria-Bertani media as described in 2.5.2 and 2.5.3. After reaching the desired OD_{600} reading of 0.6 ~ 0.8, 80% (v/v) glycerol was added to the broth culture at a 1 to 10 ratio. The culture was divided into 1 ml aliquots and stored at -80ºC. To determine the bacterial dose, one aliquot was thawed, serially diluted in PBS and appropriate dilutions were spread on LUS plates and incubated at 37ºC overnight before the colonies were enumerated. When infecting in HeLa cells, aliquots stored at -80ºC were thawed and diluted to desired concentration in DMEM-Complete media.

2.5.5 Growth conditions of *S*. Typhimurium inoculum for murine infections

All strains of *S*. Typhimurium were grown in M9 minimal media supplemented with 100 µM methionine and 100 µM histidine at 37ºC for 24 hours, with shaking at 180 rpm. After determining the OD_{600} of the culture, 80% (v/v) glycerol was added to the broth culture at a 1 to 10 ratio, and 1 ml aliquots were stored at -80ºC. To determine the number of cfu per ml, one an aliquot was thawed and serially diluted in PBS, dilutions of the aliquot were spread on LUS plates, incubated at 37ºC overnight and colonies were enumerated. For use in mice and just prior to inoculation, the stored aliquots in the -80ºC freezer were thawed and diluted in PBS as required.

2.5.6 Storage of the bacterial strains

Salmonella and *E. coli* strains were stored as streak plated on LUS plates at 4ºC for a maximum of 4 weeks. When long term storage was required, 10 ml LB-Miller broth cultures were grown overnight with shaking (180 rpm) at 37ºC with the appropriate antibiotic supplemented, then 250 µl of 80% (v/v) glycerol was added to 750 µl of the culture, which was then transferred to a cryovial and stored at -80ºC.

2.6. Testing growth kinetics of *S*. Typhimurium

S. Typhimurium SL1344 wild-type strain and mutants were grown in LB-Miller broth as described in section 2.5.2. After overnight incubation, 1 ml of the broth culture was taken into a new Eppendorf tube, the bacterial cells were pelleted by centrifugation at 16,060 ×g for 10 min and resuspended in an equal volume of PBS, diluted 1:1000 and finally from that dilution 200 µl was transferred in 20 ml M9 minimal media supplemented with histidine 100 µM and/or appropriate metabolites e.g. methionine, as required. Inoculated cultures were incubated at 37ºC with shaking at 180 rpm until the desired time point was reached. In order to quantify bacterial concentration, at each time point, 100 µl of the culture was diluted in PBS and then plated on LUS plates to determine the cfu/ml. The plates were incubated at 37ºC overnight and colonies were subsequently enumerated.

2.7 DNA methods

2.7.1 Genomic DNA extraction

Genomic DNA was extracted from bacterial strains by using a method adapted from Sambrook *et. al*. 2001 (444). Bacteria were harvested from 10 ml LB-Miller broth culture grown at 37ºC with shaking. 5 ml of the culture was centrifuged at 2,851 ×g for 10 min. The supernatant was discarded and the pellet was resuspended in 2 ml of PBS. Then 1.5 ml of 20% SDS and 25 µl of 20 mg/ml Proteinase K (Promega) were added to the resuspended bacteria. The Proteinase K digestion was incubated at 37ºC until the cell suspension was clear, approximately in 30-60 min. The suspension was transferred to a 15 ml Phase-lock tube (5prime), an equal volume of phenol: chloroform was added and the mixture was mixed gently until a milky emulsion formed. The mixture was centrifuged (2,851 ×g, 2 min), the top aqueous phase was recovered carefully without disturbing the lower phases and transferred to a fresh Phase-lock tube. The centrifugation step was repeated and the aqueous phase was collected into a sterile centrifuge tube. An equal volume of chloroform:isoamyl alcohol (24:1) was added to the aqueous portion and mixed gently until a milky emulsion formed. The suspension was centrifuged again (2,851 ×g, 2 min) to separate the emulsion, the top (aqueous) phase was recovered carefully without disturbing the lower phases and transferred into a fresh 10 ml tube. After phenol: chloroform: isoamyl alcohol extraction, 3M Sodium acetate (pH:5.2) was added to the DNA solution at a 1 to 10 ratio and mixed well. Then, ice-cold 95% ethanol was added at double the volume and the tube was inverted gently until DNA was visibly precipitated out of the solution. Precipitated

DNA was then washed with cold ethanol (70%) for 5 min by inverting the tubes several times. DNA was transferred to a new Eppendorf tube and air dried for 5-10 min and then, resuspended in 0.5 ml distilled water and stored at -20ºC.

2.7.2 Plasmid DNA extraction

Plasmid DNA was extracted from bacterial strains using the Wizard Miniprep DNA purification system (Promega), as per the manufacturer's instructions. The concentration of the plasmid DNA was determined (see section 2.7.8) and was stored at -20ºC.

2.7.3 Standard polymerase chain reaction (PCR)

All PCR amplifications were performed using a Veriti 96 well Thermal Cycler (Applied Biosystems). Depending on the purpose of the PCR, 20, 50 or 100 µl standard reaction mixtures were produced that included: 200 µM of dNTP mix (Promega), 0.5-1 µM of each oligonucleotide primer (Geneworks), 10-200 ng of template DNA, 1-10 U of DNA Polymerase (Promega or NEB), the appropriate enzyme buffer and autoclaved MiliQ water to make up the required volume. Unless stated otherwise, the following programme was used for PCR: Initial denaturation at 95ºC for 1 min followed by 30-35 cycles at 95ºC for 1 min, annealing was set at 5ºC below of the T_m of the primers for 1 min, extension at 72ºC (1 min/kb of DNA to be amplified), followed by a final extension at 72ºC for 5 min.

2.7.4 Colony PCR

Single bacterial colonies grown on solid agar were selected using a sterile pipette tip and resuspended in 50 µl MiliQ water, and then boiled for 10 min. The boiled lysate was cooled down for 5 min at room temperature and centrifuged at 9,503 ×g for 5-10 min. The supernatant was removed and transferred to a new tube for further analysis. 1 µl was used as a template in a 20 µl reaction mixture with GoTaq Green Master Mix (Promega) and 0.5 µM of each primer (Geneworks).

2.7.5 Oligonucleotide primers

All primers used in this research (for sequencing and PCR) were purchased from Geneworks and are listed in Table 2-5. The primer stocks were prepared in MilliQ water and the stock concentration was adjusted to 10 µM.

Table 2-5. Oligonucleotide primers used in this study for mutant construction and verification

Mutants	Sequence (5'-3')	Application
Δ*metA*-ISceI- F	**TAGGGATAACAGGGTAAT**CGCCAGTGTTAACGCATGTTC	Mutant construction
Δ*metA*-ISceI- R	**TAGGGATAACAGGGTAAT**CGGAATACCACGAATCTGCC	Mutant construction
Δ*metA*-Kan-F	**CTAAGGAGGATATTCATATG**CGCAGCCACGGTAATTTACTG	Mutant construction
Δ*metA*-Kan-R	**GAAGCAGCTCCAGCCTACACA**ACCTGATAACCTCACGACATACG	Mutant construction
Δ*metA*-Chk-F	ACATGCACTTATCAGACAGCG	Mutant verification
Δ*metA*-Chk-R	GGTATAGCTAATGGTGCCGTTC	Mutant verification
Δ*metB*-ISceI- F	**TAGGGATAACAGGGTAAT**CGCAGATCGGCATCATCC	Mutant construction
Δ*metB*-ISceI- R	**TAGGGATAACAGGGTAAT**CTTCATCAACCTGCGGCTG	Mutant construction
Δ*metB*-Kan-F	**CTAAGGAGGATATTCATATG**CGGTATTGAAGATGGCGAAG	Mutant construction
Δ*metB*-Kan-R	**GAAGCAGCTCCAGCCTACACA**CAGCCGTATTGTTCGTCATCG	Mutant construction
Δ*metB*-Chk-F	AGAACAATGTCGGAGATAGCC	Mutant verification
Δ*metB*-Chk-R	GTGGCGGAATAGTCGGAAC	Mutant verification
Δ*metC*-ISceI- F	**TAGGGATAACAGGGTAAT**CCTTCGTTATCTTCGCTGCC	Mutant construction
Δ*metC*-ISceI- R	**TAGGGATAACAGGGTAAT**CAGCAGAGTGCGGACAAACG	Mutant construction
Δ*metC*--Kan-F	**CTAAGGAGGATATTCATATG**GCTGGTTCGGGTGCATATTG	Mutant construction
Δ*metC*-Kan-R	**GAAGCAGCTCCAGCCTACACA**CACTATTCACTGAGCCAAGCG	Mutant construction
Δ*metC*-Chk-F	CGATCGTCGCCAGATAACC	Mutant verification
Δ*metC*-Chk-R	CATTACCTGGTCTTCATGGCG	Mutant verification
Δ*metE*-ISceI-F	**TAGGGATAACAGGGTAAT**CTACCTGCGGCCAGCTTG	Mutant construction
Δ*metE*-ISceI-R	**TAGGGATAACAGGGTAAT**CAATGCGGTCGCCACTCTG	Mutant construction
Δ*metE*--Kan-F	**CTAAGGAGGATATTCATATG**GGCGTTAGCGAACATGGTC	Mutant construction
Δ*metE*-Kan-R	**GAAGCAGCTCCAGCCTACACA**TCAACTCGCGACGCAGG	Mutant construction
Δ*metE*-Chk-F	CATCGGCGAATAATGCAGTC	Mutant verification
Δ*metE*-Chk-R	CCCACTCGTCATTCACCAGG	Mutant verification
Δ*metF*-ISceI-F	**TAGGGATAACAGGGTAAT**GCAGCCTGATGGAGCATGG	Mutant construction
Δ*metF*-ISceI-R	**TAGGGATAACAGGGTAAT**GCCACGACCATCAATAGAACG	Mutant construction
Δ*metF*--Kan-F	**CTAAGGAGGATATTCATATG**GCCGTGAAGGAGTGAAGGA	Mutant construction

Δ*metF*-Kan-R	**GAAGCAGCTCCAGCCTACACA**CTTCCGCCAGGCTCTGATTC	Mutant construction
Δ*metF*-Chk-F	GACACCCAGTTAGCGCTTAC	Mutant verification
Δ*metF*-Chk-R	CAGAATAAACAGGTCGGCC	Mutant verification
Δ*metH*-ISceI-F	**TAGGGATAACAGGGTAAT**CGGTGAGTCGTGGAATTAGGC	Mutant construction
Δ*metH*-ISceI-R	**TAGGGATAACAGGGTAAT**CGTCAGGGCGACAAGATCC	Mutant construction
Δ*metH*--Kan-F	**CTAAGGAGGATATTCATATG**GAGGATGTTGAGCGGTGGC	Mutant construction
Δ*metH*-Kan-R	**GAAGCAGCTCCAGCCTACACA**GCCGTCCAGCACCAGAATAC	Mutant construction
Δ*metH*-Chk-F	GCTACCGACGATAAACGCG	Mutant verification
Δ*metH*-Chk-R	CCAGCGCCAGTAGAATCAGG	Mutant verification
Δ*metNIQ*-ISceI- F	**TAGGGATAACAGGGTAAT**ACTGCCCTGCGGATGG	Mutant construction
Δ*metNIQ*-ISceI-R	**TAGGGATAACAGGGTAAT**CACAGCTGTGCAGCAGG	Mutant construction
Δ*metNIQ*--Kan-F	**GAAGCAGCTCCAGCCTACACA**GTCTGATGAAGTGTACGAAGCC	Mutant construction
Δ*metNIQ*--Kan-R	**CTAAGGAGGATATTCATATG**TCCCCTGCTGGAACACTT	Mutant construction
Δ*metNIQ*-Chk-F	CCATATCGATATGCAGGAAATCAC	Mutant verification
Δ*metNIQ*-Chk-R	CTCATTTCGCCGAAATATTCAGG	Mutant verification
Δ*speD*-ISceI-F	**TAGGGATAACAGGGTAAT**CGCGCTTTACGCTGGTAAT	Mutant construction
Δ*speD*-ISceI-R	**TAGGGATAACAGGGTAAT**CTGGATGCCGGTACGACAAT	Mutant construction
Δ*speD*-Kan-F	**CTAAGGAGGATATTCATATG**GATGCGCGAGATTTACTACGG	Mutant construction
Δ*speD*-Kan-R	**GAAGCAGCTCCAGCCTACACA**GCTCTTCTGCGGTTTTGGC	Mutant construction
Δ*speD*-Chk-F	CGCAATGCTACGTGAAGTTAC	Mutant verification
Δ*speD*-Chk-R	GATCAGCCGTAGTCATGGC	Mutant verification
Δ*speE*-ISceI-F	**TAGGGATAACAGGGTAAT**GTCGCTACGTTCTCAGTATGC	Mutant construction
Δ*speE*-ISceI-R	**TAGGGATAACAGGGTAAT**GAACGTTGTCTACGGCAAAG	Mutant construction
Δ*speE*-Kan-F	**CTAAGGAGGATATTCATATG**GCTATTACAACCCGGCTATTC	Mutant construction
Δ*speE*-Kan-R	**GAAGCAGCTCCAGCCTACACA**GAACGTTGTCTACGGCAAAG	Mutant construction
Δ*speE*-Chk-F	CAGGCGGGTGTCTAAGCTTAG	Mutant verification
Δ*speE*-Chk-R	CAGCGACTTCATATCTTCCGAC	Mutant verification
Δ*luxS*-ISceI-F	**TAGGGATAACAGGGTAAT**GACGTTAGGCATTGGCTGTG	Mutant construction
Δ*luxS*-ISceI-R	**TAGGGATAACAGGGTAAT**CTGCTGCTGTTTCAACGAGC	Mutant construction

Δ*luxS*--Kan-F	**CTAAGGAGGATATTCATATG**CGTCATATTCTGGAGC GTGA	Mutant construction
Δ*luxS*-Kan-R	**GAAGCAGCTCCAGCCTACACA**CAGATCAAACACGGT GATTGC	Mutant construction
Δ*luxS*-Chk-F	CGCTTCCTCGATCTGTTTATG	Mutant verification
Δ*luxS*-Chk-R	CTCGTCGATGTCAGACTACCG	Mutant verification
Δ*bioB*-ISceI-F	**TAGGGATAACAGGGTAAT**GAACGTGTCGCCATGATA ACC	Mutant construction
Δ*bioB*-ISceI-R	**TAGGGATAACAGGGTAAT**CTGTCACCACCAGTTGCT GAC	Mutant construction
Δ*bioB*-Kan-F	**CTAAGGAGGATATTCATATG**GGCAGAGGACAAGGAT CTGC	Mutant construction
Δ*bioB*-Kan-R	**GAAGCAGCTCCAGCCTACACA**CTGGCGATGAATTTG CTGC	Mutant construction
Δ*bioB*-Chk-F	CTTTCATCCCATTCGCCATC	Mutant verification
Δ*bioB*-Chk-R	CCACCAGCAACTCAGGCTTC	Mutant verification
Δ*pfs*-ISceI-F	**TAGGGATAACAGGGTAAT**GAAACCACACAGCGATCA TG	Mutant construction
Δ*pfs*-ISceI-R	**TAGGGATAACAGGGTAAT**GGTAAACAGAGGATTCAT GCC	Mutant construction
Δ*pfs*--Kan-F	**CTAAGGAGGATATTCATATG**GAAACAGTCGACTCTG ATGGTC	Mutant construction
Δ*pfs*-Kan-R	**GAAGCAGCTCCAGCCTACACA**CCGTTCAACTGGCCA GTG	Mutant construction
Δ*pfs*-Chk-F	CTGCGCCCAGGTAAGATTC	Mutant verification
Δ*pfs*-Chk-R	ACCTGCTCACGGCTGACTTG	Mutant verification
Amplification of Kan^R cassette		
pKD4-F	TGTGTAGGCTGGAGCTGCTTC	
pKD4-R	CATATGAATATCCTCCTTAG	
Complementation constructs		
metB-BamH1-F	TGGATCCGTCGCAGATGTGCGCTAATG	
metB-SalI-R	TGTCGA**C**CATAATGCCTGCGACACGC	
pfs-BamH1-F	TGGATCCCTCATGCTCCGTCTTTACACC	
pfs-Sph1-R	TGCATGCGAATAGCTGCTGACGCCAAC	
SahH-BamH1-F	TGGATCCATGGACTACAAAGACCATGACGGTGATTATAAAGATCATG ACATCGATTACAAGGATGACGATGACAAGATGGAACTGGTAGAAGAA GGAG	
SahH-Sph1-R	TGCATGCGATTTAGTTATCTTGACTAAATC	
Sequencing pGEM-Teasy		
M13-F	CGCGGGAATTCGATT	
M13-R	GAATTCACTAGTGATT	

Endonuclease restriction sites are underlined; kanamycin^R-cassette specific sequences are in bold; F, forward (5') primer; R, reverse (3') primer.

2.7.6 Agarose Gel Electrophoresis

Amplified products from PCR were analysed using agarose gel electrophoresis. For resolving PCR products, 1% -1.5% (w/v) agarose (Bio-Rad) gels were used. The agarose was melted in 1× Tris-Acetate-EDTA (TAE) electrophoresis buffer (see Table 2-2 for composition of TAE Buffer) and DNA samples were mixed with 6x Gel Loading Dye (NEB) before loading. 100 bp DNA ladder (NEB) or 1 kb DNA ladder (Promega) were used to estimate fragment size. Gels were electrophoresed at 95-100V for 45 min to 1 hour by using a Bio-Rad 200/2.0 Electrophoresis Power Supply. SYBERSafe (Life Technologies) was used to stain the DNA present in agarose gels and DNA was observed with Gel Documentation System (Syngene). Digital images were taken using GeneSnap Version 7.07 Software (Syngene).

2.7.7 Purification of DNA from an agarose gel

A Wizard Gel and PCR Clean-up System (Promega) was used for the purification of PCR-amplified DNA or DNA generated from other enzymatic reactions. DNA fragments were excised from agarose gel using a sterile scalpel blade and purified using a Gel Purification Kit (Promega) according to the manufacturer's instructions. DNA was eluted in 50 µl MiliQ water and was stored at -20ºC.

2.7.8 Determination of DNA concentration

Generally, the concentration of PCR amplified and purified DNA, genomic DNA and plasmid DNA was determined by using a Nanodrop ND-2000 spectrophotometer (Thermo Fisher Scientific) as per manufacturer's instructions.

2.7.9 Restriction endonuclease reactions

The reaction mixture of restriction enzyme digestion experiments was made up of: 0.5-2 µg of DNA, 5-10 U of restriction endonucleases (Promega or NEB), 2 µl of appropriate 10× buffer and the remaining volume (up to 20 µl) with sterile MiliQ water. The reaction mixture was incubated for 4-5 hours at the appropriate temperature (usually 37ºC). Digested DNA fragments were visualised by gel electrophoresis and subsequently purified prior to insertion into vectors.

2.7.10 dATP Tagging of PCR products

The addition of a deoxyadenosine (dATP) overhang to the 3'-ends of blunt-ended purified PCR fragments facilitated the insertion of this fragment into the pGEM-Teasy vector (Promega). To create the overhang, 20 µl reaction mixture containing 0.1- 2 µg of DNA fragment, 0.2 mM dATP (Promega), 2.5 U Taq DNA Polymerase (NEB) and 2 µl of 10× reaction buffer (NEB) was then incubated at 72ºC for 20 min.

2.7.11 DNA Ligation

The A-tailed DNA fragment was ligated into pGEM-Teasy (Promega) through TA cloning. The molar ratio of insert to vector was 3:1, as per manufacturer's instruction. The 10 µl reaction mixture consisted of 5 µl of 2× rapid ligation buffer (Promega), 50 ng pGEM-Teasy (Promega), 3U of Ligase (Promega) and the amount of insert was calculated using the formula below. When DNA was inserted into the complementation plasmid pACYC184 (NEB), the reaction mixture was prepared as per manufacturer's instruction. Ligation reactions were incubated at 4ºC overnight.

The formula to calculate the amount of insert:

[(Amount of vector (ng) × size of insert (kb) / size of vector (kb)] × insert: vector

= amount of insert (ng).

2.7.12 DNA transformation

Transformation of DNA into bacteria was mediated using either electroporation (for general plasmid DNA transformations) or TSS enhanced chemical transformation (for ligation reactions or plasmid DNA transformations).

2.7.12.1 Initial preparation of the competent cells

The transformation of DNA into *Salmonella* and *E. coli* was initiated by firstly growing the bacterial culture to mid-exponential phase. Cells were rapidly cooled by placing on ice for approximately 5 min followed by centrifugation (2,851 ×g for 10 min, 4ºC) to pellet. The pellet was resuspended in ice-cold, sterile PBS of equal volume to the original culture.

2.7.12.2 Electroporation

To induce electro competency, cells were subjected to three centrifugations at 2,851 ×g, 10 min and three washing steps with 10 ml, 5 ml and 3 ml of ice-cold sterile dH_2O after which the cells were resuspended in a final volume of 500 µl sterile dH_2O and placed on ice (according to the method described in Sambrook *et al*. 2001(444)). 80 µl of resuspended cells were mixed with 20-200 ng of DNA. The mixture was transferred into an electroporation cuvette (width 0.1 cm) and placed into ice. Electroporation was conducted in a Gene Pulser (Bio-Rad Micropulser) at 1.8 V, 25 µF and 200 Ω. 1 ml of LB-Miller broth was immediately added to the electroporated cells after the electric pulse. The cells were resuspended in the LB-Miller broth and then transferred to a fresh Eppendorf tube for incubation at 37ºC for 1.5-2 hours with shaking (180 rpm). Different dilutions were spread on agar plates with appropriate antibiotic(s) and the plates were incubated at 37ºC overnight.

2.7.12.3 TSS enhanced chemical transformation

After the initial preparation (as described in section 2.7.12.1), the 10 ml culture was centrifuged at 2,851 ×g for 10 min and the pellet was resuspended in 800 µl sterile ice-cold TSS broth (445). 20- 200 ng of DNA was resuspended in 80 µl ice cold TSS enhanced buffer which was then added to the resuspended cells in TSS broth. The mixture was incubated for 20 min on ice and 20 min at room temperature followed by the addition of 1 ml of LB broth to the cells. The cells were further incubated at 37ºC shaking (180 rpm) for 1-1.5 hours. Finally, the culture was centrifuged at 9,503 ×g for 3 min and resuspended in 0.6-0.8 ml LB-Miller broth. Different dilutions of the resulting bacterial suspension were spread on plates with appropriate antibiotic(s) and plates were incubated at 37ºC overnight.

2.8 DNA Sequencing

2.8.1 Standard DNA sequencing

DNA sequencing was performed to confirm nucleotide sequences using the ABI PRISM Big Dye Terminators v3.1 Cycle Sequencing Kit (Applied Biosystems) as per manufacturer's instructions. Reactions were analysed on an ABI3100 capillary sequencer (Applied Biosystems) at The Centre for Translational Pathology, Department of Pathology, The University of Melbourne.

2.8.2 Computer analysis of the sequence data

Sequence data was edited and analysed using the sequence analysis program Finch TV v1.4.0 to view all chromatogram files. Nucleotide and amino acid homology searches were performed using BlastN and BlastP programs available at the National Centre for Biotechnology Information (NCBI) website.

2.8.3 Whole-Genome DNA sequencing

Genomic DNA samples were isolated and quantified from *S.* Typhimurium strains of interest as described in sections 2.7.1 and 2.7.8. Whole genome sequencing was performed with MiSeq system (Illumina) according to the manufacturer's instructions. Sequencing results for the *S.* Typhimurium mutant strains are shown in the Appendix.

Velvet Assembler was used to assemble the DNA reads and to generate the initial contigs. Assembled and annotated sequences were analysed using Tablet which is a high-performance graphical viewer for alignments and assemblies. All sequences were compared to the *S.* Typhimurium SL1344 NCTC 13347 genome sequence (Wellcome Trust Sanger Institute Pathogen Genomic Group), EMBL accession number FQ312003.

2.9 Site-directed mutagenesis in *S.* Typhimurium

2.9.1 Gene gorging

The gene gorging method (446) was used to construct targeted site-directed gene deletions in *S.* Typhimurium strains. The process involves the incorporation of a DNA fragment containing a selectable antibiotic resistance marker (in this study the kanamycin resistance cassette) flanked by chromosomal sequence (approximately 500 bp at each end) homologous to the flanking regions of the target gene to be replaced. This DNA was introduced into a donor plasmid, pGEM-Teasy. The mutagenesis occurred through homologous recombination and allelic replacement, a rare event selected using kanamycin resistance, encoded by the kanamycin resistance 'cassette'.

2.9.2 The donor plasmid construction

Approximately 0.5 kb regions flanking the upstream and downstream sequence of the target genes were amplified by using SL1344 genomic DNA as a template (Figure 2-1(1)). From

pKD4, a 1.6 kb kanamycin resistance cassette, containing a FLP recognition site (FRT) at either end, was amplified using primers pKD4-F and pKD4-R (Figure 2-1(2)). The primers used in the PCR contained overhangs complementary to either end of the kanamycin resistance cassette which facilitated joining of the three fragments (upstream, kanamycin cassette and downstream) together by overlapping extension PCR (Figure 2-1(3)). The -I*Sce*I- primers used in the overlapping PCR had overhang sequences encoding the I*Sce*-I restriction site. When the three fragments were joined together by overlapping extension PCR, this resulting knockout construct containing the I*Sce*-I site was ligated into the high copy number plasmid pGEM-Teasy (Promega). The insertion site of pGEM-Teasy contained 3'-terminal thymidines at either end, and the Taq polymerase used for the amplification adds single deoxyadenosines to the 3'-end of the amplified products, which facilitated the ligation of the fragment into the targeting vector (Figure 2-1(4)).

The resulting donor plasmid was introduced into the *E. coli* strains MC4100 or DH5α. Plasmids were isolated from *E. coli* grown in the presence of kanamycin and were digested with the restriction enzyme I*Sce*-I. After restriction digestion, DNA was visualised on an agarose gel to confirm that both ends of the insert contain I*Sce*-I sites, which produced 3.0 kb and 2.5 kb fragments. The donor plasmids that showed correct restriction digests profile, were sequenced using the M13F and M13R primers.

Plasmids containing the correct sequence were transformed into *S.* Typhimurium BRD666 strain. BRD666 is a restriction-negative modification-positive ($r^- m^+$) mutant and was used to modify the plasmid DNA with a *Salmonella*-specific methylation pattern. The kanamycin resistant colonies were selected for plasmid extraction and then that BRD666-modified plasmid was transferred into target *S.* Typhimurium strains.

(1) Amplification of flanks

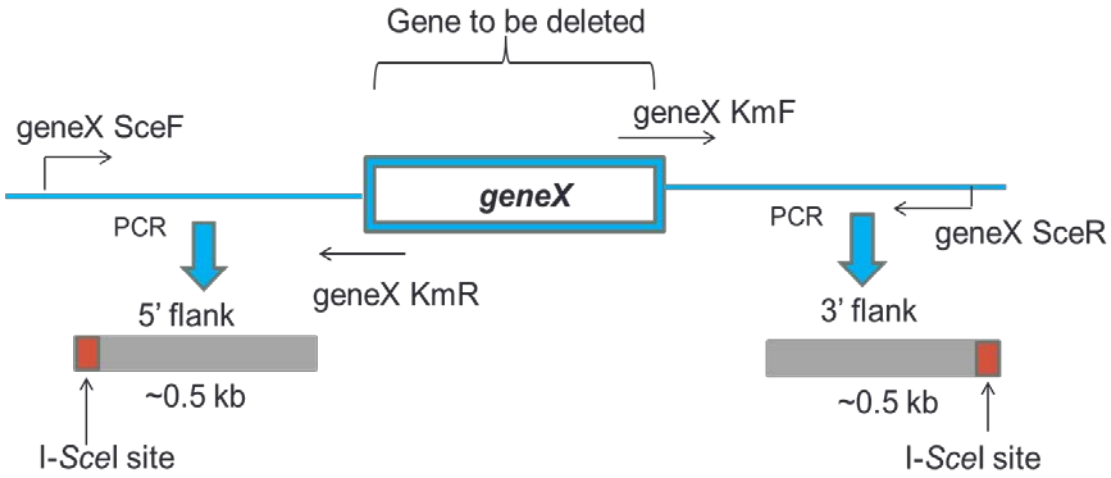

(2) Amplification of Kanamycin resistance cassette

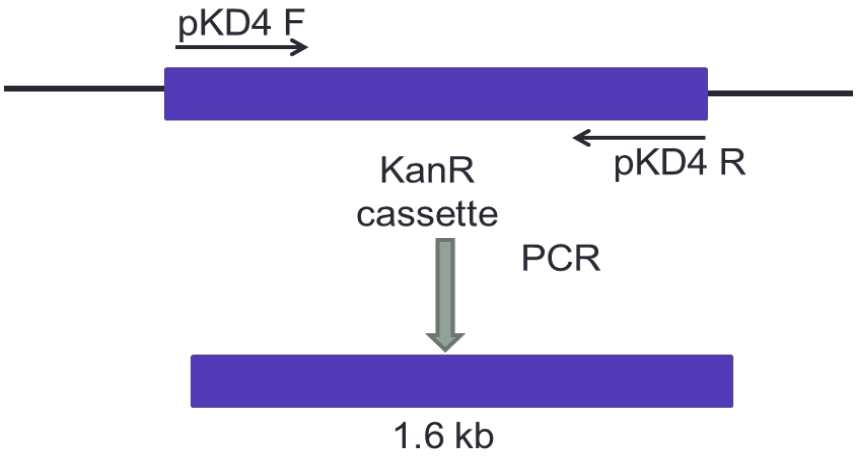

(3) Flanks + cassette joined by overlapping PCR

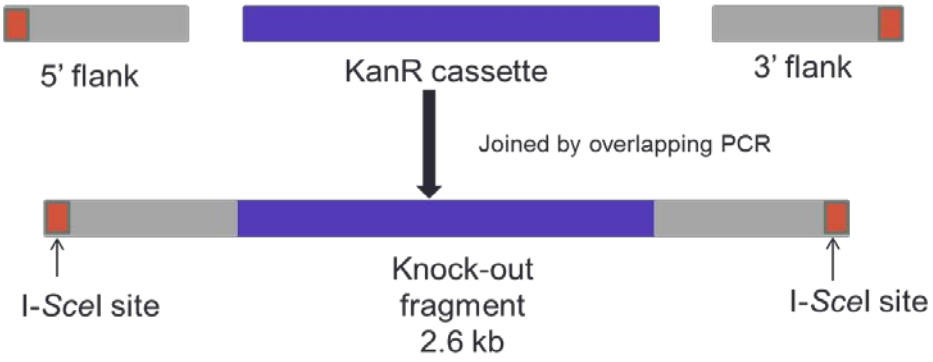

(4) Ligation of the knockout fragment into the plasmid pGEM-Teasy

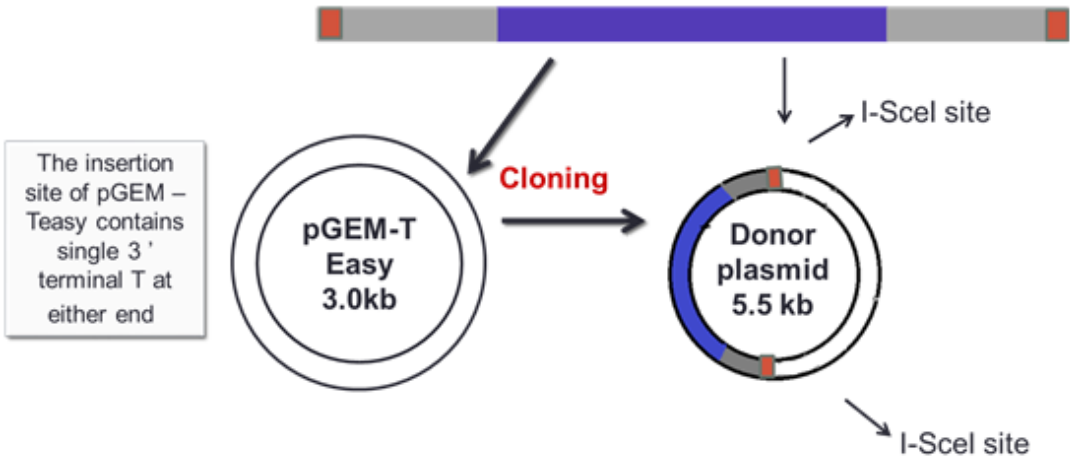

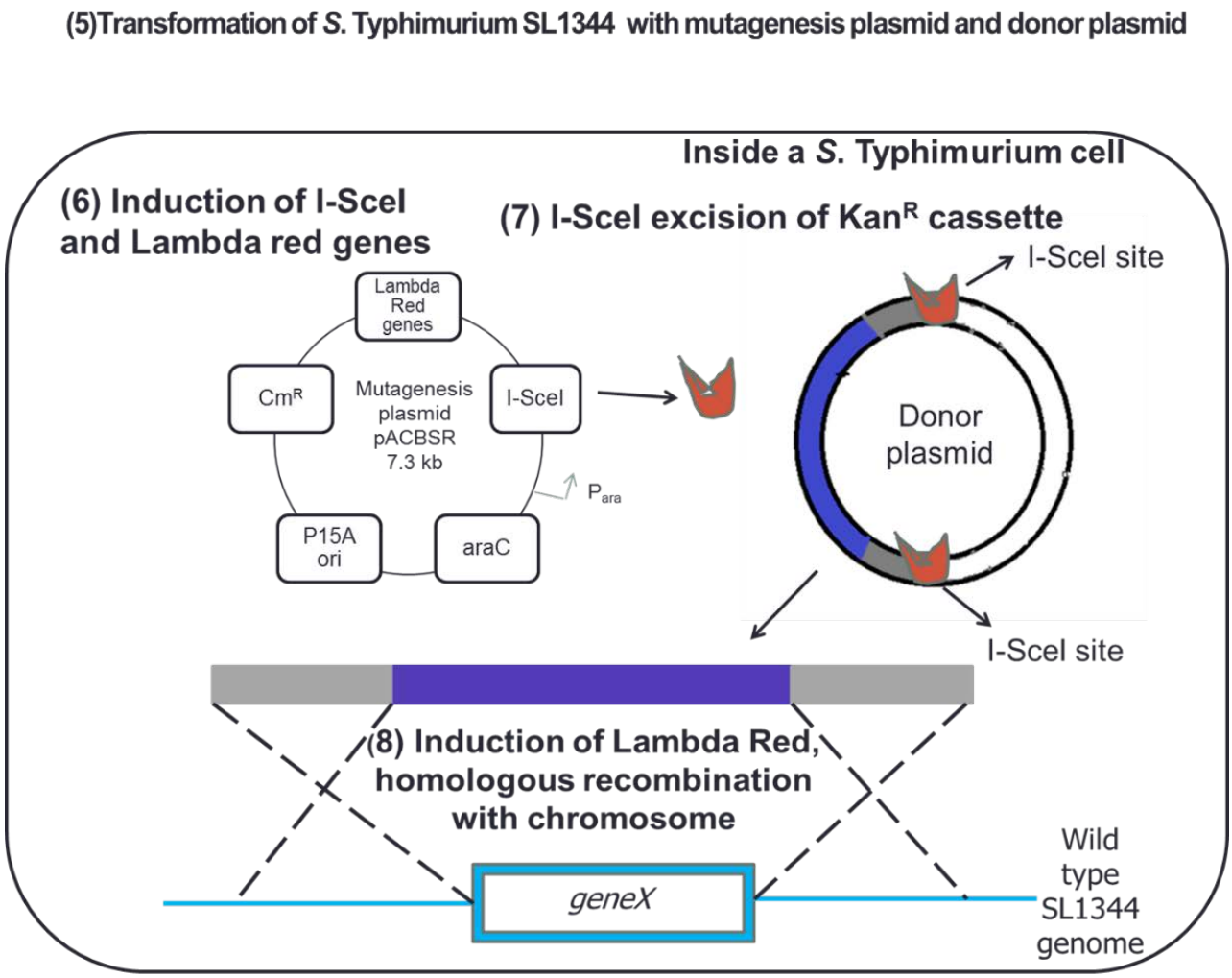

Figure 2-1: Schematic representation of the 'gene gorging' method for constructing *S.* Typhimurium deletion mutants. (1) PCR amplification of 5'and 3' flanking sequence of *geneX* from the wild-type SL1344 chromosomal DNA, (2) PCR amplification of the Kan^R cassette sequence from pKD4 plasmid, (3) the Kan^R cassette sequence was joined with 5'and 3' flanking sequence by overlapping PCR, (4) ligation of this fragment into the donor plasmid pGEM-Teasy, (5) the mutagenesis plasmid pACBSR and the donor plasmid pGEM-Teasy were transformed into *S*. Typhimurium SL1344 and transformants were selected by growing them on LB agar plates containing kanamycin (50 µg/ml) and chloramphenicol (30 µg/ml) antibiotics. A single colony was grown into LB broth containing chloramphenicol and 20% arabinose (6) to induce I-*Sce*I and λ-Red recombinase, (7) the excision of Kan^R fragment from the donor plasmid occurs and facilitates, (8) homologous recombination with the targeted region in the chromosome.

2.9.3 Mutagenesis

The mutagenesis plasmid pACBSR contains gene coding restriction endonuclease I*Sce*-I, gene coding λ-Red under the control of an arabinose inducible promoter, pBAD and a chloramphenicol resistance cassette expressed from a constitutive promoter. Induction of I*Sce*-I results in donor plasmid cleavage, generating the linear dsDNA target, which is a substrate for λ-Red gene products. Homologous recombination of this fragment with genomic DNA is promoted by λ-Red recombinase.

Donor plasmid pGEM-Teasy was transferred into *S.* Typhimurium SL1344 containing the pACBSR mutagenesis plasmid (Figure 2-1(5)) and transformed *S.* Typhimurium colonies were selected by kanamycin and chloramphenicol antibiotics at 50 µg/ml and 30 µg/ml, respectively. Single colonies were isolated and inoculated in 1 ml LB broth in an Eppendorf tube containing 3 µl of 10 mg/ml chloramphenicol and 15 µl of 20% (w/v) arabinose to induce the I*Sce*-I and λ-Red genes, and grown overnight with shaking at 30ºC, allowing for the excision of the Kan^R cassette containing fragment from the donor plasmid (Figure 2-1(7)), and homologous recombination of the cassette into the targeted region (Figure 2-1(8)). The appropriate dilutions were spread onto a LB plate containing kanamycin and incubated at 30ºC. In one typical experiment, 100-200 mutants were screened by replica plating on ampicillin and kanamycin plates, selecting for ampicillin sensitivity and kanamycin resistance which indicated the loss of donor plasmid and the integration of the Kan^R cassette into the targeted region. Mutagenesis was confirmed by colony PCR. If all deletion mutants were chloramphenicol-resistant, then one kanamycin resistant and ampicillin sensitive colony was picked, resuspended in LB broth supplemented with 15 µl of 20% (w/v) L-arabinose and incubated at 37ºC shaking overnight. This arabinose induction removed the mutagenesis pACBSR plasmid. Appropriate dilutions were spread on the kanamycin plates and 50-100 colonies were screened by replica plating on chloramphenicol and kanamycin plates for chloramphenicol sensitivity.

2.9.4 P22 phage transduction

P22 phage transduction was used to move the defined deletion sequence into a clean *S.* Typhimurium background. To generate the donor phage lysate, 50 µl of phage lysate was mixed with 1.5 ml mid-exponential culture of the donor bacterial stain and shaken (180 rpm) at 37ºC overnight. After the overnight incubation, 50 µl of chloroform was added and the suspension was shaken for 20 min at 37ºC. Then the culture was centrifuged at 16,060 ×g for

2 min at 37ºC and approximately 900 µl of supernatant was transferred to a fresh tube. 30 µl chloroform was added into that suspension which was grown shaking for 3 hours at 37ºC. After the addition of 30 µl chloroform, the donor/P22 phage suspension was filter-sterilised using a 0.2 µm filter and stored at 4ºC. 50 µl of donor/P22 phage suspension was spread plated on LB-agar plates (without antibiotic selection) and incubated at 37ºC to confirm there was no viable bacteria.

To move the mutation into a clean wild-type *S.* Typhimurium SL1344 background, 0.5 ml serial 1:10 dilutions (10^{-1}, 10^{-2}, 10^{-3}, 10^{-4}) were prepared from donor/P22 phage suspension in LB-Miller broth and each dilution (including the original) were mixed with 0.5 ml of recipient mid-log culture (equal volume) and incubated at 37ºC, 180 rpm, 30 min. After incubation, 100-200 µl culture were spread on Luria-agar plates containing kanamycin and incubated at 37ºC overnight. Kan^R colonies were confirmed by testing 5-10 colonies by colony PCR (section 2.9.6). To purify the colonies from P22 phage, colonies were streaked onto EBU (Evans Blue Uranine) plates. The dark green colonies represented the presence of phage and the white colonies represented the absence of phage (447). Ca^{2+} is essential for P22 phage adsorption. EGTA acts as chelating agent which chelates Ca^{2+} to reduce phage adsorption and reinfection (447, 448). Hence, white colonies were further streaked on LB-agar plates supplemented with EGTA 10 mM to obtain phage-free colonies.

2.9.5 Removal of the Kan^R cassette

The Kan^R cassette was excised through electroporation of kanamycin resistant mutants with plasmid pCP20 (443). pCP20 is a temperature-sensitive plasmid and contains the *flp* gene under the control of an arabinose-inducible promoter and must be maintained at 30ºC. The transformants were selected on chloramphenicol plates at 30ºC where plasmid replication occurs, and the FLP recombinase was expressed to recognise the FRT ends of the kanamycin cassette. This recombination eliminated most of the kanamycin cassette and left a small (~80 nucleotide) scar region. A single colony was grown in LB broth at 42ºC shaking overnight. Different dilutions of the culture were plated on agar plates (containing no antibiotic) and were incubated at 42ºC overnight after which 25-50 colonies were screened by replica plating on kanamycin and chloramphenicol plates, selecting for sensitivity to both antibiotics. Mutants that were sensitive to both chloramphenicol and kanamycin were confirmed by colony PCR as described in section 2.9.6.

2.9.6 Confirmation of *S*. Typhimurium mutants

The deletion mutants with Kan^R cassette were confirmed by using colony PCR that generated two bands using two sets of primers. One set of primers was the -ChkF- and -pKD4-F(RC) reverse primer pair. The -ChkF- primer corresponded to chromosomal sequence approximately 100 bp upstream of the end of 5' flanking sequence (500 bp) of the targeted gene and -pKD4-F(RC) primer corresponded to the 5'-end of the Kan^R cassette. These primers amplified a 0.7~0.8 kb product. Another set of primers -ChkF- and pKD4-Reverse pair corresponded to the 3'end of the Kan^R cassette and amplified an approximately 2.1 kb product. This result shows that the whole cassette was incorporated in the chromosome and confirmed the precise genomic location of the kanamycin cassette. After $kanamycin^R$ cassette excision, the colony PCR was conducted with primers -ChkF- and -ChkR- (Table 2-5). The primer -ChkR- was designed from sequence 100 bp upstream of the 3' end of the other flanking region (500 bp) of the gene to be replaced. For Kan^R cassette excision, both primers were used to amplify the sequence, to confirm that the sequence was cleanly deleted leaving a short 80 nucleotide "scar".

2.10 Construction of complementation plasmids

To construct complementation plasmids, the sequence of the gene to be complemented and the flanking regions that incorporated the genes' native promoter and terminator (with the exception of heterologous complementation of *sahH* from *Legionella pneumophila* into *Salmonella* Typhimurium), was amplified by Phusion High Fidelity DNA Polymerase (Promega). The promoter and terminator were identified based on genome data from *E. coli* K-12 substrain MG1655 and *S.* Typhimurium LT2 (available on www.biocyc.org). For complementation of the double mutant Δ*metNIQ*Δ*metB*, the *metB* sequence was PCR amplified with the primer pair metB-BamH1-F and metB-Sal1-R (Table 2-5) and for the complementation of the Δ*pfs* mutant, *pfs* was PCR amplified with the primer pair pfs-BamH1-F and pfs-Sph1-R (Table 2-5). The amplified DNA fragment was ligated into pGEM-Teasy, transformed into *E. coli* DH5α and sequenced. Sequencing confirmed the integrity of the gene in the complementation construct. pGEM-Teasy was digested with appropriate restriction enzymes for 4 hours at 37ºC. Under similar conditions, the vector pACYC184, a medium-copy expression plasmid that is retained in *Salmonella* in the absence of selection (449), was also digested with the same restriction enzymes. After digestion, correctly sized fragments of vector and insert were recovered from agarose electrophoresis gels and ligated together. The resulting ligation mixture was transformed into *E. coli* DH5α, and the transformants were screened for

the correct size of insert and sequenced. After confirmation by sequencing, the plasmid was transformed into *S*. Typhimurium BRD666 and mutant *S*. Typhimurium strains.

For heterologous expression of *sahH* from *L. pneumophila* into *S*. Typhimurium, a 3× FLAG-tag sequence was attached at the 5' end of *sahH*. The coding region of s*ahH* including the 3× FLAG sequence was PCR-amplified using the primers SahH-BamH1-F and SahH-Sph1-R (Table 2-5) to include the restriction endonuclease site for BamH1 and Sph1. The DNA sequence was ligated into pGEM-Teasy and sequenced. The complementation sequence was excised and cloned into the restriction sites BamH1 and Sph1 of pACYC184 within the tetracycline-resistant region using the tetracycline-resistant gene (tet^R) promoter for expression, instead of the native promoter of *sahH*, to form the complementation plasmid pACYC184 *sahH* (Lp). The plasmid pACYC184 *sahH* (Lp) was transformed into *E. coli* DH5α and sequenced. The plasmid with appropriate sequence was transformed into *S*. Typhimurium BRD666, extracted using method as described in section 2.7.2 and transformed into the *S*. Typhimurium Δ*pfs* mutant.

2.11 Western blotting

$^{3\times FLAG}$SahH expression (from pACYC184 *sahH* (Lp)) was detected by Western blot analysis using a monoclonal mouse Anti-FLAG antibody (Sigma) at a concentration of 1:2000. *S.* Typhimurium whole cell lysates were prepared from overnight cultures. Samples were separated by sodium dodecyl sulphate (SDS)-polyacrylamide gel electrophoresis (PAGE) and transferred to iBlot2 NC Regular stack nitrocellulose (Thermo Fisher Scientific) using an iBlot2 Gel Transfer Driver (Life technologies, CA) at 20 V for 6-7 min. The membrane was blocked for 1 hour at 25ºC in rotating condition using blocking buffer (Table 2-2). The primary antibody was diluted in 1:2000 in the blocking buffer and incubated with the membrane at 4ºC overnight under rotating condition. The membrane was washed with 0.05% skim-milk in Tween-20 3 times, 10 min each under rotating condition. Anti-mouse antibody conjugated with Horseradish Peroxidase (HRP) (Biorad) was used as the secondary antibody at a concentration of 1:10,000 in the blocking buffer and the membrane was incubated under rotating condition for 1 hour at 25ºC. The membrane was washed with 0.05% skim-milk in Tween-20 three times, 10 min each, under rotating condition. Bound antibody was visualised with ECL Western Blotting Detection Reagents (Amersham Biosciences) according to the manufacturer's instructions. The development step occurred typically within 2-3 minutes and the membrane was imaged by using DNR-Bioimaging System (MF-ChemiBis 3.2)

2.12 Mammalian cell culture methods

2.12.1 Maintenance of mammalian cells

HeLa epithelial cells were grown and maintained in DMEM (supplemented with 10% (v/v) heat inactivated fetal calf serum (FCS) and streptomycin 50 µg/ml) in a humidified 37°C, 5% CO_2 incubator. The cells were split into a new tissue culture flask when they were 80-90% confluent. To passage the cells, the growth media was removed from the flask and the flask was washed with PBS gently. Then 5-10 ml of Trypsin-EDTA (Media Preparation Unit, Department of Microbiology and Immunology, The University of Melbourne) was added into the flask which was incubated for 5-10 min in the humidified incubator at 37ºC and 5% CO_2. After 5-10 min, 5 ml of fresh DMEM was added and the cells were resuspended in the media. The suspension was centrifuged at 524 ×g for 5 min and the supernatant was discarded. The pellet was resuspended with in fresh DMEM (supplemented with FCS). Cells were diluted in an appropriate amount (as required, splits were mostly of a 1:3 or 1:5 ratio) in a new flask containing fresh growth media. Cells were passaged every 2-4 days.

2.12.2 Cell line storage

Cells were centrifuged at 524 ×g for 5 minutes and resuspended in DMEM media (supplemented with FCS and 5% DMSO). Cells were stored at -80ºC for short-term storage and in liquid nitrogen for long-term storage.

2.12.3 Viable cell count

To quantify cell numbers, cell suspension was diluted in 0.4% Trypan blue (Sigma). Aliquots of 10 µl were mounted in a Neubauer Improved Haemocytometer (Hausser Scientific). The cells were visualised under a light microscope. Cells in each of the four corner squares were counted and non-viable cells, permeable to the Trypan blue, were excluded.

2.12.4 Intracellular survival assay using HeLa cells

HeLa cells were grown in DMEM supplemented with 10% (v/v) FCS, in a humidified 37°C, 5% CO_2 incubator. One day prior to infection HeLa cells were seeded in 24-well plates at 2 $\times 10^5$ cells per well. For the preparation of bacterial inoculum see section 2.5.4. The bacterial inoculum was prepared such that 1×10^6 cfu/ml was obtained. Bacteria were revived from the frozen stocks, washed with PBS and resuspended in DMEM-Complete supplemented with 10%

(v/v) FCS and added to HeLa cell monolayers at a MOI of 5-10:1. The bacterial load of the inoculum was confirmed by plating out serial dilutions on LUS plates. Infected HeLa cells were centrifuged at 524 ×g for 5 min immediately after the addition of bacteria and then incubated for 1 hour at 37°C, with 5% CO_2. Extracellular bacteria were removed by aspiration and the HeLa cells were washed twice with PBS. At this point (defined as time 1 hour) fresh media (DMEM with or without Met) containing 100 µg ml^{-1} gentamicin was added to kill extracellular bacteria (450, 451). The plates were further incubated for 1 hour at 37°C, 5% CO_2 and then media was replaced with DMEM with or without Met containing 10 µg ml^{-1} gentamicin for the remainder of the experiment. To enumerate intracellular bacteria, cells were washed twice with PBS, lysed with 0.1% Triton X-100 (Sigma) for 15 min and serial dilutions were performed if necessary. The bacteria were enumerated by plating appropriate dilutions on LUS plates. The plates were incubated at 37°C, overnight. For intracellular replication/survival, intracellular bacteria were enumerated at 2, 5 and 10 hours after inoculation of tissue culture cells.

2.13 Mouse experiments

2.13.1 Housing, husbandry and ethical care

All mice were bred and housed under specific pathogen free (SPF) conditions within the Biological Research Facility (BRF) at the Department of Microbiology and Immunology at The University of Melbourne. All mouse experiments were performed with approval from The Biochemistry & Molecular Biology, Dental Science, Medicine, Microbiology & Immunology, and Surgery Animal Ethics Committee, The University of Melbourne. Unless otherwise stated, 6-8 weeks old male or female mice were used for all animal experiments. Mice were euthanised by CO_2 asphyxiation at desired time points, or when adverse event threshold was reached.

2.13.2 Mouse strains

All transgenic and knockout mice (including IFN-$\gamma^{-/-}$) were in a C57BL/6 genetic background and bred at the BRF.

2.13.3 Intravenous infection of mice

For the preparation of the bacterial inoculum, see the growth conditions (section 2.5.5). Before infection, mice were transferred into a new clean cage and the box was placed on a light-bulb

warmer box to heat up the mice for about 10-15 min which helps to dilate the blood vessels of the tail. The mice were restrained by transfer into a clean tube and held by the tail. The infection was initiated using 200 µl PBS containing 200 cfu of *S*. Typhimurium, which was injected into the tail vein using a 27gauge needle (Terumo).

2.13.4 Oral infection

For the preparation of the bacterial inoculum, see the growth conditions (section 2.5.5). Mice were first anesthetised with isoflurane and were administered with 100 µl sodium bicarbonate (10% w/v) via an 18 gauge, 50.2 cm animal feeding needle (Terumo) to neutralise stomach acidity. After 5-10 min, the mice were orally infected under anaesthesia with approximately 5×10^7 cfu of *S*. Typhimurium strains resuspended 200 µl PBS.

2.13.5 Determination of bacterial counts in the organs

Mice were euthanised on the designated day and organs (spleen and liver) were collected in sterile homogenising bags (Sarstedt) and kept on ice for a maximum of 3 hours. Five ml of ice-cold sterile PBS was added to the bags and organs were homogenised for 15 minutes in a Stomacher 80 homogeniser (Seward Medical). Serial dilutions were performed and spread onto LUS plates. The viable bacterial count was determined after incubation at 37ºC for 16-18 hours.

2.14 Liquid Chromatography Mass Spectrometry

2.14.1 Preparation of stock solutions and standards

Stock solutions of the related underivatised metabolites were prepared in appropriate solvent and with a concentration of 1.0 mg/ml. Before using, the solutions were combined and diluted with water to give an appropriate standard metabolite mix solution. $^{13}C^{15}N$-Aspartate (Cambridge Bioscience) was used as an Internal Standard at a concentration of 1 µM in water. All stock solutions were stored at -20ºC.

2.14.2 Sample harvest (Metabolic arrest) for Liquid Chromatography Mass Spectrometry

Ten ml of the exponential culture of each *Salmonella* strain was diluted into 30 ml of PBS in falcon tubes. The tubes were placed in an ice/water slurry for 5 min to chill. Then the cultures were centrifuged (931 ×g, 1ºC, 10 min). The supernatant was removed from each tube, the

pellet was resuspended in to 1 ml PBS and transferred into a 1.5 ml Eppendorf tube. The cultures were centrifuged (17,295 ×g, 30 seconds, 1ºC). The supernatant was removed and the pellet was washed with 1 ml PBS and then centrifuged again (17,295 ×g, 30 seconds, 1ºC). After this second washing step, all PBS was discarded carefully from each tube. Cell pellets were stored at -80ºC until metabolite extraction was carried out.

2.14.3 Extraction of metabolites

Cell pellets were resuspended with 400 µl of 3:1 methanol:water solution containing 1:1000 of Internal Standard. Cell lysis was ensured by repeated cycles of freeze-thaw for a total of 10 times (cooling to -80ºC). Cellular debris was pelleted by centrifugation (17,295 ×g, 5 min, 1ºC). The metabolic extract was transferred to a new tube and was stored on dry ice and transferred to Metabolomics Australia, The University of Melbourne at Bio21 Institute.

2.14.4 Instrumentation

A SeQuant ZIC-pHILIC column (5 µM, 150 x 4.6 mm, Millipore) coupled to a 1260 series HPLC system (Agilent) was used to separate metabolites. The method used was previously described (452) with slight modifications: - a flow rate of 0.3 mL/min with 20 mM ammonium carbonate in water and 100% acetonitrile as the mobile phase (452). A binary gradient was set up as follows: 0.5 min: 80% acetonitrile, 15.5 min: 50% acetonitrile, 17.5 min: 20% acetonitrile, 18.5 min: 5% acetonitrile, 21 min 5% acetonitrile, 23 min 80% acetonitrile and held at 80% acetonitrile until 29.5 min. Detection of metabolites was performed on an Agilent Q-TOF mass spectrometer 6545 operating in negative ESI mode. The scan range was 85-1200 m/z between 2 and 28.2 min at 0.8 spectra/second.

2.14.5 Calibration and validation

LC-MS.d files were converted to .mzXML files using MS convert and analysed using the LCMS R package (453, 454). Following alignment, groups were extracted with a mass window of 10 ppm and statistical analysis performed using MetaboAnalyst 3.0 (455). The dataset was uploaded, filtered using the interquartile range, log transformed and a one-way ANOVA performed with Tukey's HSD ($p < 0.01$). Data was analysed using MAVEN in parallel to validate the LCMS results (456). Following alignment, metabolites were assigned using exact mass (<10 ppm) and retention time (compared to a standards library of 150 compounds run the

same day). Scatter plots were generated for each pairwise comparison and statistical significance was determined using a *P* value < 0.05 with Benjamini correction.

2.15 Statistical analysis:

All statistical analyses were performed using GraphPad Prism version 7 (GraphPad software). For comparison of a two data groups at a single time or collection point, the two-tailed unpaired t-test was used. For comparison of three or more data groups at a single time or collection point, the two-tailed one-way ANOVA with Bonferroni's post-test was used. p values below 0.05 were considered statistically significant. Unless otherwise stated, all comparisons were made against wild-type *S.* Typhimurium SL1344 values.

Chapter 3

Role of methionine biosynthesis and transport in the virulence of *Salmonella* Typhimurium

3.1 Introduction

Methionine (Met), a sulphur-containing amino acid, is required for several important cellular functions, including the initiation of protein synthesis (285, 286). Met is adenosylated as S-adenosyl L-Met (SAM), which plays a vital role in the transfer of methyl groups to DNA, RNA and proteins, as well as the biosynthesis of cysteine, phospholipids and polyamines (228, 285). Met is a member of the aspartate family of amino acids and, in the cell, aspartate comes from oxaloactetate, a α-ketoacid of the TCA cycle (224, 228, 230). While aspartate provides the carbon backbone of Met, cysteine donates the sulphur to Met, and the methyl group of Mets is derived from the tetrahydrofolate that is produced in the one-carbon cycle (230, 457, 458) (Figure: 3-1).

The *de novo* biosynthetic pathway of Met is present in prokaryotes. Bacteria can synthesise their own Met but higher eukaryotes such as mammals obtain this amino acid through external sources, including diet and gut flora (225, 226). The purpose of this study was to investigate the essentiality of *de novo* biosynthesis and transport of Met in the growth and virulence of *Salmonella* Typhimurium *in vitro* and *in vivo*.

A model pathway for *Salmonella* Met biosynthesis has been previously reported (459) . This pathway is initiated from homoserine to form O-succinyl L-homoserine, this is followed by L-cystathionine, and then L-homocysteine and finally L-Met. The first three steps are catalysed by MetA (homoserine O-succinyltransferase), MetB (cystathionine γ-synthase) and MetC (cystathionine β-lyase). The final step of Met biosynthesis is catalysed by two alternate Met synthases MetE and MetH. The Met synthase MetH is vitamin B12-dependent and MetE is vitamin B12-independent (383, 384, 386, 460, 461). In this final step, homocysteine is condensed with methyltetrahydrofolate, which provides the methyl group. Methyltetrahydrofolate comes from one-carbon cycle (from methylenetetrahydrofolate) through methyltetrahydrofolate reductase (MetF) mediated reaction which leads to the synthesis of tetrahydrofolate and Met (Figure 3-1).

In *Salmonella*, Met also gets recycled through an activated methyl cycle (232, 285-287). The primary methyl donor, S-adenosyl L-Met (SAM), is formed by the activation of Met through the condensation reaction with ATP by an S-adenosyl methionine synthase, encoded by *metK* (231, 287). SAM is used for a variety of methylation reactions, including the methylation of

DNA, RNA, protein, lipid and other macromolecules in the bacterial cell (233, 285, 361, 372, 374, 376, 377, 380, 381, 462, 463).

Transcriptional regulation of Met biosynthesis is achieved through two different mechanisms: The MetJ repressor and the MetR activator. (464-467). MetJ and its corepressor SAM repress the transcription of all *met* genes except *metH*. MetJ binds within the "met-box", a transcriptional regulator binding site which has an eight-nucleotide consensus sequence (465, 468). On the other hand, MetR acts as an activator and is also known to control the expression of *metA, metF, metE, metH* and as well as autoregulate *metR* itself (469-471). Lastly, the presence or absence of vitamin B12 controls the function of the MetE and MetH proteins. When vitamin B12 is available, MetH which is more efficient than MetE, catalyses Met synthesis. When vitamin B12 is unavailable, MetE catalyses the reaction. *Salmonella* can only synthesise vitamin B12 under anaerobic conditions (382, 467, 472, 473).

3.1.1 Met Biosynthesis

Succinylation of Homoserine

The first step in Met biosynthesis is the succinylation of homoserine, which comes from aspartate (224, 228, 230). This step is catalysed by homoserine O-succinyl-transferase (MetA), which is a 35.6 kDa protein encoded by *metA*. Both D- and L-homoserine are substrate for MetA (474, 475). Succinyl-CoA reacts with MetA to form a succinylated enzyme intermediate, which is then transferred to the γ-oxygen of homoserine to form O-succinyl L-homoserine (474, 475). Homoserine is subsequently activated for condensation with cysteine to form cystathionine.

Cystathionine synthesis

In the second step of Met biosynthesis, cystathionine γ-synthase (MetB), the *metB* gene product, catalyses a γ-replacement reaction. The reaction involves the targeting of O-succinyl L-homoserine by L-cysteine and the subsequent formation of L-cystathionine and succinate. Cystathionine γ-synthase is a homotetramer, where each subunit is 40 kDa (476-478).

Homocysteine synthesis

The β-elimination of L-cystathionine is catalysed by cystathionine β-lyase (MetC), the *metC* product, and after the β-elimination of L-homocysteine, pyruvate and ammonia are formed

(479, 480). Active cystathionine β-lyase exists as a homotetramer and the molecular weight of each subunit is 43 kDa (479, 480).

Methyltetrahydrofolate synthesis

For Met biosynthesis, one-carbon units are derived from methyltetrahydrofolate that forms part of one-carbon cycle (481, 482). Methylenetetrahydrofolate reductase (MetF), which is the *metF* gene product, catalyses the reduction of methylenetetrahydrofolate to methyltetrahydrofolate using NADH (481, 482). The active enzyme is a tetramer composed of identical 33 kDa subunits (481, 482).

Synthesis of Met

The last step of Met biosynthesis is the formation of Met from homocysteine. This reaction can be catalysed by two different enzymes, either vitamin B12-dependent Met synthase or vitamin B12-independent Met synthase which are the products of *metH* and *metE*, respectively (483). The methyl cycle and the one-carbon pathway are linked at this step. The methyl group is transferred from methyltetrahydrofolate to the sulphur of L-homocysteine to produce Met (483). The two Met synthases function differentially as described previously. The reaction catalysed by MetH is much faster than the reaction catalysed by MetE, which means that the vitamin B12-independent enzyme is less efficient than vitamin B12-dependent Met synthase MetH (473). The molecular weights of MetH and MetE are136 kDa and 84 kDa, respectively (483, 484).

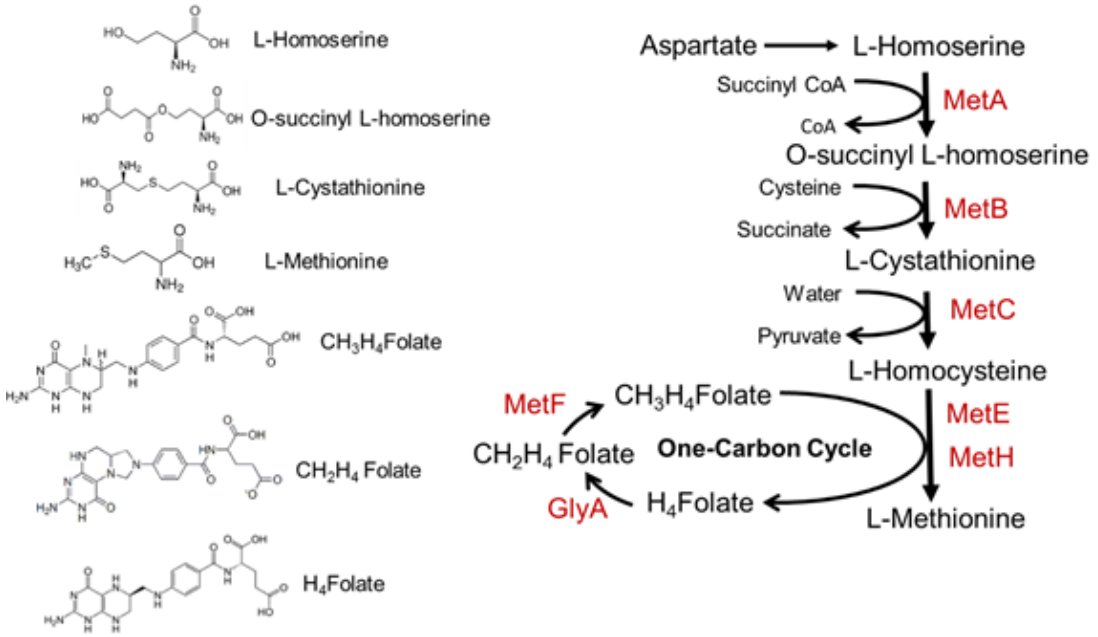

Figure 3-1: The biosynthetic pathway of Met in *S.* Typhimurium. MetA syccinylates homoserine to form O-succinyl L-homoserine, which undergoes condensation reaction with cysteine to form L-cystathionine. This condensation reaction is catalysed by MetB. MetC catalyses the conversion of L-cystathionine to L-homocysteine, pyruvate and ammonia. The final step of Met biosynthesis is catalysed by two alternate Met synthases; MetE and MetH that function differentially; MetE is vitamin B12-independent and MetH is vitamin B12-dependent. In this final step, L-homocysteine is condensed with methyltetrahydrofolate, which provides the methyl group. Methyltetrahydrofolate comes from methylenetetrahydrofolate in the one-carbon cycle, through the methyltetrahydrofolate reductase (MetF) mediated reaction tetrahydrofolate and Met are synthesised. Enzymes in this pathway are shown in red. Arrows indicate the direction of catalytic reactions. The chemical structure of the metabolites has been shown on the left. Figure adapted from (259) .

3.1.2 Transport of Met

Salmonella spp. can import Met into the cell though two different systems: high-affinity and low-affinity transport (263-265, 485). The high-affinity transporter (K_m~0.1 μM) is composed of three proteins: an ATPase (encoded by *abc*), a permease (encoded by *yaeE*) and a substrate binding protein (encoded by *yaeC*), which are known as MetN, MetI and MetQ, respectively (260-262). The MetNIQ is a member of the Met Uptake Transporter (MUT) family (262). On the other hand, it is postulated that there is at least one cryptic low-affinity transporter, putatively called MetP (K_m~20 to 40 μM) (263-265). The chromosomal location of the low affinity-transporter(s) remains unknown. In the absence of the high-affinity transporter, the low-affinity transporter is able to provide the cell with sufficient Met to grow *in vitro* (485),

however it is unclear whether this happens *in vivo*. It has been shown that *S.* Typhimurium lacking the high-affinity transporter was significantly attenuated in C3H/HeN mice, suggesting that *de novo* Met biosynthesis may not be sufficient for growth in mice (270).

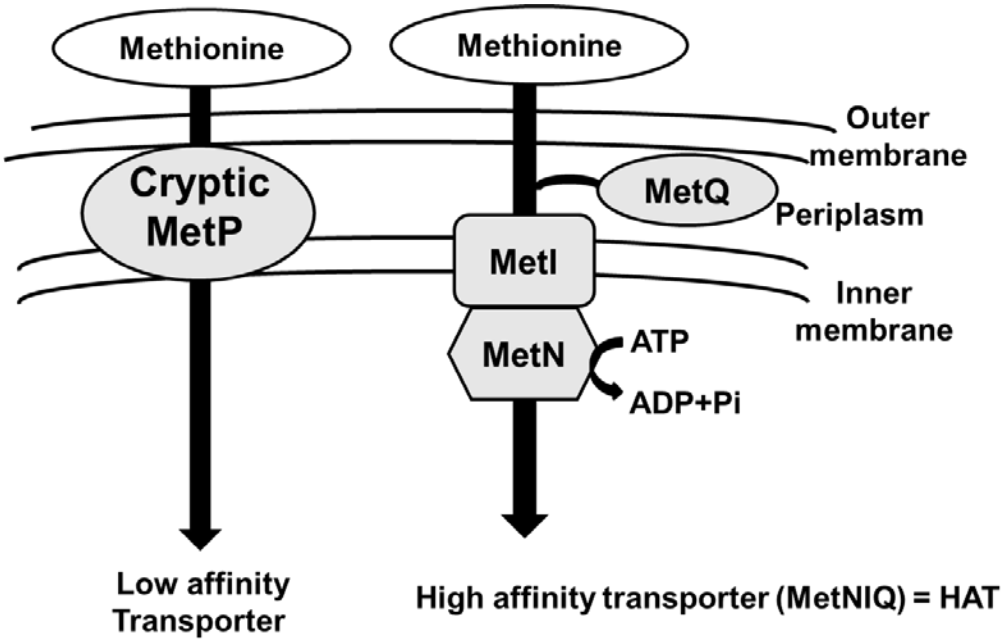

Figure 3-2: Schematic diagram of Met transport in *S.* Typhimurium. Met is transported in *S.* Typhimurium through two types of transporters. The high-affinity transporter is composed of three different proteins, MetN, MetI and MetQ; and low-affinity transporter/s (MetP) is cryptic. Adapted from (486).

3.2 Results

3.2.1 Construction and confirmation of *S*. Typhimurium *met* mutants

Defined deletions of sequence encoding the *met* biosynthesis genes *metA, metB, metC, metE, metF, metH* and Met high-affinity transporter *metNIQ* were generated in *S*. Typhimurium SL1344. In total, 12 different mutant strains were constructed for this study: Δ*metA,* Δ*metB,* Δ*metC,* Δ*metE,* Δ*metF*, Δ*metH*, Δ*metE*Δ*metH*, Δ*metNIQ*, Δ*metNIQ*Δ*metB,* Δ*metNIQ*Δ*metE,* Δ*metNIQ*Δ*metH* and Δ*metNIQ*Δ*metE*Δ*metH.*

"Gene gorging" (described in section 2.9) was used to remove defined chromosomal sequence to construct Δ*metA,* Δ*metB,* Δ*metC,* Δ*metE*. Δ*metF*, Δ*metH* and Δ*metNIQ.* The *met* gene sequences are single cistrons located at different sites on the bacterial chromosome except *metB* is the first gene in a two-gene operon with *metL* (based on genome data from *E. coli* substrain MG1655 and *S*. Typhimurium LT2 available in www.biocyc.org). The three genes, *metN*, *metI* and *metQ*, that form the high-affinity transporter are in an operon. The target sequence to be deleted was replaced with Kan^R cassette by homologous recombination. To reduce the chance of affecting the expression of downstream genes, at least ~50 bp at the 3' ends of the gene to be deleted, including the stop codon, was retained. Gene deletions were validated by PCR using primers that bind to the flanking regions of the deletion site. The mutants were confirmed by a colony PCR (described in section 2.9.6).

The targeted deleted region of the mutants Δ*metA,* Δ*metB,* Δ*metC,* Δ*metE*. Δ*metF*, Δ*metH* and Δ*metNIQ* was shown in Figure 3-3. Kan^R cassette was excised from the mutants Δ*metA,* Δ*metB,* Δ*metC,* Δ*metE*. Δ*metF* and Δ*metH* (shown in 3-4(A)). The purpose of the removal of the Kan^R cassette was to reduce the possible polar effect of the Kan^R cassette on the downstream genes. Also, the excision of the Kan^R cassette allowed construction of additional double and triple mutants (Δ*metE*Δ*metH*, Δ*metNIQ*Δ*metB,* Δ*metNIQ*Δ*metE,* Δ*metNIQ*Δ*metH* and Δ*metNIQ*Δ*metE*Δ*metH*). The excision of the Kan^R cassette was done using pCP20, which is a temperature-sensitive plasmid that contains the *flp* gene (FLP recombinase) under the control of an inducible promoter (described in section 2.9.5). The recombination event excises the Kan^R cassette, replacing it with an 80-nucleotide scar sequence. The P22 phage was used to transduce the Kan^R mutation to a kanamycin-sensitive strain (described in section 2.9.4) and thus, the double and triple mutants Δ*metE*Δ*metH*, Δ*metNIQ*Δ*metB*, Δ*metNIQ*Δ*metE,* Δ*metNIQ*Δ*metH* and Δ*metNIQ*Δ*metE*Δ*metH* were generated. The Δ*metE*::*kan* was added to

the kanamycin sensitive Δ*metH* mutant and the high-affinity transporter mutation Δ*metNIQ*::*kan* was added to the Kan-sensitive biosynthetic mutants Δ*metB*, Δ*metE*, Δ*metH* and Δ*metE*Δ*metH* to construct the double and triple knockout strains: Δ*metNIQ*Δ*metB*, Δ*metNIQ*Δ*metE*, Δ*metNIQ*Δ*metH* and Δ*metNIQ*Δ*metE*Δ*metH* (shown in Figure 3-4(B, C, D, E)).

The resulting Kan-sensitive Δ*metA*, Δ*metB*, Δ*metC*, Δ*metE*. Δ*metF* and Δ*metH* were confirmed by colony PCR using Chk-F and Chk-R primers (shown in Figure 3-4(A)). The Kan-excised mutants showed a smaller PCR product (size: 1.2-1.5 kb) than the wild-type SL1344 strain due to the Kan^R cassette removal. But the high-affinity transporter mutant Δ*metNIQ* retained the Kan^R cassette and it also facilitated the construction of double and triple mutants. The confirmatory PCR was done using the same primers and the resulting product size was still smaller with the Kan^R Δ*metNIQ* mutant than the wild-type because of the long sequence of the targeted *metNIQ* operon (shown in Figure 3-3(G) and 3-4(A)). All the PCR products shown in Figure 3-4 have been generated using Chk-F and Chk-R primers (listed in Table 2-5). The product size along with the description of the mutant strains are listed in the Table 3-1. The whole genome sequencing results of the mutant strains Δ*metA*, Δ*metB*, Δ*metC*, Δ*metE*, Δ*metF*, Δ*metH* and Δ*metNIQ* has been described in the Appendix.

Table 3-1. The PCR product sizes (using Chk-F and Chk-R primers) with the respective mutant strains (Figure 3-4)

Strain	Description	Product size
Δ*metA*	*metA* (Kan^R cassette excised)	1,441 bp (Figure 3-4A)
Δ*metB*	*metB* (Kan^R cassette excised)	1,523 bp (Figure 3-4A)
Δ*metC*	*metC* (Kan^R cassette excised)	1,605 bp (Figure 3-4A)
Δ*metE*	*metE* (Kan^R cassette excised)	1,635 bp (Figure 3-4A)
Δ*metF*	*metF* (Kan^R cassette excised)	1,635 bp (Figure 3-4A)
Δ*metH*	*metH* (Kan^R cassette excised)	1,473 bp (Figure 3-4A)
Δ*metNIQ*	Δ*metNIQ::kan* (Kan-resistant)	2,700 bp (Figure 3-4A)
Δ*metE*Δ*metH*	Δ*metE::kan* Δ*metH* (Kan^R cassette excised)	3,135 bp (Figure 3-4B) 1,473 bp (Figure 3-4B)
Δ*metNIQ*Δ*metB*	Δ*metNIQ::kan* Δ*metB* (Kan^R cassette excised)	2,700 bp (Figure 3-4C) 1,523 bp (Figure 3-4C)
Δ*metNIQ*Δ*metE*	Δ*metNIQ::kan* Δ*metE* (Kan^R cassette excised)	2,700 bp (Figure 3-4D) 1,635 bp (Figure 3-4D)
Δ*metNIQ*Δ*metH*	Δ*metNIQ::kan* Δ*metH* (Kan^R cassette excised)	2,700 bp (Figure 3-4D) 1,473 bp (Figure 3-4D)
Δ*metNIQ*Δ*metE*Δ*metH*	Δ*metNIQ::kan* Δ*metE* (Kan^R cassette excised) Δ*metH* (Kan^R cassette excised)	2,700 bp (Figure 3-4E) 1,635 bp (Figure 3-4E) 1,473 bp (Figure 3-4E)

A)

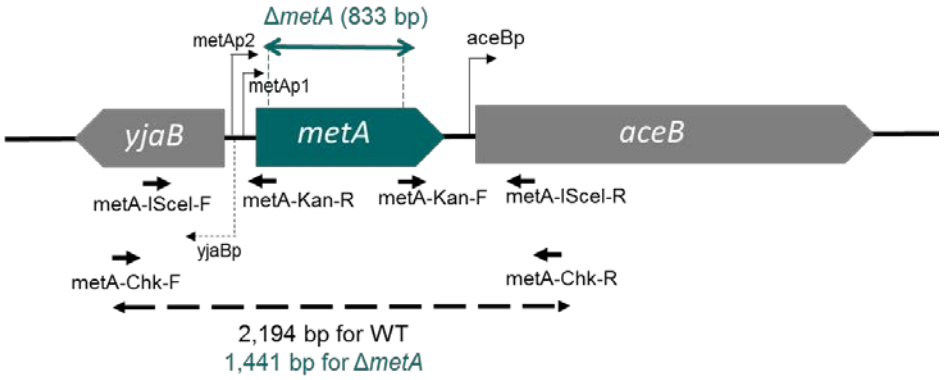
ΔmetA (833 bp)
metAp2
metAp1
aceBp
yjaB
metA
aceB
metA-ISceI-F
metA-Kan-R
metA-Kan-F
metA-ISceI-R
yjaBp
metA-Chk-F
metA-Chk-R
2,194 bp for WT
1,441 bp for ΔmetA

B)

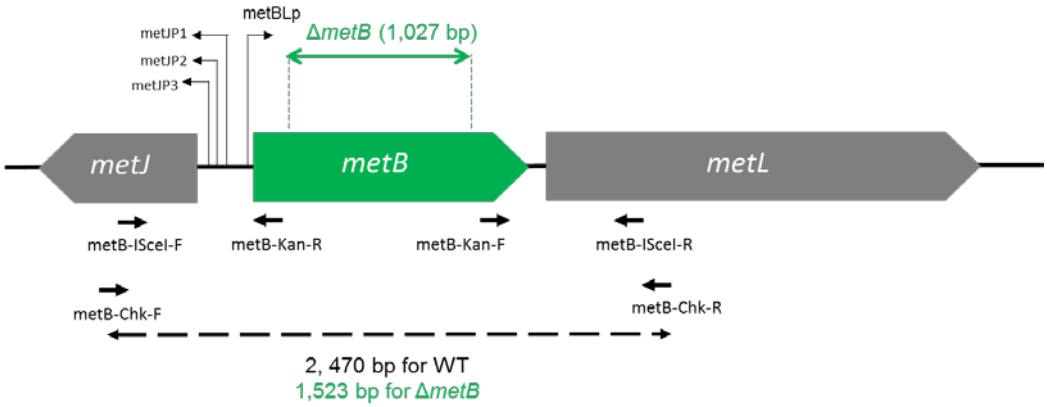
metBLp
metJP1
metJP2
metJP3
ΔmetB (1,027 bp)
metJ
metB
metL
metB-ISceI-F
metB-Kan-R
metB-Kan-F
metB-ISceI-R
metB-Chk-F
metB-Chk-R
2, 470 bp for WT
1,523 bp for ΔmetB

C)

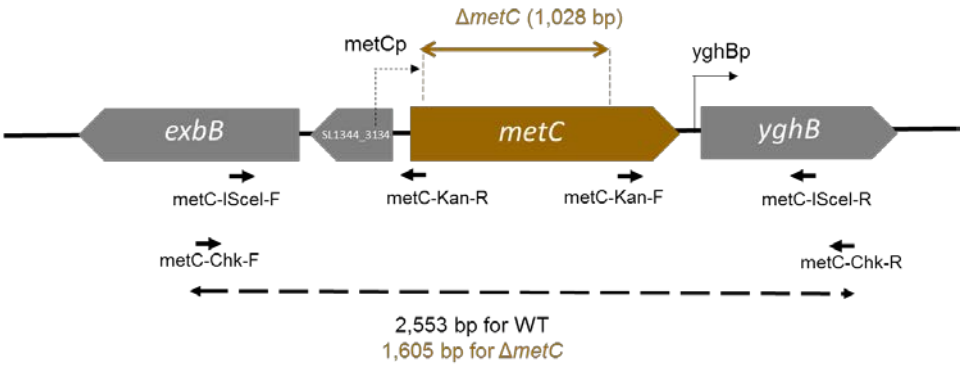
ΔmetC (1,028 bp)
metCp
yghBp
exbB
SL1344_3134
metC
yghB
metC-ISceI-F
metC-Kan-R
metC-Kan-F
metC-ISceI-R
metC-Chk-F
metC-Chk-R
2,553 bp for WT
1,605 bp for ΔmetC

D)

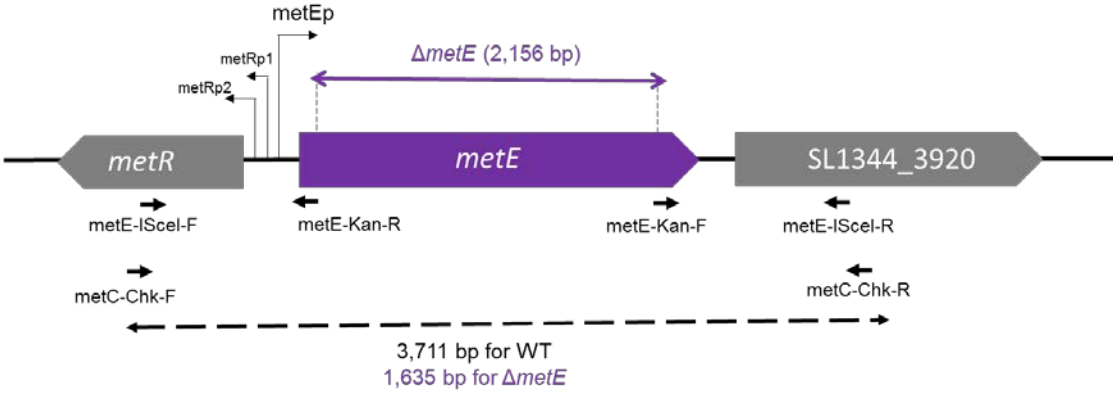
metEp
metRp1
metRp2
ΔmetE (2,156 bp)
metR
metE
SL1344_3920
metE-ISceI-F
metE-Kan-R
metE-Kan-F
metE-ISceI-R
metC-Chk-F
metC-Chk-R
3,711 bp for WT
1,635 bp for ΔmetE

E)

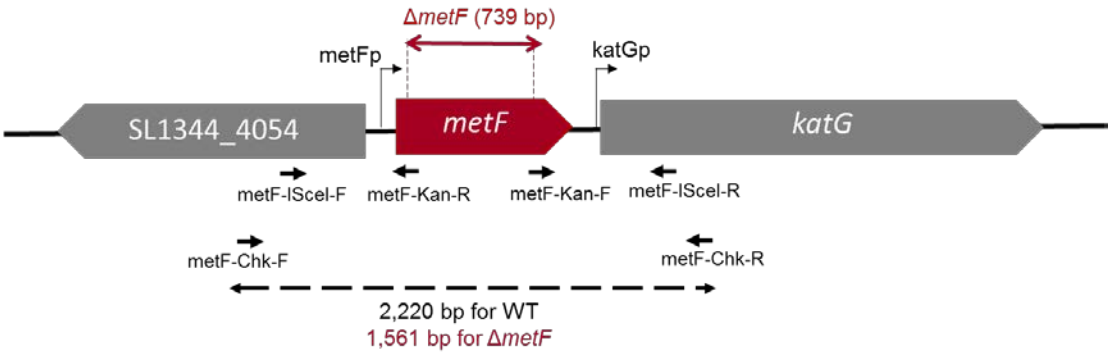
ΔmetF (739 bp)
metFp
katGp
SL1344_4054
metF
katG
metF-ISceI-F
metF-Kan-R
metF-Kan-F
metF-ISceI-R
metF-Chk-F
metF-Chk-R
2,220 bp for WT
1,561 bp for ΔmetF

F)

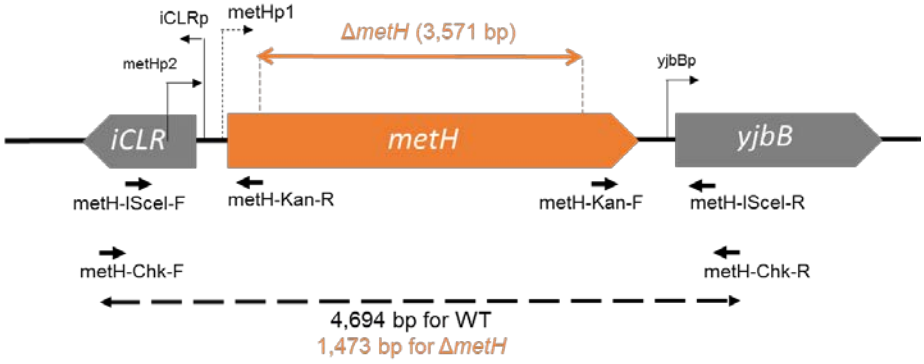
iCLRp
metHp1
ΔmetH (3,571 bp)
metHp2
yjbBp
iCLR
metH
yjbB
metH-ISceI-F
metH-Kan-R
metH-Kan-F
metH-ISceI-R
metH-Chk-F
metH-Chk-R
4,694 bp for WT
1,473 bp for ΔmetH

G)

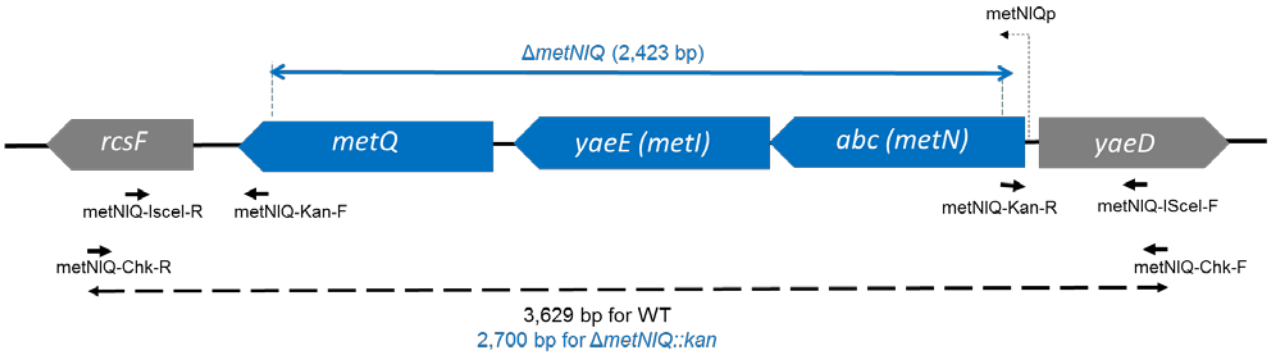

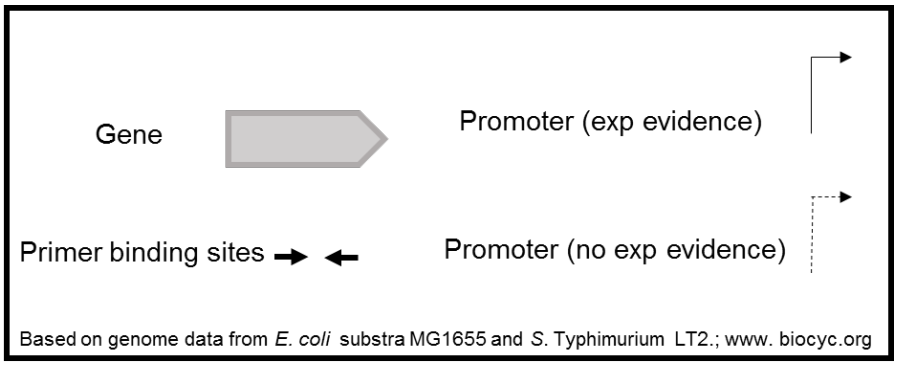

Figure 3-3: Schematic representation of targeted deletions in *metA*, *metB*, *metC*, *metE*, *metF*, *metH* and *metNIQ* gene loci of *S*. Typhimurium SL1344 using gene gorging. The target gene *metA* (**A**); *metB* (**B**); *metC* (**C**); *metE* (**D**); *metF* (**E**); *metH* (**F**) and *metNIQ* (**G**) is represented in the 5' to 3' orientation as block arrow box in colour. Angled line arrow indicates the position of the promoter region (based on experimental and non-experimental evidence from the database of *E. coli* substrain MG1655 and *S*. Typhimurium LT2 available in www.biocyc.org**)** for targeted genes. The sites of flanking genes are shown as block arrow boxes in grey. The region of chromosomal DNA deleted in the mutant is represented between dashed colour lines, the boundaries of which were defined by the binding sites of Kan-R and Kan-F primers, indicated as short black arrows. Chk-F and Chk-R primers were designed to be ~100 bp upstream and downstream of the region that underwent homologous recombination and the size of the PCR product was used to confirm gene deletion, as shown in Figure 3-4.

A)

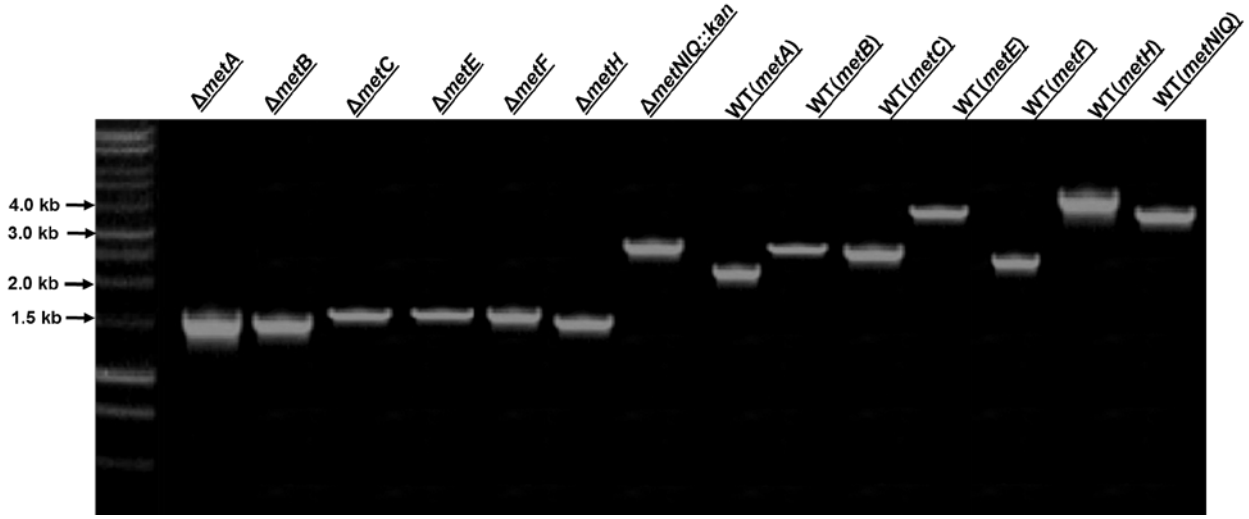
ΔmetA
ΔmetB
ΔmetC
ΔmetE
ΔmetF
ΔmetH
ΔmetNIQ::kan
WT(metA)
WT(metB)
WT(metC)
WT(metE)
WT(metF)
WT(metH)
WT(metNIQ)
4.0 kb
3.0 kb
2.0 kb
1.5 kb

B)

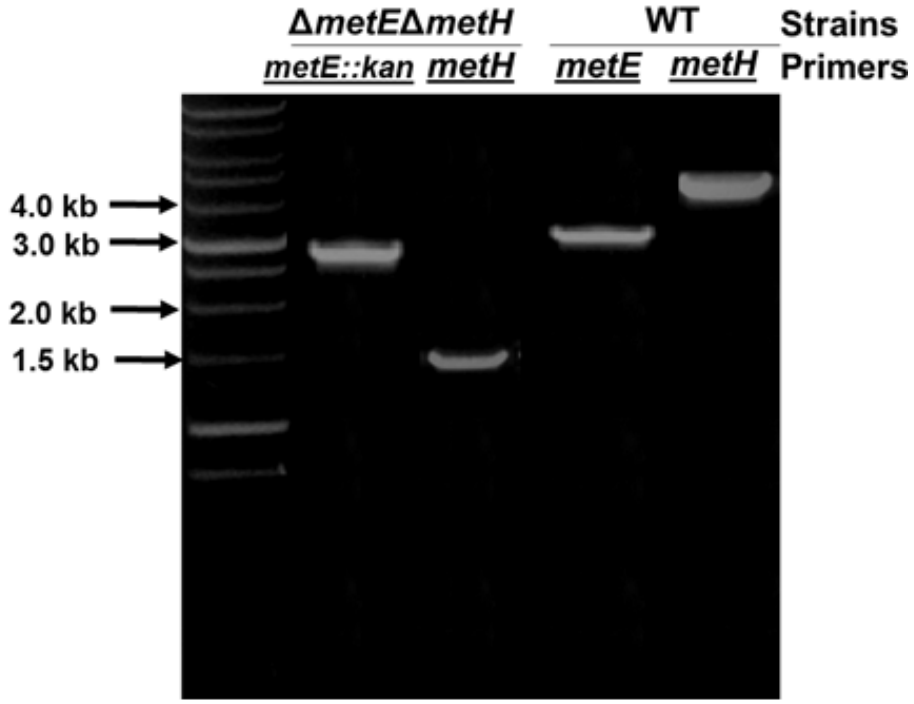
ΔmetEΔmetH
WT
Strains
metE::kan
metH
metE
metH
Primers
4.0 kb
3.0 kb
2.0 kb
1.5 kb

C)

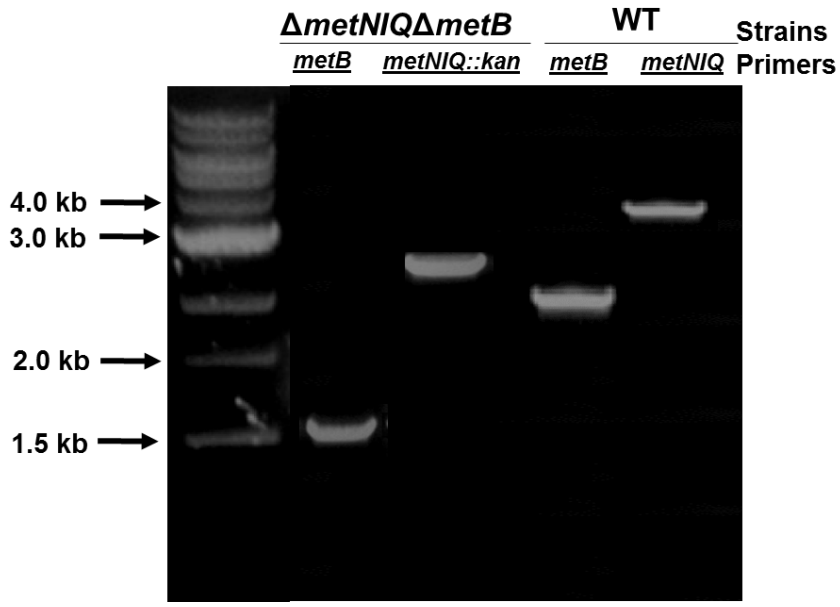
ΔmetNIQΔmetB
WT
Strains
metB
metNIQ::kan
metB
metNIQ
Primers
4.0 kb
3.0 kb
2.0 kb
1.5 kb

D)

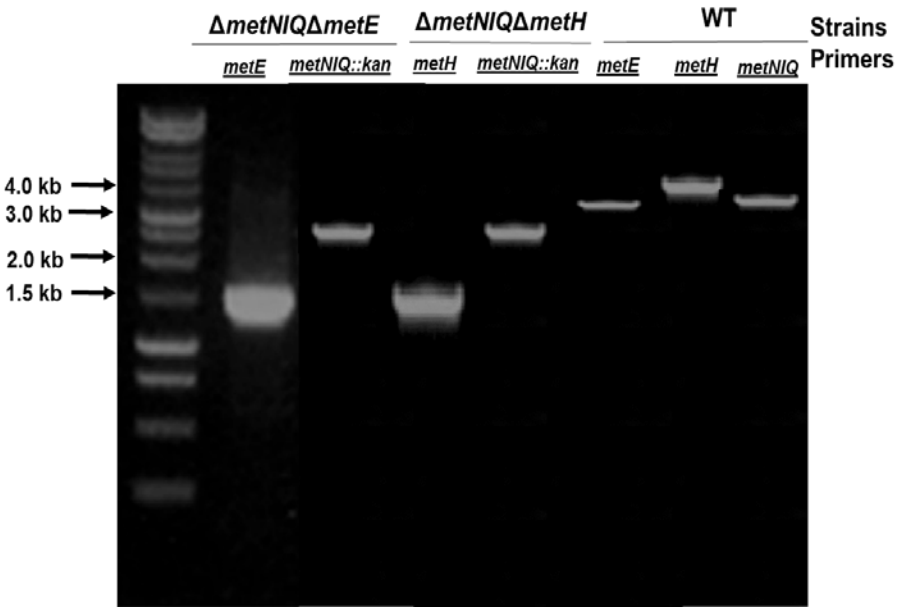
ΔmetNIQΔmetE
ΔmetNIQΔmetH
WT
Strains
metE
metNIQ::kan
metH
metNIQ::kan
metE
metH
metNIQ
Primers
4.0 kb
3.0 kb
2.0 kb
1.5 kb

E)

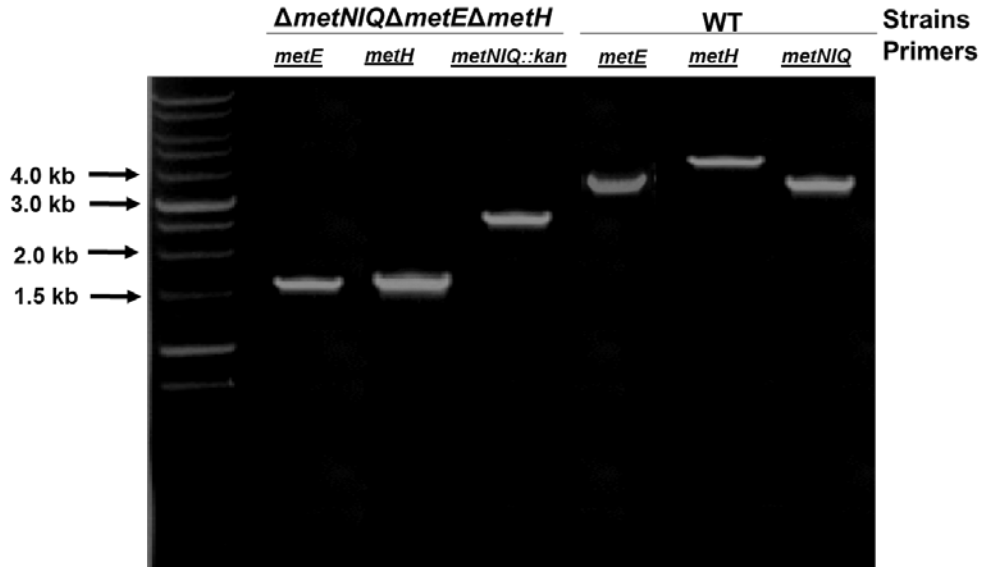

Figure 3-4: PCR validation of site-targeted deletion of *metA, metB, metC, metE. metF, metH* and *metNIQ* genes in *S.* Typhimurium SL1344. The PCR products (using Chk-F and Chk-R primers and corresponding sizes are mentioned in Table 3-1) which confirmed the target gene deletion in the mutants **A)** *de novo* biosynthetic single mutants and high-affinity transporter mutant; **B)** Δ*metE*Δ*metH*; **C)** Δ*metNIQ*Δ*metB*; **D)** Δ*metNIQ*Δ*metE* and Δ*metNIQ*Δ*metH*; **E)** Δ*metNIQ*Δ*metE*Δ*metH*. BenchTop 1 kb DNA Ladder (Promega) was used.

3.2.2 *De novo* Met biosynthesis is essential for *S.* Typhimurium in M9 minimal media

With the defined collection of mutants in the Met biosynthesis pathway, the importance of Met for *in vitro* growth was determined. All mutants were tested for their ability to grow in minimal media (M9) with and without Met, and in rich media (LB). Where Met was supplied, the mutants grew as efficiently as wild-type in Met-supplemented M9 media (Figure 3-5) as well as in LB (data not shown), indicating that the mutants generated are capable of normal growth in the presence of available Met. In M9 minimal media, the Δ*metA*, Δ*metB*, Δ*metC*, Δ*metE,* Δ*metF* and Δ*metE*Δ*metH* mutants became Met auxotrophs whereas Δ*metH* showed substantial growth over the 24-hour period, suggesting that MetH is not essential for *de novo* biosynthesis of Met under aerobic conditions (Figure 3-5). The growth of Δ*metH* in M9 media was compensated by a functional Met synthase MetE.

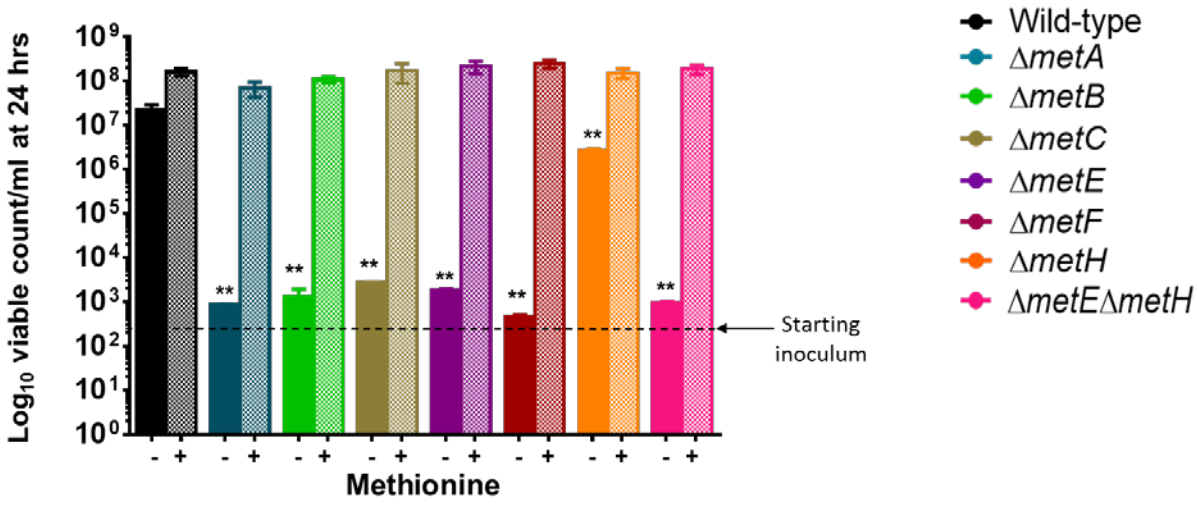

Figure 3-5: The *de novo* biosynthetic mutants demonstrate Met-dependent growth in M9 minimal media. The *de novo* biosynthetic mutants Δ*metA*, Δ*metB*, Δ*metC*, Δ*metE*, Δ*metF*, Δ*metH* and Δ*metE*Δ*metH* were tested for growth in M9 minimal media with or without (+/-) Met supplemented at 100 µM concentration. Viable counts were determined after 24 hours of aerobic growth (shaking at 180 rpm) at 37ºC. WT wild-type; Statistics: One-way ANOVA using Bonferroni's Post-test. Error bar shows mean ± standard error of the mean. Data is pooled from two independent experiments.
** $p < 0.01$ compared with wild-type.

3.2.3 The demonstration of vitamin B12-dependency of *S.* Typhimurium Δ*metE* strain

To demonstrate the vitamin B12-dependency of MetH, the growth of the double mutant Δ*metE*Δ*metH* was tested along with the individual mutants Δ*metE* and Δ*metH* for growth in M9, with or without vitamin B12 (Figure 3-6A). The individual mutants Δ*metE* and Δ*metH* grew in the presence of vitamin B12, however, Δ*metE*Δ*metH* did not show any growth in the presence or absence of vitamin B12. The Δ*metE* mutant which was reliant on MetH to synthesise Met, did not grow in absence of vitamin B12 but grew in presence of vitamin B12 which validates the vitamin B12-dependency of MetH.

As *S.* Typhimurium only synthesises vitamin B12 under anaerobic condition (383, 472, 473), the growth of the Δ*metE*Δ*metH*, Δ*metE* and Δ*metH* were tested under anaerobic and aerobic condition in M9 media (without Met and vitamin B12 supplemented) in (Figure 3-6B). The Δ*metE* mutant showed growth in the absence of oxygen, which supports the hypothesis that *Salmonella* can synthesise vitamin B12 only under anaerobic condition. In contrast, the Δ*metE*Δ*metH* mutant did not grow under aerobic or anaerobic conditions.

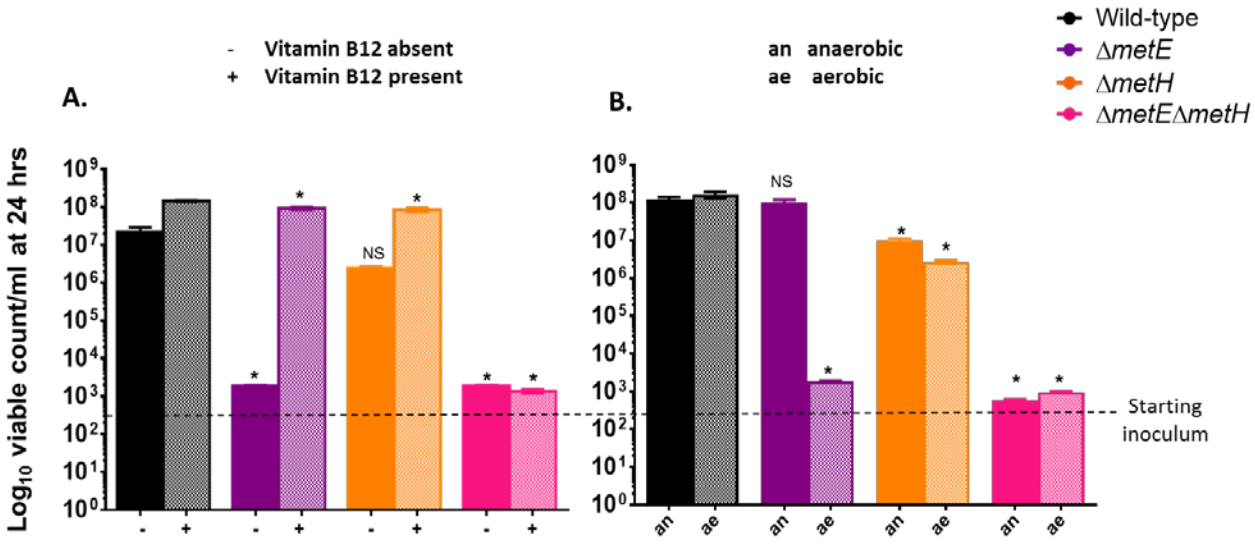

Figure 3-6: The demonstration of vitamin B12-dependency in Met synthase MetH. A) Δ*metE*, Δ*metH* and Δ*metE*Δ*metH* mutants were tested for growth in M9 minimal media supplemented with or without vitamin B12 supplemented at 100 µM concentration. **B)** Δ*metE*, Δ*metH* and Δ*metE*Δ*metH* mutants were tested for growth in M9 minimal media under anaerobic and aerobic conditions at 37ºC. Viable counts were determined at 24 hours. WT wild-type; statistics: One-way ANOVA using Bonferroni's Post-test; Error bars represent mean ± standard error of the mean. Data is pooled from two independent experiments. NS Not significant, * $p < 0.05$ compared with wild-type.

3.2.4 The Met synthase genes *metE* and *metH* are highly conserved in the *Salmonella* genus

To investigate the frequency of sequence variation within key Met synthases *metE* and *metH*, a database of 2490 genome sequences was compiled from complete genome sequences from the NCBI and also draft genome sequences associated with population-based genomic datasets. This database constitutes genome sequences from *S. bongori* and *S. enterica*, and three of the seven *S. enterica* subspecies including *enetrica*, *arizonae* and *diarizonae*. The majority of genome sequences available were representatives of *Salmonella enterica* subsp *enterica*, predominantly *S.* Typhi (487) and *S.* Typhimurium NTS (488); a reflection of their clinical relevance to human health.

Carriage of *S.* Typhimurium SL1344 *metE* (vitamin B12-independent) and *metH* (vitamin B12-dependent) genes within the assembled genome database (n = 2490) was determined through BlastN analysis (blastn 2.3.0+) using the parameters of 80% sequence identity over a minimum of 80% length of the *metE* and *metH* gene sequence. Both *metE* and *metH* were present in >99% of genome sequences (Figure 3-7, bar blot) including representatives of *S. bongori* and *S. enterica* subspecies *arizonae* and *diarizonae*. Low levels of gene sequence variation were observed in *metE* and *metH* (Figure 3-7, whisker plot). This data highlights that MetE and

MetH are highly conserved, and their functionality is retained in this ecologically diverse pathogen. Thus, the ability to synthesise Met in vitamin B12-dependent anaerobic conditions (through MetH) and during aerobic growth (through MetE) is an important biological tool for *Salmonella*.

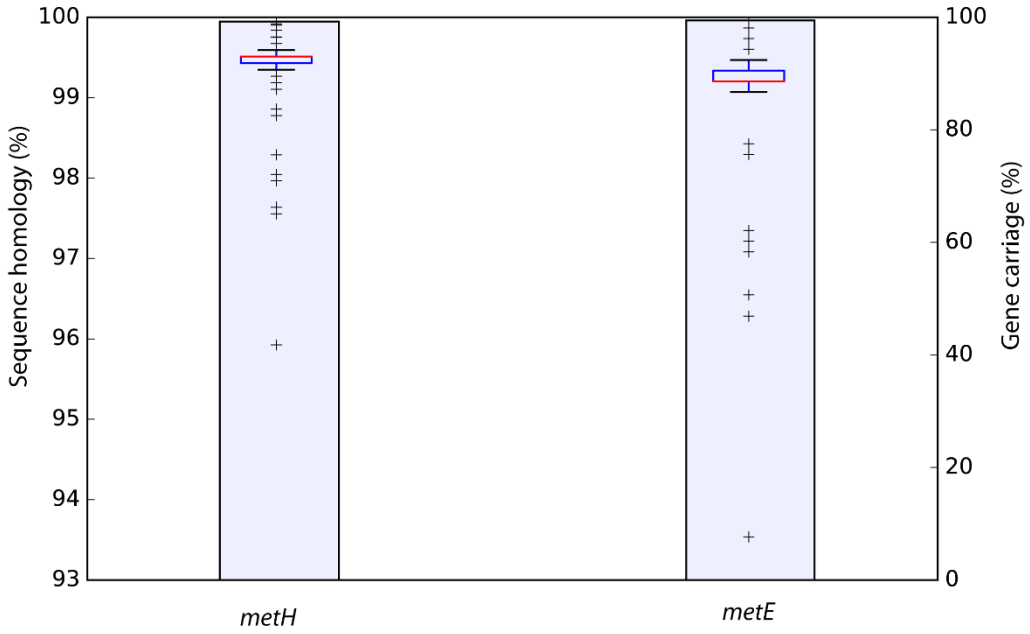

Figure 3-7: *metE* and *metH* genes are highly conserved in *Salmonella*. Bar-and-whisker plot showing the frequency and nucleotide sequence variation of *metE* and *metH* from SL1344 within 2490 genome sequences encompassing different *Salmonella* species and subspecies. The Right Y-axis refers to the bar plot (blue) showing the percent carriage of *metE* and *metH* within 2490 genome sequences. The left Y-axis refers to the whisker plot showing a high level of sequence conservation (%) within the *metE* and *metH* gene sequences. Error bars represent mean ± standard error of the mean with outliers (+) representing sequences beyond the SEM.

3.2.5 In the absence of Met, *de novo* biosynthetic mutants become defective for intracellular replication

The ability of *Salmonella* to survive and replicate in host cells within the SCV is considered as a key virulence trait (209). The role of Met in intracellular survival and replication was therefore assessed by enumerating intracellular bacteria at 2, 5 and 10 hours after infection of HeLa cells. The growth media used for the assay were DMEM-No Met (which did not contain Met) and DMEM-Complete (which contained Met) (described in section 2.2). When DMEM-No Met was used, Δ*metA*, Δ*metB*, Δ*metC* and Δ*metF* showed significant attenuation for intracellular growth compared with the wild-type control (Figure 3-8). In contrast, Δ*metE* displayed an increased lag, and then started to grow slowly after 5 hours because of the

functional MetH. Δ*metH* also showed growth comparable to wild-type, indicating that a functional MetE is sufficient for supporting intracellular growth in HeLa cells (Figure 3-8A).

When DMEM-complete was used as a growth medium where Met is present, none of the mutants showed any intracellular growth defect (Figure 3-8B), indicating that the presence of Met could fully restore the growth of the mutants.

A.

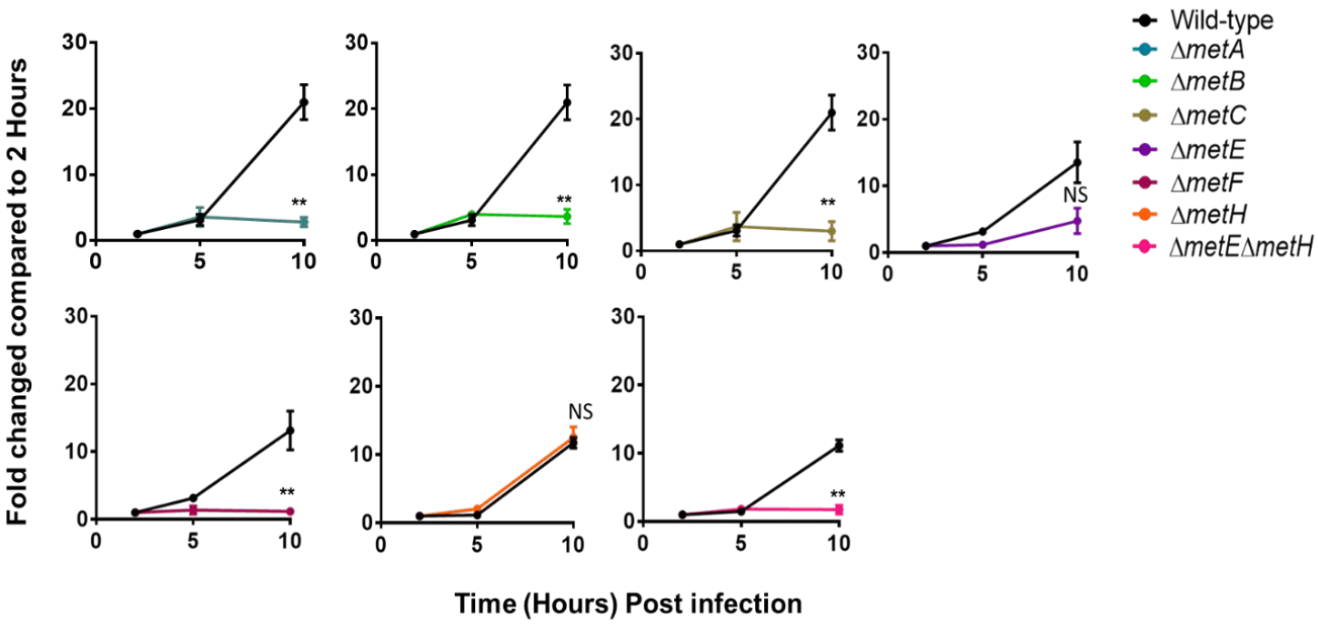

B.

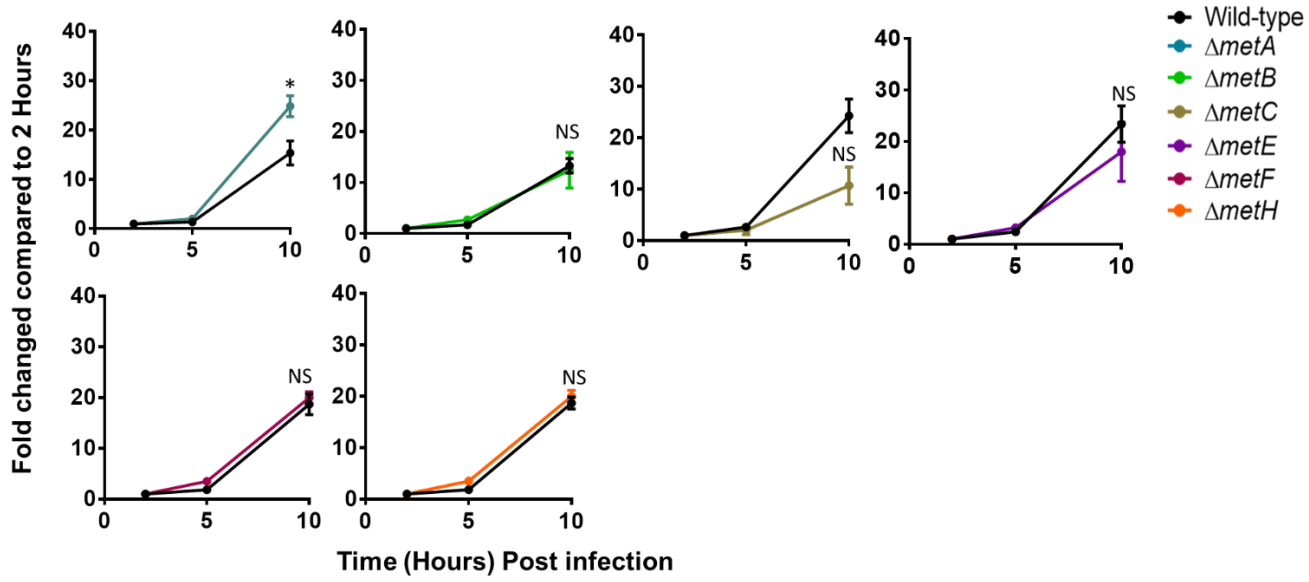

Figure 3-8: The *de novo* Met biosynthetic mutants become defective for intracellular replication in HeLa cells when Met is absent in the tissue culture media. *Salmonella* strains were grown to exponential phase in LB and used to infect HeLa cells for 1 hour at 37ºC (MOI: 5-10). At this point, non-adherent bacteria were removed and extracellular bacteria were killed by gentamicin. To determine the intracellular survival/replication, intracellular bacteria were enumerated at 2, 5 and 10 hours post-infection. **A)** The tissue culture media used for this experiment was DMEM-No Met; **B)** The tissue culture media used for this experiment was DMEM-Complete. Experiments were repeated at least three times independently and the data was pooled from all experiments. The difference was statistically tested at 10 hours using unpaired t-test. Error bars represent mean ± standard error of the mean. NS Not Significant $p > 0.05$; significant * $p < 0.05$; ** $p < 0.01$.

3.2.6 *De novo* Met biosynthesis is not essential for *S*. Typhimurium virulence in mice

The result from the intracellular survival assay experiments suggested that the absence of Met in the tissue culture media reduced the growth of bacteria in cells. Met present in the tissue culture media fully restored the intracellular growth of the mutants. Previous reports suggested that there is a connection between Met biosynthesis and virulence of the *Salmonella* in host (266, 268). The virulence of individual *de novo* biosynthetic mutants were examined in C57BL/6 mice infected intravenously and orally (Figure 3-9).

Mice were infected with 200 cfu intravenously and, at day 5 post-infection, mice were culled and the bacterial load in the spleen and liver was determined as viable counts. The number of bacteria recovered from mice infected with the mutants was comparable to those from mice infected with the wild-type *Salmonella* (Figure 3-9A). None of the mutants showed any virulence defect in mice in the case of intravenous infection.

Oral infection was conducted to test the virulence of the *de novo* Met biosynthesis mutants Δ*metB*, Δ*metE*, Δ*metH* and Δ*metE*Δ*metH*. Mice were infected with 5×10^7 cfu and, at day 6 post-infection, the bacterial loads in the spleen and liver was determined as viable counts. The number of the bacteria from mice infected with Δ*metB*, Δ*metE*, Δ*metH* and Δ*metE*Δ*metH* was comparable to those from mice infected with the wild-type *S.* Typhimurium (Figure 3-9B). None of these mutants showed any growth defect in mice in the case of oral infection.

These data showed that *de novo* Met biosynthesis is not essential for the growth of *S.* Typhimurium in C57BL/6 mice regardless of the route of infection.

A.

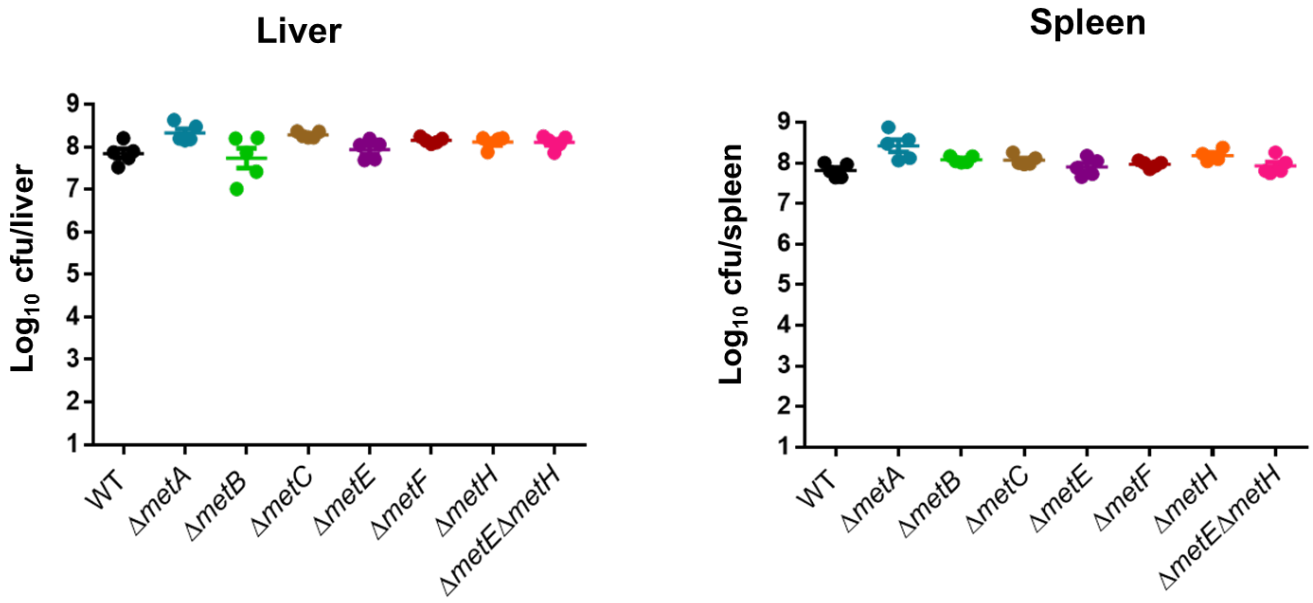

B.

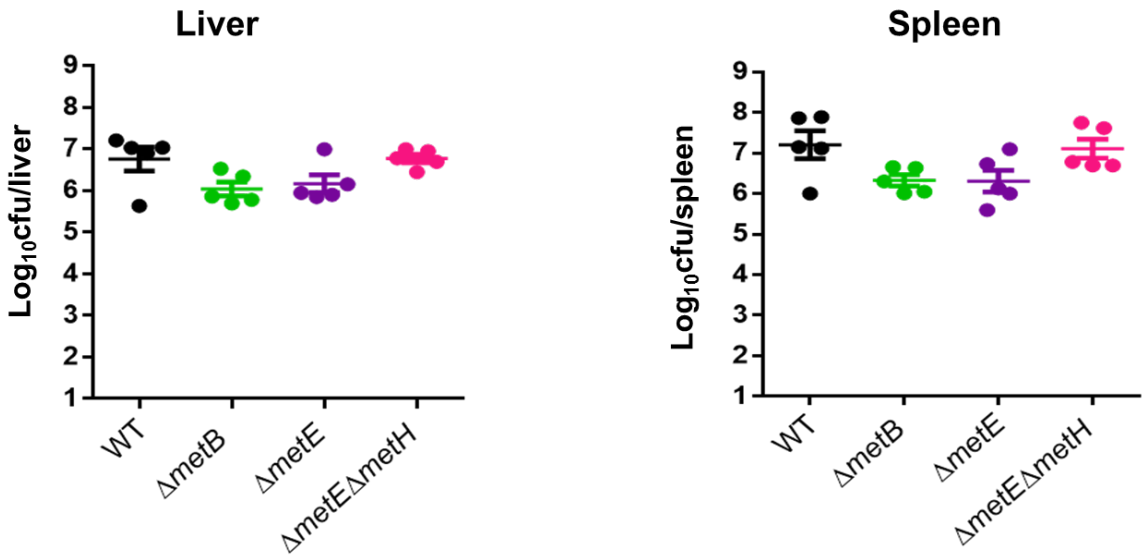

Figure 3-9: *De novo* Met biosynthesis is not essential for *S.* Typhimurium virulence. A) C57BL/6 mice were intravenously infected with 200 cfu of indicated strains of *S.* Typhimurium. At day 5 post-infection, the liver and spleen were harvested and plated on Luria agar + streptomycin (LUS) media to determine the bacterial burden in the organs. **B)** C57BL/6 mice were infected via oral gavage with 5×10^7 cfu of indicated strains of *S.* Typhimurium. The liver and spleen were harvested and plated to determine the bacterial burden at day 6 post-infection. Error bars represent mean ± standard error of the mean. Statistics: One-way ANOVA with Bonferroni's multiple comparison test; all comparisons were not statistically different $p > 0.05$.

3.2.7 The high-affinity transporter mutant Δ*metNIQ* is not growth attenuated in M9 minimal media

The *de novo* biosynthetic *met* mutants of *S.* Typhimurium were able to grow *in vitro* and *in vivo* in presence of Met because a highly efficient Met transport system could support the growth of *S.* Typhimurium. The high-affinity transporter mutant Δ*metNIQ* was tested for its ability to grow in M9 minimal media with or without Met. The Δ*metNIQ* mutant showed growth to levels equivalent to the wild-type in M9 minimal media without Met (Figure 3-10), indicating that this strain retains a fully functional *de novo* Met biosynthesis pathway.

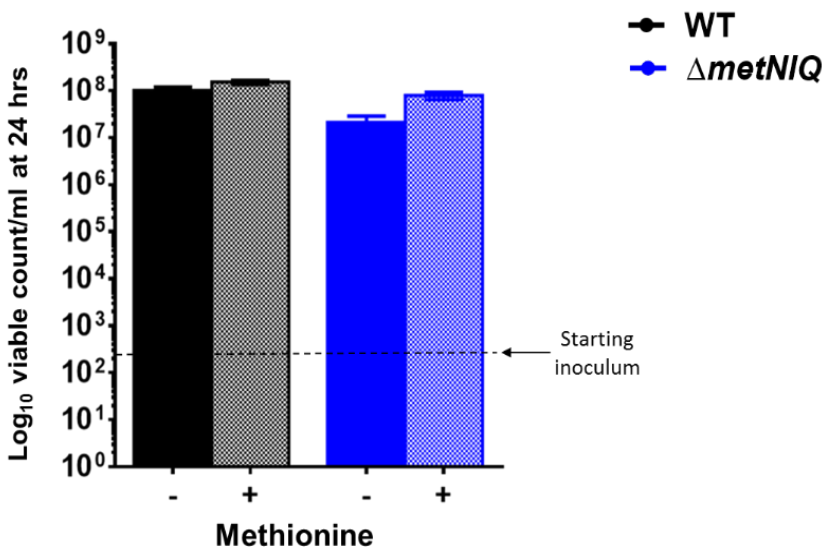

Figure 3-10: The high-affinity transporter mutant Δ*metNIQ* is able to grow in M9 minimal media. The high-affinity transporter mutant Δ*metNIQ* and WT *S.* Typhimurium were tested for growth in M9 minimal media with or without Met supplementation. The growth was tested under these conditions: 37ºC, aerobic growth, shaking. Viable count was determined at 24 hours. WT wild-type; Error bars represent mean ± standard error of the mean. Data is pooled from three independent experiments. Statistics: unpaired T-test; all comparisons were not statistically different; $p > 0.05$.

3.2.8 The high-affinity transporter mutant Δ*metNIQ* is not attenuated for intracellular growth

The high-affinity transporter mutant Δ*metNIQ* was tested for intracellular growth in HeLa cells. The role of Met transport in intracellular survival and replication was assessed by enumerating intracellular bacteria at 2, 5 and 10 hours after infection of HeLa cells (Figure 3-11). The growth media used for the assay was DMEM-No Met and DMEM-Complete (described in Table 2-2). The Δ*metNIQ* mutant did not show any attenuation for intracellular growth regardless of the tissue culture media used. This result suggests that *de novo* Met biosynthesis supports the intracellular growth of *S.* Typhimurium transporter mutant at the same rate as wild-type *S.* Typhimurium.

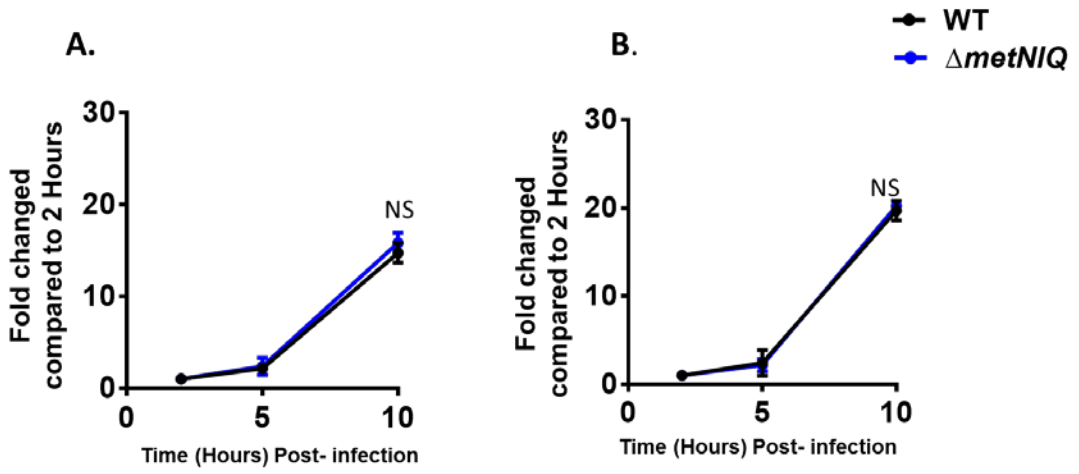

Figure 3-11: The high-affinity transporter-deficient *S.* Typhimurium mutant Δ*metNIQ* is not attenuated for intracellular replication in HeLa cells. HeLa cells were infected with exponential LB cultures of *S.* Typhimurium Δ*metNIQ* for 1 hour at 37ºC (MOI: 5-10). At this point, non-adherent bacteria were removed and extracellular bacteria were killed by gentamicin. To determine the intracellular survival/replication, intracellular bacteria were enumerated at 2, 5 and 10 hours. **A)** The tissue culture media used for this experiment was DMEM-No Met; **B)** The tissue culture media used for this experiment was DMEM-Complete. Experiments were repeated at least three times independently and the data was pooled from all experiments. The difference was tested at 10 hours. Error bars represent mean ± standard error of the mean. Statistics: unpaired T-test; NS Not Significant $p > 0.05$.

3.2.9 The high-affinity transporter is not essential for virulence of *S.* Typhimurium in mice

Previous studies have shown that the *S.* Typhimurium lacking the high-affinity transporter Δ*metNIQ* is significantly attenuated in C3H/HeN mice. C3H/HeN mice are resistant to *Salmonella* infection because they carry the resistant allele named "Immunity to typhimurium" and denoted by (*Ity*) (Ity^r dominant) which controls resistance and susceptibility to *S.* Typhimurium (489). This indicates that the *de novo* Met biosynthesis may not be sufficient for growth in some strains of mice (270). Although in our study the Δ*metNIQ* was not attenuated for intracellular survival in mice carrying *Ity*-sensitive allele (ie. C57BL/6 mice), the virulence was tested in mice to see if it supports the previous data. The virulence of high-affinity transporter mutant Δ*metNIQ* was tested in C57BL/6 murine host after intravenous and oral inoculation (Figure 3-12).

Mice were infected with 200 cfu of Δ*metNIQ* intravenously and, at day 5 post-infection, the animals were culled and the bacterial load in the spleen and liver was determined as viable counts. The number of bacteria recovered from mice organs infected with Δ*metNIQ* was equivalent to the bacterial load from the mice infected with the wild-type strain (Figure 3-12A).

Mice were also infected with 5×10^7 cfu of Δ*metNIQ* orally and at day 6 post-infection, the bacterial load in the spleen and liver was determined as viable counts. The number of bacteria recovered from mice organs infected with Δ*metNIQ* was equivalent with those from mice infected with the wild-type strain (Figure 3-12B).

Given the above results, it could be hypothesised that the transport of Met through the high-affinity transporter is not required for the virulence of *S.* Typhimurium because of the presence of a fully functional Met biosynthesis system, which can provide the Met that the bacteria require.

A.

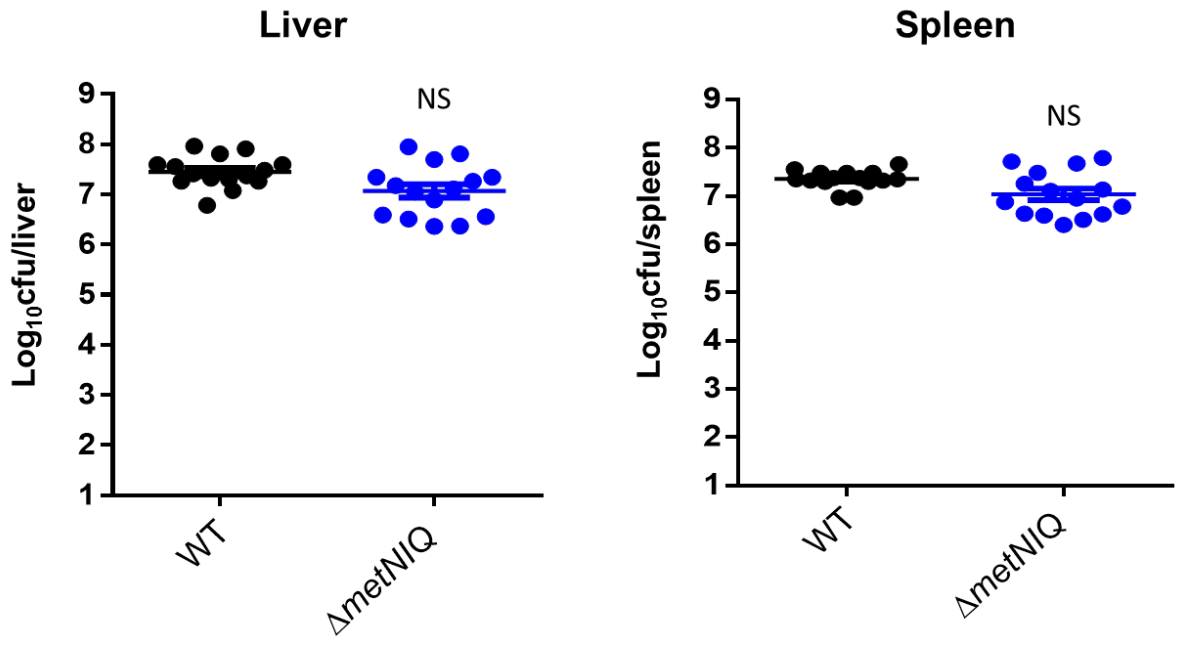

B.

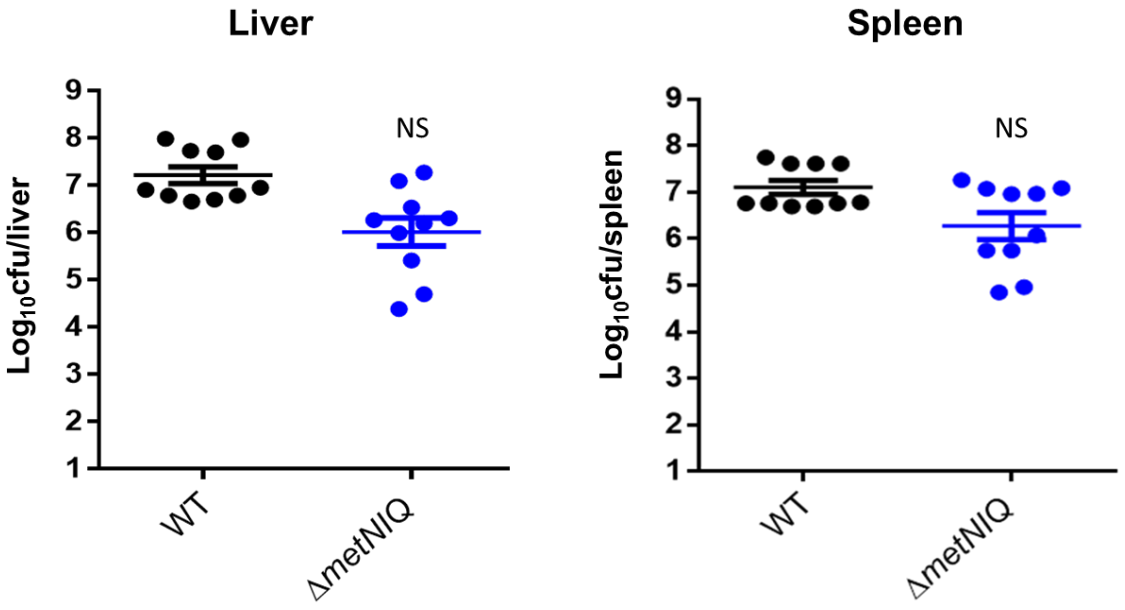

Figure 3-12: The high-affinity transporter-deficient *S.* Typhimurium Δ*metNIQ* remains virulent in mice. A) C57BL/6 mice were infected intravenously with 200 cfu of wild-type. *S.* Typhimurium or Δ*metNIQ.* The liver and spleen were harvested for plating to determine the bacterial burden at day 5 post-infection. Data are pooled from three independent experiments. **B)** C57BL/6 mice were infected orally with 5×10^7 cfu of wild-type *S.* Typhimurium or Δ*metNIQ*. On day 6 post-infection, the liver and spleen were harvested for plating to determine the bacterial burden in the organs. Data are pooled from two independent experiments. Error bars represent mean ± standard error of the mean. Statistics: unpaired T-test; NS Not significant $p > 0.05$.

3.2.10 The Δ*metNIQ*Δ*metB*, Δ*metNIQ*Δ*metE* and Δ*metNIQ*Δ*metE*Δ*metH* are Met auxotrophs in M9 minimal medium but Δ*metNIQ*Δ*metH* is not

To characterise the growth and virulence trait of *S.* Typhimurium when both Met biosynthesis and high-affinity transport were absent from the bacterium, double and triple knockout strains that lack both high-affinity transport and *de novo* biosynthesis of Met were generated: Δ*metNIQ*Δ*metB*, Δ*metNIQ*Δ*metE*, Δ*metNIQ*Δ*metH* and Δ*metNIQ*Δ*metE*Δ*metH* by following the P22 phage transduction (section 3.2.1 and section 2.9.4). The Δ*metNIQ*Δ*metB* strain was complemented by expressing the *metB* gene with the putative *metB* promoter on the pACYC184 plasmid (section 2.10).

The four mutant strains (i.e. combined mutants having deletion in biosynthesis and the high-affinity transporter) Δ*metNIQ*Δ*metB,* Δ*metNIQ*Δ*metE,* Δ*metNIQ*Δ*metH* and Δ*metNIQ*Δ*metE*Δ*metH*, and the complemented strain Δ*metNIQ*Δ*metB* pACYC184 *metB,* were tested for their growth in M9 minimal media with or without Met (Figure 3-13).

Δ*metNIQ*Δ*metB* and Δ*metNIQ*Δ*metE*Δ*metH* mutants showed Met auxotrophy in M9 media without Met. This observation suggests a combined deficiency in both biosynthesis and high-affinity transport in M9 minimal media (when no Met is present) is attenuating, as expected. The complementation with *metB* restored the growth of Δ*metNIQ*Δ*metB* pACYC184 *metB* strain to wild-type levels, indicating that the biosynthesis can fully restore the growth of the double mutant Δ*metNIQ*Δ*metB.*

The Δ*metNIQ*Δ*metE* mutant was not able to grow in M9 media without supplemented Met. The Δ*metE* mutant was not able to grow under aerobic condition (section 3.2.3) and that is most likely due to a dysfunctional MetH in the absence of its B12 cofactor. The Δ*metNIQ*Δ*metH* mutant did not show Met auxotrophy in M9 media (i.e. where no Met is supplemented) most probably because it had the functional, vitamin B12-independent Met synthase MetE which can fully compensate for the loss of MetH. The addition of Met into the media restored the growth of all these mutant strains, suggesting that the presence and activity of the putative low-affinity transporter ('MetP') was sufficient to enable Met uptake and facilitate growth (Figure 3-13).

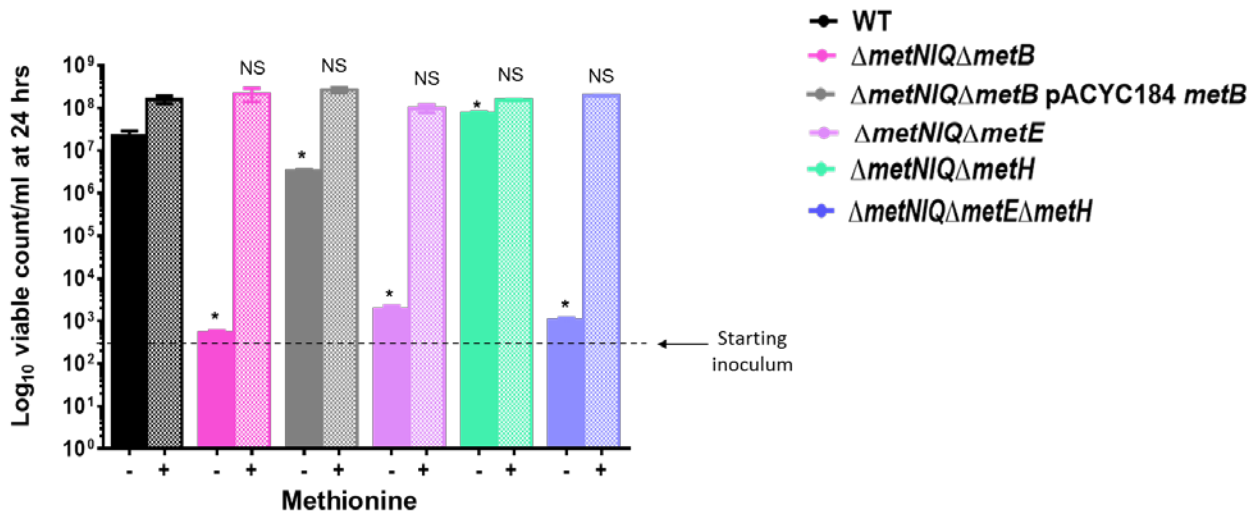

Figure 3-13: The mutants deficient in *de novo* Met biosynthesis and high-affinity transport show Met auxotrophy in M9 minimal media. The double and triple mutants Δ*metNIQ*Δ*metB*, Δ*metNIQ*Δ*metE*, Δ*metNIQ*Δ*metH*, Δ*metNIQ*Δ*metE*Δ*metH* and a complemented mutant strain Δ*metNIQ*Δ*metB* pACYC184 *metB* were tested for growth in M9 minimal media (with and without Met supplementation). The growth was tested under conditions of 37ºC, aerobic growth, shaking. Viable count was determined at 24 hours. WT wild-type; Statistics: One-way ANOVA with Bonferroni's multiple comparison test. Error bars represent mean ± standard error of the mean. Data is pooled from two different experiments. NS Not significant.
* $p < 0.05$ compared with wild-type under the same condition.

3.2.11 The Δ*metNIQ*Δ*metB* and Δ*metNIQ*Δ*metE*Δ*metH* strains are attenuated for intracellular survival but Δ*metNIQ*Δ*metE* and Δ*metNIQ*Δ*metH* are not

Four mutant strains, comprising of the 3 double Δ*metNIQ*Δ*metB*, Δ*metNIQ*Δ*metE*, Δ*metNIQ*Δ*metH* and the triple mutant Δ*metNIQ*Δ*metE*Δ*metH* were tested for intracellular growth in HeLa cells over 2 hours, 5 hours and 10 hours (Figure 3-14). DMEM-No Met and DMEM-complete were used as the tissue culture media (described in section 2.2). The mutants deficient in both biosynthesis and high-affinity transport, Δ*metNIQ*Δ*metB* and Δ*metNIQ*Δ*metE*Δ*metH*, were attenuated for intracellular growth in HeLa cells when DMEM-No Met was used as tissue culture media (Figure 3-14A). The presence of Met in DMEM restored the growth of these two strains to wild-type levels (Figure 3-14B). The two other double mutants Δ*metNIQ*Δ*metE* and Δ*metNIQ*Δ*metH* grew to wild-type levels in HeLa cells.

A.

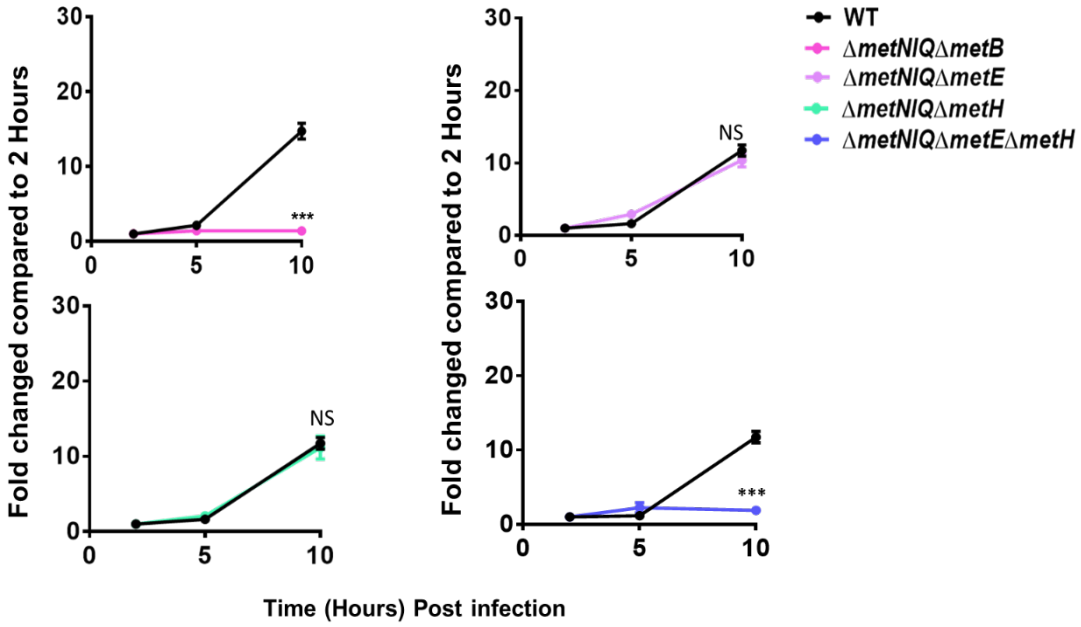

B.

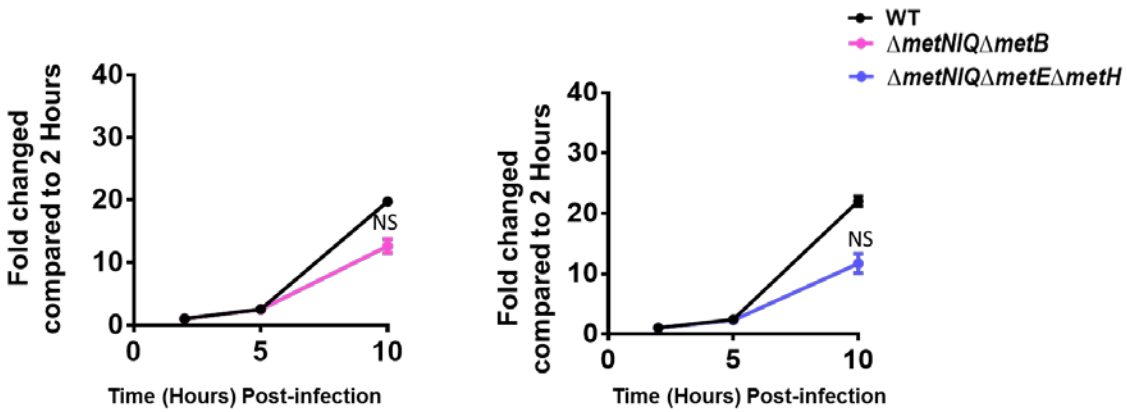

Figure 3-14: The mutants deficient in *de novo* Met biosynthesis and high-affinity transport become defective for intracellular growth and replication in HeLa cells when Met is absent in tissue culture media. HeLa cells were infected with exponential LB cultures of the indicated strains of *S.* Typhimurium for 1 hour at 37ºC (MOI: 5-10). At this point, non-adherent bacteria were removed and extracellular bacteria were killed by gentamicin. To determine the intracellular survival/replication, intracellular bacteria were enumerated at 2 hours, 5 hours and 10 hours. The strains tested were: Δ*metNIQ*Δ*metB*, Δ*metNIQ*Δ*metE*, Δ*metNIQ*Δ*metH* and Δ*metNIQ*Δ*metE*Δ*metH*. The tissue culture media used for this experiment was **A)** DMEM-No Met supplemented and **B)** DMEM-Complete. Δ*metNIQ*Δ*metE* and Δ*metNIQ*Δ*metH* were tested using only DMEM-No Met. The experiments were repeated at least three times independently and the data were pooled from all experiments. The difference was statistically tested at 10 hours. Error bars represent mean ± standard error of the mean. Statistics: unpaired T-test; NS Not Significant $p > 0.05$; *** $p < 0.001$

3.2.12 Δ*metNIQ*Δ*metB* and Δ*metNIQ*Δ*metE*Δ*metH* are attenuated in mice

The virulence of the mutant strains Δ*metNIQ*Δ*metB*, Δ*metNIQ*Δ*metE*Δ*metH* and the complemented strain Δ*metNIQ*Δ*metB* pACYC184 *metB* were tested in C57BL/6 mice (Figure 3-15).

Mice were infected with 200 cfu of Δ*metNIQ*Δ*metB*, Δ*metNIQ*Δ*metE*Δ*metH* and Δ*metNIQ*Δ*metB* pACYC184 *metB* intravenously (Figure 3-15A). At day 5 post-infection, the mice were culled and the bacterial load in the spleen and liver was determined by viable count. The bacterial number of the mutants deficient in biosynthesis and high-affinity transport i.e. Δ*metNIQ*Δ*metB* and Δ*metNIQ*Δ*metE*Δ*metH* were approximately 10^5 and 10^4 in the organs which showed 1000-fold and 10,000-fold reductions in the bacterial load in the spleen and liver compared to the wild-type strain. This data suggests that these mutants are severely attenuated for growth in mice. In contrast, analysis of the Δ*metNIQ*Δ*metE*Δ*metH* mutant showed approximately 10-fold reduction in bacterial burden compared to Δ*metNIQ*Δ*metB*, suggesting

a role for the active cycling of Met in optimal growth in sensitive mice (when high-affinity transporter is absent).

In case of the oral infection, the mice were infected with 5×10^7 cfu of the Δ*metNIQ*Δ*metB* and Δ*metNIQ*Δ*metE*Δ*metH* (Figure 3-15B, 3-15C and 3-15D). Bacterial fecal shedding was assessed for Δ*metNIQ*Δ*metB* compared to wild-type over the infection period (Figure 3-13C). This data shows that at day 6 post-infection, the Δ*metNIQ*Δ*metB* mutant was found in a lower number (10^5 cfu) in the infected mice than in the wild-type (10^6 cfu) although the difference was not statistically significant. This data indicates that there was not any substantial difference in the fecal shedding of the Δ*metNIQ*Δ*metB* mutant and wild-type. At day 6 post-infection, mice were culled and the bacterial burden was determined from the spleen and liver (Figure 3-15B and 3-15D). The viable bacterial number in the spleen and liver for Δ*metNIQ*Δ*metB* and Δ*metNIQ*Δ*metE*Δ*metH* is approximately 10^4 and 10^3 cfu, respectively (1,000-fold to 10,000-fold reduced compared to the wild-type). This resembles the result found from intravenous infection with the Δ*metNIQ*Δ*metB* and Δ*metNIQ*Δ*metE*Δ*metH*, indicating that Δ*metNIQ*Δ*metB* and Δ*metNIQ*Δ*metE*Δ*metH* are attenuated in mice regardless of the route of infection.

A.

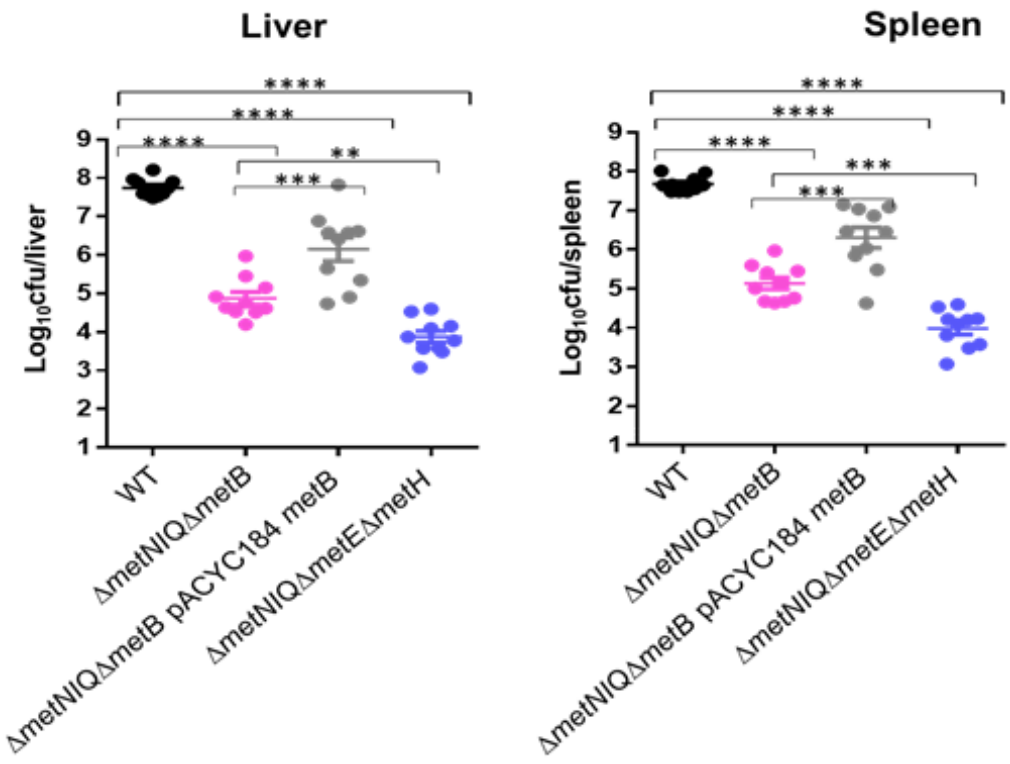

B.

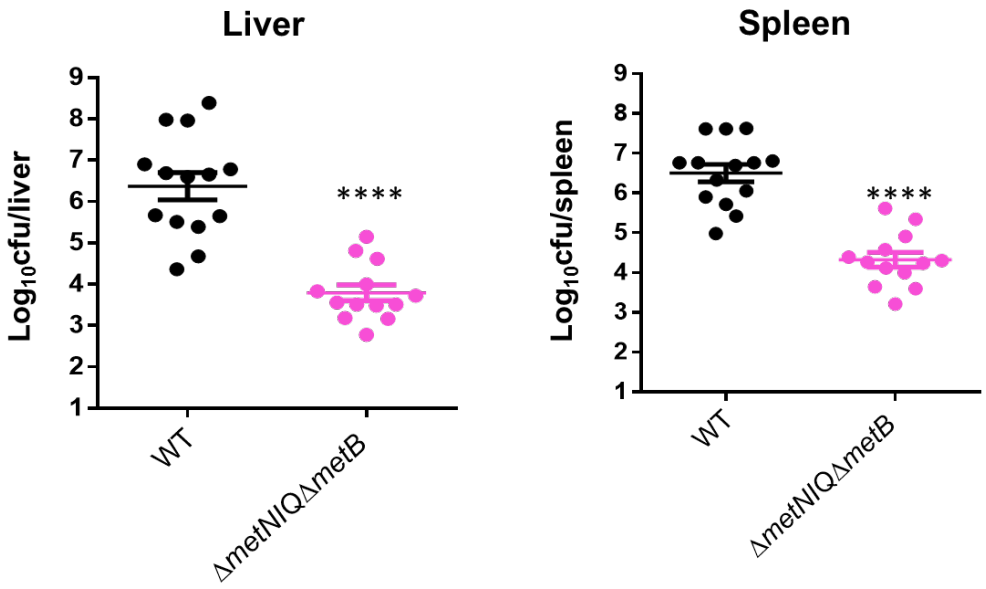
Liver
Spleen
Log10cfu/liver
Log10cfu/spleen
****
****
WT
ΔmetNIQΔmetB
WT
ΔmetNIQΔmetB

C.

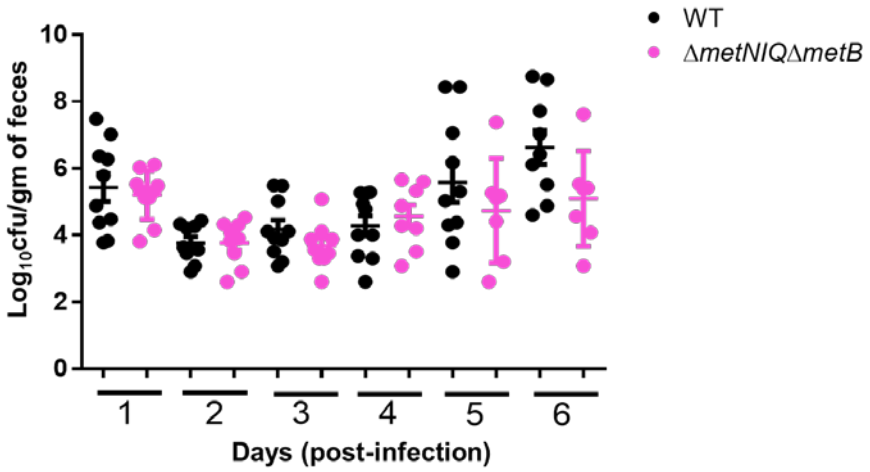
WT
ΔmetNIQΔmetB
Log10cfu/gm of feces
Days (post-infection)

D.

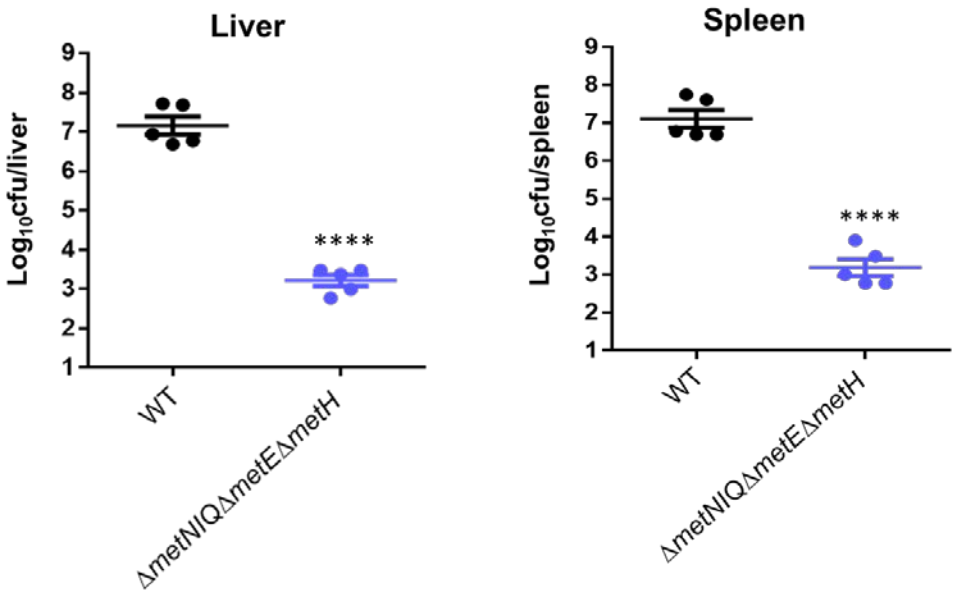

Figure 3-15: *S.* Typhimurium mutants lacking the biosynthesis and high-affinity transport of Met are attenuated in mice. A) C57BL/6 mice were infected intravenously with 200 cfu of different strains of *S.* Typhimurium. At day 5 post-infection, the liver and spleen were harvested for plating to determine the bacterial burden in the organs. Results are pooled from two independent experiments. **B)** C57BL/6 mice were infected orally with 5×10^7 cfu of different strains of *S.* Typhimurium. At day 6 post-infection, liver and spleen were harvested for plating to determine the bacterial burden in the organs. Results were pooled from three independent experiments. **C)** The fecal burden was determined every 24 hours. Results were pooled from two independent experiments. **D)** C57BL/6 mice were infected intravenously with 200 cfu of indicated strains of *S.* Typhimurium. Error bars represent mean ± standard error of the mean. Statistics: One-way ANOVA with Bonferroni's multiple comparison test (3-15A) and unpaired T-test (3-15B, C and D); significant ** $p < 0.01$; **** $p < 0.0001$.

3.2.13 The Δ*metNIQ*Δ*metE* and Δ*metNIQ*Δ*metH* are virulent in mice

The virulence of the mutant strains Δ*metNIQ*Δ*metE* and Δ*metNIQ*Δ*metH* was tested in C57BL/6 mice (Figure 3-16). Mice were infected with 200 cfu of Δ*metNIQ*Δ*metE* or Δ*metNIQ*Δ*metH* intravenously and, at day 5 post-infection, the bacterial load in the spleen and liver was determined as viable counts. The mutants showed bacterial load equivalent to those of the wild-type *S.* Typhimurium in the spleen and liver, suggesting that these mutants are virulent for systemic infection in mice and demonstrated the redundancy of the two Met synthases MetE and MetH.

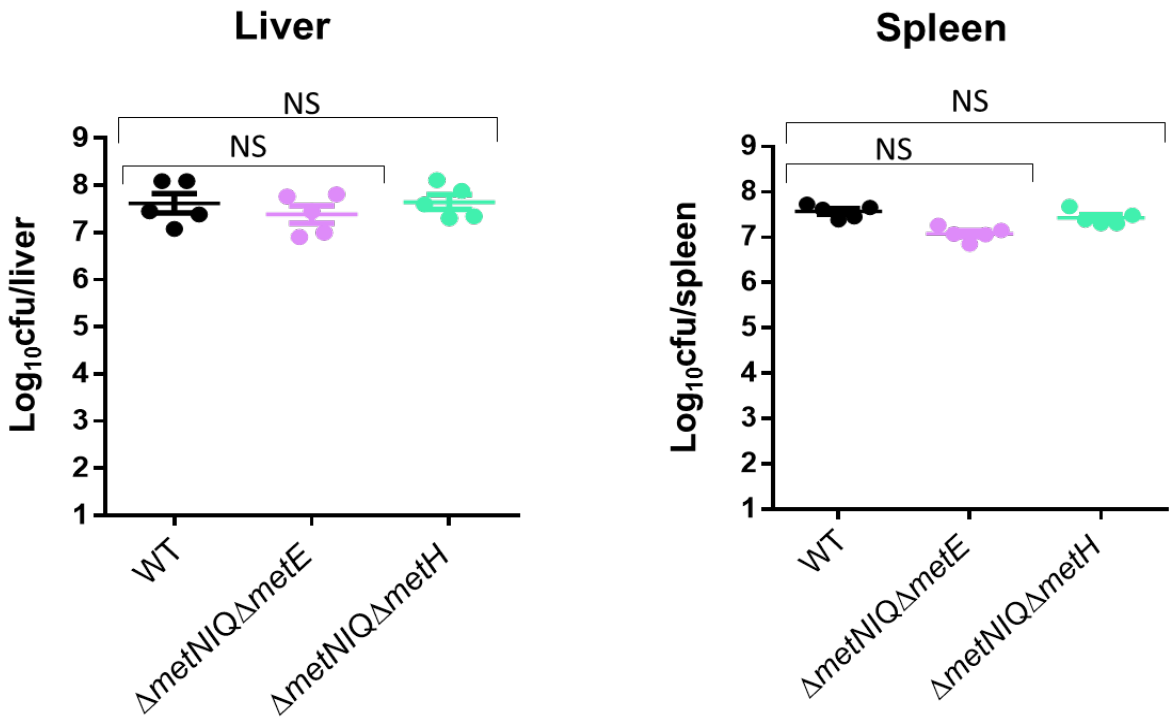

Figure 3-16: The Δ*metNIQ*Δ*metE* and Δ*metNIQ*Δ*metH* mutants are virulent in mice. C57BL/6 mice were intravenously infected with 200 cfu of indicated strains of *S.* Typhimurium. At day 5 post-infection, the liver and spleen were harvested for plating to determine the bacterial burden in the organs. Error bars represent mean ± standard error of the mean. Statistics: One-way ANOVA with Bonferroni's multiple comparison test; Not Significant $p > 0.05$.

3.2.14 The role of the cryptic low-affinity transporter in a concentration-dependent L-Met transport

In addition to the characterised high-affinity Met transporter, MetNIQ, *S.* Typhimurium can take up Met through a cryptic low-affinity transporter/s, putatively referred to as MetP (263, 264). This transporter/s is cryptic because the chromosomal location is still unidentified and it is unclear whether this capacity to import Met is dependent on one or more unknown transporters. This study shows that the supplementation of Met in M9 and DMEM media fully restores the growth of the *S.* Typhimurium double mutant Δ*metNIQ*Δ*metB* and triple mutant Δ*metNIQ*Δ*metE*Δ*metH*, hence validating the existence of another transporter which can transport L-Met (section 3.2.10, 3.2.11 and 3.2.12). To understand the concentration-dependent L-Met transport, the mutant strains Δ*metB*, Δ*metNIQ* and Δ*metNIQ*Δ*metB* were tested for their growth in M9 minimal media supplemented with 10 µM, 1.0 µM and 0.1 µM L-Met in comparison to wild-type (Figure 3-17). Δ*metB* shows growth in M9 minimal media with L-Met supplemented with 10 µM, 1.0 µM and 0.1 µM and this represents the efficient Met

transport mediated by the high-affinity transporter. MetNIQ can transport Met even when the concentration is as low as 0.1 µM. The Δ*metNIQ*Δ*metB* mutant was able to grow in M9 minimal media supplemented with 10 µM L-Met, although not as efficiently as the wild-type ($p > 0.5$) but cannot grow in L-Met when supplemented at 0.1 µM concentration over 96 hours ($p < 0.01$). This supports the previous studies showing that the putative low-affinity transporter is not as efficient as it's high-affinity counterpart and the K_m of this low-affinity transporter for L-Met is much higher than MetNIQ (263, 264). Δ*metNIQ* did not show any growth attenuation because of the functional *de novo* Met biosynthetic pathway.

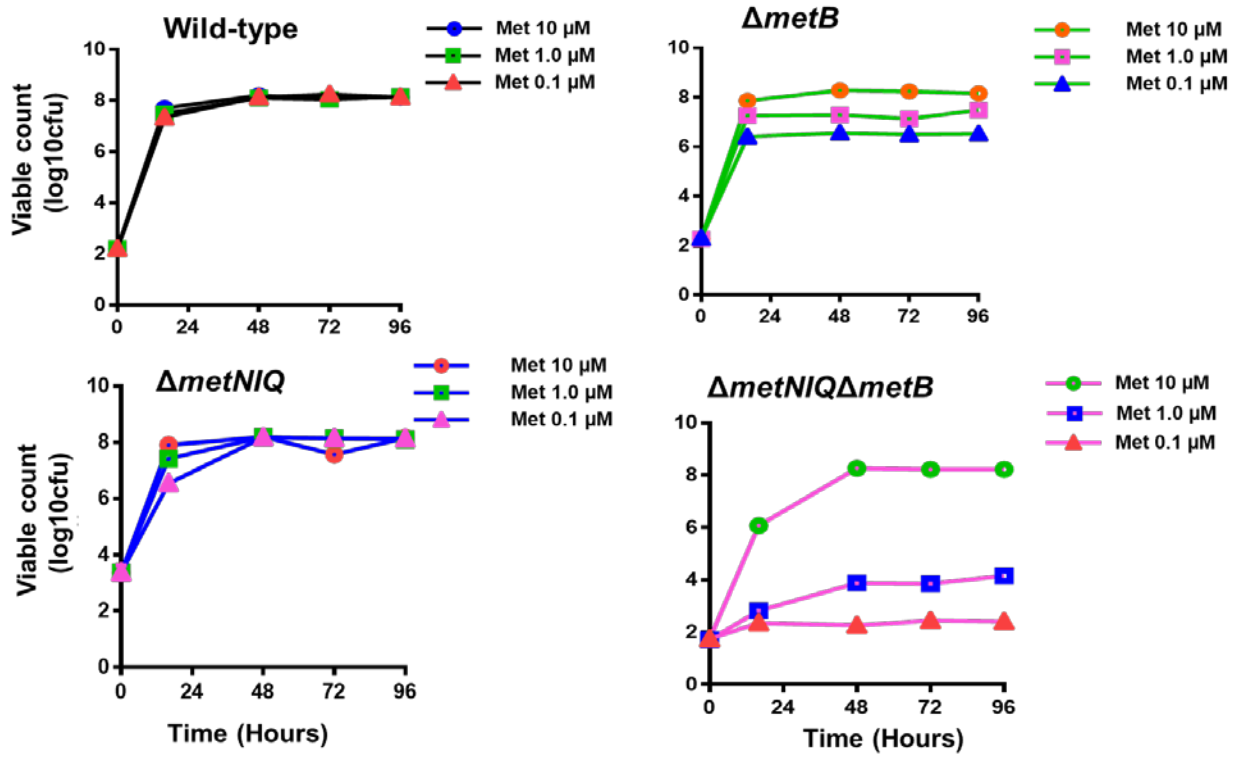

Figure 3-17: Uptake of L-Met by low-affinity transporter "MetP" depends on L-Met concentration. Growth of Δ*metB*, Δ*metNIQ* and Δ*metNIQ*Δ*metB* was monitored in M9 media with different concentration of L-Met added for up to 96 hours. Viable counts were determined at every 24 hours. Error bars represent mean ± standard error of the mean. For Δ*metNIQ*Δ*metB*, in 1 µM Met: $p < 0.01$; in 0.1 µM Met: $p < 0.05$ when compared with wild-type.

3.2.15 The low-affinity transporter "MetP" ineffectively transports D-Met

It has been shown that *E. coli* high-affinity transporter mutant Δ*metNIQ* is unable to grow in D-Met (485). There is also evidence that *S.* Typhimurium Δ*metNIQ*Δ*metB* shows a slow response to D-Met when the concentration is increased to 670 µM and depicts that low-affinity transporter has a higher K_m for D-Met compare to L-Met (264). To test whether the low-affinity transporter can transport D-Met, the Δ*metB* and Δ*metNIQ*Δ*metB* mutants were grown in M9

minimal media supplemented with D-Met in two different concentrations, 100 µM and 700 µM, and growth was monitored for 96 hours (Figure 3-18). The Δ*metB* mutant showed growth in M9 minimal media supplemented with D-Met at 100 µM and 700 µM, demonstrating that high-affinity transporter can take up the D-isomer of Met, which supports *Salmonella* growth. On the other hand, the Δ*metNIQ*Δ*metB* mutant displayed growth deficiency in M9 media containing D-Met at 100 µM, but showed restored growth when the concentration was increased to 700 µM, indicating that the low-affinity transporter MetP is in fact able to take up the D-isomer when D-Met, but the uptake of D-Met occurs less efficiently than L-Met.

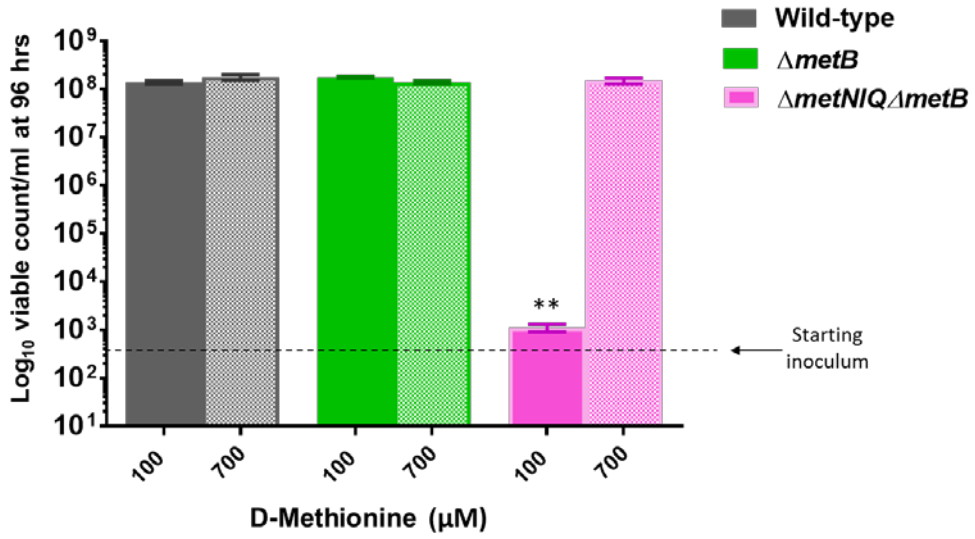

Figure 3-18: The low-affinity transporter inefficiently imports D-Met. The growth of Δ*metB* and Δ*metNIQ*Δ*metB* was monitored in M9 minimal media with D-Met for 96 hours. Viable count was determined at 96 hours. Statistics: Unpaired t-test. Error bars represent mean ± standard error of the mean. Data is pooled from two independent experiments. ** $p < 0.001$

3.2.16 Metabolite profiling in *S.* Typhimurium Met biosynthetic and high-affinity transporter mutants

To generate novel insights about the Met biosynthesis pathway in *S.* Typhimurium, the change in the intracellular concentration of the metabolites were examined through liquid-chromatography- mass spectrometry (LC-MS). A well-established method was used to extract, identify and quantify intracellular pool size of the intermediates of the Met biosynthesis pathway in *S.* Typhimurium wild-type SL1344 and mutants lacking either or both of the *de novo* biosynthesis pathway and the high-affinity transporter of Met. The intracellular level of the metabolites was compared between *S.* Typhimurium SL1344 mutants and the wild-type.

The conditions for growing the *S.* Typhimurium SL1344 mutants and the wild-type have been described in section 2.5.2 and 2.5.3.

The Δ*metB* mutant exhibited a significantly elevated pool of O-succinylhomoserine compared to the wild-type strain, consistent with the disruption of the conversion of O-succinylhomoserine to cystathionine via MetB enzyme and concomitant build-up of the enzyme's substrate (Figure 3-19A). Accumulation of O-succinylhomoserine was also observed in the Δ*metNIQ*Δ*metB* mutant but the levels were not significantly different compared to wild-type. Analysis of the mutant strains Δ*metE*, Δ*metH*, Δ*metNIQ* and Δ*metNIQ*Δ*metE*Δ*metH* failed to reveal any intracellular accumulation of this metabolite (Figure 3-19A).

The conversion of homocysteine to Met is mediated by two Met synthases: MetE and MetH. Disruption of MetE led to no noticeable change in any observable intermediates. In contrast, Δ*metH* and Δ*metNIQ*Δ*metE*Δ*metH* mutants carried an approximately 10-fold and a 15 to 30-fold increase of 5-methyltetrahydrofolate levels, respectively, compared with wild-type which were significantly different (Figure 3-19A). Significant accumulation of 5-methyltetrahydrofolate, a mediator of the methyl group transfer, suggested that the one-carbon cycle is perturbed in these strains.

The Δ*metB* mutant also had an increased S-adenosylmethionine (SAM) pool (up ~ 5.5-fold higher than wild-type). Intracellular accumulation of SAM was also found in Δ*metNIQ*Δ*metB* (up ~ 5-fold higher than wild-type). Both mutants had elevated SAM pool but for the Δ*metB* mutant it was significantly higher (p-value < 0.01) whereas for the Δ*metNIQ*Δ*metB* mutant this change was not statistically significant.

An untargeted mass/charge (m/z) feature analysis was performed to detect any unexpected metabolite changes due to each mutant (Figure 3-19B). Pair-wise comparisons were performed and a p-value of <0.05 (with multiple hypothesis testing corrected; Benjamini) was used to filter interesting m/z features. Several unexpected features were significantly elevated in the Δ*metB* mutant compared to the wild type (Figure 3-19B), including glycerate, adenine, hexose-6-phosphate, 3-phosphoglycerate and gluconate. The concentration of these metabolites significantly increased in the Δ*metB* mutant compared to the wild type. In comparison, Δ*metE* did not show any significantly different m/z features (Figure 3-19C); whereas only the m/z feature corresponding to 5-methyltetrahydrofolate was significantly different in the Δ*metH* mutant (Figure 3-19D).

Interestingly, several m/z features corresponding to peptidoglycan biosynthetic intermediates were significantly different for the Δ*metB* mutant, including UDP-N-acetyl-muraminate-alanine-glutamate (Figure 3-19B), suggesting an association between Met biosynthesis and peptidoglycan biosynthesis. Disruption of *metB* led to a decrease in intracellular concentrations of UDP-N-acetylmuraminate and a dramatic increase of UDP-N-acetylmuramoyl-L-alanine (12-fold), UDP-N-acetylmuramoyl-L-alanyl-D-glutamate (1400-fold) and UDP-N-acetyl-muramoyl-L-alanyl-D-γ-glutamyl-meso-2,6-diaminopimelate (4-fold) (Figure 3-19E). A decrease in UDP-N-acetylmuraminate and an increase in UDP-N-acetylmuramoyl-L-alanine (9-fold), UDP-N-acetylmuramoyl-L-alanyl-D-glutamate (1000-fold) and UDP-N-acetylmuramoyl-L-alanyl-D-γ-glutamyl-meso-2,6-diaminopimelate (5-fold) was also observed in the double mutant Δ*metNIQ*Δ*metB* (Figure 3-19E).

A.

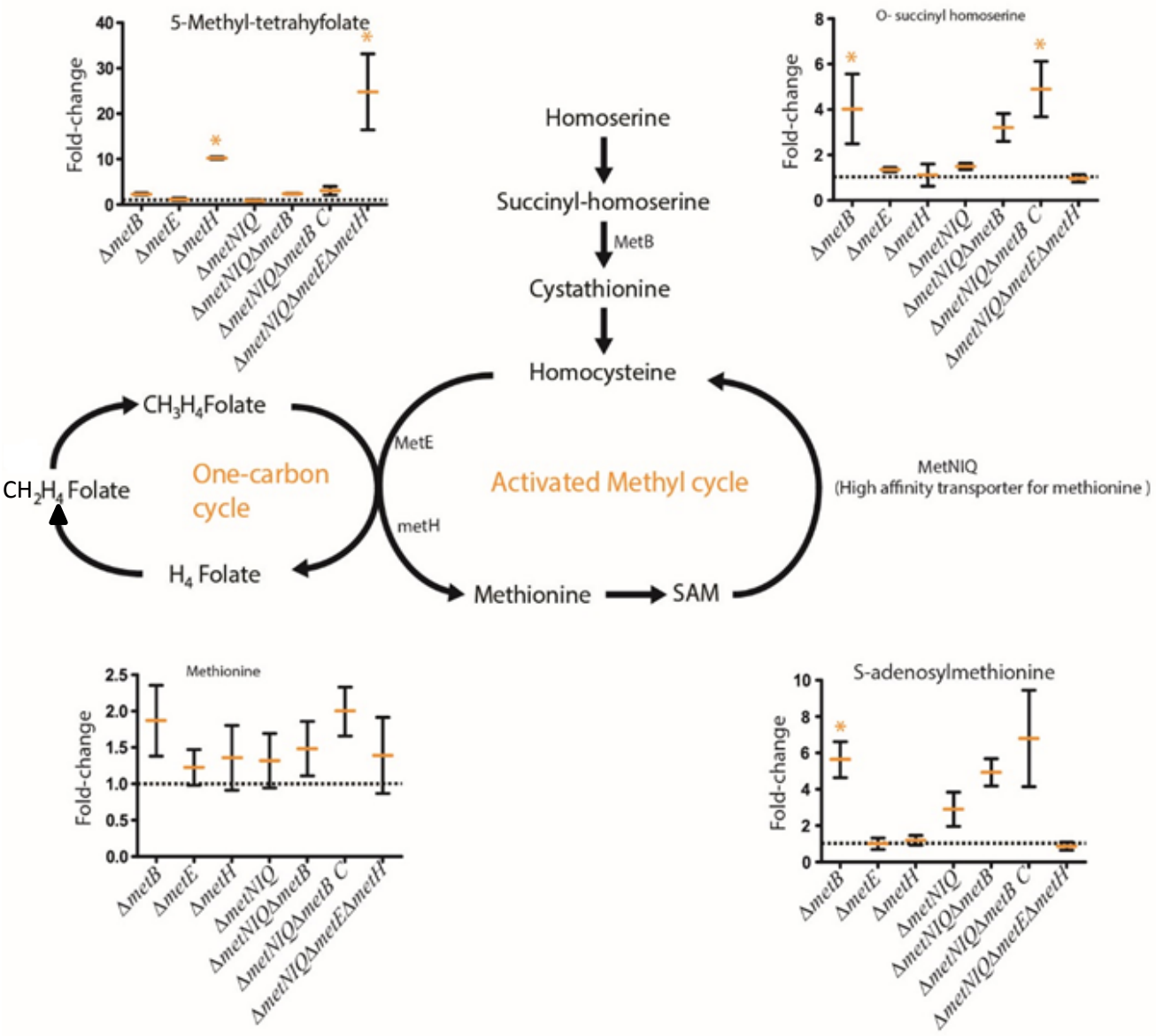

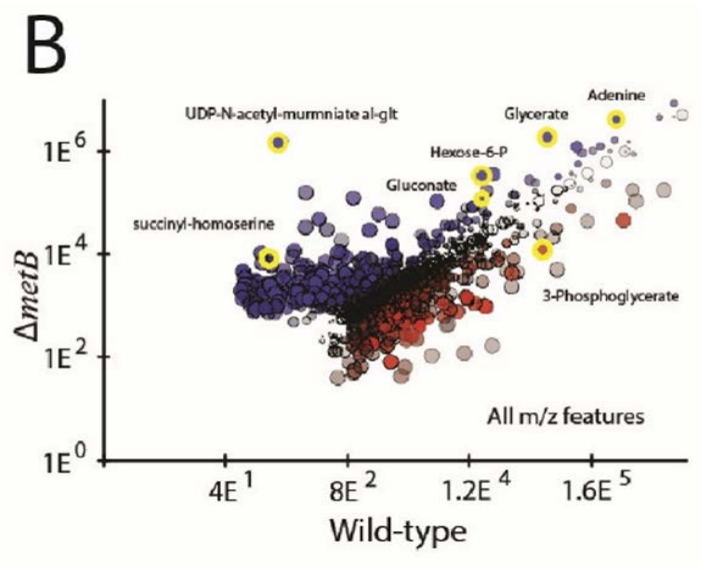
B
UDP-N-acetyl-murmniate al-glt
Glycerate
Adenine
Hexose-6-P
Gluconate
succinyl-homoserine
3-Phosphoglycerate
ΔmetB
All m/z features
Wild-type

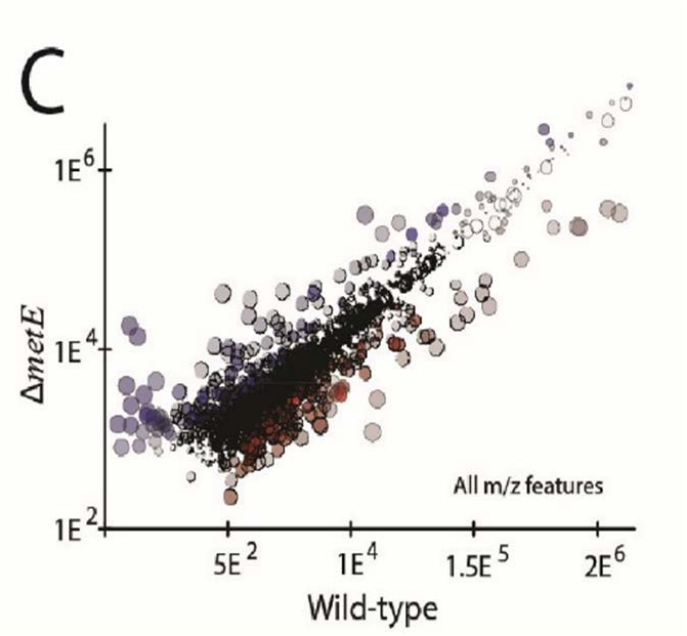
C
ΔmetE
All m/z features
Wild-type

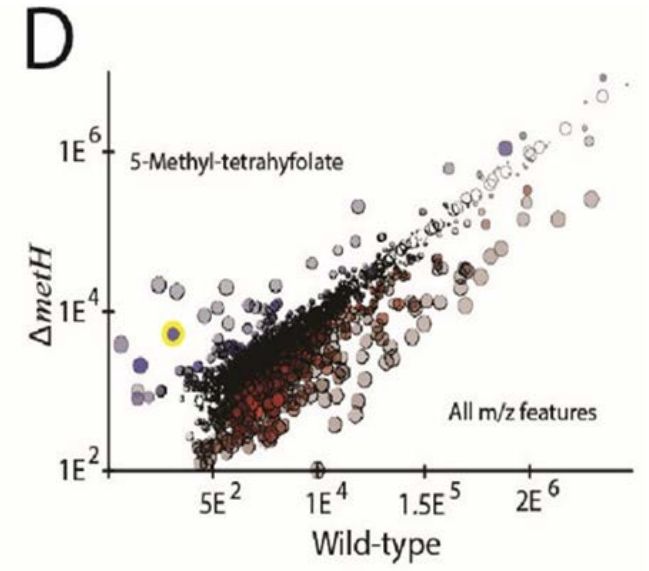
D
5-Methyl-tetrahyfolate
ΔmetH
All m/z features
Wild-type

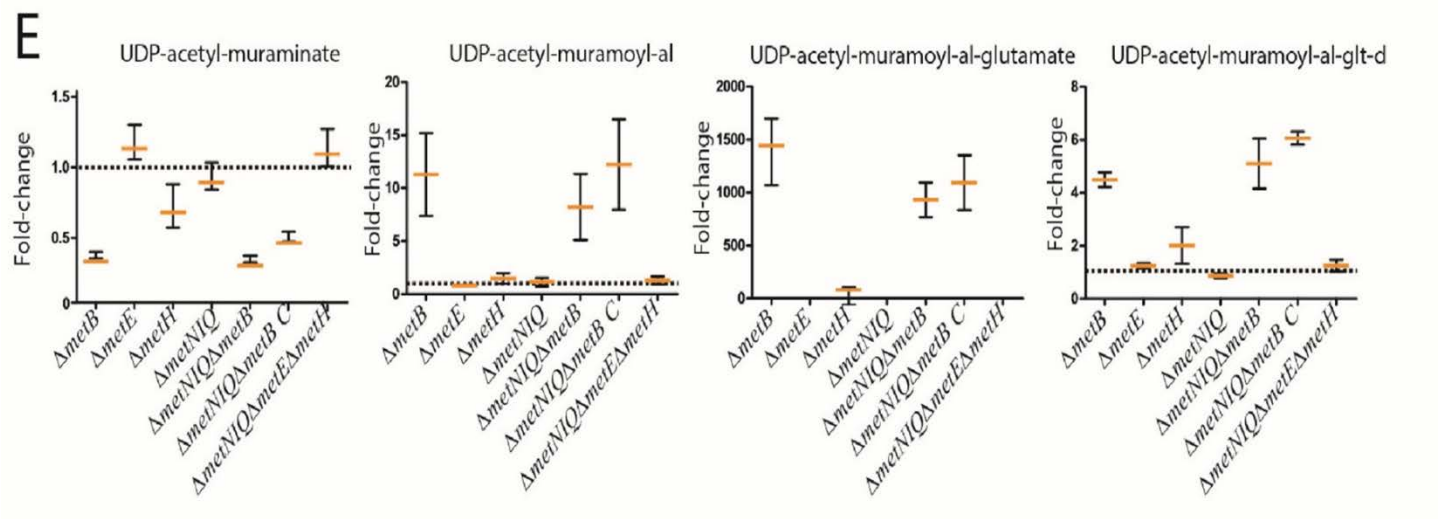

Figure 3-19: Metabolite perturbations following genetic disruption to Met biosynthesis, one-carbon cycle and activated methyl cycle. Total metabolite pools in each strain were detected and quantitated using an LC-QTOF (Liquid Chromatography-Quadrupole Time-of-flight)**.** (A) Intermediates of the Met biosynthetic pathway, activated methyl cycle and one-carbon cycle: O-succinylhomoserine, 5-methyl-tetrahydrofolate, Met and S-adenosylmethionine. Data are presented as the mean fold change of each mutant strain compared to the wild-type from three independent biological replicates (± SEM). * represents statistical significance as determined by a one-way ANOVA ($p < 0.01$), except for S-adenosylmethionine (SAM) which was not extracted via LC-MS (Liquid Chromatography-Mass Spectrometry). For this metabolite, statistical testing was performed in MAVEN using a $p < 0.05$ with Benjamini correction. (B-D) depicts the scatter plots of wild-type compared to Δ*metB*, Δ*metE*, and Δ*metH* respectively. Each dot represents a single extracted m/z feature with each axis depicting the arbitrary ion count. m/z features which are no different between conditions plot along the diagonal. The colour intensity indicates the confidence of the difference (greater intensity equates to lower variance across biological replicates). Yellow highlight indicates a subset of confirmed metabolites with a statistically significant difference in a pair-wise comparison ($p < 0.05$ with Benjamini correction. (E) The four metabolites associated with peptidoglycan synthesis- (Left to right) UDP-acetyl-muraminate, UDP-acetyl-muramoyl-alanine, UDP-acetyl-muramoyl-alanine-glutamate, UDP-acetyl-muramoyl-alanine-glutamate-diaminopimelic acid; Data are presented as the mean fold change of each knockout line compared to the wild-type line from three independent biological replicates (± SEM). * represents statistical significance as determined by a one-way ANOVA ($p < 0.01$).

3.3 Discussion:

Met metabolism and transport is an important part of the interconnected and interdependent amino acid metabolism of bacteria (269). In this study, we investigated the essentiality of Met biosynthesis and transport in *Salmonella* Typhimurium virulence.

De novo biosynthetic mutants Δ*metA*, Δ*metB*, Δ*metC*, Δ*metE*, Δ*metF* and Δ*metE*Δ*metH* grown under aerobic conditions required Met supplementation in M9 minimal media (Figure 3-5), as expected based on a previous report that a *S.* Typhimurium Δ*metC* mutant showed Met auxotrophy (266). *Salmonella* either synthesise vitamin B12 under anaerobic conditions or they derive it exogenously (383, 385, 472, 473). In this study, the Δ*metE* mutant, which retains the B12-dependent Met synthase, did not grow in M9 media under aerobic conditions (Figure 3-6). In contrast, Δ*metH* was able to grow in absence of Met in M9, through the use of MetE (Figure 3-6). The use of two Met synthases, expressed and active in different environments, is seen in most bacteria (490, 491). It was also depicted from the bioinformatics analysis (section 3.2.4) that *metE* and *metH* are highly conserved in *Salmonella* which may reflect an ecological strategy with which *Salmonella* are associated.

Met is present in all living cells including eukaryotic cells such as HeLa cells and *S.* Typhimurium can access this amino acid during intracellular proliferation, where it is provided in excess, e.g. in the tissue culture media. When the media is depleted of Met, lack of *de novo* synthesis within *S.* Typhimurium reduced the intracellular growth of the bacteria. *De novo* Met biosynthetic mutants Δ*metA*, Δ*metB*, Δ*metC*, Δ*metF* and Δ*metE*Δ*metH* were defective for intracellular replication when compared with wild-type in HeLa cells but the addition of Met in DMEM fully restored the growth of *met* mutants (Figure 3-8). Mutants Δ*metE* and Δ*metH* did not show any defect for intracellular survival and replication even under Met depleted conditions (Figure 3-8), suggesting that MetH could complement a Δ*metE* mutant through either the exogenous acquisition of vitamin B12 (from fetal calf serum which is a good source of vitamin B12 and supplemented in DMEM), or through anaerobic growth within the SCV and the production of vitamin B12.

Previous studies found that Met auxotrophs became defective for intracellular survival in macrophages and epithelial cells (209, 215). *Ejim et. al* showed that Met auxotrophy was linked with *S.* Typhimurium avirulence when a Δ*metC* mutant of *S.* Typhimurium LT2 was inoculated into mice. After 3 days, there was a 100-fold reduction in bacterial spleen and liver counts

(266). It was also observed that mice that were orally inoculated with wild-type *S.* Typhimurium died earlier than those infected with the *metC* mutant strain, suggesting that *metC* has a role in the virulence of *S.* Typhimurium in mice. Subsequently, a high throughput screen for inhibitors of *E. coli* MetC revealed several compounds that inhibited MetC function, but the *in vitro* or *in vivo* activity of these compounds was not reported (267). A *metC* mutation in *S.* Gallinarum, a poultry pathogen, was found to be attenuated in 1-day old chickens (268). Previously, it was shown that mutations in the regulation of Met metabolism, affecting MetR and MetJ, attenuated *Vibrio cholerae* in suckling mice and that MetR plays a role in colonisation of the mouse intestine (269). A recent study also concluded that a *S.* Typhimurium Δ*metE*Δ*metH* mutant was avirulent in mice and the Met transport system could not fully compensate for the lack of the biosynthesis system (492). These data supported a hypothesis that the enzymes in the Met biosynthesis pathway play an important role in *S.* Typhimurium virulence, and the systematic analysis of *in vitro* and *in vivo* "essentiality" of the genes involved in Met biosynthesis in *S.* Typhimurium, using the mouse as a model system, was conducted in this thesis.

Mice resistance or susceptibility to intracellular pathogens, such as *Salmonella* spp. and *Mycobacteria* spp., is largely conferred by an important macrophage/monocyte-expressed gene known as natural resistance associated protein-1 (*Nramp-1*) (493-495). C57BL/6 mice strains possess a sensitive allele of *Nramp-1* (496). Loss of the Met biosynthetic pathway did not affect the fitness of bacteria for *in vivo* replication in these mice, when compared with wild-type *S.* Typhimurium, and there was no loss of virulence after five-six days (following i.v. infection and oral infection) (Figure 3-9). This data conflicts with the above-mentioned reports (266, 492). The mouse assay used in this study was different from one of the above-mentioned studies (492). In the studies reported here, mice were infected with a single strain, whereas previous studies typically used competitive infections, where wild-type and mutant strains compete in the same infected animal. The latter assay may put more pressure on the performance of the mutant to grow in this competitive environment, and it is not uncommon to have divergent results from single infection and competitive infection (497, 498).

In *S.* Typhimurium, Met can be transported through a highly efficient high-affinity transporter MetNIQ and a cryptic low-affinity transporter/s named in the literature as MetP (485). A previous report found that high-affinity transporter mutant was attenuated in C3H/HeN female mice, which are more resistant to *S.* Typhimurium infection because they carry the resistant

allele named “Immunity to typhimurium” denoted as (*Ity*) *Ity*^{r}/*Nramp-1*. This allele controls mice resistance and susceptibility to *S.* Typhimurium (270, 489). Studies reported in this chapter show that *S*. Typhimurium *de novo* Met biosynthetic mutants were fully virulent in C57BL/6 mice suggesting that the pool of Met available in the animal was sufficient for normal growth; where the MetNIQ transporter was absent, *de novo* synthesis could satisfy the requirements for the amino acid. The high-affinity transporter mutant Δ*metNIQ* was equivalent, measured by *in vitro* and *in vivo* fitness, to wild-type *S.* Typhimurium in M9 minimal media, HeLa cells and mice (Figure 3-10, 3-11 and 3-12).

In section 3.2.6, it was shown that *de novo* Met biosynthesis is not required for *S*. Typhimurium virulence. The high-affinity transporter was also not essential for *in vivo* fitness (section 3.2.9). Studies were conducted to determine whether the putative and cryptic low-affinity Met transporter, MetP, could replace the requirements for *de novo* Met synthesis or acquisition through the high-affinity transporter. The sub-terminal and terminal steps of *de novo* Met biosynthesis is blocked in double Δ*metNIQ*Δ*metB* and triple mutants Δ*metNIQ*Δ*metE*Δ*metH*, respectively. These mutants were able to grow in M9 minimal media supplemented with L-Met which supports the presence of MetP (Figure 3-13 and 3-17). They showed a 3-log and a 4-log reduction of the bacterial load in spleen and liver following intravenous or oral infection, respectively (Figure 3-15). This suggests that the host-supply of Met, acquired through MetP, is insufficient to sustain the growth observed with the wild-type *S.* Typhimurium. Although the complemented strain Δ*metNIQ*Δ*metB* pACYC184 *metB* did not fully restore the growth to the level of the MetNIQ mutation alone, growth was significantly increased. The reduced growth and intracellular proliferation of Δ*metNIQ*Δ*metB* and Δ*metNIQ*Δ*metE*Δ*metH* during the survival in epithelial cells (when DMEM-No Met used) (Figure 3-14) also suggests that insufficient Met may be present to sustain maximal replication during the proliferation within the SCV itself. These results also demonstrated that the high-affinity transporter MetNIQ was not essential for growth of *S*. Typhimurium in animals provided *de novo* Met biosynthesis was intact and the growth of Δ*metNIQ*Δ*metB* and Δ*metNIQ*Δ*metE*Δ*metH* was reduced during the survival in HeLa cells (when DMEM-No Met used) (Figure 3-12 and Figure 3-14).

The differences in *in vivo* growth between the Δ*metNIQ*Δ*metE*Δ*metH* and Δ*metNIQ*Δ*metB* mutants suggest that the Met recycling through the activated methyl cycle, missing in the former mutant with Met synthase block, is required for full virulence (when high-affinity transporter is absent), even if Met is acquired extrinsically through low-affinity transporter/s.

The literature suggests that *S.* Typhimurium spp. have at least one low-affinity transporter which is cryptic and can provide the pathogen with Met when the high-affinity transporter is absent (264). In this chapter, it was shown that the presence of L-Met *in vitro* could fully restore the growth of Δ*metNIQ*Δ*metB* and triple mutant Δ*metNIQ*Δ*metE*Δ*metH* where the bacteria are dependent on the low-affinity transporter for Met acquisition (Figure 3-13). This data confirms the existence of at least one low-affinity Met transporter. But this transporter is not as efficient as high-affinity transporter because it could not fully compensate the bacterial virulence *in vitro* and in the murine host when *de novo* biosynthesis and high-affinity transporter were both absent.

S. Typhimurium has two Met synthases, MetE and MetH, which can catalyse the last step in Met biosynthesis. They are differentially functional – MetH is vitamin B12-dependent whereas MetE is not. When vitamin B12 is not present MetH is not functional (383, 385, 472, 473). The presence of vitamin B12 represses constitutive *metE* expression by forming a B12-MetH-Holoenzyme, which represses transcription of *metE* (460, 467, 499). There is also a previous report demonstrating that B12-MetH-Holoenzyme produces sufficient Met and diminishing the level of homocysteine which is an activator of *metE* gene in *S.* Typhimurium (500). *Salmonella* spp. can either synthesise vitamin B12 under anaerobic condition or obtain the vitamin exogenously (385).

Previous global analysis of the metabolism of *S.* Typhimurium highlighted the redundancy in the key metabolic pathway (185); MetE and MetH are examples of this redundancy. The single Δ*metE* and Δ*metH* mutants grew at wild-type rates in HeLa cells and mice, though, depending on the growth conditions, replication in minimal media in the absence of added Met revealed differences that were very likely attributable to the production of vitamin B12 since the growth differences in the single mutants in M9 were abrogated when vitamin B12 was added. In HeLa cells, neither of the mutants were growth attenuated. In mice, both mutants (ie. Δ*metE* and Δ*metH*) grew at levels equivalent to the wild-type suggesting that the growth attenuation seen in Δ*metE* in the absence of added vitamin B12 in M9, was not mirrored in mice (Figure 3-9). This suggests that either B12 levels were sufficient or the conditions necessary for more optimal *metH* expression within Δ*metE* were found *in vivo* – anaerobiosis and/or the presence of B12, like wild-type. For further confirmation, the high-affinity transporter mutant was combined with either of the Met synthases individually, ie. Δ*metNIQ*Δ*metE* and Δ*metNIQ*Δ*metH* were generated. Neither of these mutants showed any attenuation in mice

which again supports the hypothesis that the two Met synthases are functionally redundant in C56BL/6 mice (Figure 3-16).

To generate novel insights about the Met biosynthesis pathway in *S.* Typhimurium, the change in the intracellular concentration of the metabolites (when some key steps are inactivated the pathway) was examined (Figure 3-19). This analysis allowed us to revalidate the proposed model of Met biosynthesis pathway. A validated mass spectrometry method was used to identify and quantify the intracellular intermediates of the pathway of the *S.* Typhimurium SL1344 Met biosynthetic mutants Δ*metB*, Δ*metE*, Δ*metH;* a high-affinity transporter mutant Δ*metNIQ* and mutants lacking both Met *de novo* biosynthesis and the high-affinity transporter Δ*metNIQ*Δ*metB*. The data obtained from the untargeted m/z feature analysis of *S.* Typhimurium SL1344 Δ*metB* to wild type led to many putative metabolite identifications. Some of them were across disparate metabolic pathways, making it unclear how disruption to a single enzyme in Met biosynthesis could be causing such widespread perturbations. This analysis revealed that, surprisingly, the intracellular concentration of several metabolites such as UDP-acetyl-muramoyl-alanine, UDP-N-acetylmuramoyl-L-alanyl-D-glutamate and UDP-N-acetylmuramoyl-L-alanyl-D-γ-glutamyl-meso-2,6-diaminopimelate, linked with peptidoglycan synthesis, were profoundly increased in the Δ*metB* and Δ*metNIQ*Δ*metB* mutants (Figure 3-19E).

In *E. coli* (representative of the *Enterobacteriaceae* family), the glycan backbone of peptidoglycan consists of alternating molecules of N-acetylglucosamine and N-acetylmuramic acid and that are linked by a beta 1,4-glycoside bond. N-acetylmuramic acid have an attached tetrapeptide of L-alanine, D-glutamate, diaminopimelic acid (DAP) and D-alanine. The tetrapeptide chains that stretch out from the backbone, can be connected by an interpeptide bridge between a free amino group on DAP and a free carboxyl group on a nearby D-Alanine (in Gram-positive bacteria, this corresponds to pentaglycine bridge) (501). Because Met biosynthesis and meso-diaminopimelic acid biosynthesis are interconnected and linked with aspartate (502, 503), the perturbation of the intracellular metabolite pool related to Met biosynthesis could also impact peptidoglycan synthesis. The alteration in the peptidoglycan-related metabolites could have some implications on the antibiotic sensitivity and resistance, and therefore, the Δ*metB* is subjected for future study to determine any alteration in antibiotic sensitivity and resistance phenotype.

O-succinylhomoserine condenses with cysteine to form cystathionine in a reaction catalysed by MetB. Disruption of *metB* leads to the observed increased intracellular concentration of the glycolytic intermediates e.g. hexose-6-phosphate, gluconate and 3-phosphoglycerate (3-PG). Presumably, disturbance of the TCA cycle might occur when serine is accumulated - serine is synthesised from 3-PG by a pathway of reversible reactions. Because serine can be directly converted: (1) to pyruvate and from there can enter the TCA cycle or be metabolised through pyruvate metabolism; and or (2) to glycine and can enter one-carbon cycle; and/or (3) to O-phosphatidyl-serine and can enter glycerophospholipid metabolism pathways; (4) to 3-PG hydroxyl-pyruvate (on its way to 3-PG), and can enter glyoxylate metabolism (504).

The intracellular pool size of S-adenosylmethionine (SAM) is significantly higher in Δ*metB* compared to wild-type, indicating that Δ*metB* may be unable to metabolize SAM efficiently. However, Δ*metE* and Δ*metH* mutants did not show any significant change in intracellular concentration of SAM. This observation may reflect that in the Δ*metB* mutant, homocysteine (which will be eventually converted into SAM) cannot be derived through the *de novo* biosynthesis and fed into the activated methyl cycle. Moreover, accumulation of homocysteine is toxic for the bacterial cell (505, 506). In this scenario, there is a reduced need for the provision of homocysteine through the activated methyl cycle, leading a build-up of SAM. In Δ*metE* and Δ*metH* mutants, *de novo* homocysteine biosynthesis is fully functional and homocysteine feeds into the activated methyl cycle. As a result, there is a requirement for continuous running of the activated methyl cycle to prevent intracellular homocysteine accumulation which, in turn, would inhibit SAM accumulation. The Δ*metB* mutant showed a statistically significant (5.5-fold) increase in intracellular SAM concentration. The Δ*metNIQ*Δ*metB* double mutant showed a 5-fold increase, albeit this difference was not statistically significant. The lack of statistical significance may reflect the variation observed in the biological replicates and suggests that the experiments were underpowered to extract all the biologically-relevant differences. In the Δ*metNIQ*Δ*metE*Δ*metH* triple mutant, Met can only be transported from the growth medium into the cell through the putative low-affinity transporter. The loss of the activated methyl cycle in Δ*metNIQ*Δ*metE*Δ*metH* possibly could account for the observed increased intracellular pool of SAM.

The deletion of vitamin B12-dependent Met synthase MetH either in Δ*metH* or in Δ*metNIQ*Δ*metE*Δ*metH* leads to a profound difference in 5-methyltetrahydrofolate level, a metabolite in the one carbon cycle (Figure 3-19). As can be expected, in the Δ*metH* mutant

the deletion of MetH (in presence of the vitamin B12-independent MetE) leads to a 10-fold higher intracellular concentration of the substrate (5-methyltetrahydrofolate), because MetE is much less efficient than MetH (473, 507). The Δ*metNIQ*Δ*metE*Δ*metH* mutant (i.e. deficient in both Met synthases) is unable to metabolize 5-methyltetrahydrofolate because of the loss of the activated methyl cycle and hence shows 25-fold higher pool size than the wild-type for this metabolite.

The data obtained from the mass spectrometry analysis with the complemented mutant Δ*metNIQ*Δ*metB* (denoted as Δ*metNIQ*Δ*metB* C in the Figure 3-19A and 3-19E) carrying pACYC184 *metB* did not completely restore the metabolite levels as seen in the Δ*metNIQ* mutant. However, this is not unusual since genetic complementation using a plasmid will differ from the native level due to plasmid copy number; this might therefore account for the partially complemented phenomena that is observed.

3.4 Summary of findings

The research described in this chapter has significantly contributed to the knowledge of *S. enterica* Met metabolism within the mammalian host. Previous studies had shown a relationship between Met biosynthesis and *S. enterica* virulence in host. The findings from this comprehensive analysis would suggest that *de novo* Met biosynthesis is unlikely to represent high value targets for antibiotic development. Met acquisition *in vivo* was observed in mutants unable to synthesise Met. The putative cryptic low-affinity transporter termed MetP cannot fully compensate when *de novo* biosynthesis and high-affinity Met transport both are absent. Lastly, the individual Met synthases, MetE and MetH, are functionally redundant during *S.* Typhimurium growth in murine host.

Chapter 4

Exploring the importance of the activated methyl cycle and an incomplete methionine salvage pathway in *Salmonella* Typhimurium

4.1 Introduction

The prevalence of antibiotic resistance of *Salmonella* Typhimurium has, like many other pathogens, increased, highlighting the need for new antimicrobial drug targets (17, 182, 185, 508-511). The metabolic differences between prokaryotes and eukaryotes can be exploited to provide novel drug targets. The activated methyl cycle is the central metabolic pathway, responsible for providing the methyl donor for the methylation of cellular components, and for the recycling of methionine (Met) (232, 233). S-adenosylmethionine (SAM) is an essential component in the activated methyl cycle and is synthesised from Met (232, 285). The methyl group of Met is activated by ATP to form SAM, and this reaction is catalysed by the enzyme SAM synthetase (MetK) (512) (Figure 4-1). SAM is essential to the bacterial cell; as the enteric bacteria such as *E. coli* and *S.* Typhimurium have no transporter for SAM, non-functional mutation or deletion of SAM synthetase (MetK) is lethal (293-296). Within the methyl cycle, the methyl group is transferred from SAM to form S-adenosylhomocysteine (SAH), which is then immediately converted to homocysteine and is finally recycled to Met to complete the methyl cycle (Figure 4-1). SAM is the predominant methyl donor in the cell and is responsible for methylation of a variety of macromolecules including DNA, RNA, proteins, hormones, lipids and metabolites by a variety of SAM-dependent methyltransferases (232, 285, 286) (Figure 4-1).

In *S.* Typhimurium and *E. coli*, the conversion of SAH to homocysteine is a two-step process. SAH is converted to S-ribosylhomocysteine (SRH) and then from SRH to homocysteine by MTA/SAH nucleosidase (Pfs) and S-ribosylhomocysteine lyase (LuxS), respectively. During the conversion of SRH to homocysteine, autoinducer-2 (AI-2) is produced which is an integral component of quorum-sensing. AI-2 purportedly functions in intraspecies and interspecies communication, which is driven by cell density and the metabolic potential of the environment (339, 340). In eukaryotes and some bacteria, SAH is converted to homocysteine through a one-step process by S-adenosylhomocysteine hydrolase (SahH) (232, 303).

Besides methylation, SAM also participates in other reactions; most importantly, it provides a critical activated methyl group donor for the synthesis of polyamines, predominantly spermidine and spermine (232, 288). Spermidine synthesis proceeds with the decarboxylation of SAM and is catalysed by SAM decarboxylase (SpeD). Decaroboxylated SAM donates an aminopropyl group to putrescine to produce spermidine and 5'-methylthioadenosine (MTA), and this reaction is catalysed by spermidine synthase (SpeE). MTA is further converted to

methylthioribose (MTR) by Pfs (Figure 4-1). *E. coli* and *Salmonella* excrete the MTR from the cell (234-236, 431, 432) and do not possess any functional Met salvage system due to the lack of a kinase; hence MTR is thought to be the dead-end of an incomplete salvage pathway in *E. coli* and *Salmonella* (234-236, 431, 432).

MTA/SAH nucleosidase is encoded by *pfs*, which is present in many bacteria including *E. coli* and *Salmonella.* Pfs catalyses the conversion of SAH to SRH to quickly remove it from the cell. Pfs also catalyses the hydrolysis of 5'-methylthioadenosine (MTA) to 5'-methylthioribose (MTR) and adenine (313, 322, 513). Previous studies have shown that the deletion of Pfs causes a growth defect in *E. coli* (312, 417) and *E. coli* Δ*pfs* was shown to phenocopy a biotin synthase (*bioB* gene product) mutant (312, 417). BioB is a member of SAM-dependent enzymes, and uses SAM as an oxidizing agent to accomplish sulphur insertion. BioB inserts sulphur into dethiobiotin to produce biotin and a highly reactive by-product 5'-deoxyadenosine (5'-DOA) (Figure 4-2). 5'-DOA is a potent inhibitor of BioB function, and accumulated 5'-DOA levels inhibit biotin synthesis (514). Deletion mutants of *pfs* are unable to perform adenine salvage from 5'-DOA, which is otherwise used as a substrate to form adenine and 5'-deoxyribose. Therefore, the lack of Pfs leads to accumulation of 5'-DOA which inhibits BioB function, and biotin supplementation can restore the normal growth of a *E. coli* Δ*pfs* strain (312, 417).

Based on previous studies, the hypothesis is that the activated methyl cycle and the incomplete Met salvage pathway, which are also involved in Met and SAM recycling and utilisation, are essential for *Salmonella* virulence *in vivo* and may be exploited as a novel antibiotic target. *Salmonella* mutants with defined mutation in every enzyme of these pathways were generated, phenotypically validated using defined growth media, tested for their ability to grow intracellularly *in vitro,* and to cause systemic disease in the murine host.

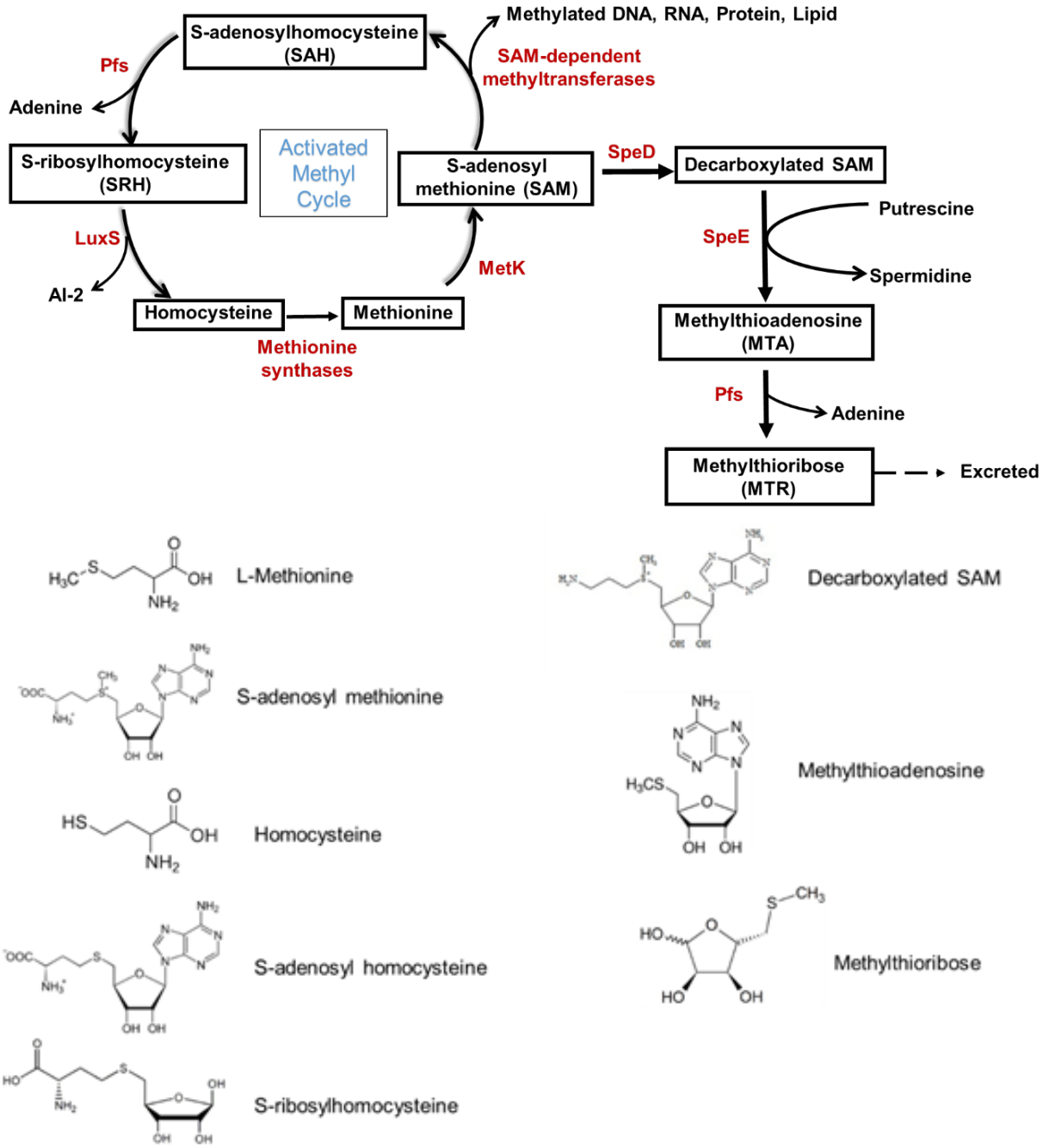

Figure 4-1: Proposed activated methyl cycle and incomplete Met salvage pathway in *S.* Typhimurium. Boxes represent metabolites and arrows represent the direction of enzymatic reactions. MetK, S-adenosylmethionine synthetase; Pfs, S-adenosylhomocysteine/methylthioadenosine nucleosidase; LuxS, S-ribosylhomocytseine lyase; SpeD, S-adenosylmethionine decarboxylase; SpeE, Spermidine synthase.

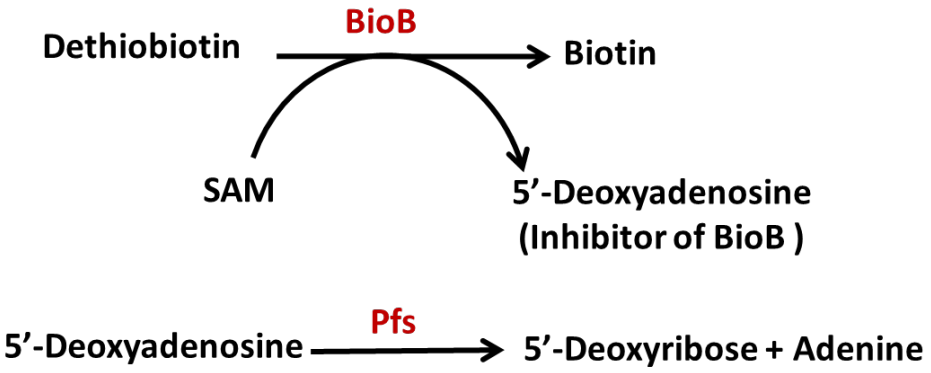

Figure 4-2: Proposed relationship between biotin synthesis and Pfs in *S.* Typhimurium. BioB, biotin synthase; Pfs, S-adenosylhomocysteine/Methylthioadenosine nucleosidase; SAM, S-adenosylmethionine; BioB uses SAM and inserts sulphur into dethiobiotin to produce biotin and a highly reactive component 5'-deoxyadenosine (5'-dADO). 5'-dADO is a potent inhibitor of BioB enzyme and is converted to 5'-deoxyribose and adenine by Pfs. The deletion of Pfs leads to accumulation of 5'-dADO.

4.2 Results

4.2.1 Construction and confirmation of *S.* Typhimurium mutants

"Gene gorging" (described in section 2.9) was used to remove defined chromosomal sequences to construct Δ*speD*, Δ*speE*, Δ*luxS*, Δ*bioB* and Δ*pfs* in *S.* Typhimurium SL1344. The *speD* and *speE* are in an operon, and the *pfs* is the first gene in a three-gene operon which consists of *pfs*, *btuf* and *yadS*. The remaining sequences were single cistrons located at different sites around the chromosome (based on genome data from *E. coli* substrain MG1655 and *S.* Typhimurium LT2 available in www.biocyc.org). The target sequence to be deleted is replaced with Kan^R cassette by homologous recombination. To limit the impact of the deletions on downstream genes, at least ~50 bp at the 3' ends of the gene to be deleted including the stop codons, was left intact. Gene deletions were validated by PCR using primers that bind to flanking regions of the deletion site. The Kan^R mutants were selcted by antibiotic selection and were confirmed by a colony PCR (described in section 2.9.6).

The targeted deleted region of the mutants Δ*speD*, Δ*speE*, Δ*luxS*, Δ*bioB* and Δ*pfs* is shown in Figure 4-3. The Kan^R cassette was excised from all mutants (except Δ*pfs*). The resistance cassette was removed to reduce possible polar effect of the Kan^R cassette on downstream genes. Plasmid pCP20 mediated the excision of the cassette. Kan^R mutants were transformed with pCP20, which carries a temperature-sensitive plasmid replicon and encodes *flp* (FLP recombinase) under the control of an inducible promoter. The recombination event excises the

Kan^R cassette, leaving an 80 nt 'scar' sequence (section 2.9.5). The resulting Kan-sensitive mutants were confirmed by colony PCR using Chk-F primer and a downstream chromosome-annealing primer termed Chk-R (shown in Figure 4-4). The Chk-F and Chk-R primers are listed in Table 2-5. The Kan-excised mutants showed a smaller PCR product (size: 1.2-1.5 kb) than the wild-type SL1344 strain due to deletion created through the Kan^R cassette removal. For Δ*pfs* which contained the Kan^R cassette, the confirmatory PCR was done using the same primers, and the resulting product size was bigger with the Kan^R Δ*pfs* mutant than the wild-type because the Kan^R cassette which replaced the sequence of *pfs* gene, was retained (shown in Figure 4-4). The product size along with the description of the mutant strains are listed in the Table 4-1.

Table 4-1. The PCR product sizes (using Chk-F and Chk-R primers) with the respective mutant strains (Figure 4-4)

Strain	Description	Product size
Δ*speD*	*speD* (Kan^R cassette excised)	1,484 bp (Figure 4-4A)
Δ*speE*	*speE* (Kan^R cassette excised)	1,479 bp (Figure 4-4A)
Δ*luxS*	*luxS* (Kan^R cassette excised)	1,627 bp (Figure 4-4A)
Δ*bioB*	*bioB* (Kan^R cassette excised)	1,674 bp (Figure 4-4A)
Δ*pfs*	*pfs::kan* (Kan resistant)	2,974 bp (Figure 4-4A)

A)

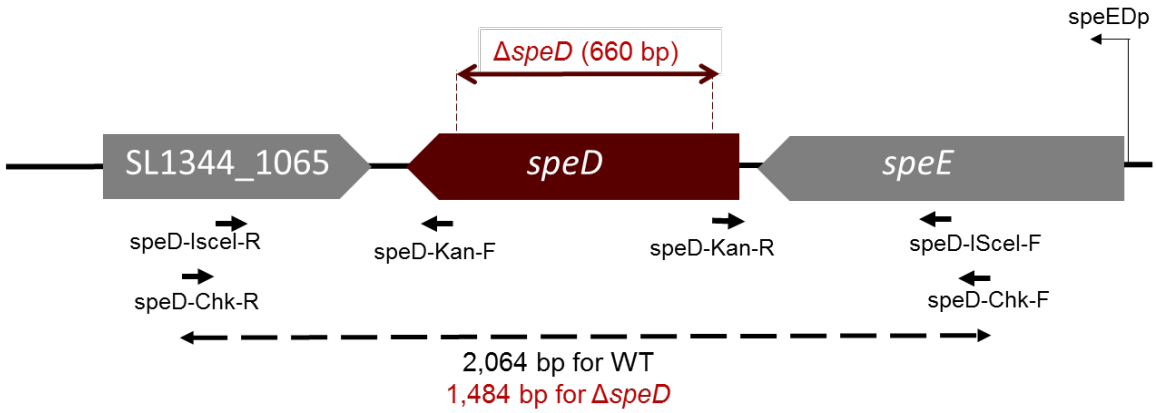
speEDp
ΔspeD (660 bp)
SL1344_1065
speD
speE
speD-IsceI-R
speD-Kan-F
speD-Kan-R
speD-ISceI-F
speD-Chk-R
speD-Chk-F
2,064 bp for WT
1,484 bp for ΔspeD

B)

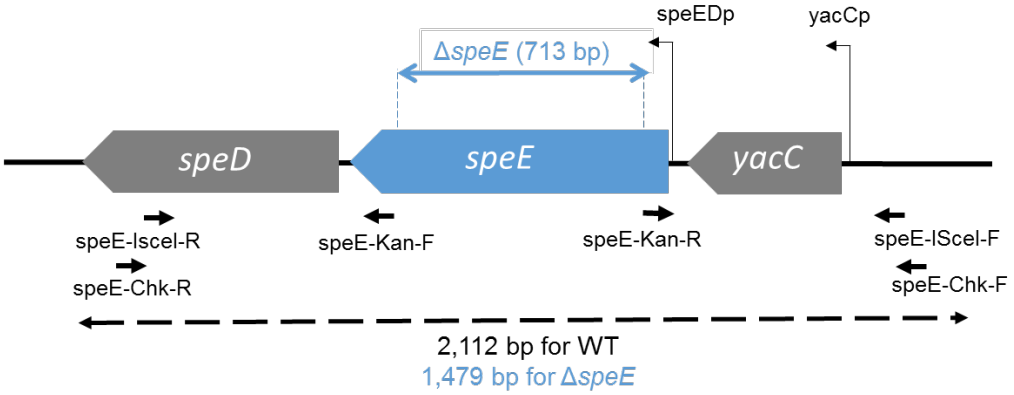
speEDp
yacCp
ΔspeE (713 bp)
speD
speE
yacC
speE-IsceI-R
speE-Kan-F
speE-Kan-R
speE-ISceI-F
speE-Chk-R
speE-Chk-F
2,112 bp for WT
1,479 bp for ΔspeE

C)

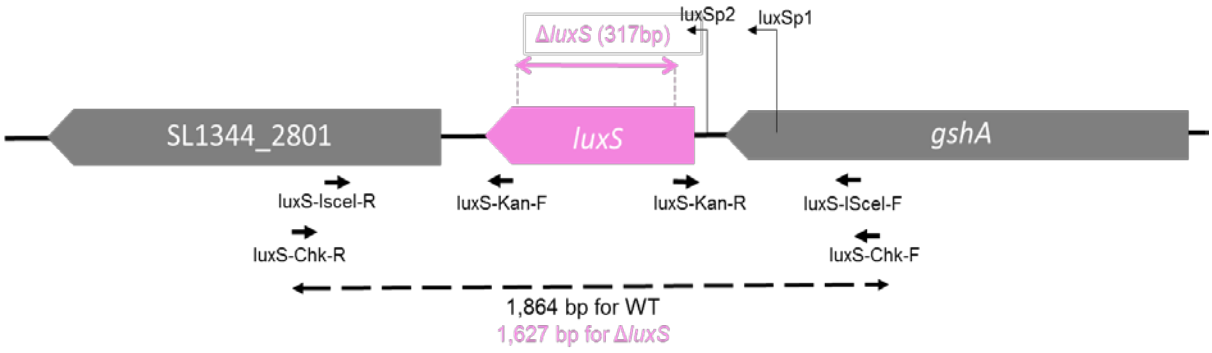
luxSp2
luxSp1
ΔluxS (317bp)
SL1344_2801
luxS
gshA
luxS-IsceI-R
luxS-Kan-F
luxS-Kan-R
luxS-ISceI-F
luxS-Chk-R
luxS-Chk-F
1,864 bp for WT
1,627 bp for ΔluxS

D)

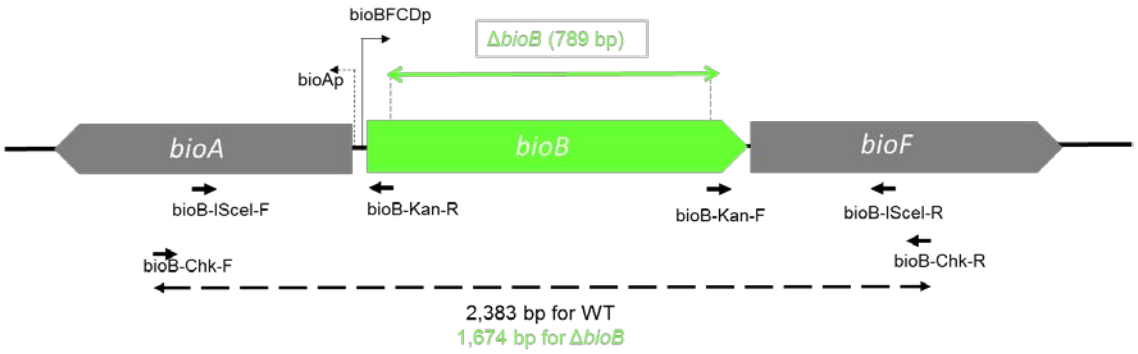

E)

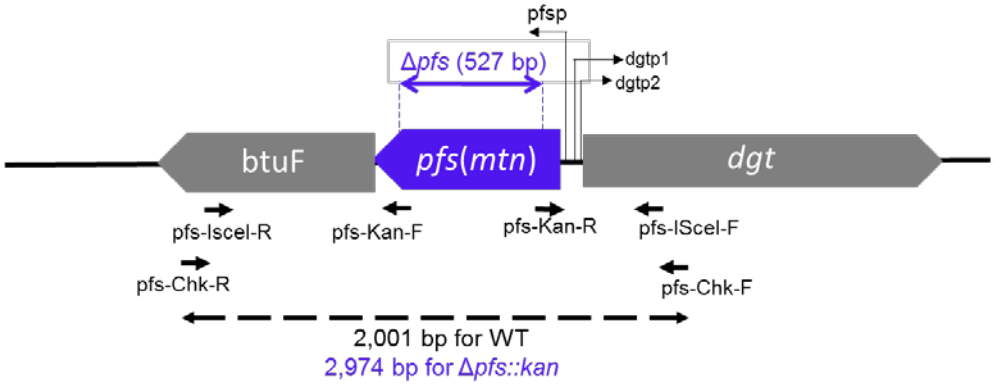

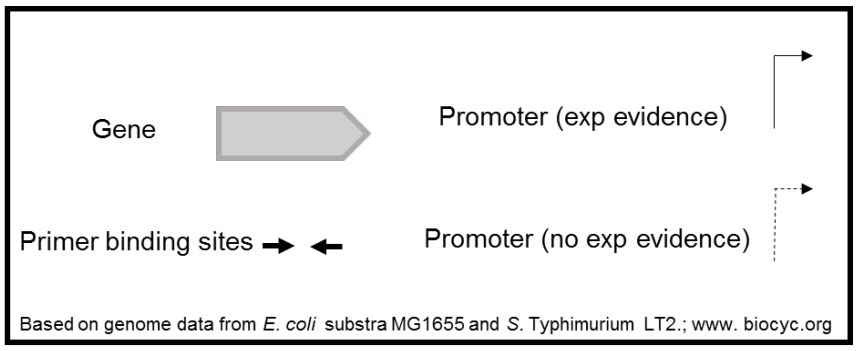

Figure 4-3: Schematic representation of the targeted deletions in *speD*, *speE*, *luxS*, *bioB* and *pfs* gene loci of *S*. Typhimurium SL1344 using gene gorging. The target gene *speD* (**A**), *speE* (**B**), *luxS* (**C**), *bioB* (**D**) and *pfs* (**E**) is represented in the 5' to 3' orientation by the arrowed corresponding coloured box. Angled line arrow indicates the position of promoter regions (based on experimental and non-experimental evidence from the database of *E. coli* substrain MG1655 and *S.* Typhimurium LT2 available in www.biocyc.org**)** for the targeted genes. The sites of flanking genes are shown as grey arrow boxes. The region of chromosomal DNA deleted in the mutant is represented between the dashed coloured lines, the boundaries of which were defined by the binding sites of Kan-R and Kan-F primers, indicated as short black arrows. Chk-F and Chk-R primers were designed to be ~100 bp upstream and downstream of the region that underwent homologous recombination and the size of the PCR product was used to confirm gene deletion, as shown in Figure 4-4.

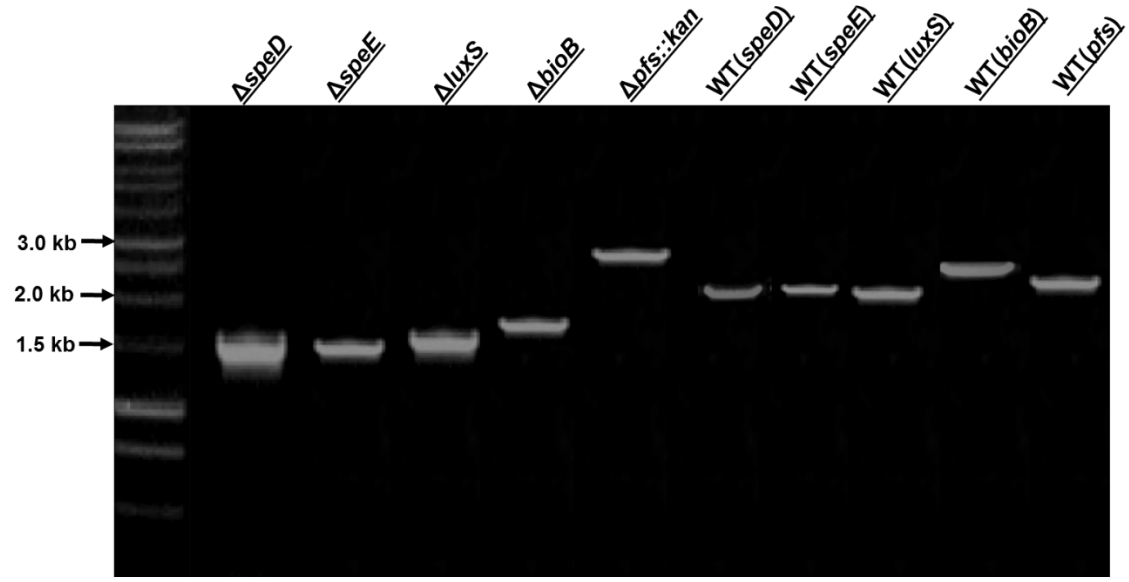

Figure 4-4: Confirmation of site-targeted deletion of *speD, speE, luxS, bioB* and *pfs* in *S.* Typhimurium SL1344. The PCR products (using Chk-F and Chk-R primers and corresponding sizes are mentioned in table 4-1) which confirmed the target gene deletion in the mutants Δ*speD* (**4-3A**), Δ*speE* **(4-3B**), Δ*luxS* (**4-3C**), Δ*bioB* (**4-3D**) and Δ*pfs::kan* (**4-3E**). The ladder used: BenchTop 1 kb DNA Ladder (Promega).

4.2.2 *S.* Typhimurium Δ*speD*, Δ*speE* and Δ*luxS* mutants do not show defective growth in M9 minimal media

The metabolic phenotype of *S.* Typhimurium Δ*speD*, Δ*speE* and Δ*luxS* mutants was verified by assessing their capacity to grow in M9 minimal media in comparison with the wild-type *Salmonella*. The Δ*speD*, Δ*speE* and Δ*luxS* mutants were able to grow in M9 minimal media without requiring additional supplement, and the growth over time was indistinguishable from that of the wild-type, as all four strains demonstrated similar growth kinetics, reached exponential phase growth at a similar time, and achieved similar maximal viable counts at stationary phase (Figure 4-5).

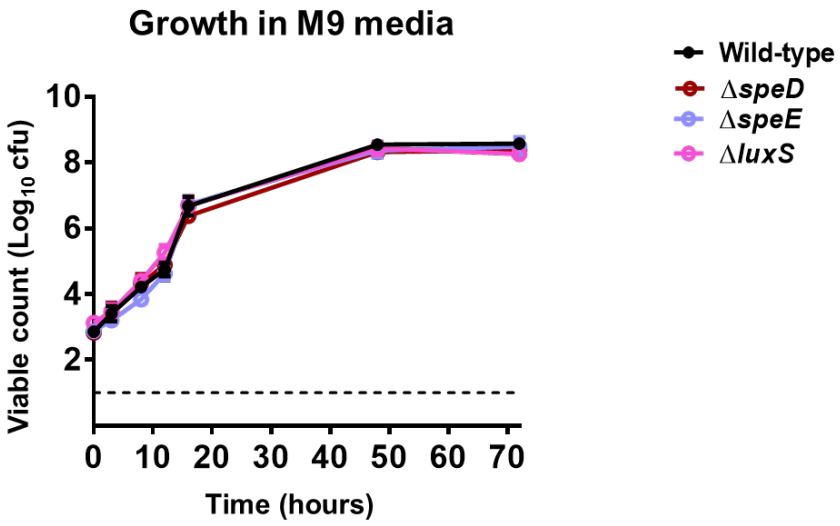

Figure 4-5: *S*. Typhimurium Δ*speD*, Δ*speE* and Δ*luxS* mutants can grow in M9 minimal media. Δ*speD*, Δ*speE* and Δ*luxS* were grown in M9 minimal media, at 37ºC shaking, and compared to wild-type. The viable bacterial count was determined at 3, 8, 12, 16, 48 and 72 hours in M9 minimal media. Error bar represents mean ± standard error of the mean. Data is pooled from three independent experiments. The broken line denotes the limit of detection of the viable count.

4.2.3 *S*. Typhimurium Δ*speD*, Δ*speE* and Δ*luxS* mutants are not attenuated for intracellular growth

Intracellular growth is strongly correlated with virulence in the development of systemic salmonellosis in the murine host (209). A variety of cells of the reticuloendothelial system, such as the spleen and liver, provides *Salmonella* with an intracellular growth niche (108, 134, 515). The intracellular replication and survival of *S*. Typhimurium Δ*speD*, Δ*speE* and Δ*luxS* mutants was assessed in HeLa cells and intracellular bacteria number was quantified as an indication of bacterial growth over a 10-hour period. After 1 hour of initial infection, non-adherent bacteria were removed by washing with PBS and gentamicin was added to kill extracellular bacteria. Intracellular survival and multiplication was determined by enumerating intracellular bacteria at 2, 5 and 10 hours post-infection. The three mutant strains (Δ*speD*, Δ*speE* and Δ*luxS*) grew at similar rates to the wild-type (Figure 4-6).

The data suggests that the spermidine decarboxylase (SpeD) and spermidine synthase (SpeE), responsible for polyamine, particularly spermidine, synthesis (288, 391, 415), are not required for *Salmonella* to replicate in mammalian cells. Similarly, the Δ*luxS* mutant did not show any detectable growth defect, when compared with wild-type. These data indicate that S-ribosylhomocysteine lyase (LuxS) is not essential for intracellular growth and survival of *S*. Typhimurium in HeLa cells.

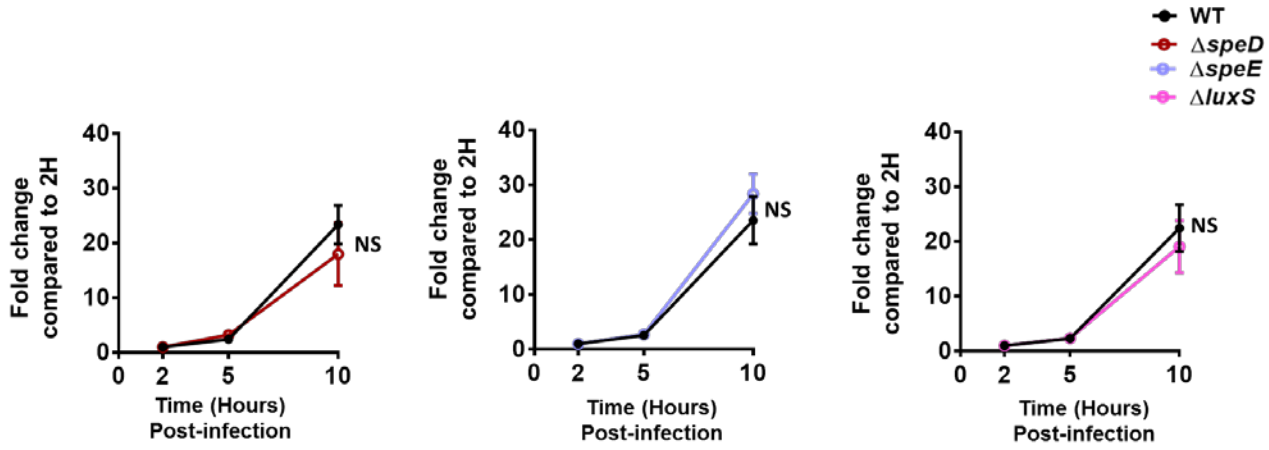

Figure 4-6: *S.* Typhimurium Δ*speD*, Δ*speE* and Δ*luxS* mutants are not attenuated for intracellular growth in HeLa cells. HeLa cells were infected with exponential LB cultures of the indicated strains of *S.* Typhimurium for 1 hour at 37ºC (MOI: 5-10). At this point, non-adherent bacteria were removed and gentamicin was added to kill extracellular bacteria. To determine the intracellular survival and replication, intracellular bacteria were enumerated at 2, 5 and 10 hours post-infection. The cell culture media used for this experiment was DMEM-Complete. 2H on the Y-axis means 2 hours; The experiment was performed at least three times independently and the data are pooled from the three experiments. Error bars represent mean ± standard error of the mean. Statistical differences were analysed at 10 hours by unpaired T-test. NS Not Significant $p > 0.05$.

4.2.4 *S.* Typhimurium Δ*speD*, Δ*speE* and Δ*luxS* are virulent in mice

The role of SpeD, SpeE and LuxS enzymes in the virulence of *S.* Typhimurium was examined by testing the growth of each of the mutants in C57BL/6 mice. Mice were infected with 200 cfu intravenously, and at day 5 post-infection mice were culled and the bacterial load in the spleen and liver was determined as viable counts. There was no significant difference in the number of bacteria recovered from the spleen and liver of mice infected with Δ*speD*, Δ*speE* and Δ*luxS* when compared with the bacterial burden found in the organs of mice infected with wild-type. This result indicates that the enzymes SpeD, SpeE and LuxS are not essential for growth of *S.* Typhimurium in C57BL/6 mice (Figure 4-7).

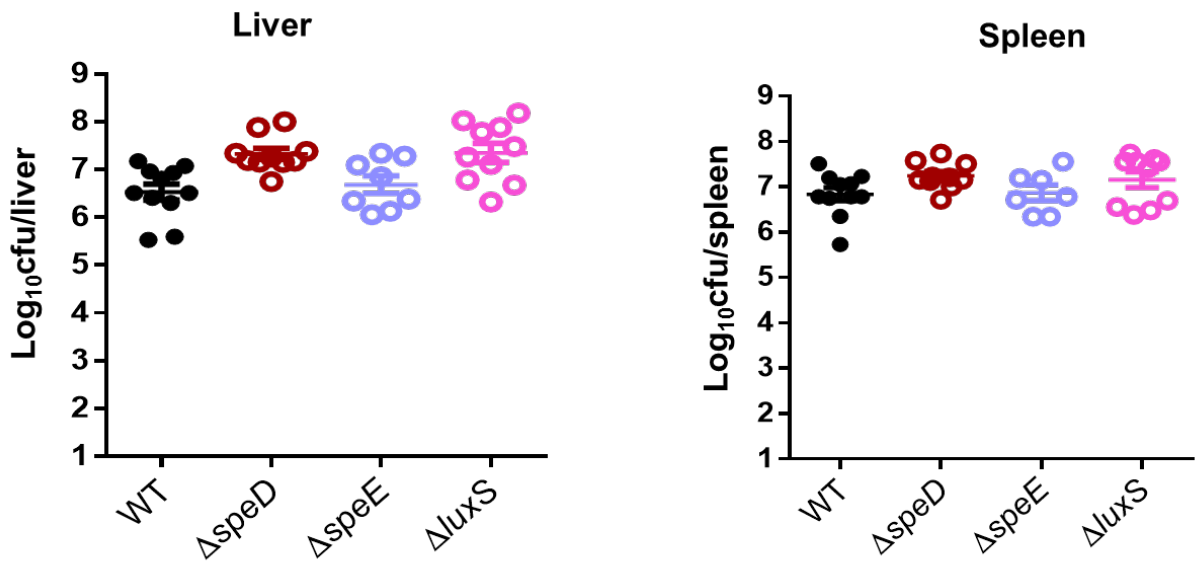

Figure 4-7: *S.* Typhimurium Δ*speD*, Δ*speE* and Δ*luxS* are not attenuated in mice. C57BL/6 mice were infected intravenously with 200 cfu of indicated strains of *S.* Typhimurium. At least five mice were infected per group. At day 5 post-infection, the liver and spleen were harvested and plated to determine the bacterial burden. Data points represent individual mice, and data are pooled from two independent experiments. WT, wild-type. Error bars represent mean ± standard error of the mean. Statistical differences were analysed by One-way ANOVA with Bonferroni's post-test. Groups were not statistically different $p > 0.05$.

4.2.5 *S.* Typhimurium Δ*pfs* mutant shows severe growth defect in M9 minimal media

The metabolic phenotype of the *S.* Typhimurium Δ*pfs* mutant was determined by assessing the ability of the deletion mutant to grow in M9 minimal media. The *S.* Typhimurium Δ*pfs* mutant was unable to grow in M9 minimal media (without Met and biotin) (Figure 4-8A) but was able to grow in nutrient-rich LB media (Figure 4-8D), indicating that the Δ*pfs* mutant is an auxotroph that requires additional nutrient to support growth in culture. To confirm that the deleted *pfs* gene was responsible for this loss of growth capacity, a complementation plasmid was constructed, where Pfs was expressed under the control of the *pfs* promoter in pACYC184 (described in section 2.10) and reintroduced into the Δ*pfs* mutant. The complemented strain, named Δ*pfs* pACYC184 *pfs*, was able to grow in M9 minimal media at levels comparable to the wild-type (Figure 4-8A) demonstrating that the restored phenotype was associated with having functional *pfs* gene present.

To further characterise the specificity of auxotrophy in the Δ*pfs* mutant, it was grown in M9 media supplemented with either Met (100 µM) or biotin (100 µM), and supplementation of either was able to support the growth of the Δ*pfs* mutant (Figure 4-8B and 4-8C). This result indicates that the presence of Met and biotin can support the growth of the Δ*pfs* mutant.

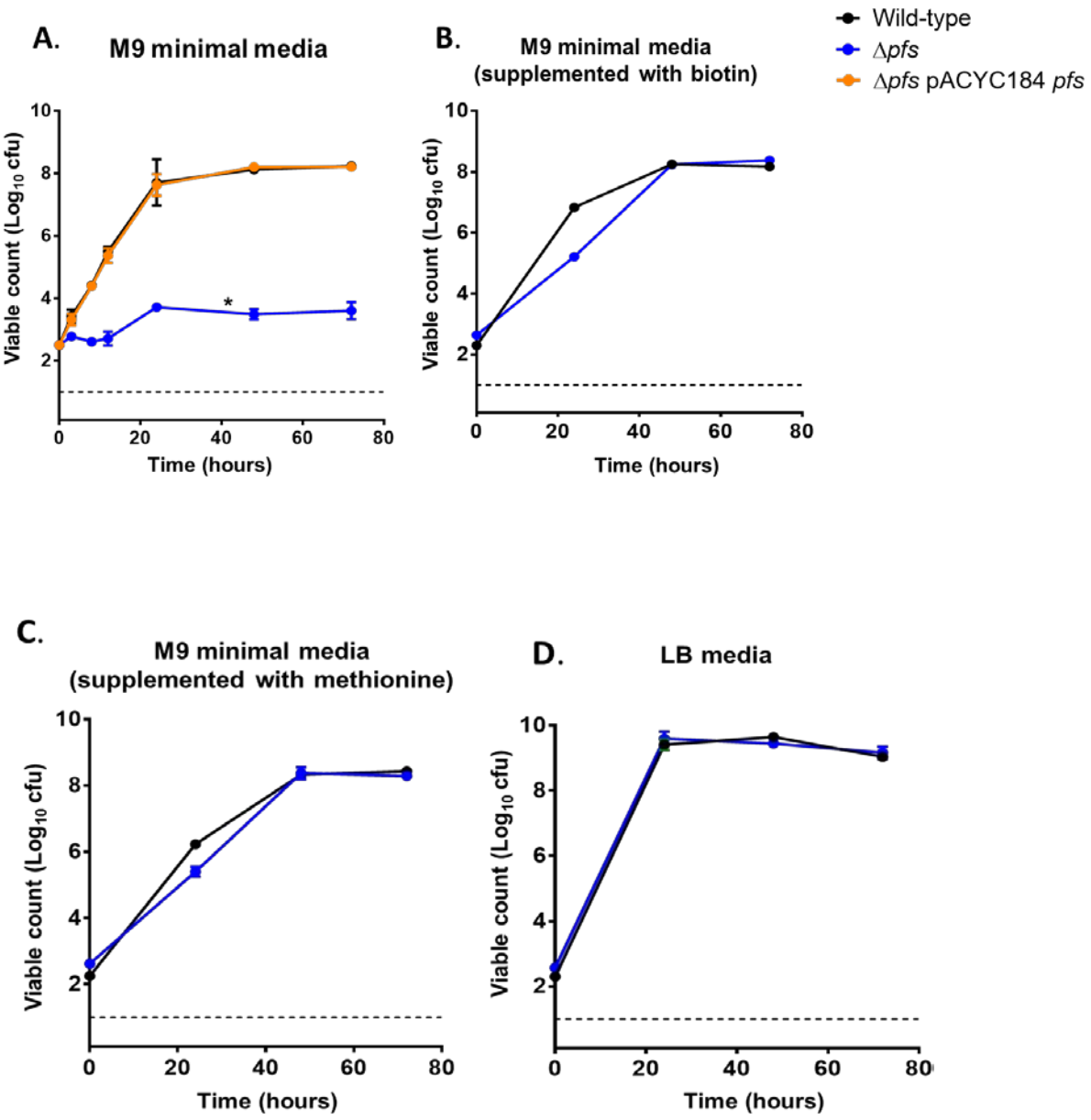

Figure 4-8: The *S.* Typhimurium Δ*pfs* mutant requires supplementation of either biotin or Met to grow in M9 minimal media. A) *S.* Typhimurium wild-type, Δ*pfs* and Δ*pfs* pACYC184 *pfs* were grown in M9 minimal media (without Met and biotin), at 37ºC shaking, compared to wild-type. The genetically complemented mutant strain Δ*pfs* pACYC184 *pfs* grew at an equivalent rate to wild-type. **B), C) and D):** *S.* Typhimurium wild-type and Δ*pfs* mutant were grown in M9 minimal media with biotin (100 µM) and Met (100 µM) supplemented, and in LB broth respectively. Viable count was determined at 24, 48 and 72 hours. The inoculum was plated on LUS (Luria Agar + streptomycin) plated at indicated time-point to determine the viable count. Statistics: Mann-Whitney test. Error bars represent mean ± standard error of the mean. Data is pooled from three independent experiments. Significant * $p < 0.05$. The broken line denotes the limit of detection of the viable count.

4.2.6 The *S.* Typhimurium Δ*pfs* mutant is attenuated for intracellular growth and replication

The intracellular replication of *S.* Typhimurium Δ*pfs* mutant was assessed in HeLa cells over a 10-hour period as described previously (section 4.2.3). The cell culture media used for this assay was DMEM-Complete. The deletion of the MTA/SAH nucleosidase (Pfs) led to a significant attenuation of intracellular survival and replication in HeLa cells, in contrast with the parent wild-type *S.* Typhimurium SL1344. Over 10 hours, the bacterial number of Δ*pfs* within HeLa cells remained approximately constant whereas, for wild-type, the bacterial count increased over 15-fold (Figure 4-9). This attenuated growth phenotype of Δ*pfs* was complemented by expression of *pfs* from its native promoter on pACYC184 (Δ*pfs* pACYC184 *pfs*) confirming that Pfs activity is required for intracellular survival and replication in HeLa cells (Figure 4-9). The complementation of the mutant by pACYC184 *pfs* restored growth of Δ*pfs* mutant in HeLa cells to the similar level seen with wild-type. This data demonstrates that the MTA/SAH nucleosidase known as Pfs is essential for bacterial replication in mammalian cells.

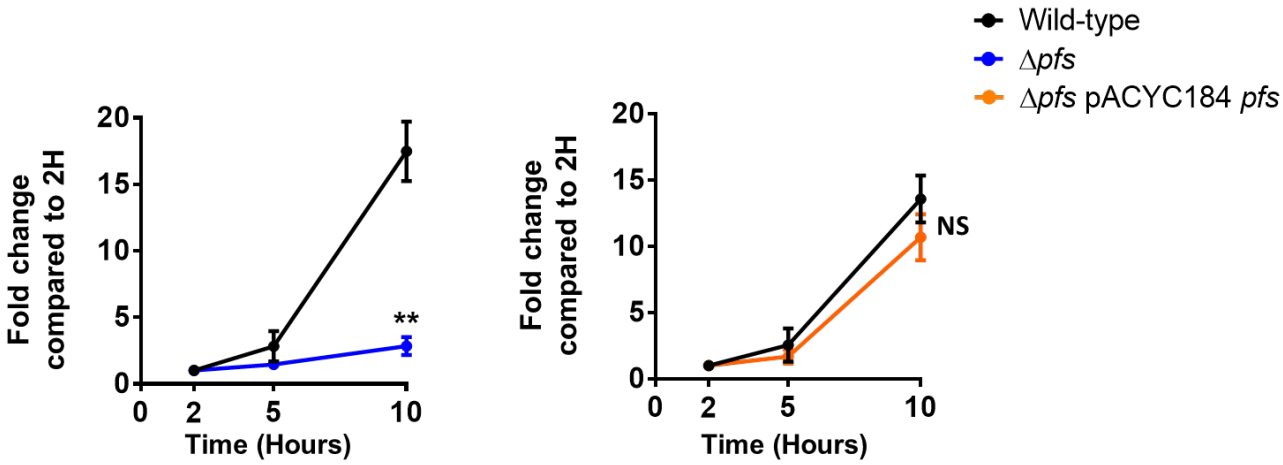

Figure 4-9: *S.* Typhimurium Δ*pfs* mutant is attenuated for intracellular growth in HeLa cells. HeLa cells were infected with exponential LB cultures of the wild-type, Δ*pfs* and complemented strain Δ*pfs* pACYC184 *pfs* of *S.* Typhimurium for 1 hour at 37ºC (MOI: 5-10). At this point, non-adherent bacteria were removed and extracellular bacteria were killed by gentamicin. To determine the intracellular survival/replication, intracellular bacteria were enumerated at 2, 5 and 10 hours post-infection. The strains tested were: Δ*pfs* and complemented strain Δ*pfs* pACYC184 *pfs*. The cell culture media used for this experiment was DMEM-Complete. 2H at Y-axis means 2 hours. The experiments were repeated at least three independent times and the data is pooled from all experiments. Error bars represent mean ± standard error of the mean. Statistical differences were analysed at 10 hours by unpaired T-test. NS Not Significant $p > 0.05$, Significant ** $p < 0.01$

4.2.7 The *S.* Typhimurium Δ*pfs* mutant is attenuated in mice

The role of Pfs in the virulence of *S.* Typhimurium was examined by testing the growth of the mutant in C57BL/6 mice and comparing it to that of the wild-type strain. C57BL/6 mice were infected with the Δ*pfs* mutant intravenously and orally (Figure 4-10).

C57BL/6 mice were infected intravenously with 200 cfu of the wild-type strain, Δ*pfs* mutant or the complemented strain Δ*pfs* pACYC184 *pfs* (Figure 4-10A) and at day 5 post-infection, mice were culled, the spleen and liver were removed and bacteria in the organs were enumerated as viable counts. There was 4-fold less Δ*pfs* mutant recovered compared to wild-type and there were equivalent numbers of bacteria recovered from liver and spleen for each of the strains tested. The results showed that the growth of the Δ*pfs* mutant was significantly attenuated in mice.

Another group of C57BL/6 mice were infected orally with 5×10^7 cfu of wild-type and the Δ*pfs* mutant (Figure 4-10B). To determine the bacterial burden, the mice were culled on day 6 post-infection, and the spleen and liver was removed and the number of bacteria enumerated by viable count. There was 4-fold less Δ*pfs* mutant recovered compared to wild-type and there were equivalent numbers of bacteria recovered from liver and spleen for each of the strains tested. The results showed that the growth of the Δ*pfs* mutant was significantly attenuated in mice.

This data indicates that MTA/SAH nucleosidase (Pfs) is essential for replication of *S.* Typhimurium in mice.

A.

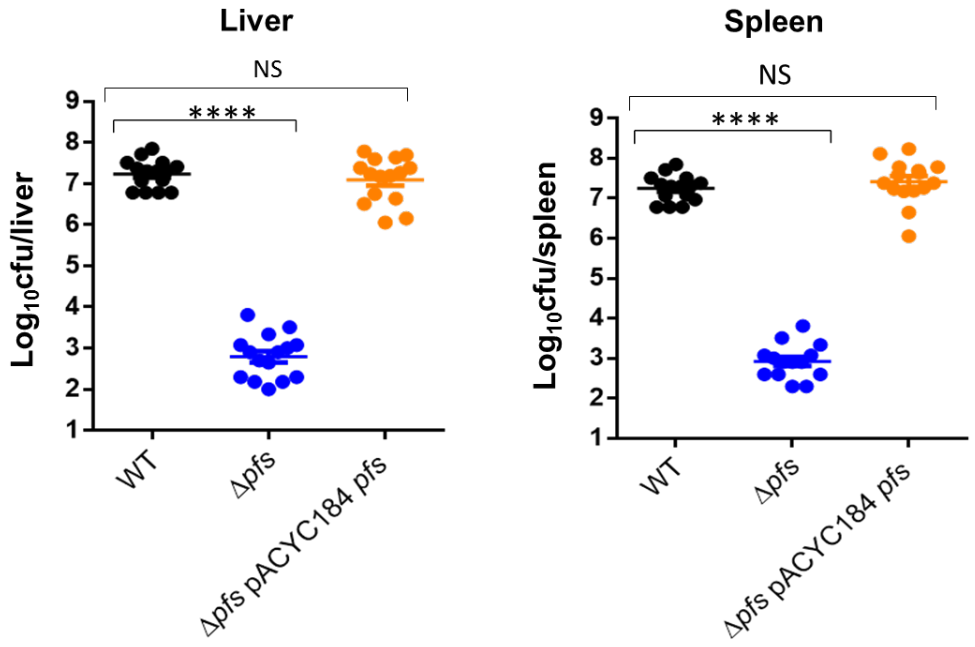

B.

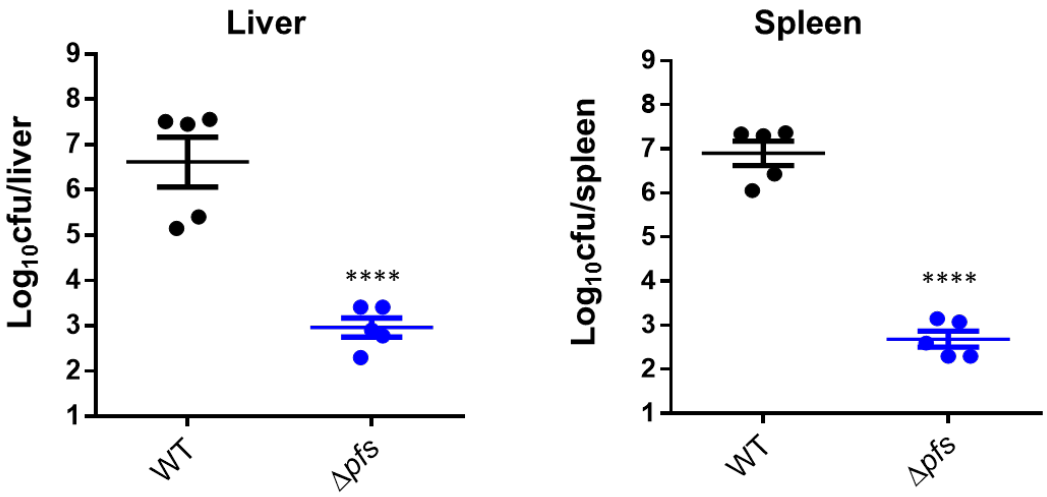

Figure 4-10: *S.* Typhimurium Δ*pfs* is severely attenuated in mice. A) C57BL/6 mice were infected intravenously with 200 cfu of different strains of *S.* Typhimurium. The strains tested were Δ*pfs* mutant and the complemented strain Δ*pfs* pACYC184 *pfs* and compared with wild-type. Data represents from three independent experiments. At least five mice were infected per group. On day five post-infection, liver and spleen were harvested and plated to determine the bacterial burden in the organs. The experiments were repeated at least three independent times and the data is pooled from all experiments. At least five mice were infected per group. Statistical differences were analysed by One-way ANOVA Bonferroni's post-test; Error bars represent mean ± standard error of the mean; NS Not significant $p > 0.05$; significant **** $p < 0.0001$. **B)** C57BL/6 mice were infected orally with 5×10^7 cfu of wild-type *S.* Typhimurium and the Δ*pfs* mutant**.** At least five mice were infected per group. Six days after infection, liver and spleen were harvested and plated to determine the bacterial burden in the organs. WT, wild-type. Error bars represent mean ± standard error of the mean. Statistical differences were analysed by unpaired t-test; Significant **** $p < 0.0001$.

4.2.8 Met and biotin support the growth of *S.* Typhimurium Δ*pfs* in a concentration-dependent manner

The growth of *S.* Typhimurium Δ*pfs* was assessed in M9 media in the presence of biotin and Met at different concentrations in order to identify the lowest concentration of biotin or Met that can support the growth of the Δ*pfs* mutant. Growth was defined as increased vible bacterial count, which were enumerated by plating serial dilutions of bacteria on LUS (Luria agar + streptomycin) every 24 hours (Figure 4-11A and 4-11B). The growth of the Δ*pfs* mutant lags behind that of the wild-type, but reach at the level similar to the wild-type in the presence of 100 uM biotin or Met after 40 hours. The data suggests a slowing of the growth of the mutant, even in high concentrations (<100 µM) of biotin or Met.

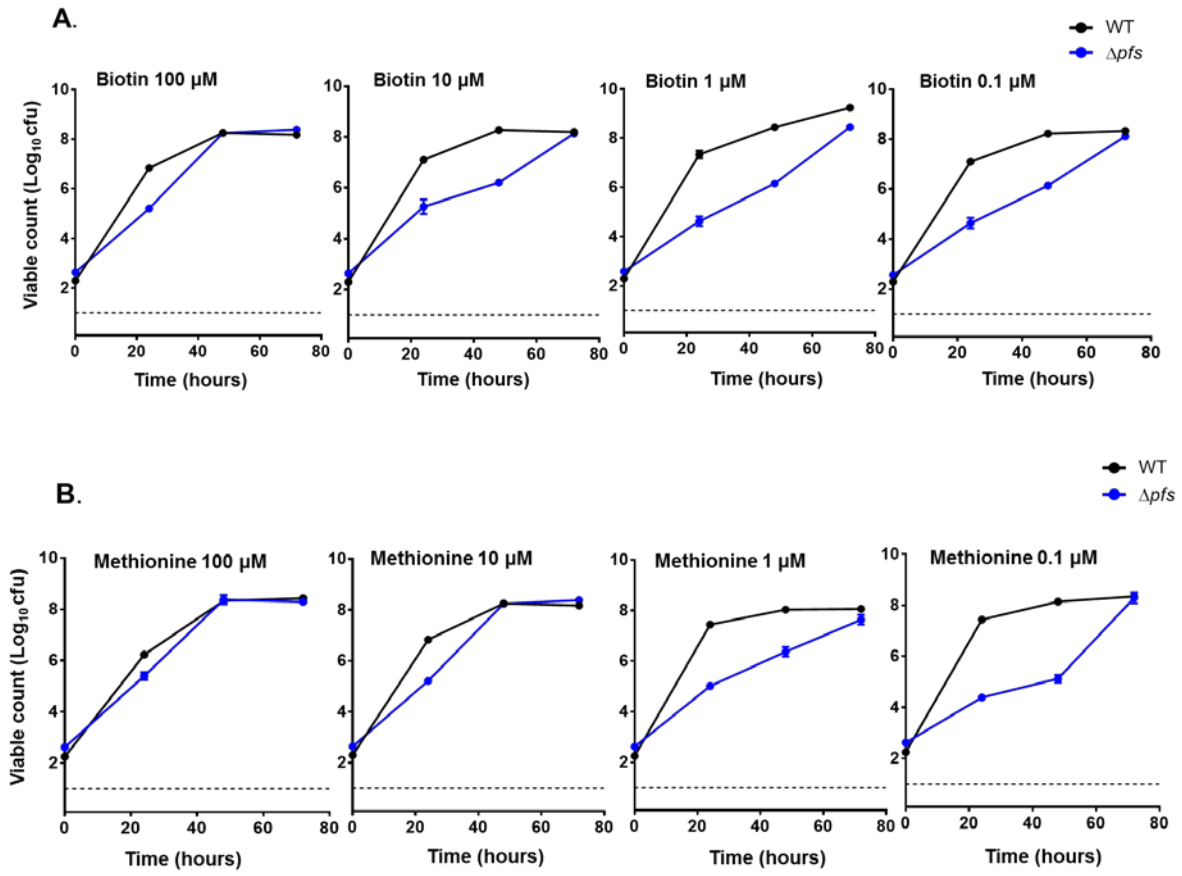

Figure 4-11: The growth kinetics of the *S.* Typhimurium Δ*pfs* mutant in M9 minimal media supplemented with different concentration of biotin and Met. *S.* Typhimurium wild-type and Δ*pfs* mutant were grown in M9 minimal media with various biotin and Met concentration, at 37ºC shaking. **A)** Viable count was determined at every 24 hours in M9 minimal media with biotin supplemented at concentration 100 µM, 10 µM, 1 µM and 0.1 µM and **B)** with Met supplemented at concentration 100 µM, 10 µM, 1 µM and 0.1 µM. The inoculum was plated on LUS (Luria Agar + streptomycin) plates at every time-point. Error bars represent mean ± standard error of the mean. Data is pooled from two independent experiments. The broken line denotes the limit of detection of the viable count.

4.2.9 *S.* Typhimurium Δ*bioB* mutant is unable to grow in M9 minimal media

E. coli Δ*pfs* was shown to phenocopy a biotin synthase (*bioB* gene product) mutant (312, 417) and the proposed relationship between Pfs and BioB is shown in Figure 4-2. As the addition of biotin restored the growth of *S.* Typhimurium Δ*pfs* in minimal media, the *S.* Typhimurium Δ*bioB* mutant, which is unable to convert dethiobiotin to biotin using SAM as a donor (as depicted in Figure 4-2), was characterised in M9 minimal media to compare the growth levels with that of the wild-type (Figure 4-12). As expected, the Δ*bioB* mutant was unable to grow in minimal media when compared with wild-type ($p < 0.01$), but the supplementation with biotin (100 µM) restored the growth of Δ*bioB* to levels similar to those of the wild-type (Figure 4-12).

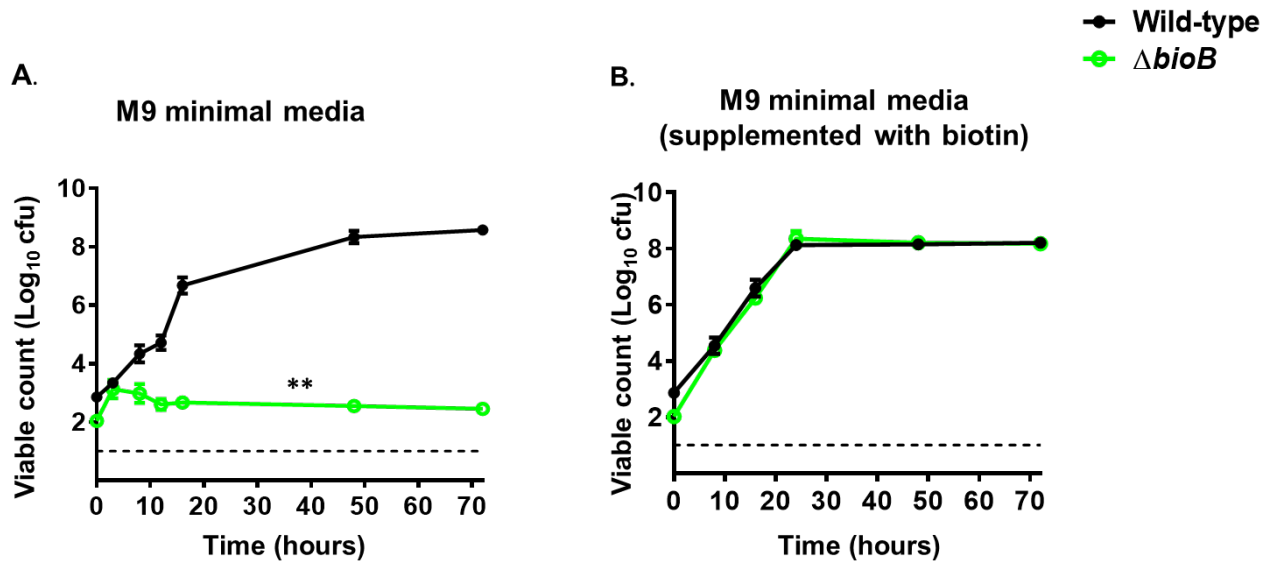

Figure 4-12: The *S.* Typhimurium Δ*bioB* mutant is unable to grow in M9 minimal media. **A)** The Δ*bioB* mutant was tested in M9 minimal media (without biotin) at 37ºC shaking and compared with wild-type. The viable bacterial count was determined at 3, 8, 12, 16, 48 and 72 hours in M9 minimal media (no biotin). Statistical difference was analysed using Mann-Whitney test. ** $p < 0.01$. **B)** The viable bacterial count was determined by 8, 16, 24, 48 and 72 hours in M9 minimal media with biotin supplemented (100 µM). The addition of biotin restored the growth of the Δ*bioB* mutant like wild-type strain. Error bars represent mean ± standard error of the mean. Statistics: Mann-Whitney test. Data is pooled from three independent experiments. The broken line denotes the limit of detection of the viable count. Significant ** $p < 0.01$.

4.2.10 *S*. Typhimurium Δ*bioB* is not attenuated for intracellular growth and replication

The intracellular replication of *S*. Typhimurium Δ*bioB* mutant and wild-type was investigated in HeLa cells over a 10-hour period as described previously (section 4.2.3). The cell culture media used for this assay was DMEM-Complete. The Δ*bioB* mutant showed a similar intracellular growth pattern to wild-type (Figure 4-13), suggesting that biotin synthase is not required for *Salmonella* to grow inside of HeLa cells. Perhaps the mutant acquired biotin from FCS (Foetal Calf Serum) which was supplemented in DMEM-Complete (516).

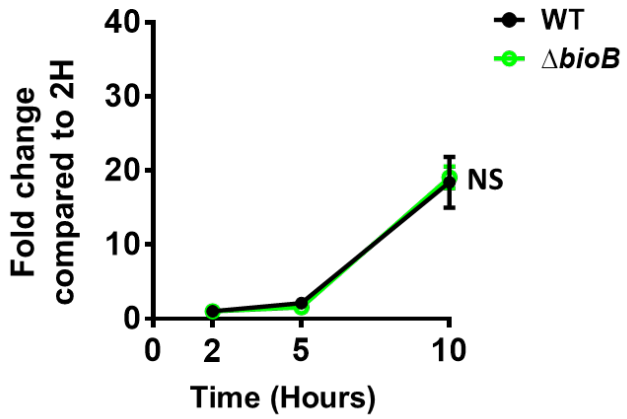

Figure 4-13: The *S*. Typhimurium Δ*bioB* mutant is not attenuated for intracellular growth in HeLa cells. HeLa cells were infected with exponential LB cultures of *S*. Typhimurium Δ*bioB* and wild-type for 1 hour at 37ºC (MOI: 5-10). At this point, non-adherent bacteria were removed, and extracellular bacteria were killed by gentamicin. To determine the intracellular survival/replication, intracellular bacteria were enumerated at 2, 5 and 10 hours. The cell culture media used for this experiment was DMEM-Complete. 2H at Y-axis means 2 hours. The experiments were repeated at least three independent times and the data is pooled from all experiments. Error bars represent mean ± standard error of the mean. Statistical differences were analysed at 10 hours by unpaired T-test. NS Not Significant $p > 0.05$.

4.2.11 The *S*. Typhimurium Δ*bioB* mutant is virulent in mice

As the *S*. Typhimurium Δ*pfs* mutant showed severe attenuation in mice and showed biotin auxotrophy in M9 minimal media, the Δ*bioB* mutant was tested for growth in the murine host. C57BL/6 mice were infected intravenously with 200 cfu of the Δ*bioB* mutant or wild-type (Figure 4-14). The bacterial load in the organs from the mice infected with the Δ*bioB* mutant was a moderately (but significantly) higher than the wild-type bacterial load. This shows that Δ*bioB* was fully virulent over five days of systemic infection.

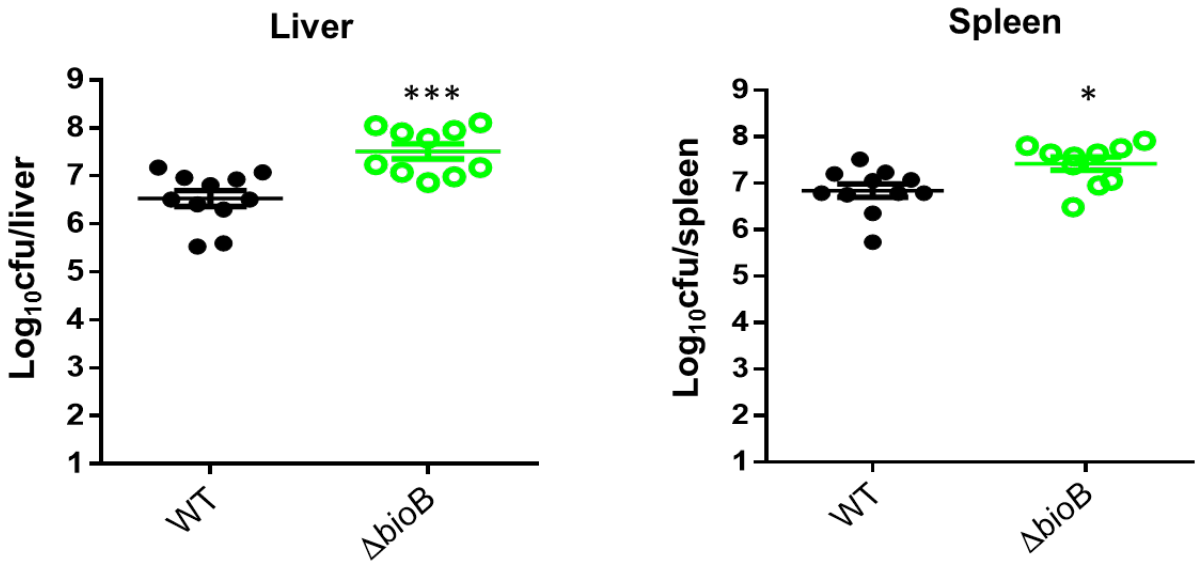

Figure 4-14: *S.* Typhimurium Δ*bioB* mutant is virulent in mice. C57BL/6 mice were infected intravenously with 200 cfu of *S.* Typhimurium wild-type and Δ*bioB* mutant. On day five post-infection, the liver and spleen were harvested and plated to determine the bacterial burden in the organs. Data are pooled from two independent experiments. At least five mice were infected per group. WT, wild-type; Error bars represent mean ± standard error of the mean. Statistical differences were analysed by unpaired t-test. *** p= 0.0004 and * p= 0.01

4.2.12 Investigating the importance of removal of S-adenosylhomocysteine (SAH) from the *S.* Typhimurium Δ*pfs* mutant

It was previously established that SpeD, SpeE and LuxS are not essential for *S.* Typhimurium growth in *vitro* and *in vivo* (Section 4.2.2, 4.2.3 and 4.2.4). SpeD and SpeE are upstream of Pfs in the incomplete Met salvage pathway (as depicted in Figure: 4-1) where SAM acts as aminopropyl group donor, and LuxS is located downstream of Pfs in the activated methyl cycle (Figure: 4-1). The lack of attenuation in the upstream and downstream mutants (i.e. Δ*luxS*, Δ*speE* and Δ*speD*) suggests that the severe attenuation of *S.* Typhimurium Δ*pfs* mutant is unlikely to be due to the deficiency of the enzymes which are located upstream (such as SpeD and SpeE) and downstream (such as LuxS) of Pfs in the pathway.

In *E. coli* and *Salmonella*, the conversion of SAH to homocysteine is a two-step process that occurs via S-ribosylhomocysteine (SRH) (232, 303). SAH, through Pfs, is converted to SRH, and SRH is converted into homocysteine via LuxS, liberating the quorum sensing autoinducer-2 (AI-2) (Figure 4-1). This cycle is then reinitiated when Met is synthesised from homocysteine by one or both Met synthases, and the one carbon cycle. In some prokaryotes and many eukaryotes, this pathway is different, and the SAH is converted directly to homocysteine through S-adenosylhomocysteine hydrolase (SahH) (300, 311). Previous reports suggest that

SAH is a potent inhibitor of SAM-dependent methyltransferases (315-317). The immediate removal of SAH from the cell may support optimal methylation (232, 285, 286).

It is hypothesised that the heterologous expression of an exogenous SAH hydrolase (SahH) in *S.* Typhimurium Δ*pfs* might resolve whether the accumulation of the inhibitory metabolite, SAH, is important in the attenuation of the Δ*pfs* mutant. To address this specifically, the heterologous expression of an exogenous SAH hydrolase (SahH) that restores one of the three enzymatic functions of Pfs is used to complement the *S.* Typhimurium Δ*pfs* mutant. To do this, a heterologous complemented strain, *S.* Typhimurium Δ*pfs* pACYC184 *sahH*(Lp), was constructed. DNA encoding SahH from *Legionella pneumophila* was ligated with DNA encoding a 3× FLAG-Tag at its N-termimus, to facilitate detection of the expression of SahH. The *L. pneumophila* protein was expressed under the promoter of the tet^R gene in pACYC184. FLAG is a hydrophilic eight-residue tag that acts as an antigenic region to which a FLAG-specific antibody binds (517). Given that the FLAG tag is a short peptide, there is reduced possibility that it will interfere with the function of the tagged protein (517). The construction of the pACYC184 *sahH*(Lp) FLAG fusion is described in section 2.10.

Western blot was used to confirm the expression of S-adenosylhomocysteine hydrolase (SahH) from *L. pneumophila* in *S.* Typhimurium Δ*pfs* pACYC184 *sahH*(Lp) by detecting whether FLAG-SahH was expressed in the complemented strain. Cell pellets collected from 1 ml culture of the Δ*pfs* mutant, the complemented strain Δ*pfs* pACYC184 *pfs*, the heterologously complemented strain Δ*pfs* pACYC184 *sahH*(Lp) strain and the wild-type strain grown in M9 minimal media supplemented with Met and biotin were used to analyse the SahH protein expression (Figure 4-15). Cell lysate was resuspended in Laemmli sample buffer and proteins were separated by SDS-PAGE. Proteins were transferred on to nitrocellulose and probed with an antibody against the FLAG-Tag. The result indicates that the 48 kDa S-adenosylhomocysteine hydrolase (SahH) was expressed in the complemented strain Δ*pfs* pACYC184 *sahH*(Lp).

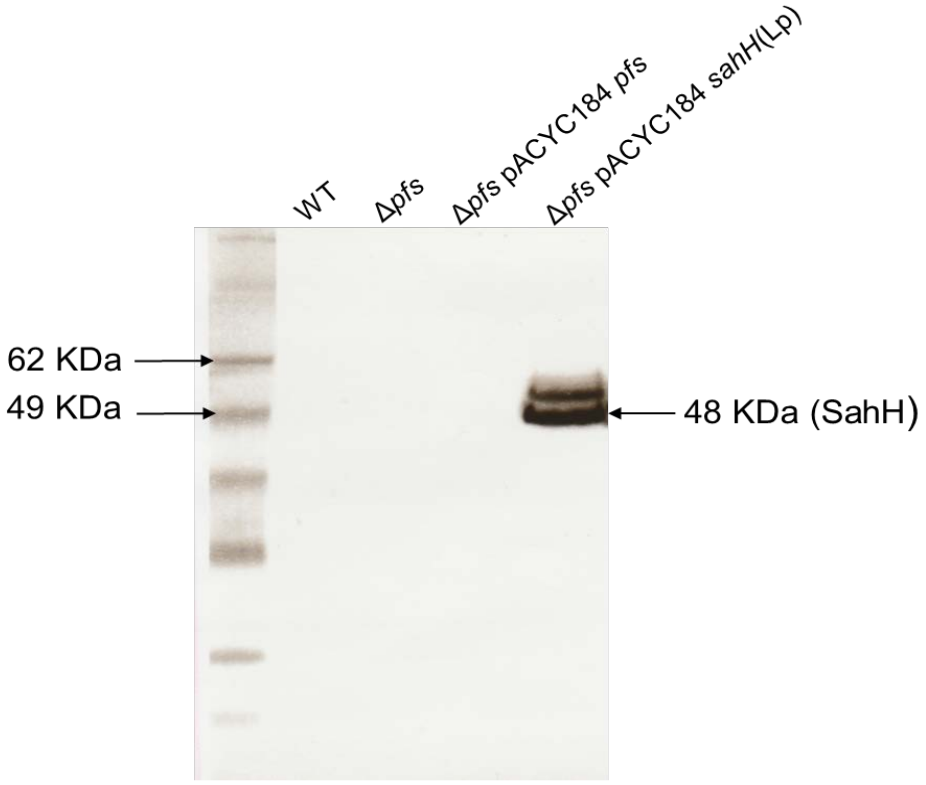

Figure 4-15: Western blot confirms the expression of S-adenosylhomocysteine hydrolase (SahH) in *S.* Typhimurium Δ*pfs* pACYC184 *sahH*(Lp). Pellets were collected from 1 ml culture of the Δ*pfs* mutant, the complemented mutant Δ*pfs* pACYC184 *pfs*, the heterologously complemented strain Δ*pfs* pACYC184 *sahH*(Lp) and wild-type strain, grown in M9 minimal media supplemented with Met (100 µM) and biotin (100 µM). The western blot was probed against the FLAG-Tag on SahH protein. SahH is observed as a 48 KDa protein which has two bands, possibly because of some post-translational modifications.

4.2.13 *S.* Typhimurium Δ*pfs* pACYC184 *sahH*(Lp) can grow in M9 minimal media

The growth of Δ*pfs* pACYC184 *sahH*(Lp) in M9 minimal media was compared with that of the Δ*pfs* mutant, the complemented strain Δ*pfs* pACYC184 *pfs* and wild-type (Figure 4-16). The data showed that heterologous complementation rescued growth of the Δ*pfs* mutant because it grew in M9 minimal media at a similar rate to the Δ*pfs* pACYC184 *pfs* strain, and to the wild-type, SL1344.

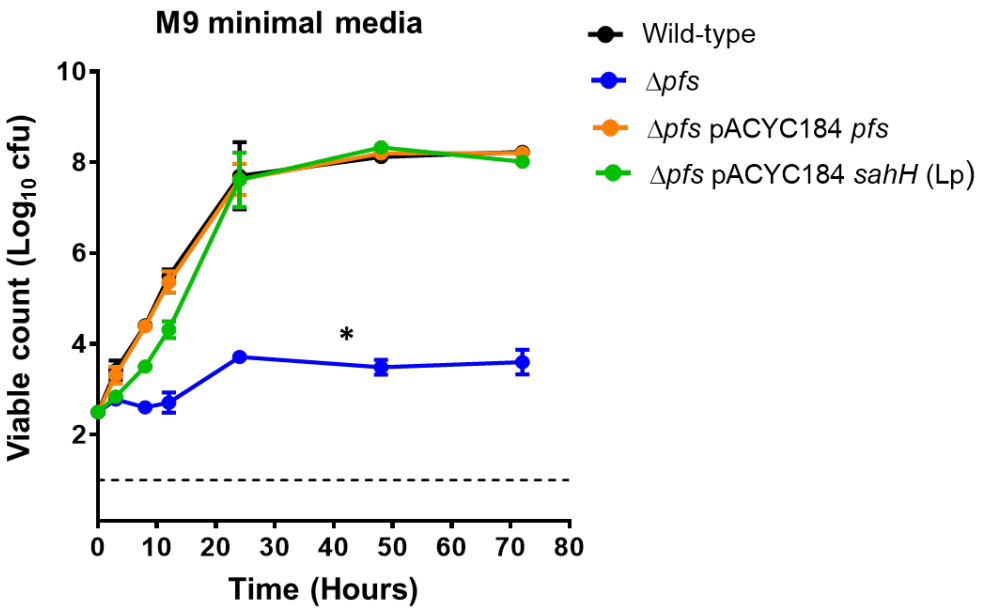

Figure 4-16: The heterologously complemented strain Δ*pfs* pACYC184 *sahH*(Lp) can grow in M9 minimal media. The indicated strains of *S.* Typhimurium were grown in M9 minimal media at 37ºC shaking compared to wild-type. Viable count was determined at 3, 8, 12, 24, 48, 72 hours (without Met, without biotin). The inoculum was plated on LUS (Luria Agar + streptomycin) plates at every time-point. Error bars represent mean ± standard error of the mean. Statistics: Mann-Whitney test. Data is pooled from three independent experiments. The broken line denotes the limit of detection of the viable count. Significant * $p < 0.05$

4.2.14 *S.* Typhimurium Δ*pfs* pACYC184 *sahH*(Lp) is not attenuated for intracellular replication

Using a systematic approach as with other *Salmonella* studied earlier in this chapter, the HeLa cell infection model was used to determine whether the heterologous complementation with SahH restores the intracellular growth capacity for the Δ*pfs* mutant. Similar as described before, HeLa cells were infected with exponential LB cultures of *S.* Typhimurium wild-type and Δ*pfs* pACYC184 *sahH*(Lp) over a 10-hour period post-infection (Figure: 4-17). *S.* Typhimurium Δ*pfs* pACYC184 *sahH*(Lp) replicated to levels comparable to those of the wild-type in HeLa cells, suggesting that the removal of SAH is important for intracellular growth.

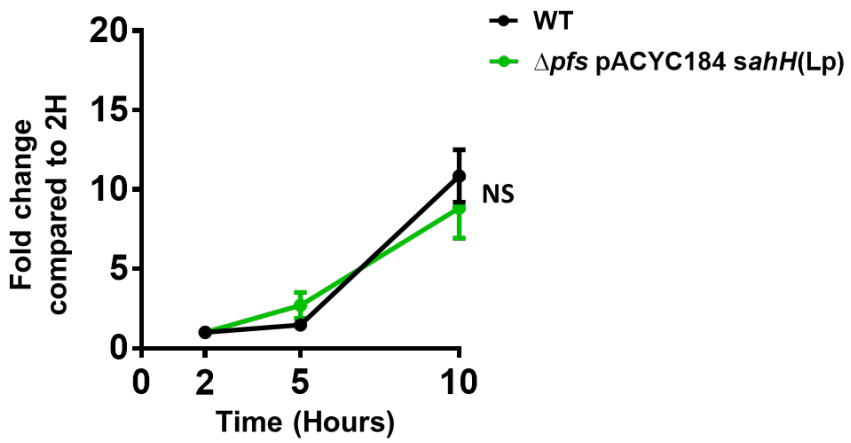

Figure 4-17: *S.* Typhimurium Δ*pfs* pACYC184 *sahH*(Lp) is not attenuated for intracellular growth. HeLa cells were infected with exponential LB cultures of the strains Δ*pfs* pACYC184 *SahH*(Lp) and wild-type for 1 hour at 37ºC (MOI: 5-10). At this point, non-adherent bacteria were removed and extracellular bacteria were killed by gentamicin. To determine the intracellular survival/replication, intracellular bacteria were enumerated at 2, 5 and 10 hours. The cell culture media used for this experiment was DMEM-Complete. The experiments were repeated at least three independent times and the data is pooled from all experiments. 2H at Y-axis means 2 hours. Error bars represent mean ± standard error of the mean. Statistical differences were analysed at 10 hours by unpaired T-test; NS Not Significant $p > 0.05$.

4.2.15 *S.* Typhimurium Δ*pfs* pACYC184 *sahH*(Lp) is virulent in mice

To examine the virulence of *S.* Typhimurium Δ*pfs* pACYC184 *sahH*(Lp) in the murine host, C57BL/6 mice were intravenously infected with the *S.* Typhimurium wild-type, the Δ*pfs* mutant, Δ*pfs* mutant complemented with endogenous *pfs* gene (Δ*pfs* pACYC184 *pfs*) or the heterologous *sahH* gene (Δ*pfs* pACYC184 *sahH*(Lp)). The bacterial burden in the spleen and liver was determined by organ removal and viable count on day 5 post-infection (Figure: 4-18). The bacterial counts from the organs showed that complementation with the *sahH* gene in *S.* Typhimurium Δ*pfs* fully restored growth in the mice. This result suggests that the accumulation of SAH in the Δ*pfs* mutant may be attenuating *in vivo*.

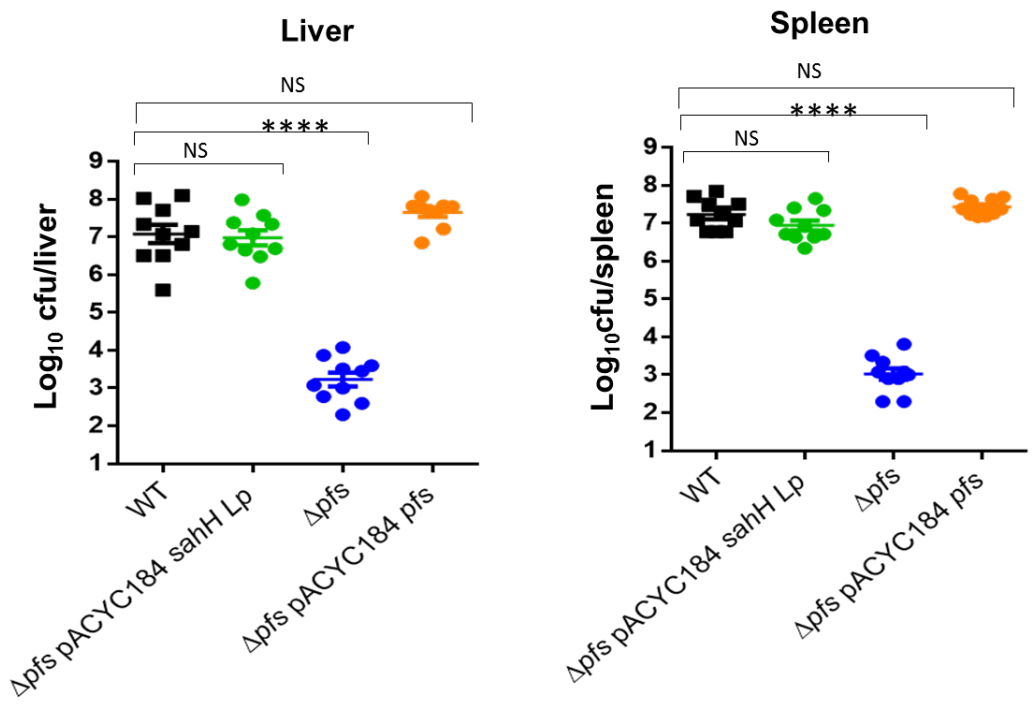

Figure 4-18: Virulence phenotype of *S.* Typhimurium Δ*pfs* pACYC184 *sahH*(Lp) in mice. C57BL/6 mice were infected intravenously with 200 cfu of different strains of *S.* Typhimurium. The strains tested were wild-type, Δ*pfs* mutant, Δ*pfs* pACYC184 *pfs* and Δ*pfs* pACYC184 *sahH*(Lp). The experiments were repeated at least two independent times and the data is pooled from all experiments. Five days after infection, the mice were killed and the liver and spleen were removed for plating to determine the bacterial burden in the organs. WT, wild-type. Error bars represent mean ± standard error of the mean. Statistical analyses were done by One-way ANOVA with Bonferroni's post-test. NS Not Significant $p > 0.05$; significant **** $p < 0.0001$

4.2.16 *S.* Typhimurium Δ*pfs* causes delayed systemic infection in IFN-γ deficient mice

IFN-γ is a key cytokine in the control of *Salmonella* infections (518, 519). To determine whether the growth attenuation observed in the Δ*pfs* mutant was intrinsic, or whether it required host innate intervention to control the infection, experiments were conducted to contrast the growth of the well-documented aromatic amino acid biosynthesis deletion mutant of *S.* Typhimurium SL1344, known as BRD509 (*aroA*$^{-}$) (180, 436), with that of the Δ*pfs* mutant of *S.* Typhimurium SL1344.

In the first experiment, groups of IFN-γ$^{-/-}$ mice were intravenously infected with one of four strains of *S.* Typhimurium: wild-type, the Δ*pfs* mutant, the complemented strain Δ*pfs* pACYC184 *pfs*, and the aromatic amino acid mutant (BRD509) (Figure 4-19). Up until day five post-infection, mice infected with either the Δ*pfs* mutant or BRD509 did not show any disease symptoms. IFN-γ$^{-/-}$ mice infected with *S.* Typhimurium Δ*pfs* pACYC184 *pfs* showed weight loss equivalent to those infected with wild-type bacteria (Figure 4-19A). At day five

post-infection, the bacterial burden in the spleen and liver of IFN-$\gamma^{-/-}$ mice infected with the Δ*pfs* mutant was smilar to those infected with BRD509 ($p > 0.05$), whereas the Δ*pfs* pACYC184 *pfs* strain grew in both liver and spleen at levels comparable to the wild-type strain. This result indicated that *S.* Typhimurium Δ*pfs* and BRD509 (*aro*$^{-}$) show a similar level of attenuation in IFN-γ deficient mice during the first 5 days of infection.

A.

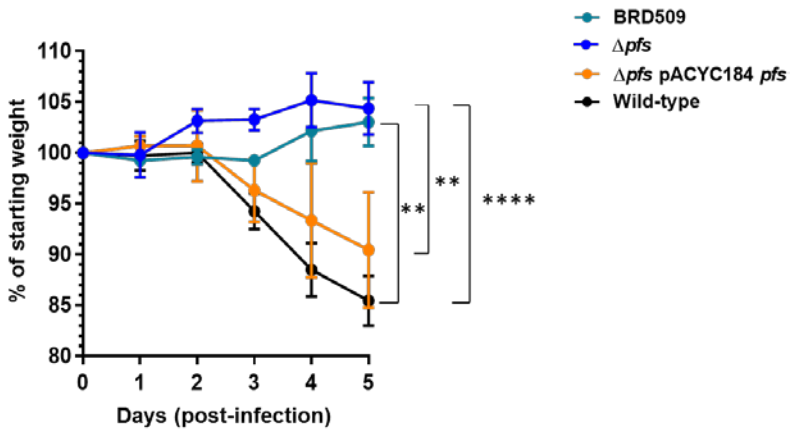

B.

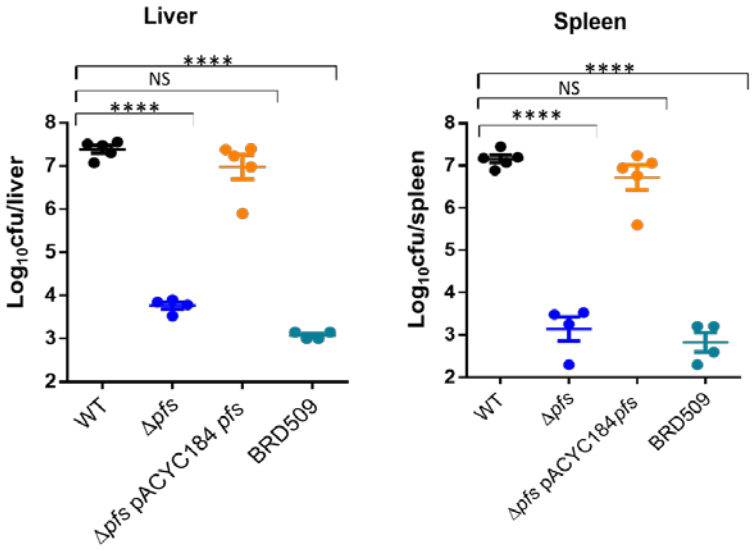

Figure 4-19: *S.* Typhimurium Δ*pfs* and BRD509 (*aro*$^{-}$) show a similar level of attenuation in IFN-γ deficient mice during the first 5 days of infection. IFN-$\gamma^{-/-}$ mice were infected intravenously 200 cfu of Δ*pfs* mutant, Δ*pfs* pACYC184 *pfs*, BRD666 and wild-type. **A)** Mice were weighed daily and the pattern of weight loss over the course of the infection. Statistical analyses: Two-way ANOVA with Bonferroni's post-test. **B)** The liver and spleen were harvested and plated to determine the bacterial burden at day 5 post-infection. WT, wild-type. Error bars represent mean ± standard error of the mean. Statistical analyses: One-way ANOVA with Bonferroni's post-test. NS Not Significant $p > 0.05$; significant** $p < 0.01$; **** $p < 0.0001$

In the second experiment, the growth of the Δ*pfs* mutant in mice was compared with that of BRD509 in IFN-$\gamma^{-/-}$ mice over ten days of infection (Figure 4-20). IFN-$\gamma^{-/-}$ mice infected intravenously with Δ*pfs* started to lose weight after day five. From day eight post-infection the mice infected with Δ*pfs* became visibly unwell with ruffled fur and started showing common disease symptoms such as weight loss, hunching and reduced activity. No disease signs were observed in the IFN-$\gamma^{-/-}$ mice infected with BRD509 (Figure 4-20A). All mice were culled at day ten, and the organs were collected to determine the bacterial load. Viable count from the spleen and liver demonstrated that when the host is deficient for IFN-γ, the Δ*pfs* mutant was capable of growing and causing disease albeit significantly delayed compared to wild-type (Figure 4-20B).

A.

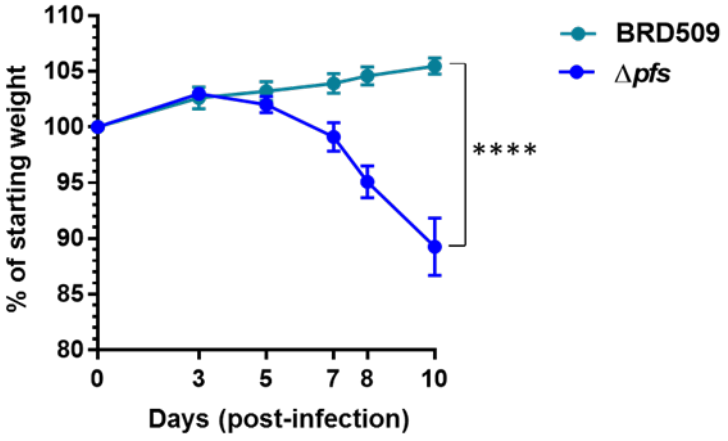

B.

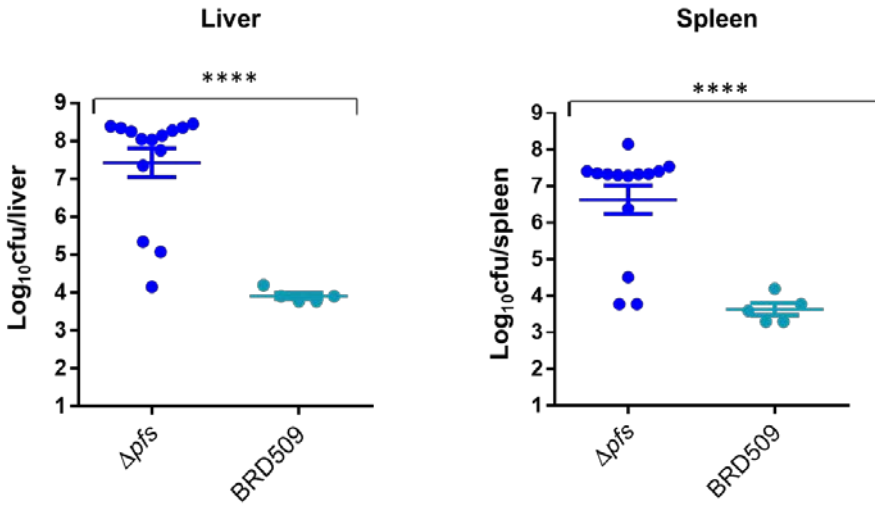

Figure 4-20: Mice lacking IFN-γ have increased sensitivity to *S.* Typhimurium Δ*pfs* mutant compared to BRD509 over the course of a 10-day infection. IFN-$\gamma^{-/-}$ mice were infected intravenously with 200 cfu of the Δ*pfs* mutant or BRD509. **A)** The pattern of weight loss over the course of the infection. Statistical analyses: Two-way ANOVA with Bonferroni's post-test. **B)** The liver and spleen were harvested and plated to determine the bacterial burden at day 10 post-infection. WT, wild-type. Error bars represent mean ± standard error of the mean. Statistical analyses: Unpaired t-test. NS Not Significant $p > 0.05$; significant **** $p < 0.0001$

In the third experiment, the growth of the Δ*pfs* mutant was studied in IFN-$\gamma^{-/-}$ mice and wild-type C57BL/6 mice (Figure 4-21). In C57BL/6 mice, no disease symptom or weight loss was observed during the experimental period, whereas IFN-$\gamma^{-/-}$ mice started to lose weight after day five (Figure 4-21A). On day ten post-infection, both groups of mice were culled, and the bacterial numbers in the liver and spleen were estimated by viable count. The viable count of the Δ*pfs* mutant from the organs of IFN-$\gamma^{-/-}$ mice were higher than the number obtained from organs of wild-type C57BL/6 mice. This data suggests that IFN-γ plays a major role in controlling growth and multiplication of the Δ*pfs* mutant in C57BL/6 mice (Figure 4-21B).

A.

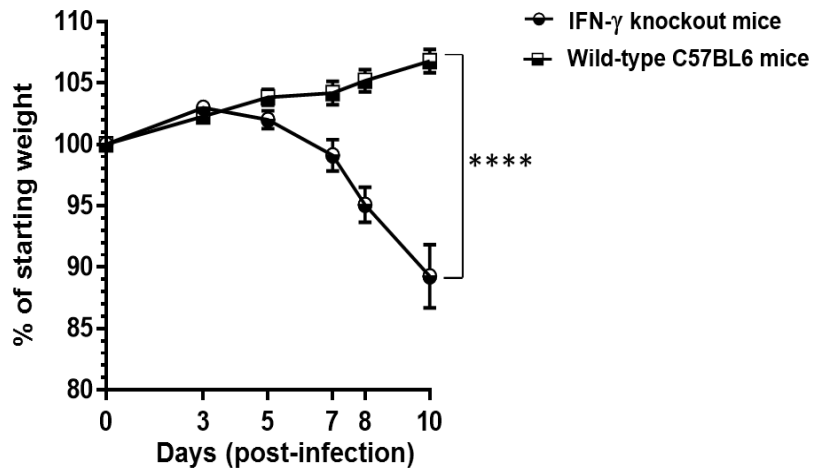

B.

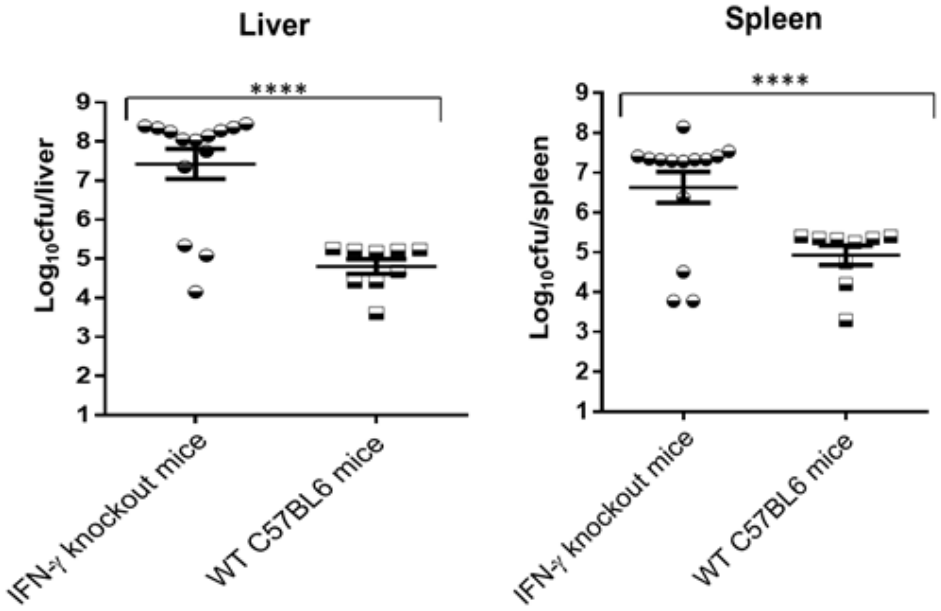

Figure 4-21: Mice deficient of IFN-γ are sensitive to *S.* Typhimurium Δ*pfs*, but the wild-type mice are not. Wild-type C57BL/6 mice and IFN-$\gamma^{-/-}$ mice were infected intravenously 200 cfu of *S.* Typhimurium Δ*pfs* mutant. **A)** The pattern of weight loss over the course of the infection. Statistical analyses: Two-way ANOVA with Bonferroni's post-test. **B)** The liver and spleen were harvested and plated to determine the bacterial burden at day 10 post-infection. WT, wild-type. Error bars represent mean ± standard error of the mean. Statistical analyses: Unpaired t-test. NS Not Significant $p > 0.05$; significant **** $p < 0.0001$.

4.3 Discussion

Knowledge of pathways involving Met that are critical to the growth of *S.* Typhimurium and its virulence *in vivo* could be applied to the development of a novel antibiotic against *S.* Typhimurium and related pathogens. The findings presented in this chapter address several important points regarding the essentiality of recycling of Met through the activated methyl cycle. Additionally, this chapter also revealed the utilisation of Met (via SAM) during polyamine particularly spermidine synthesis, and the requirement of the SAH/MTA nucleosidase (Pfs), in the virulence of the pathogen. Site-directed mutagenesis and complementation, *in vitro* intracellular growth assay and murine infection, were employed to create an understanding of the individual components of Met metabolism that contribute to virulence.

Polyamines are present in all living cells including in epithelial cells and macrophages. In this study, it was shown that *S.* Typhimurium Δ*speD* and Δ*speE*, which are purportedly unable to synthesise spermidine, can grow in M9 minimal media (Figure 4-5). The Δ*speD* and Δ*speE* mutants did not show any defect for intracellular growth when compared with wild-type in HeLa epithelial cells (Figure 4-6). When these strains were tested in the murine host, they were as virulent as wild-type in mice, causing a systemic infection (Figure 4-7). Together these data demonstrate that spermidine biosynthesis is not essential for *S.* Typhimurium virulence.

Previous studies have shown that polyamine mutants in *S.* Typhimurium and *S.* Gallinarum were able to grow in minimal media (410, 415), similar to the data presented here. *S.* Gallinarum spermidine mutants were not defective for intracellular replication in chicken macrophages (415). In contrast, a *S.* Typhimurium polyamine mutant, with deletion of *speB, speC, speE* and *speF*, showed reduced intracellular growth and replication in epithelial cells and also had reduced competitive fitness compared to the wild-type (410). In the later study, the polyamine mutant had a deletion of the four different genes and was not able to synthesise either spermidine and putrescine. The single mutants in the present study reported here, Δ*speD* and Δ*speE,* were designed to allow the bacterium to retain *de novo* putrescine biosynthesis, and the transport systems for putrescine and spermidine, encoded by *potABCD* and *potFGHI* were left intact. The ability to synthesise putrescine, when spermidine biosynthesis is absent, and transport of polyamines from the environment would likely not lower the intracellular concentration of polyamines and could be sufficient to support the growth of the bacterium during systemic infection in mice. In *E. coli*, putrescine is the most predominant polyamine in

terms of intracellular concentration, followed by spermidine (520). Also, the order of preference for extracellular polyamine uptake in *E. coli* is putrescine > spermidine > spermine (520). It is therefore not unexpected that *S.* Typhimurium spermidine biosynthetic mutants were still fit to grow and exihibited full virulence in the murine host. Interestingly, spermidine biosynthesis was shown to be essential for virulence of *S.* Gallinarum in chicken (415), through examination of a Δ*speE* mutant, but complementation was not reported (415). The gastrointestinal environments of birds and mammals are quite different (521) which could account for the different phenotypes reported in different hosts. Moreover, a recent study has shown that spermidine biosynthesis is not required for virulence of *S.* Typhimurium in mice (522). In concert with the research presented here, that study revealed that spermidine biosynthesis might be dispensable for virulence of *S.* Typhimurium because of the functional spermidine uptake system (522).

While the data presented here suggests that spermidine biosynthesis is not essential for the virulence of *S.* Typhimurium *in vivo*, this study, which focussed on Met and SAM metabolism, did not address whether putrescine is required for virulence in the host. Putrescine biosynthesis occurs through a separate pathway, which is not dependent on SAM (288, 391, 410, 523).

LuxS was also found to be not essential for growth of *S.* Typhimurium in minimal media (Figure 4-5), which suggests that Met recycling through the activated methyl cycle is not an essential process for growth *in vitro* under minimal nutrients. This observation is supported by some previous studies where it has been shown that *E. coli* and *Salmonella* lacking LuxS do not show any growth defect *in vitro* (308, 333, 334, 524). The present study shows that the Δ*luxS* mutant was not defective for intracellular growth in HeLa cells compared with wild-type (Figure 4-6). Finally, the virulence of the Δ*luxS* mutant was also found to be equivalent to wild-type in its ability to cause systemic infection in C57BL/6 mice (Figure 4-7). LuxS appeared as dispensable for the virulence of *S.* Typhimurium in mice, which also supported a previous report where female BALB/c mice were orally infected with *S.* Typhimurium Δ*luxS*, and the Δ*luxS* mutant was found to be virulent (337).

LuxS plays a potential role in two different aspects of *S.* Typhimurium pathogenesis; in the recycling of Met and in quorum sensing. Many pathogenic bacteria synthesise LuxS and, in some bacteria, LuxS is involved in the control of virulence gene expression such as in *Vibrio cholarae*, *Streptococcus pyogenes*, *Shigella flexneri* and *Clostridium perfringenes* (525-528). Even though *Streptococcus pneumoniae* Δ*luxS* could colonise the nasopharynx of mice, the

Δ*luxS* mutant was not able to disseminate to the lungs and the bloodstream (307). In *Neisseria meningitidis*, LuxS is required for bacteraemia and meningococcal pathogenesis in mice (304). In *E. coli* and *Salmonella*, LuxS is required to complete the activated methyl cycle which can replenish Met from homocysteine (303, 305-308). It was shown, in the present study, that Met recycling and Met replenishment through LuxS is not essential for *S.* Typhimurium virulence *in vivo*. Also, it can be concluded that AI-2 mediated quorum sensing is also dispensable for *S.* Typhimurium growth and virulence during systemic infection in mice (Figure 4-7).

In the present study reported in this chapter, it has been shown that Pfs (SAH/MTA nucleosidase) is essential for growth of *S.* Typhimurium in minimal media (Figure 4-8). The growth phenotype of *S.* Typhimurium Δ*pfs* in M9 minimal media was restored, with different kinetics, by the addition of Met and biotin to M9 (Figure 4-8). These results suggested that the deletion of *pfs* led to a Met and biotin auxotrophy in *S.* Typhimurium. Additionally, the Δ*pfs* mutant was significantly attenuated for intracellular survival and replication in the *Salmonella*-containing vacuole in HeLa cells (Figure 4-9). Most importantly, Pfs was found to be essential for virulence in *S.* Typhimurium to cause systemic disease in the murine model. The Δ*pfs* mutant showed a 10,000-fold reduction in the bacterial load in spleen and liver compared with wild-type in C57BL/6 mice, after intravenous or oral infection (Figure 4-10). This result suggests that the murine supply of Met or biotin is insufficient to offset the growth defects of the Δ*pfs* mutant. The complemented strain of the Δ*pfs* mutant grew with similar kinetics to the wild-type *in vitro* in M9 media and in HeLa cells, and *in vivo* in C57BL/6 mice (Figure 4-8, 4-9 and 4-10).

Previous reports have shown that the *E. coli* Δ*pfs* mutant is growth defective in minimal media (417) and the addition of Met or biotin partially restored the growth of the *E. coli* Δ*pfs* mutant (312). Recent findings in some other bacteria such as in *Staphylococcus aureus, Neisseria meningitides* and *Borrelia burgdorferi* suggested that Pfs is essential for their virulence (329, 338, 529).

How might the mouse infection attenuation of the Pfs mutant be explained if mutation of the downstream activated methyl cycle (LuxS), polyamines (SpeD, SpeE) and biotin synthetic pathway (BioB) showed full virulence? Presumably, deletion of Pfs leads to the accumulation of SAH and MTA in the cell (300, 302, 421). The elevated level of SAH leads to the inhibition of the SAM-dependent methyltransferases (315-317). The elevated level of MTA is inhibitory for polyamine synthases and SAM-dependent methyltransferases (422, 530). Having shown

that SpeD, SpeE, LuxS and BioB are dispensable (Figure: 4-7), the hypothesis that SAH accumulation is attenuating was tested through the heterologous expression of SahH.

It is argued that the heterologous expression of SahH (S-adenosylhomocysteine hydrolase) enzyme from *Legionella pneumophila* into the *S.* Typhimurium Δ*pfs* mutant, helped to remove SAH from the cell while leaving MTA unaffected (Figure 4-16, 4-17, 4-18). Removal of SAH restored the growth and virulence of the Δ*pfs* mutant in M9 minimal media, HeLa cells and the murine host (Figure 4-16, 4-17, 4-18). This result suggests that accumulated SAH is likely to suppress the SAM-dependent methyltransferases and that the removal of SAH helps to restore growth *in vitro* and *in vivo*. While the expressed level of MTA was not examined directly, it is expected that this intermediate is unaffected by SahH expression, because SahH lacks the multifunctional, and multi-substrate activities of Pfs (300-302, 310, 423).

Cytokines play a key role in the control of *S.* Typhimurium infections, none more so than IFN-γ (518, 519, 531) IFN-γ is predominantly produced by T cells and natural killer cells (532). IFN-γ controls infection by activating the ability of the macrophages to inhibit *Salmonella* growth (531, 533-535). In the present study, IFN-γ was also implicated in controlling infection of *S.* Typhimurium Δ*pfs* mutant as is evident from its severe attenuation in C57BL/6 mice compared to IFN-$\gamma^{-/-}$ mice that showed significant body weight loss and hugher bacterial load in spleen and liver (Figure 4-21).

Th effect of Δ*pfs* mutant on the health of IFN-$\gamma^{-/-}$ mice was compared to a well-known vaccine strain BRD509 which is an avirulent aromatic amino acid biosynthetic mutant with a deletion of the *aroA* gene affecting the pre-chorismate pathway (180, 436). BRD509 was initially designated as an *aroA aroD* double mutant. BRD509 lacks the ability to synthesise three aromatic amino acids tryptophan, phenylalanine and tyrosine, as well as para- amino benzoate, and di-hydroxy benzoate (180, 436). In IFN-$\gamma^{-/-}$ mice, the Δ*pfs* mutant and BRD509 grew to similar numbers in the spleen and liver during the first five days of infection but by day 10 post-infection, the IFN-$\gamma^{-/-}$ mice were more sensitive to the Δ*pfs* mutant than BRD509 (Figure 4-19 and 4-20). The Δ*pfs* mutant caused systemic disease in those mice, whereas BRD509 remained at a lower level throughout the 10-days infection. Previous studies by Kupz *et al*. suggested that BRD509 would be controlled in IFN-γ deficient mice for approximately for 3-4 weeks after which the mice succumb to infection (518). This present study reveals that the Δ*pfs* mutant acts differently from BRD509 when IFN-γ is absent in the host. The Δ*pfs* mutant can grow faster than BRD509, meaning that the attenuation resulting from SAH accumulation

(which may reflect a slow growth) is ultimately absent in IFN-γ deficient mice. Also, both being a metabolic mutant, the virulence trait of the Δ*pfs* mutant depends on the host (the presence or absence of IFN-γ) for attenuation. IFN-γ controls the intracellular growth of the pathogens but the cytokine's function usually does not kill the bacteria making IFN-γ more bacteriostatic than bacteriocidal (535, 536). IFN-γ works at the early stage of the infection, but the clearance of the pathogen is not dependent on this cytokine (535, 536). Therefore, it can be assumed that the absence of IFN-γ results in an inadequate host immune response which in turn leads to uncontrolled growth of the Δ*pfs* mutant and eventually progression to a high bacterial burden at the later stage of the infection. In wild-type C57BL/6 mice, IFN-γ elicits a desired immune response that can assert control over the growth of the Δ*pfs* mutant in the initial stage of the infection, but this growth attenuation in the absence of this cytokine is not sustained over a longer period of time.

4.4 Summary of finding

The importance of the activated methyl cycle and an incomplete Met salvage pathway in virulence of *S*. Typhimurium, SAM recycling and Met replenishment through activated methyl cycle, was found to be non-essential for bacterial growth and virulence in the murine host. Autoinducer-2 mediated quorum sensing was not essential for bacterial growth and virulence *in vitro* and *in vivo*. Similarly, spermidine synthesis was also dispensable during growth and virulence of *S*. Typhimurium. Pfs (S-adenosylhomocysteine/Methylthioadenosine nucleodsidase), a multi-functional enzyme, was found to be essential for bacterial growth in the murine host, and represents a potential target for novel therapeutics. The removal of S-adenosylhomocysteine (SAH) from the *S*. Typhimurium Δ*pfs* mutant through expression of a putative monofunctional S-adenosylhomocysteine hydrolase (SahH) from *L. pneumophila* suggests that accumulation of SAH was responsible for the severe attenuation of the Δ*pfs* mutant. This accumulation of SAH is likely to suppress essential SAM-dependent methyltransferase(s).

Chapter 5

General Discussion

General Discussion

Salmonella enterica is a faecal-orally transmitted bacterial pathogen that, depending on serovar, causes a range of local and systemic diseases in humans, ranging from gastroenteritis, diarrhoea, bacteraemia to enteric (typhoid) fever. In addition to the 200,000 deaths caused by typhoid fever annually (5, 6, 537), infection with invasive non-typhoidal *Salmonella* (iNTS) serovars is responsible for significant morbidity and mortality in sub-Saharan Afirica, where co-infection with HIV results in an estimated 1 million deaths every year (30, 538). Antibiotics are used to treat *S. enterica* infections, however, strains of *S. enterica* that are resistant to drugs are now wide spread and increasing in incidence (17, 509). The increasing prevalence of antibiotic resistance in *S. enterica* is already limiting treatment options (e.g. typhoid and ciprofloxacin (55, 59, 539, 540)) and poses a significant threat to public health. There is an urgent need to identify novel antibiotic targets against this pathogen (17, 509).

To address this growing crisis of resistance, it is necessary to identify drug targets in microbial physiology that will provide alternatives to the current drugs targets where antibiotic resistance has occurred. Current antibiotics target three broad areas including cell wall synthesis and remodelling (e.g., beta-lactams), nucleic acid synthesis (e.g., quinolones) and protein synthesis (e.g., chloramphenicol) (181, 509).

Metabolism is essential in all living cells. Currently, a small number of antibiotics target microbial metabolism such as folate synthesis (e.g., sulphonamides and trimethoprim) (181, 182). Metabolic pathways which are conserved across both microbes and their hosts are often not suitable for the antibiotic target, as inhibitors designed to block the bacterial pathways can interfere with host metabolism, resulting in toxicity (183). On the other hand, a number of metabolic pathways exist exclusively in microbes and it is likely that such metabolic pathways can make ideal targets for novel antimicrobial therapy.

The virulence of intracellular bacterial pathogens such as *Salmonella* and *Mycobacterium* is largely linked with their growth *in vivo* though the recent discovery of a toxin in *S.* Typhi (541) might impact this thinking. Therefore, the ability of these pathogen to synthesise and/or acquire nutrients is absolutely critical to their capacity to cause disease. There are reports which showed that pathogens might acquire and metabolise nutrients differently *in vivo* compared to growth under nutrient-rich *in vitro* conditions (182, 183, 542). *S. enterica* has a diverse metabolic network and it has access to a variety of host nutrients during infection, adding to the challenge

of developing specific growth targeting inhibitors (184, 195). This diversity in substrate choice leads to an extensively redundant *S. enterica* metabolism in the host and renders this pathogen independent of individual biosynthetic and catabolic pathways (184, 195). Some of this putative redundancy comes only from metabolic modelling; the experimental data that show *in vivo* "essentiality" or redundancy is lacking (184). Becker *et al*. (2006) suggested that, due to considerable amount of differences between *S. enterica* and their human and animal host, viable antimicrobial targets remain and majority of these metabolic pathways should be thoroughly and systematically investigated in this pathogen (184).

Methionine (Met) is a sulphur-containing amino acid that participates in a number of important biological processes in a living cell. Formylated Met is required for the initiation of protein translation (228, 229). Met reacts with ATP to form S-adenosylmethionine (SAM), a major methyl donor in the cell (285, 286, 348). It is classed as an "essential" amino acid in mammals because they are forced to acquire it from diet and gut flora (225, 226). In contrast, *de novo* Met biosynthesis is present in prokaryotes. Therefore, this unique pathway in *S.* Typhimurium was chosen for essentiality studies and to determine the need for various metabolites in the synthesis of Met, and in its subsequent use in the activated methyl cycle and polyamine synthesis, in growth by the bacterium in the laboratory mouse, and in tissue culture. The studies presented in this thesis were therefore designed to explore Met metabolism of *S.* Typhimurium and contribute to the existing knowledge of bacterial metabolism. If essentiality can be proven, then the pathway can be explored further for antibiotics that inhibit the pathway and hence growth of *S. enterica.*

It was hypothesised that Met is essential for *S.* Typhimurium growth and virulence in host. In support of this hypothesis, there are some previous reports that showed Met biosynthesis is essential for virulence of *S.* Typhimurium in mice (266) and *S.* Gallinarum in new-born chicken (268). It was also shown that the *S.* Typhimurium Met high-affintiy transporter mutant was attenuated in C3H/HeN mice (270). The essentiality of the key enzymes specifically required for Met biosynthesis and transport in *S.* Typhimurium virulence was systematically analysed in this study. In Chapter 3, it was shown that *de novo* Met biosynthesis does not have any impact on the virulence of *S.* Typhimurium in mice. This result indicated that the apparent redundancy is due to the ability of the bacteria to acquire Met from the host when they cannot synthesise the amino acid. The high-affinity Met transport system was also found dispensable *in vivo*. However, some attenuation of growth occurred when both *de novo* biosynthesis and

the high-affinity transporter were absent. This data suggests that Met biosynthesis pathway does not offer any obvious novel drug targets. The *in vitro* and *in vivo* data also suggested that the low-affinity transporter, termed MetP (263-265, 485), can at least partially replace the function of the high-affinity transporter, since the putative low-affinity transporter cannot fully compensate for the requirement of Met *in vivo* when both *de novo* biosynthesis and transport are absent. The cryptic MetP was not identified, though a strategy to find the transporter was developed, assuming that MetP is a single transporter, and not the function of promiscuous transporters of other related amino acids. In this approach, the *S.* Typhimurium Δ*metNIQ*Δ*metB* mutant strain is complemented with a pBAD cloning vector where *metB* gene is placed under control of the arabinose promoter. Following transposon mutagenesis, mutant trains that were capable of growing on arabinose (ie. intrinsic production of Met) but which were incapable of growing on minimal medium complemented by L-Met, would be selected and characterised. Growth of these mutants is rescued by arabinose selection, and they can be enriched by adding e.g. ampicillin to minimal medium cultures grown with L-Met (ie. killing all dividing bacteria).

The role of two Met synthases MetE and MetH (vitamin B12-independent and vitamin B12-dependent, respectively) *in vivo* was also analysed. *S. enterica* either synthesise vitamin B12 under anaerobic conditions or they derive it exogenously (383, 467). In Chapter 3, it was shown that the Δ*metE* mutant grew in presence of vitamin B12 and under anaerobic condition but Δ*metE*Δ*metH* did not, which clearly demonstrated the *in vitro* dependency of MetH function on vitamin B12, and on the absence of oxygen. It was also found that the two Met synthases are redundant for *S.* Typhimurium virulence *in vivo*. The requirement for vitamin B12 for MetH activity highlights the complexity and interconnectivity within the network of different metabolic pathways in *S. enterica*. The murine host can either 1) supply enough vitamin B12 to *S. enterica* during infection, and/or *S. enterica* converts the microenvironment in *Salmonella* Containing Vacuole (SCV) to be low oxygen, which enables synthesis of vitamin B12 and makes MetH functional, which then efficiently catalyses Met biosynthesis. Met is recycled and replenished through the activated methyl cycle (232, 285-287) where SAM is synthesised from Met. The methyl group of SAM is used for methylation of cellular macromolecules such as DNA, RNA, proteins and lipids (232, 285-287). An integral metabolite of the activated methyl cycle is autoinducer-2 (AI-2), which plays a role in quorum sensing (303-305, 332, 339, 340). Once SAM is synthesised, it also donates the aminopropyl group for spermidine synthesis (349, 391, 407, 409, 543); following donation of the aminopropyl group, the remainder of the SAM

proceeds through a quasi-salvage pathway as *S. enterica* lacks a 5'-methylthioribose kinase (234, 235, 432, 434). 5'-methylthioribose kinase is required to run a functional salvage pathway; this pathway is present in some bacteria such as *Klebsiella pneumoniae* and *Bacillus subtilis*, and facilitates the recycling of Met (234, 235, 432, 434). In Chapter 4, the essentiality of the activated methyl cycle and the incomplete Met salvage pathway in *S.* Typhimurium virulence was investigated.

Polyamines were found to be essential in *S.* Typhimurium (410) and *S.* Gallinarum (415) in some recent reports. In Chapter 4, it was shown that spermidine synthesis is not required for *S.* Typhimurium virulence in the murine host which supports a recent study which was conducted by Jelsbak and colleagues (522). However, this thesis focussed on the utilisation of SAM and the role of the enzymes involved in putrescine biosynthesis in *S.* Typhimurium were not explored. AI-2 mediated quorum sensing was also found to be non-essential to the pathogenesis of *S.* Typhimurium infection in the murine host.

One important finding of the research in this dissertation is that SAH/MTA nucleosidase (Pfs) is essential for virulence of *S.* Typhimurium in mice, suggesting that Pfs represents a potential antibiotic target. Recent studies in other bacteria such as *Staphylococcus aureus, Neisseria meningitides* and *Borrelia burgdorferi* also suggested that Pfs could be a novel drug target (338, 423, 529). The X-ray crystal structure of Pfs from *E. coli* has been solved to show the active site of the enzyme (318, 319, 544). Several highly effective inhibitors such as imidazole, purine and deazopurine-based chemicals were identified for Pfs by screening virtual compound libraries (545, 546). However, the antimicrobial activity e.g., against *N. meningitides* of these inhibitors was only modest perhaps due to poor drug transport (545, 546). One future activity might be the screening of Pfs inhibitors specifically for growth inhibition of *S. enterica.*

As the Pfs is involved in multiple pathways it is necessary to understand which are critical for virulence. To test the hypothesis that S-adenosylhomocysteine (SAH) accumulation plays a role in the attenuation observed in the *S.* Typhimurium Δ*pfs* mutant, SahH was expressed in the mutant. By complementing with the SahH from *Legionella pneumophila,* it was demonstrated that the removal of accumulated SAH from the cell is necessary for full virulence of *S.* Typhimurium. Accumulation of SAH is likely to suppress SAM-dependent methyltransferases which are responsible for methylation of DNA, RNA, proteins and lipids. In future studies, the methylation level in DNA in the Δ*pfs* mutant and wild-type *S.*

Typhimurium might be determined, which could act as a proxy for the intracellular accumulation of SAH, if the levels of SAH cannot be determined.

Generally, during an infection the net bacterial load observed in host tissues represents the result of total bacterial growth in that tissue less the bacteria removed by host defences. IFN-γ is a major immune cytokine, produced by T cells and natural killer cells, and plays a critical role in controlling *Salmonella* infection (531, 533-535). IFN-γ works at the early stage of the infection, but the eventual clearance of the pathogen is not dependent on this cytokine (535, 536). To determine if the attenuation of the *S.* Typhimurium Δ*pfs* mutant is dependent on host clearance mediated through IFN-γ, the Δ*pfs* mutant was tested in immunocompromised mice (IFN-$\gamma^{-/-}$) and the *in vivo* growth compared with the well characterised pre-chorismate mutant of S. Typhimurium strain BRD509. The *S.* Typhimurium Δ*pfs* mutant was similarly attenuated as BRD509 in IFN-$\gamma^{-/-}$ mice early in infection, but began growing more quickly when the infection was prolonged for 10 days. The ability of the Δ*pfs* mutant to grow despite the toxic levels of SAH suggests that the strain may have adapted to the accumulation of SAH. This hypothesis was not tested but future work could look at sequencing of the Δ*pfs* mutants recovered from the mice to determine whether there were point mutations in the genes of the Met biosynthesis or activated methyl cycle pathways that could account for bacterial growth. In the wild-type mice, the *S.* Typhimurium Δ*pfs* infection was controlled and the progression of the disease was stopped.

S. enterica is an excellent model organism to study bacterial pathogenesis and metabolic requirements on a model mammalian host. This study made a contribution with the first comprehensive analysis of Met biosynthesis, the transport and downstream usage of Met in *S. enterica.* By deleting each known enzyme in the Met pathway, transport and metabolism, this research systematically explored this component of *Salmonella* metabolism. It must be acknowledged that the work has been carried out using just one strain of *S.* Typhimurium and the mouse infection differs from infections of humans and possibly other animal species, so the generalizability of the findings are not fully resolved. Equally, it is also recognised that results generated from a single cell line, HeLa in this study, speak to growth of the bacteria in all mammalian cells types. The characterisation of *S.* Typhimurium metabolic mutants described in this thesis will add to the existing knowledge of *S. enterica* metabolism in the host. This study demonstrated the role of Pfs in virulence of *S.* Typhimurium and showed that it could be an attractive target for an antibiotic against *S.* Typhimurium, albeit the loss of

attenuation seen in the IFN-γ deficient mice suggests that, like many other antibiotics, an antibiotic targeting the synthesis or function of Pfs could be dependent on the function of host defences for efficacy (547). This work also opens up opportunities for further investigation of the ability of a *S*. Typhimurium Δ*pfs* mutant to act as a vaccine for *S. enterica* infections.

References:

1. Mastroeni P, Maskell D. Salmonella Infections: Clinical, Immunological and Molecular Aspects: Cambridge University Press; 2006.

2. Parthasarathy A. Textbook of pediatric infectious diseases: JP Medical Ltd; 2013.

3. Everest P, Wain J, Roberts M, Rook G, Dougan G. The molecular mechanisms of severe typhoid fever. Trends in microbiology. 2001;9(7):316-20.

4. Buckle GC, Walker CLF, Black RE. Typhoid fever and paratyphoid fever: Systematic review to estimate global morbidity and mortality for 2010. Journal of global health. 2012;2(1).

5. Crump JA, Luby SP, Mintz ED. The global burden of typhoid fever. Bulletin of the World Health Organization. 2004;82(5):346-53.

6. Bhan MK, Bahl R, Bhatnagar S. Typhoid and paratyphoid fever. Lancet. 2005;366(9487):749-62.

7. Haeusler GM, Curtis N. Non-typhoidal Salmonella in children: microbiology, epidemiology and treatment. Hot Topics in Infection and Immunity in Children IX: Springer; 2013. p. 13-26.

8. Gilks CF. Acute bacterial infections and HIV disease. British medical bulletin. 1998;54(2):383-93.

9. Watera C, Nakiyingi J, Miiro G, Muwonge R, Whitworth JA, Gilks CF, et al. 23-Valent pneumococcal polysaccharide vaccine in HIV-infected Ugandan adults: 6-year follow-up of a clinical trial cohort. Aids. 2004;18(8):1210-3.

10. van Oosterhout JJ, Laufer MK, Graham SM, Thumba F, Perez MA, Chimbiya N, et al. A community-based study of the incidence of trimethoprim-sulfamethoxazole-preventable infections in Malawian adults living with HIV. JAIDS Journal of Acquired Immune Deficiency Syndromes. 2005;39(5):626-31.

11. Stevens MP, Humphrey TJ, Maskell DJ. Molecular insights into farm animal and zoonotic Salmonella infections. Philosophical Transactions of the Royal Society of London B: Biological Sciences. 2009;364(1530):2709-23.

12. Hohmann EL. Nontyphoidal salmonellosis. Clinical infectious diseases : an official publication of the Infectious Diseases Society of America. 2001;32(2):263-9.

13. Mermin J, Hutwagner L, Vugia D, Shallow S, Daily P, Bender J, et al. Reptiles, amphibians, and human Salmonella infection: a population-based, case-control study. Clinical Infectious Diseases. 2004;38(Supplement 3):S253-S61.

14. Braden CR. Salmonella enterica serotype Enteritidis and eggs: a national epidemic in the United States. Clinical Infectious Diseases. 2006;43(4):512-7.

15. Antunes P, Mourão J, Campos J, Peixe L. Salmonellosis: the role of poultry meat. Clinical Microbiology and Infection. 2016;22(2):110-21.

16. Aoki Y, Kitazawa K, Kobayashi H, Senda M, Arahata Y, Homma R, et al. Clinical features of children with nontyphoidal Salmonella bacteremia: A single institution survey in rural Japan. PloS one. 2017;12(6):e0176990.

17. Bush K, Courvalin P, Dantas G, Davies J, Eisenstein B, Huovinen P, et al. Tackling antibiotic resistance. Nature Reviews Microbiology. 2011;9(12):894-6.

18. Edelman R, Levine MM. Summary of an international workshop on typhoid fever. Reviews of infectious diseases. 1986;8(3):329-49.

19. Kauffmann F. The classification and nomenclature of salmonella-species. Zentralblatt für Bakteriologie, Parasitenkunde, Infektionskrankheiten und Hygiene Erste Abteilung Originale Reihe A: Medizinische Mikrobiologie und Parasitologie. 1973;223(4):508.

20. Le Minor L, Popoff MY. Designation of Salmonella enterica sp. nov., nom. rev., as the Type and Only Species of the Genus Salmonella: Request for an Opinion. International Journal of Systematic and Evolutionary Microbiology. 1987;37(4):465-8.

21. SKERMAN VBD, McGowan V, Sneath PHA. Approved lists of bacterial names. International Journal of Systematic and Evolutionary Microbiology. 1980;30(1):225-420.

22. Crosa J, Brenner D, Ewing W, Falkow S. Molecular relationships among the Salmonelleae. Journal of bacteriology. 1973;115(1):307-15.

23. Reeves M, Evins G, Heiba A, Plikaytis B, Farmer JJ. Clonal nature of Salmonella typhi and its genetic relatedness to other salmonellae as shown by multilocus enzyme electrophoresis, and proposal of Salmonella bongori comb. nov. Journal of clinical microbiology. 1989;27(2):313-20.

24. Tindall B, Grimont P, Garrity G, Euzeby J. Nomenclature and taxonomy of the genus Salmonella. International journal of systematic and evolutionary microbiology. 2005;55(1):521-4.

25. Thomas L, Gerald T. Baron's Medical Microbiology. shigella. 2000:389-400.

26. Todar K. Salmonella and salmonellosis. Todar’s online textbook of bacteriology. 2005.

27. Su L, Chiu C. Salmonella: clinical importance and evolution of nomenclature. Chang Gung medical journal. 2007;30(3):210.

28. Brenner F, Villar R, Angulo F, Tauxe R, Swaminathan B. Salmonella nomenclature. Journal of clinical microbiology. 2000;38(7):2465-7.

29. Grimont PA, Weill F-X. Antigenic formulae of the Salmonella serovars. WHO collaborating centre for reference and research on Salmonella. 2007;9.

30. Gilchrist JJ, MacLennan CA, Hill AV. Genetic susceptibility to invasive Salmonella disease. Nature Reviews Immunology. 2015;15(7):452-63.

31. Crump JA, Luby SP, Mintz ED. The global burden of typhoid fever. Bulletin of the World Health Organization. 2004;82(5):346-53.

32. Mogasale V, Maskery B, Ochiai RL, Lee JS, Mogasale VV, Ramani E, et al. Burden of typhoid fever in low-income and middle-income countries: a systematic, literature-based update with risk-factor adjustment. The Lancet Global health. 2014;2(10):e570-e80.

33. Crump JA, Sjölund-Karlsson M, Gordon MA, Parry CM. Epidemiology, clinical presentation, laboratory diagnosis, antimicrobial resistance, and antimicrobial management of invasive Salmonella infections. Clinical microbiology reviews. 2015;28(4):901-37.

34. Kirk MD, Pires SM, Black RE, Caipo M, Crump JA, Devleesschauwer B, et al. World Health Organization estimates of the global and regional disease burden of 22 foodborne bacterial, protozoal, and viral diseases, 2010: a data synthesis. PLoS medicine. 2015;12(12):e1001921.

35. Crump JA, Mintz ED. Global trends in typhoid and paratyphoid fever. Clinical Infectious Diseases. 2010;50(2):241-6.

36. Maskell D. Salmonella infections: clinical, immunological and molecular aspects: Cambridge University Press; 2006.

37. Parry CM. Epidemiological and clinical aspects of human typhoid fever. Salmonella infections: clinical, immunological and molecular aspects. 2006.

38. Bhutta ZA. Current concepts in the diagnosis and treatment of typhoid fever. BMJ. 2006;333(7558):78-82.

39. Sattar AA, Yusuf MA, Islam MB, Jahan WA. Different diagnostic procedure of typhoid fever: A review update. Journal of Current and Advance Medical Research. 2014;1(2):35-41.

40. Arnold A, Griffin GE. Challenging Concepts in Infectious Diseases and Clinical Microbiology: Oxford University Press (UK); 2014.

41. Jones C, Darton TC, Pollard AJ. Why the development of effective typhoid control measures requires the use of human challenge studies. Frontiers in microbiology. 2014;5:707.

42. Marathe SA, Lahiri A, Negi VD, Chakravortty D. Typhoid fever & vaccine development: a partially answered question. Indian Journal of Medical Research. 2012;135(2):161.

43. Zhang W, Sack DA. Progress and hurdles in the development of vaccines against enterotoxigenic Escherichia coli in humans. Expert review of vaccines. 2012;11(6):677-94.

44. Olarte J, Galindo E. Salmonella typhi resistant to chloramphenicol, ampicillin, and other antimicrobial agents: strains isolated during an extensive typhoid fever epidemic in Mexico. Antimicrobial agents and chemotherapy. 1973;4(6):597-601.

45. Butler T, Arnold K, Linh N, Pollack M. Chloramphenicol-resistant typhoid fever in Vietnam associated with R factor. The Lancet. 1973;302(7836):983-5.

46. Chun D, Seol SY, Cho DT, Tak R. Drug resistance and R plasmids in Salmonella typhi isolated in Korea. Antimicrobial agents and chemotherapy. 1977;11(2):209-13.

47. Paniker C, Vimala K. Transferable chloramphenicol resistance in Salmonella typhi. Nature. 1972;239:109-10.

48. Mukhtar ED. Trimethoprim-sulphamethoxazole in the treatment of enteric fever in the Sudan. Transactions of the Royal Society of Tropical Medicine and Hygiene. 1981;75(6):771.

49. Ling J, Chau P. Plasmids mediating resistance to chloramphenicol, trimethoprim, and ampicillin in Salmonella typhi strains isolated in the Southeast Asian region. Journal of Infectious Diseases. 1984;149(4):652-.

50. Kamili M, Ali G, Shah M, Rashid S, Khan S, Allaqaband G. Multiple drug resistant typhoid fever outbreak in Kashmir Valley. Indian journal of medical sciences. 1993;47(6):147-51.

51. Bavdekar S. Antimicrobial therapy of multidrug resistant typhoid fever in children: pediatricians' opinion. Journal of postgraduate medicine. 1996;42(3):65.

52. Smith MD, Duong NM, Hoa N, Wain J, Ha HD, Diep TS, et al. Comparison of ofloxacin and ceftriaxone for short-course treatment of enteric fever. Antimicrobial agents and chemotherapy. 1994;38(8):1716-20.

53. Parry CM. The treatment of multidrug-resistant and nalidixic acid-resistant typhoid fever in Viet Nam. Transactions of the Royal Society of Tropical Medicine and Hygiene. 2004;98(7):413-22.

54. Shirakawa T, Acharya B, Kinoshita S, Kumagai S, Gotoh A, Kawabata M. Decreased susceptibility to fluoroquinolones and gyrA gene mutation in the Salmonella enterica serovar Typhi and Paratyphi A isolated in Katmandu, Nepal, in 2003. Diagnostic microbiology and infectious disease. 2006;54(4):299-303.

55. Renuka K, Sood S, Das BK, Kapil A. High-level ciprofloxacin resistance in Salmonella enterica serotype Typhi in India. Journal of medical microbiology. 2005;54(10):999-1000.

56. Pang T, Levine MM, Ivanoff B, Wain J, Finlay BB. Typhoid fever—important issues still remain. Trends in microbiology. 1998;6(4):131-3.

57. Butler T. Treatment of typhoid fever in the 21st century: promises and shortcomings. Clinical Microbiology and Infection. 2011;17(7):959-63.

58. Basnyat B. The treatment of enteric fever. Journal of the Royal Society of Medicine. 2007;100(4):161-2.

59. Gaind R, Paglietti B, Murgia M, Dawar R, Uzzau S, Cappuccinelli P, et al. Molecular characterization of ciprofloxacin-resistant Salmonella enterica serovar Typhi and Paratyphi A causing enteric fever in India. Journal of Antimicrobial Chemotherapy. 2006;58(6):1139-44.

60. Asna SZH, Haq JA. Decrease of antibiotic resistance in Salmonella typhi isolated from patients attending hospitals of Dhaka City over a 3 year period. International journal of antimicrobial agents. 2000;16(3):249-51.

61. Control CfD, Prevention. Antibiotic resistance threats in the United States, 2013. Atlanta: CDC; 2013. 2015.

62. Bayer C, Bernard H, Prager R, Rabsch W, Hiller P, Malorny B, et al. An outbreak of Salmonella Newport associated with mung bean sprouts in Germany and the Netherlands, October to November 2011. 2014.

63. Jackson BR. Outbreak-associated Salmonella enterica Serotypes and Food Commodities, United States, 1998–2008-Volume 19, Number 8—August 2013-Emerging Infectious Disease journal-CDC. 2013.

64. Lienemann T, Niskanen T, Guedes S, Siitonen A, Kuusi M, Rimhanen-Finne R. Iceberg lettuce as suggested source of a nationwide outbreak caused by two Salmonella serotypes, Newport and Reading, in Finland in 2008. Journal of food protection. 2011;74(6):1035-40.

65. Shahunja K, Leung DT, Ahmed T, Bardhan PK, Ahmed D, Qadri F, et al. Factors associated with non-typhoidal Salmonella bacteremia versus typhoidal Salmonella bacteremia in patients presenting for care in an urban diarrheal disease hospital in Bangladesh. PLoS Negl Trop Dis. 2015;9(9):e0004066.

66. McGovern V, Slavutin L. Pathology of salmonella colitis. The American journal of surgical pathology. 1979;3(6):483-90.

67. Majowicz SE, Musto J, Scallan E, Angulo FJ, Kirk M, O'Brien SJ, et al. The global burden of nontyphoidal Salmonella gastroenteritis. Clinical Infectious Diseases. 2010;50(6):882-9.

68. Cherubin CE, Neu HC, Imperato PJ, Harvey RP, Bellen N. Septicemia with non-typhoid salmonella. Medicine. 1974;53(5):365-76.

69. Todd W, Murdoch JM. Salmonella virchow: a cause of significant bloodstream invasion. Scottish medical journal. 1983;28(2):176-8.

70. Keddy K, Goldsmid JM, Frean J. Tropical gastrointestinal infections. Primer of tropical medicine 1st edn Brisbane: ACTM. 2005.

71. Anderson E. Drug resistance in Salmonella typhimurium and its implications. Br Med J. 1968;3(5614):333-9.

72. Oloya J, Doetkott D, Khaitsa M. Antimicrobial drug resistance and molecular characterization of Salmonella isolated from domestic animals, humans, and meat products. Foodborne pathogens and disease. 2009;6(3):273-84.

73. Phillips I, Casewell M, Cox T, De Groot B, Friis C, Jones R, et al. Does the use of antibiotics in food animals pose a risk to human health? A critical review of published data. Journal of Antimicrobial Chemotherapy. 2004;53(1):28-52.

74. Threlfall E, Day M, De Pinna E, Charlett A, Goodyear K. Assessment of factors contributing to changes in the incidence of antimicrobial drug resistance in Salmonella enterica serotypes Enteritidis and Typhimurium from humans in England and Wales in 2000, 2002 and 2004. International journal of antimicrobial agents. 2006;28(5):389-95.

75. Mather A, Reid S, Maskell D, Parkhill J, Fookes M, Harris S, et al. Distinguishable epidemics of multidrug-resistant Salmonella Typhimurium DT104 in different hosts. Science. 2013;341(6153):1514-7.

76. Glynn MK, Bopp C, Dewitt W, Dabney P, Mokhtar M, Angulo FJ. Emergence of Multidrug-Resistant Salmonella enterica SerotypeTyphimurium DT104 Infections in the United States. New England Journal of Medicine. 1998;338(19):1333-9.

77. Weill F-X, Guesnier F, Guibert V, Timinouni M, Demartin M, Polomack L, et al. Multidrug resistance in Salmonella enterica serotype Typhimurium from humans in France (1993 to 2003). Journal of clinical microbiology. 2006;44(3):700-8.

78. Erdem B, Ercis S, Hascelik G, Gur D, Gedikoglu S, Aysev A, et al. Antimicrobial resistance patterns and serotype distribution among Salmonella enterica strains in Turkey, 2000–2002. European Journal of Clinical Microbiology and Infectious Diseases. 2005;24(3):220-5.

79. Gordon MA, Graham SM, Walsh AL, Wilson L, Phiri A, Molyneux E, et al. Epidemics of invasive Salmonella enterica serovar enteritidis and S. enterica Serovar typhimurium infection associated with multidrug resistance among adults and children in Malawi. Clinical Infectious Diseases. 2008;46(7):963-9.

80. Gayle HD, Hill GL. Global impact of human immunodeficiency virus and AIDS. Clinical microbiology reviews. 2001;14(2):327-35.

81. Feasey NA, Dougan G, Kingsley RA, Heyderman RS, Gordon MA. Invasive non-typhoidal salmonella disease: an emerging and neglected tropical disease in Africa. The Lancet. 2012;379(9835):2489-99.

82. Gordon MA. Invasive Non-typhoidal Salmonella Disease–epidemiology, pathogenesis and diagnosis. Current opinion in infectious diseases. 2011;24(5):484.

83. Galanakis E, Bitsori M, Maraki S, Giannakopoulou C, Samonis G, Tselentis Y. Invasive non-typhoidal salmonellosis in immunocompetent infants and children. International journal of infectious diseases. 2007;11(1):36-9.

84. Morpeth SC, Ramadhani HO, Crump JA. Invasive non-typhi Salmonella disease in Africa. Clinical Infectious Diseases. 2009;49(4):606-11.

85. Dandekar S, George MD, Bäumler AJ. Th17 cells, HIV and the gut mucosal barrier. Current Opinion in HIV and AIDS. 2010;5(2):173-8.

86. MacLennan CA, Gilchrist JJ, Gordon MA, Cunningham AF, Cobbold M, Goodall M, et al. Dysregulated humoral immunity to nontyphoidal Salmonella in HIV-infected African adults. Science. 2010;328(5977):508-12.

87. Kingsley RA, Msefula CL, Thomson NR, Kariuki S, Holt KE, Gordon MA, et al. Epidemic multiple drug resistant Salmonella Typhimurium causing invasive disease in sub-Saharan Africa have a distinct genotype. Genome research. 2009;19(12):2279-87.

88. Gröschel DH, Hornick RB. Who Introduced Typhoid Vaccination: Almroth Wright or Richard Pfeiffer? Review of Infectious Diseases. 1981;3(6):1251-4.

89. Borgoño JM, Corey G, Engelhardt H. Field trials with killed oral typhoid vaccines. Developments in biological standardization. 1975;33:80-4.

90. Chuttani C, Prakash K, Gupta P, Grover V, Kumar A. Controlled field trial of a high-dose oral killed typhoid vaccine in India. Bulletin of the World Health Organization. 1977;55(5):643.

91. Chuttani C, Prakash K, Vergese A, Gupta P, Chawla R, Grover V, et al. Ineffectiveness of an oral killed typhoid vaccine in a field trial. Bulletin of the World Health Organization. 1973;48(6):754.

92. Chuttani C, Prakash K, Vergese A, Sharma U, Singha P, Ray BG. Effectiveness of oral killed typhoid vaccine. Bulletin of the World Health Organization. 1971;45(4):445.

93. Paterson GK, Maskell DJ. Recent advances in the field of Salmonella Typhi vaccines. Human vaccines. 2010;6(5):379-84.

94. Klugman K, Koornhof H, Schneerson R, Cadoz M, Gilbertson I, Robbins J, et al. Protective activity of Vi capsular polysaccharide vaccine against typhoid fever. The Lancet. 1987;330(8569):1165-9.

95. Robbins JD, Robbins JB. Reexamination of the protective role of the capsular polysaccharide (Vi antigen) of Salmonella typhi. Journal of infectious diseases. 1984;150(3):436-49.

96. Looney RJ, Steigbigel RT. Role of the Vi antigen of Salmonella typhi in resistance to host defense in vitro. The Journal of laboratory and clinical medicine. 1986;108(5):506-16.

97. Tran QT, Gomez G, Khare S, Lawhon SD, Raffatellu M, Bäumler AJ, et al. The Salmonella enterica serotype Typhi Vi capsular antigen is expressed after the bacterium enters the ileal mucosa. Infection and immunity. 2010;78(1):527-35.

98. Germanier R, Fiirer E. Isolation and characterization of Gal E mutant Ty 21a of Salmonella typhi: a candidate strain for a live, oral typhoid vaccine. Journal of infectious diseases. 1975;131(5):553-8.

99. Germanier R, Fürer E. Characteristics of the attenuated oral vaccine strain" S. typhi" Ty 21a. Developments in biological standardization. 1982;53:3-7.

100. Fraser A, Paul M, Goldberg E, Acosta CJ, Leibovici L. Typhoid fever vaccines: systematic review and meta-analysis of randomised controlled trials. Vaccine. 2007;25(45):7848-57.

101. Griot-Wenk M, Hartmann K, Herzog C, Ackermann J, Maspes B. Excellent long-term safety data established in a recent post-marketing surveillance for the oral typhoid fever vaccine, Vivotif. Ital J Trop Med. 2001;6:104-5.

102. Levine MM, Ferreccio C, Black RE, Tacket CO, Germanier R, Committee CT. Progress in vaccines against typhoid fever. Review of Infectious Diseases. 1989;11(Supplement 3):S552-S67.

103. Lanh MN, Van Bay P, Ho VA, Thanh TC, Lin FYC, Bryla DA, et al. Persistent efficacy of Vi conjugate vaccine against typhoid fever in young children. New England Journal of Medicine. 2003;349(14):1390-1.

104. Szu SC, Taylor DN, Trofa AC, Clements JD, Shiloach J, Sadoff JC, et al. Laboratory and preliminary clinical characterization of Vi capsular polysaccharide-protein conjugate vaccines. Infection and immunity. 1994;62(10):4440-4.

105. Kossaczka Z, Lin F-YC, Ho VA, Thuy NTT, Van Bay P, Thanh TC, et al. Safety and immunogenicity of Vi conjugate vaccines for typhoid fever in adults, teenagers, and 2-to 4-year-old children in Vietnam. Infection and immunity. 1999;67(11):5806-10.

106. Lin FYC, Ho VA, Khiem HB, Trach DD, Bay PV, Thanh TC, et al. The efficacy of a Salmonella typhi Vi conjugate vaccine in two-to-five-year-old children. New England Journal of Medicine. 2001;344(17):1263-9.

107. Jensen VB, Harty JT, Jones BD. Interactions of the Invasive PathogensSalmonella typhimurium, Listeria monocytogenes, and Shigella flexneri with M Cells and Murine Peyer's Patches. Infection and immunity. 1998;66(8):3758-66.

108. Jepson MA, Clark MA. The role of M cells in Salmonella infection. Microbes and infection / Institut Pasteur. 2001;3(14-15):1183-90.

109. Jones BD, Ghori N, Falkow S. Salmonella typhimurium initiates murine infection by penetrating and destroying the specialized epithelial M cells of the Peyer's patches. The Journal of experimental medicine. 1994;180(1):15-23.

110. Penheiter KL, Mathur N, Giles D, Fahlen T, Jones BD. Non-invasive Salmonella typhimurium mutants are avirulent because of an inability to enter and destroy M cells of ileal Peyer's patches. Molecular microbiology. 1997;24(4):697-709.

111. Vazquez-Torres A, Jones-Carson J, Bäumler AJ, Falkow S, Valdivia R, Brown W, et al. Extraintestinal dissemination of Salmonella by CD18-expressing phagocytes. Nature. 1999;401(6755):804-8.

112. Sinnott C, Teall A. Persistent gallbladder carriage of Salmonella typhi. The Lancet. 1987;329(8539):976.

113. Monack DM. Salmonella persistence and transmission strategies. Current opinion in microbiology. 2012;15(1):100-7.

114. Haraga A, Ohlson MB, Miller SI. Salmonellae interplay with host cells. Nature reviews Microbiology. 2008;6(1):53-66.

115. Santos RL, Zhang S, Tsolis RM, Kingsley RA, Adams LG, Bäumler AJ. Animal models of Salmonella infections: enteritis versus typhoid fever. Microbes and Infection. 2001;3(14):1335-44.

116. Pasetti MF, Levine MM, Sztein MB. Animal models paving the way for clinical trials of attenuated Salmonella enterica serovar Typhi live oral vaccines and live vectors. Vaccine. 2003;21(5):401-18.

117. Strugnell RA, Scott TA, Wang N, Yang C, Peres N, Bedoui S, et al. Salmonella vaccines: lessons from the mouse model or bad teaching? Current opinion in microbiology. 2014;17:99-105.

118. Nakoneczna I, Hsu H. The comparative histopathology of primary and secondary lesions in murine salmonellosis. British journal of experimental pathology. 1980;61(1):76.

119. Richter-Dahlfors A, Buchan AM, Finlay BB. Murine salmonellosis studied by confocal microscopy: Salmonella typhimurium resides intracellularly inside macrophages and exerts a cytotoxic effect on phagocytes in vivo. Journal of Experimental Medicine. 1997;186(4):569-80.

120. Khan SA, Everest P, Servos S, Foxwell N, Zähringer U, Brade H, et al. A lethal role for lipid A in Salmonella infections. Molecular microbiology. 1998;29(2):571-9.

121. Sprinz H, Gangarosa E, Williams M, Hornick R, Woodward T. Histopathology of the upper small intestines in typhoid fever. The American journal of digestive diseases. 1966;11(8):615-24.

122. Steele-Mortimer LAKaO. Taking Possesion: Biogenesis of the Salmonella-Containing Vacuole. Traffic. 2003().

123. Garcia-del Portillo F, Foster JW, Finlay B. Role of acid tolerance response genes in Salmonella typhimurium virulence. Infection and immunity. 1993;61(10):4489-92.

124. Prouty A, Gunn J. Salmonella enterica serovar typhimurium invasion is repressed in the presence of bile. Infection and immunity. 2000;68(12):6763-9.

125. Prouty A, Brodsky I, Manos J, Belas R, Falkow S, Gunn J. Transcriptional regulation of Salmonella enterica serovar Typhimurium genes by bile. FEMS Immunology & Medical Microbiology. 2004;41(2):177-85.

126. Bajaj V, Lucas RL, Hwang C, Lee CA. Co-ordinate regulation of Salmonella typhimurium invasion genes by environmental and regulatory factors is mediated by control of hilA expression. Molecular microbiology. 1996;22(4):703-14.

127. Kim JY, Young JA, Gunther NW, Lee JL. Inhibition of Salmonella by bacteriocin-producing lactic acid bacteria derived from US kimchi and broiler chicken. Journal of Food Safety. 2015;35(1):1-12.

128. Makras L, Triantafyllou V, Fayol-Messaoudi D, Adriany T, Zoumpopoulou G, Tsakalidou E, et al. Kinetic analysis of the antibacterial activity of probiotic lactobacilli towards Salmonella enterica serovar Typhimurium reveals a role for lactic acid and other inhibitory compounds. Research in Microbiology. 2006;157(3):241-7.

129. Lawhon SD, Maurer R, Suyemoto M, Altier C. Intestinal short-chain fatty acids alter Salmonella typhimurium invasion gene expression and virulence through BarA/SirA. Molecular microbiology. 2002;46(5):1451-64.

130. Alvarez-Ordonez A, Begley M, Prieto M, Messens W, Lopez M, Bernardo A, et al. Salmonella spp. survival strategies within the host gastrointestinal tract. Microbiology. 2011;157(Pt 12):3268-81.

131. Bäumler AJ, Sperandio V. Interactions between the microbiota and pathogenic bacteria in the gut. Nature. 2016;535(7610):85-93.

132. Sansonetti PJ, Phalipon A, editors. M cells as ports of entry for enteroinvasive pathogens: mechanisms of interaction, consequences for the disease process. Seminars in immunology; 1999: Elsevier.

133. Hapfelmeier S, Stecher B, Barthel M, Kremer M, Müller AJ, Heikenwalder M, et al. The Salmonella pathogenicity island (SPI)-2 and SPI-1 type III secretion systems allow Salmonella serovar typhimurium to trigger colitis via MyD88-dependent and MyD88-independent mechanisms. The Journal of Immunology. 2005;174(3):1675-85.

134. de Jong HK, Parry CM, van der Poll T, Wiersinga WJ. Host-pathogen interaction in invasive Salmonellosis. PLoS pathogens. 2012;8(10):e1002933.

135. Gordon MA. Salmonella infections in immunocompromised adults. Journal of Infection. 2008;56(6):413-22.

136. Watson KG, Holden DW. Dynamics of growth and dissemination of Salmonella in vivo. Cellular microbiology. 2010;12(10):1389-97.

137. Swart AL, Hensel M. Interactions of Salmonella enterica with dendritic cells. Virulence. 2012;3(7):660-7.

138. Voedisch S, Koenecke C, David S, Herbrand H, Förster R, Rhen M, et al. Mesenteric lymph nodes confine dendritic cell-mediated dissemination of Salmonella enterica serovar Typhimurium and limit systemic disease in mice. Infection and immunity. 2009;77(8):3170-80.

139. Geddes K, Cruz III F, Heffron F. Analysis of cells targeted by Salmonella type III secretion in vivo. PLoS pathogens. 2007;3(12):e196.

140. Crawford RW, Rosales-Reyes R, de la Luz Ramírez-Aguilar M, Chapa-Azuela O, Alpuche-Aranda C, Gunn JS. Gallstones play a significant role in Salmonella spp. gallbladder colonization and carriage. Proceedings of the National Academy of Sciences. 2010;107(9):4353-8.

141. Crawford RW, Gibson DL, Kay WW, Gunn JS. Identification of a bile-induced exopolysaccharide required for Salmonella biofilm formation on gallstone surfaces. Infection and immunity. 2008;76(11):5341-9.

142. Sheppard M, Webb C, Heath F, Mallows V, Emilianus R, Maskell D, et al. Dynamics of bacterial growth and distribution within the liver during Salmonella infection. Cellular microbiology. 2003;5(9):593-600.

143. Mastroeni P, Sheppard M. Salmonella infections in the mouse model: host resistance factors and in vivo dynamics of bacterial spread and distribution in the tissues. Microbes and infection. 2004;6(4):398-405.

144. Steele-Mortimer O. The Salmonella-containing vacuole: moving with the times. Current opinion in microbiology. 2008;11(1):38-45.

145. Hansen-Wester I, Hensel M. Salmonella pathogenicity islands encoding type III secretion systems. Microbes and Infection. 2001;3(7):549-59.

146. Kaur J, Jain S. Role of antigens and virulence factors of Salmonella enterica serovar Typhi in its pathogenesis. Microbiological research. 2012;167(4):199-210.

147. Srikanth C, Mercado-Lubo R, Hallstrom K, McCormick BA. Salmonella effector proteins and host-cell responses. Cellular and Molecular Life Sciences. 2011;68(22):3687.

148. Hardt W-D, Chen L-M, Schuebel KE, Bustelo XR, Galán JE. S. typhimurium encodes an activator of Rho GTPases that induces membrane ruffling and nuclear responses in host cells. Cell. 1998;93(5):815-26.

149. Bakshi C, Singh V, Wood M, Jones P, Wallis T, Galyov E. Identification of SopE2, a Salmonellasecreted protein which is highly homologous to SopE and involved in bacterial invasion of epithelial cells. Journal of bacteriology. 2000;182(8):2341-4.

150. Friebel A, Ilchmann H, Aepfelbacher M, Ehrbar K, Machleidt W, Hardt W-D. SopE and SopE2 from Salmonella typhimurium activate different sets of RhoGTPases of the host cell. Journal of Biological Chemistry. 2001;276(36):34035-40.

151. Zhou D, Chen LM, Hernandez L, Shears SB, Galan JE. A Salmonella inositol polyphosphatase acts in conjunction with other bacterial effectors to promote host cell actin cytoskeleton rearrangements and bacterial internalization. Molecular microbiology. 2001;39(2):248-60.

152. Zhou D, Mooseker MS, Galán JE. Role of the S. typhimurium actin-binding protein SipA in bacterial internalization. Science. 1999;283(5410):2092-5.

153. McGhie EJ, Hayward RD, Koronakis V. Cooperation between actin-binding proteins of invasive Salmonella: SipA potentiates SipC nucleation and bundling of actin. The EMBO journal. 2001;20(9):2131-9.

154. Patel JC, Galán JE. Differential activation and function of Rho GTPases during Salmonella–host cell interactions. The Journal of cell biology. 2006;175(3):453-63.

155. Chen L-M, Hobbie S, Galan JE. Requirement of CDC42 for Salmonella-induced cytoskeletal and nuclear responses. Science. 1996;274(5295):2115.

156. Hobbie S, Chen LM, Davis R, Galan J. Involvement of mitogen-activated protein kinase pathways in the nuclear responses and cytokine production induced by Salmonella typhimurium in cultured intestinal epithelial cells. The Journal of Immunology. 1997;159(11):5550-9.

157. Boyle EC, Brown NF, Finlay BB. Salmonella enterica serovar Typhimurium effectors SopB, SopE, SopE2 and SipA disrupt tight junction structure and function. Cellular microbiology. 2006;8(12):1946-57.

158. Alpuche-Aranda CM, Racoosin EL, Swanson JA, Miller SI. Salmonella stimulate macrophage macropinocytosis and persist within spacious phagosomes. Journal of Experimental Medicine. 1994;179(2):601-8.

159. Rathman M, Sjaastad MD, Falkow S. Acidification of phagosomes containing Salmonella typhimurium in murine macrophages. Infection and immunity. 1996;64(7):2765-73.

160. Carrol M, Jackett P, Aber V, Lowrie D. Phagolysosome formation, cyclic adenosine 3′: 5′-monophosphate and the fate of Salmonella typhimurium within mouse peritoneal macrophages. Microbiology. 1979;110(2):421-9.

161. Oh Y-K, Alpuche-Aranda C, Berthiaume E, Jinks T, Miller SI, Swanson JA. Rapid and complete fusion of macrophage lysosomes with phagosomes containing Salmonella typhimurium. Infection and immunity. 1996;64(9):3877-83.

162. Buchmeier NA, Heffron F. Inhibition of macrophage phagosome-lysosome fusion by Salmonella typhimurium. Infection and immunity. 1991;59(7):2232-8.

163. Drecktrah D, Knodler LA, Howe D, Steele-Mortimer O. Salmonella trafficking is defined by continuous dynamic interactions with the endolysosomal system. Traffic. 2007;8(3):212-25.

164. Bernal-Bayard J, Ramos-Morales F. Salmonella type III secretion effector SlrP is an E3 ubiquitin ligase for mammalian thioredoxin. Journal of Biological Chemistry. 2009;284(40):27587-95.

165. Shiloh MU, MacMicking JD, Nicholson S, Brause JE, Potter S, Marino M, et al. Phenotype of mice and macrophages deficient in both phagocyte oxidase and inducible nitric oxide synthase. Immunity. 1999;10(1):29-38.

166. Nathan C, Shiloh MU. Reactive oxygen and nitrogen intermediates in the relationship between mammalian hosts and microbial pathogens. Proceedings of the National Academy of Sciences. 2000;97(16):8841-8.

167. Chakravortty D, Hansen-Wester I, Hensel M. Salmonella pathogenicity island 2 mediates protection of intracellular Salmonella from reactive nitrogen intermediates. The Journal of experimental medicine. 2002;195(9):1155-66.

168. Vazquez-Torres A, Xu Y, Jones-Carson J, Holden DW, Lucia SM, Dinauer MC, et al. Salmonella pathogenicity island 2-dependent evasion of the phagocyte NADPH oxidase. Science. 2000;287(5458):1655-8.

169. Gallois A, Klein JR, Allen L-AH, Jones BD, Nauseef WM. Salmonella pathogenicity island 2-encoded type III secretion system mediates exclusion of NADPH oxidase assembly from the phagosomal membrane. The journal of immunology. 2001;166(9):5741-8.

170. Aranda CA, Swanson JA, LooMIs WP, Miller SI. Salmonella typhimurium activates virulence gene transcription within acidified macrophage phagosomes. Proceedings of the National Academy of Sciences. 1992;89(21):10079-83.

171. Deiwick J, Nikolaus T, Erdogan S, Hensel M. Environmental regulation of Salmonella pathogenicity island 2 gene expression. Molecular microbiology. 1999;31(6):1759-73.

172. Knodler LA, Vallance BA, Hensel M, Jäckel D, Finlay BB, Steele-Mortimer O. Salmonella type III effectors PipB and PipB2 are targeted to detergent-resistant microdomains on internal host cell membranes. Molecular microbiology. 2003;49(3):685-704.

173. Brawn LC, Hayward RD, Koronakis V. Salmonella SPI1 effector SipA persists after entry and cooperates with a SPI2 effector to regulate phagosome maturation and intracellular replication. Cell host & microbe. 2007;1(1):63-75.

174. Drecktrah D, Knodler LA, Galbraith K, Steele-Mortimer O. The Salmonella SPI1 effector SopB stimulates nitric oxide production long after invasion. Cellular microbiology. 2005;7(1):105-13.

175. Poncet S, Milohanic E, Maze A, Abdallah JN, Ake F, Larribe M, et al. Correlations between carbon metabolism and virulence in bacteria. Bacterial Sensing and Signaling. 16: Karger Publishers; 2009. p. 88-102.

176. Görke B, Stülke J. Carbon catabolite repression in bacteria: many ways to make the most out of nutrients. Nature Reviews Microbiology. 2008;6(8):613-24.

177. Song C, Chiasson MA, Nursimulu N, Hung SS, Wasmuth J, Grigg ME, et al. Metabolic reconstruction identifies strain-specific regulation of virulence in Toxoplasma gondii. Molecular systems biology. 2013;9(1):708.

178. Abu Kwaik Y, Bumann D. Microbial quest for food in vivo:'nutritional virulence'as an emerging paradigm. Cellular microbiology. 2013;15(6):882-90.

179. Ding Y, Liu X, Chen F, Di H, Xu B, Zhou L, et al. Metabolic sensor governing bacterial virulence in Staphylococcus aureus. Proceedings of the National Academy of Sciences. 2014;111(46):E4981-E90.

180. Hoiseth SK, Stocker BA. Aromatic-dependent Salmonella typhimurium are non-virulent and effective as live vaccines. Nature. 1981;291(5812):238-9.

181. Lewis K. Platforms for antibiotic discovery. Nature reviews Drug discovery. 2013;12(5):371-87.

182. Walsh C. Where will new antibiotics come from? Nature Reviews Microbiology. 2003;1(1):65-70.

183. Muñoz-Elías EJ, McKinney JD. Carbon metabolism of intracellular bacteria. Cellular microbiology. 2006;8(1):10-22.

184. Becker D, Selbach M, Rollenhagen C, Ballmaier M, Meyer TF, Mann M, et al. Robust Salmonella metabolism limits possibilities for new antimicrobials. Nature. 2006;440(7082):303-7.

185. Becker D, Selbach M, Rollenhagen C, Ballmaier M, Meyer TF, Mann M, et al. Robust Salmonella metabolism limits possibilities for new antimicrobials. Nature. 2006;440(7082):303-7.

186. Ferreyra JA, Ng KM, Sonnenburg JL. The Enteric Two-Step: nutritional strategies of bacterial pathogens within the gut. Cellular microbiology. 2014;16(7):993-1003.

187. Allen A. Structure and function of gastrointestinal mucus. Physiology of the gastrointestinal tract. 1981;1:617-39.

188. Florey H. The Croonian Lecture: Mucin and the protection of the body. Proceedings of the Royal Society of London Series B, Biological sciences. 1955;143(911):147-58.

189. Linden S, Sutton P, Karlsson N, Korolik V, McGuckin M. Mucins in the mucosal barrier to infection. Mucosal immunology. 2008;1(3):183-97.

190. Cohen P, Rossoll R, Cabelli V, Yang S, Laux D. Relationship between the mouse colonizing ability of a human fecal Escherichia coli strain and its ability to bind a specific mouse colonic mucous gel protein. Infection and immunity. 1983;40(1):62-9.

191. Schrager J, Oates M. Relation of human gastro-intestinal mucus to disease states. British medical bulletin. 1978;34(1):79-82.

192. McGuckin MA, Lindén SK, Sutton P, Florin TH. Mucin dynamics and enteric pathogens. Nature Reviews Microbiology. 2011;9(4):265-78.

193. Hapfelmeier S, Hardt W-D. A mouse model for S. typhimurium-induced enterocolitis. Trends in microbiology. 2005;13(10):497-503.

194. Ng KM, Ferreyra JA, Higginbottom SK, Lynch JB, Kashyap PC, Gopinath S, et al. Microbiota-liberated host sugars facilitate post-antibiotic expansion of enteric pathogens. Nature. 2013;502(7469):96-9.

195. Steeb B, Claudi B, Burton NA, Tienz P, Schmidt A, Farhan H, et al. Parallel exploitation of diverse host nutrients enhances Salmonella virulence. PLoS pathogens. 2013;9(4):e1003301.

196. Koichi K, Michiya F, Makoto N. Lipid components of two different regions of an intestinal epithelial cell membrane of mouse. Biochimica et Biophysica Acta (BBA)-Lipids and Lipid Metabolism. 1974;369(2):222-33.

197. Bertin Y, Girardeau J, Chaucheyras-Durand F, Lyan B, Pujos-Guillot E, Harel J, et al. Enterohaemorrhagic Escherichia coli gains a competitive advantage by using ethanolamine as a nitrogen source in the bovine intestinal content. Environmental microbiology. 2011;13(2):365-77.

198. Winter SE, Thiennimitr P, Winter MG, Butler BP, Huseby DL, Crawford RW, et al. Gut inflammation provides a respiratory electron acceptor for Salmonella. Nature. 2010;467(7314):426-9.

199. Thiennimitr P, Winter SE, Winter MG, Xavier MN, Tolstikov V, Huseby DL, et al. Intestinal inflammation allows Salmonella to use ethanolamine to compete with the microbiota. Proceedings of the National Academy of Sciences. 2011;108(42):17480-5.

200. Cummings J, Macfarlane G. The control and consequences of bacterial fermentation in the human colon. Journal of Applied Bacteriology. 1991;70(6):443-59.

201. Horswill AR, Escalante-Semerena JC. Salmonella typhimurium LT2 catabolizes propionate via the 2-methylcitric acid cycle. Journal of bacteriology. 1999;181(18):5615-23.

202. Goepfert J, Hicks R. Effect of volatile fatty acids on Salmonella typhimurium. Journal of bacteriology. 1969;97(2):956.

203. McHan F, Shotts EB. Effect of feeding selected short-chain fatty acids on the in vivo attachment of Salmonella typhimurium in chick ceca. Avian Diseases. 1992:139-42.

204. Van Immerseel F, Boyen F, Gantois I, Timbermont L, Bohez L, Pasmans F, et al. Supplementation of coated butyric acid in the feed reduces colonization and shedding of Salmonella in poultry. Poultry science. 2005;84(12):1851-6.

205. Boyen F, Haesebrouck F, Vanparys A, Volf J, Mahu M, Van Immerseel F, et al. Coated fatty acids alter virulence properties of Salmonella Typhimurium and decrease intestinal colonization of pigs. Veterinary microbiology. 2008;132(3):319-27.

206. Cardenal-Muñoz E, Ramos-Morales F. Analysis of the expression, secretion and translocation of the Salmonella enterica type III secretion system effector SteA. PloS one. 2011;6(10):e26930.

207. Gantois I, Ducatelle R, Pasmans F, Haesebrouck F, Hautefort I, Thompson A, et al. Butyrate specifically down-regulates Salmonella pathogenicity island 1 gene expression. Applied and environmental microbiology. 2006;72(1):946-9.

208. Huang Y, Suyemoto M, Garner CD, Cicconi KM, Altier C. Formate acts as a diffusible signal to induce Salmonella invasion. Journal of bacteriology. 2008;190(12):4233-41.

209. Leung K, Finlay B. Intracellular replication is essential for the virulence of Salmonella typhimurium. Proceedings of the National Academy of Sciences. 1991;88(24):11470-4.

210. Gahring LC, Heffron F, Finlay B, Falkow S. Invasion and replication of Salmonella typhimurium in animal cells. Infection and immunity. 1990;58(2):443-8.

211. Finlay BB, Gumbiner B, Falkow S. Penetration of Salmonella through a polarized Madin-Darby canine kidney epithelial cell monolayer. J Cell Biol. 1988;107(1):221-30.

212. Finlay BB, Falkow S. Salmonella interactions with polarized human intestinal Caco-2 epithelial cells. Journal of Infectious Diseases. 1990;162(5):1096-106.

213. Bowden SD, Rowley G, Hinton JC, Thompson A. Glucose and glycolysis are required for the successful infection of macrophages and mice by Salmonella enterica serovar Typhimurium. Infection and immunity. 2009;77(7):3117-26.

214. Mercado-Lubo R, Leatham MP, Conway T, Cohen PS. Salmonella enterica serovar Typhimurium mutants unable to convert malate to pyruvate and oxaloacetate are avirulent and immunogenic in BALB/c mice. Infection and immunity. 2009;77(4):1397-405.

215. Fields PI, Swanson RV, Haidaris CG, Heffron F. Mutants of Salmonella typhimurium that cannot survive within the macrophage are avirulent. Proceedings of the National Academy of Sciences of the United States of America. 1986;83(14):5189-93.

216. Stocker B. Aromatic-dependent salmonella as anti-bacterial vaccines and as presenters of heterologous antigens or of DNA encoding them. Journal of biotechnology. 2000;83(1):45-50.

217. Stocker BA. Attenuation of Salmonella by auxotrophy. Biology of Salmonella: Springer; 1993. p. 309-22.

218. Eriksson S, Lucchini S, Thompson A, Rhen M, Hinton JC. Unravelling the biology of macrophage infection by gene expression profiling of intracellular Salmonella enterica. Molecular microbiology. 2003;47(1):103-18.

219. Faucher SP, Porwollik S, Dozois CM, McClelland M, Daigle F. Transcriptome of Salmonella enterica serovar Typhi within macrophages revealed through the selective capture of transcribed sequences. Proceedings of the National Academy of Sciences of the United States of America. 2006;103(6):1906-11.

220. Hautefort I, Thompson A, Eriksson-Ygberg S, Parker M, Lucchini S, Danino V, et al. During infection of epithelial cells Salmonella enterica serovar Typhimurium undergoes a time-dependent transcriptional adaptation that results in simultaneous expression of three type 3 secretion systems. Cellular microbiology. 2008;10(4):958-84.

221. Jelsbak L, Hartman H, Schroll C, Rosenkrantz JT, Lemire S, Wallrodt I, et al. Identification of metabolic pathways essential for fitness of Salmonella Typhimurium in vivo. PloS one. 2014;9(7):e101869.

222. Shi L, Adkins JN, Coleman JR, Schepmoes AA, Dohnkova A, Mottaz HM, et al. Proteomic analysis of Salmonella enterica serovar Typhimurium isolated from RAW 264.7 macrophages identification of a novel protein that contributes to the replication of serovar Typhimurium inside macrophages. Journal of Biological Chemistry. 2006;281(39):29131-40.

223. Mueller JH. A new sulphur-containing amino acid isolated from casein. Experimental Biology and Medicine. 1922;19(4):161-3.

224. Barger G, Coyne FP. The amino-acid methionine; constitution and synthesis. Biochemical Journal. 1928;22(6):1417.

225. Morowitz MJ, Carlisle EM, Alverdy JC. Contributions of intestinal bacteria to nutrition and metabolism in the critically ill. Surgical Clinics of North America. 2011;91(4):771-85.

226. Neis EP, Dejong CH, Rensen SS. The role of microbial amino acid metabolism in host metabolism. Nutrients. 2015;7(4):2930-46.

227. Catoni GL. S-Adenosylmethionine; a new intermediate formed enzymatically from L-methionine and adenosinetriphosphate. The Journal of biological chemistry. 1953;204(1):403-16.

228. Adams JM, Capecchi MR. N-formylmethionyl-sRNA as the initiator of protein synthesis. Proceedings of the National Academy of Sciences of the United States of America. 1966;55(1):147-55.

229. Clark B, Marcker K. The role of N-formyl-methionyl-sRNA in protein biosynthesis. Journal of molecular biology. 1966;17(2):394IN6-406IN7.

230. Flavin M, Delavier-Klutchko C, Slaughter C. Succinic ester and amide of homoserine: some spontaneous and enzymatic reactions. Science. 1964;143(3601):50-2.

231. Markham GD, Hafner EW, Tabor CW, Tabor H. S-Adenosylmethionine synthetase from Escherichia coli. The Journal of biological chemistry. 1980;255(19):9082-92.

232. Kraus J. The Biochemistry of Adenosylmethionine. The Yale journal of biology and medicine. 1978;51(6):669.

233. Chiang P, Gordon RK, Tal J, Zeng G, Doctor B, Pardhasaradhi K, et al. S-Adenosylmethionine and methylation. The FASEB Journal. 1996;10(4):471-80.

234. Sekowska A, Dénervaud V, Ashida H, Michoud K, Haas D, Yokota A, et al. Bacterial variations on the methionine salvage pathway. BMC microbiology. 2004;4(1):9.

235. Albers E. Metabolic characteristics and importance of the universal methionine salvage pathway recycling methionine from 5′-methylthioadenosine. IUBMB life. 2009;61(12):1132-42.

236. Sauter M, Moffatt B, Saechao MC, Hell R, Wirtz M. Methionine salvage and S-adenosylmethionine: essential links between sulfur, ethylene and polyamine biosynthesis. Biochemical Journal. 2013;451(2):145-54.

237. Bourhy P, Martel A, Margarita D, Saint Girons I, Belfaiza J. Homoserine O-acetyltransferase, involved in the Leptospira meyeri methionine biosynthetic pathway, is not feedback inhibited. Journal of bacteriology. 1997;179(13):4396-8.

238. Park S-D, Lee J, Kim Y, Kim J, Lee H. Isolation and analysis of metA, a methionine biosynthetic gene encoding homoserine acetyltransferase in corynebacterium glutamicum. Molecules and cells. 1998;8(3):286-94.

239. Yamagata S. Partial purification and some properties of homoserine O-acetyltransferase of a methionine auxotroph of Saccharomyces cerevisiae. Journal of bacteriology. 1987;169(8):3458-63.

240. Kerr DS, Flavin M. The regulation of methionine synthesis and the nature of cystathionine γ-synthase in Neurospora. Journal of Biological Chemistry. 1970;245(7):1842-55.

241. Rowbury R, Woods D. O-Succinylhomoserine as an intermediate in the synthesis of cystathionine by Escherichia coli. Microbiology. 1964;36(3):341-58.

242. Foglino M, Borne F, Bally M, Ball G, Patte J. A direct sulfhydrylation pathway is used for methionine biosynthesis in Pseudomonas aeruginosa. Microbiology. 1995;141(2):431-9.

243. Datko AH, Giovanelli J, Mudd SH. Homocysteine Biosynthesis in Green Plants O-PHOSPHORYLHOMOSERINE AS THE PHYSIOLOGICAL SUBSTRATE FOR CYSTATHIONINE γ-SYNTHASE. Journal of Biological Chemistry. 1974;249(4):1139-55.

244. Kerr DS. O-Acetylhomoserine Sulfhydrylase from Neurospora Purification and consideration of its function in homocysteine and methionine synthesis Journal of Biological Chemistry. 1971;246(1):95-102.

245. Hwang B-J, Yeom H-J, Kim Y, Lee H-S. Corynebacterium glutamicum utilizes both transsulfuration and direct sulfhydrylation pathways for methionine biosynthesis. Journal of bacteriology. 2002;184(5):1277-86.

246. Vermeij P, Kertesz MA. Pathways of Assimilative Sulfur Metabolism inPseudomonas putida. Journal of bacteriology. 1999;181(18):5833-7.

247. Giovanelli J, Mudd SH. Enzymatic synthesis of cystathionine by extracts of spinach, requiring O-acetylhomoserine or O-succinylhomoserine. Biochemical and biophysical research communications. 1966;25(3):366-71.

248. Clausen T, Wahl MC, Fuhrmann JC, Laber B, Streber W, Steegborn C. Cloning, purification and characterisation of cystathionine γ-synthase from Nicotiana tabacum. Biological chemistry. 1999;380(10):1237-42.

249. Martel A, de la Tour CB, Le Goffic F. Pyridoxal 5′ phosphate binding site of Escherichia coli beta cystathionase and cystathionine gamma synthase comparison of their sequences. Biochemical and biophysical research communications. 1987;147(2):565-71.

250. Brzywczy J, Sieńko M, Kucharska A, Paszewski A. Sulphur amino acid synthesis in Schizosaccharomyces pombe represents a specific variant of sulphur metabolism in fungi. Yeast. 2002;19(1):29-35.

251. Hacham Y, Gophna U, Amir R. In vivo analysis of various substrates utilized by cystathionine γ-synthase and O-acetylhomoserine sulfhydrylase in methionine biosynthesis. Molecular biology and evolution. 2003;20(9):1513-20.

252. Rodionov DA, Vitreschak AG, Mironov AA, Gelfand MS. Comparative genomics of the methionine metabolism in Gram-positive bacteria: a variety of regulatory systems. Nucleic acids research. 2004;32(11):3340-53.

253. Krungkrai J, Webster HK, Yuthavong Y. Characterization of cobalamin-dependent methionine synthase purified from the human malarial parasite, Plasmodium falciparum. Parasitology research. 1989;75(7):512-7.

254. Goulding CW, Matthews RG. Cobalamin-dependent methionine synthase from Escherichia coli: involvement of zinc in homocysteine activation. Biochemistry. 1997;36(50):15749-57.

255. Evans JC, Huddler DP, Hilgers MT, Romanchuk G, Matthews RG, Ludwig ML. Structures of the N-terminal modules imply large domain motions during catalysis by methionine synthase.

Proceedings of the National Academy of Sciences of the United States of America. 2004;101(11):3729-36.

256. Whitfield CD, Steers EJ, Weissbach H. Purification and properties of 5-methyltetrahydropteroyltriglutamate-homocysteine transmethylase. Journal of Biological Chemistry. 1970;245(2):390-401.

257. Eichel J, González JC, Hotze M, Matthews RG, Schröder J. Vitamin-B12-Independent Methionine Synthase from a Higher Plant (Catharanthus Roseus). European journal of biochemistry. 1995;230(3):1053-8.

258. Kacprzak MM, Lewandowska I, Matthews RG, Paszewski A. Transcriptional regulation of methionine synthase by homocysteine and choline in Aspergillus nidulans. Biochemical Journal. 2003;376(2):517-24.

259. Hondorp ER, Matthews RG. Methionine. EcoSal Plus. 2006;2(1).

260. Kadner RJ, Winkler HH. Energy coupling for methionine transport in Escherichia coli. Journal of bacteriology. 1975;123(3):985-91.

261. Merlin C, Gardiner G, Durand S, Masters M. The Escherichia coli metD locus encodes an ABC transporter which includes Abc (MetN), YaeE (MetI), and YaeC (MetQ). Journal of bacteriology. 2002;184(19):5513-7.

262. Zhang Z, Feige JN, Chang AB, Anderson IJ, Brodianski VM, Vitreschak AG, et al. A transporter of Escherichia coli specific for L-and D-methionine is the prototype for a new family within the ABC superfamily. Archives of microbiology. 2003;180(2):88-100.

263. Ayling P, Bridgeland E. Methionine transport in wild-type and transport-defective mutants of Salmonella typhimurium. Microbiology. 1972;73(1):127-41.

264. Ayling P, Mojica-a T, Klopotowski T. Methionine transport in Salmonella typhimurium: evidence for at least one low-affinity transport system. Microbiology. 1979;114(2):227-46.

265. Kadner RJ. Transport systems for L-methionine in Escherichia coli. Journal of bacteriology. 1974;117(1):232-41.

266. Ejim LJ, D'Costa VM, Elowe NH, Loredo-Osti JC, Malo D, Wright GD. Cystathionine beta-lyase is important for virulence of Salmonella enterica serovar Typhimurium. Infection and immunity. 2004;72(6):3310-4.

267. Ejim LJ, Blanchard JE, Koteva KP, Sumerfield R, Elowe NH, Chechetto JD, et al. Inhibitors of bacterial cystathionine beta-lyase: leads for new antimicrobial agents and probes of enzyme structure and function. Journal of medicinal chemistry. 2007;50(4):755-64.

268. Shah DH, Shringi S, Desai AR, Heo E-J, Park J-H, Chae J-S. Effect of metC mutation on Salmonella Gallinarum virulence and invasiveness in 1-day-old White Leghorn chickens. Veterinary microbiology. 2007;119(2):352-7.

269. Bogard RW, Davies BW, Mekalanos JJ. MetR-regulated Vibrio cholerae metabolism is required for virulence. mBio. 2012;3(5).

270. Richardson AR, Payne EC, Younger N, Karlinsey JE, Thomas VC, Becker LA, et al. Multiple targets of nitric oxide in the tricarboxylic acid cycle of Salmonella enterica serovar typhimurium. Cell host & microbe. 2011;10(1):33-43.

271. Rowe PB, Lewis GP. Mammalian folate metabolism. Regulation of folate interconversion enzymes. Biochemistry. 1973;12(10):1962-9.

272. Finkelstein JD. Methionine metabolism in mammals. The Journal of nutritional biochemistry. 1990;1(5):228-37.

273. Mitchell HK, Snell EE, Williams RJ. The concentration of "folic acid". Journal of the American Chemical Society. 1941;63(8):2284-.

274. Cossins E. Folates in biological materials. 1984.

275. Schirch V, Strong WB. Interaction of folylpolyglutamates with enzymes in one-carbon metabolism. Archives of biochemistry and biophysics. 1989;269(2):371-80.

276. Naumova AK, Taketo T. Epigenetics in Human Reproduction and Development: World Scientific; 2016.

277. Mozzi F, Vignolo GM. Biotechnology of lactic acid bacteria: novel applications: John Wiley & Sons; 2010.

278. Ghrist AC, Stauffer GV. The Escherichia coli glycine transport system and its role in the regulation of the glycine cleavage enzyme system. Microbiology. 1995;141(1):133-40.

279. Mudd S, Cantoni G. Biological transmethylation methyl-group neogenesis and other one carbon metabolic reactions dependent upon tetrahydrofolic acid. Comprehensive biochemistry. 1964;15:1-47.

280. Sagers RD, Gunsalus I. INTERMEDIARY METABOLISM OF DIPLOCOCCUS GLYCINOPHILUS I.: Glycine Cleavage and One-Carbon Interconversions1. Journal of bacteriology. 1961;81(4):541.

281. Kikuchi G. The glycine cleavage system: composition, reaction mechanism, and physiological significance. Molecular and cellular biochemistry. 1973;1(2):169-87.

282. Locasale JW. Serine, glycine and one-carbon units: cancer metabolism in full circle. Nature Reviews Cancer. 2013;13(8):572-83.

283. Tong X, Zhao F, Thompson CB. The molecular determinants of de novo nucleotide biosynthesis in cancer cells. Current opinion in genetics & development. 2009;19(1):32-7.

284. Cantoni G, Borchardt R, Creveling C, Ueland P. Biological methylation and drug design. The centrality of S-adenosylhomocysteinase in the regulation of the biological utilization of S-adenosylmethionine. 1986:227-38.

285. Cantoni GL. Biological methylation: selected aspects. Annual review of biochemistry. 1975;44(1):435-51.

286. Chiang PK, Gordon RK, Tal J, Zeng G, Doctor B, Pardhasaradhi K, et al. S-Adenosylmethionine and methylation. The FASEB Journal. 1996;10(4):471-80.

287. Hobson AC. The regulation of methionine and S-adenosylmethionine biosynthesis and utilization in mutants of Salmonella typhimurium with defects in S-adenosylmethionine synthetase. Molecular and General Genetics MGG. 1974;131(3):263-73.

288. Cohen SS. Guide to the Polyamines: Oxford University Press; 1998.

289. Jarrett JT. The novel structure and chemistry of iron–sulfur clusters in the adenosylmethionine-dependent radical enzyme biotin synthase. Archives of biochemistry and biophysics. 2005;433(1):312-21.

290. Layer G, Heinz DW, Jahn D, Schubert W-D. Structure and function of radical SAM enzymes. Current opinion in chemical biology. 2004;8(5):468-76.

291. Winans SC, Bassler BL. Mob psychology. Journal of bacteriology. 2002;184(4):873-83.

292. Fuqua C, Greenberg EP. Listening in on bacteria: acyl-homoserine lactone signalling. Nature Reviews Molecular Cell Biology. 2002;3(9):685-95.

293. Wei Y, Newman E. Studies on the role of the metK gene product of Escherichia coli K-12. Molecular microbiology. 2002;43(6):1651-6.

294. Kimchi B, Ron EZ. A mutant of Escherichia coli temperature sensitive in the biosynthesis of S-adenosylmethionine. FEMS microbiology letters. 1987;43(1):101-6.

295. Tucker AM, Winkler HH, Driskell LO, Wood DO. S-Adenosylmethionine transport in Rickettsia prowazekii. Journal of bacteriology. 2003;185(10):3031-5.

296. Binet R, Fernandez RE, Fisher DJ, Maurelli AT. Identification and characterization of the Chlamydia trachomatis L2 S-adenosylmethionine transporter. mBio. 2011;2(3):e00051-11.

297. Hafner EW, Tabor C, Tabor H. Isolation of a metK mutant with a temperature-sensitive S-adenosylmethionine synthetase. Journal of bacteriology. 1977;132(3):832-40.

298. Stauffer GV, Brenchley JE. Influence of methionine biosynthesis on serine transhydroxymethylase regulation in Salmonella typhimurium LT2. Journal of bacteriology. 1977;129(2):740-9.

299. Chattopadhyay M, Ghosh A, Sengupta S. Control of methionine biosynthesis in Escherichia coli K12: a closer study with analogue-resistant mutants. Microbiology. 1991;137(3):685-91.

300. Walker R, Duerre J. S-adenosylhomocysteine metabolism in various species. Canadian journal of biochemistry. 1975;53(3):312-9.

301. Hanzelka BL, Greenberg EP. Quorum sensing in Vibrio fischeri: evidence that S-adenosylmethionine is the amino acid substrate for autoinducer synthesis. Journal of bacteriology. 1996;178(17):5291-4.

302. SHIMIZU S, SHIOZAKI S, OHSHIRO T, YAMADA H. Occurrence of S-adenosylhomocysteine hydrolase in prokaryote cells. European Journal of Biochemistry. 1984;141(2):385-92.

303. Winzer K, Hardie KR, Burgess N, Doherty N, Kirke D, Holden MT, et al. LuxS: its role in central metabolism and the in vitro synthesis of 4-hydroxy-5-methyl-3 (2H)-furanone. Microbiology. 2002;148(4):909-22.

304. Winzer K, Sun Y-h, Green A, Delory M, Blackley D, Hardie KR, et al. Role of Neisseria meningitidis luxS in cell-to-cell signaling and bacteremic infection. Infection and immunity. 2002;70(4):2245-8.

305. Xavier KB, Bassler BL. LuxS quorum sensing: more than just a numbers game. Current opinion in microbiology. 2003;6(2):191-7.

306. Taga ME, Semmelhack JL, Bassler BL. The LuxS-dependent autoinducer AI-2 controls the expression of an ABC transporter that functions in AI-2 uptake in Salmonella typhimurium. Molecular microbiology. 2001;42(3):777-93.

307. Joyce EA, Kawale A, Censini S, Kim CC, Covacci A, Falkow S. LuxS is required for persistent pneumococcal carriage and expression of virulence and biosynthesis genes. Infection and immunity. 2004;72(5):2964-75.

308. Wang L, Li J, March JC, Valdes JJ, Bentley WE. luxS-dependent gene regulation in Escherichia coli K-12 revealed by genomic expression profiling. Journal of bacteriology. 2005;187(24):8350-60.

309. Vendeville A, Winzer K, Heurlier K, Tang CM, Hardie KR. Making'sense'of metabolism: autoinducer-2, LuxS and pathogenic bacteria. Nature Reviews Microbiology. 2005;3(5):383-96.

310. Sun J, Daniel R, Wagner-Döbler I, Zeng A-P. Is autoinducer-2 a universal signal for interspecies communication: a comparative genomic and phylogenetic analysis of the synthesis and signal transduction pathways. BMC Evolutionary Biology. 2004;4(1):36.

311. Duerre JA. A hydrolytic nucleosidase acting on S-adenosylhomocysteine and on 5'-methylthioadenosine. Journal of Biological Chemistry. 1962;237(12):3737-41.

312. Choi-Rhee E, Cronan JE. A nucleosidase required for in vivo function of the S-adenosyl-L-methionine radical enzyme, biotin synthase. Chemistry & biology. 2005;12(5):589-93.

313. Ferro AJ, Barrett A, Shapiro SK. Kinetic properties and the effect of substrate analogues on 5′-methylthioadenosine nucleosidase from Escherichia coli. Biochimica et Biophysica Acta (BBA)-Enzymology. 1976;438(2):487-94.

314. Halliday N, Hardie K, Williams P, Winzer K, Barrett D. Quantitative liquid chromatography–tandem mass spectrometry profiling of activated methyl cycle metabolites involved in LuxS-dependent quorum sensing in Escherichia coli. Analytical biochemistry. 2010;403(1):20-9.

315. Reich N, Mashhoon N. Inhibition of EcoRI DNA methylase with cofactor analogs. Journal of Biological Chemistry. 1990;265(15):8966-70.

316. Reich NO, Mashhoon N. Kinetic mechanism of the EcoRI DNA methyltransferase. Biochemistry. 1991;30(11):2933-9.

317. Simms S, Subbaramaiah K. The kinetic mechanism of S-adenosyl-L-methionine: glutamylmethyltransferase from Salmonella typhimurium. Journal of Biological Chemistry. 1991;266(19):12741-6.

318. Lee JE, Cornell KA, Riscoe MK, Howell PL. Structure of E. coli 5′-methylthioadenosine/S-adenosylhomocysteine nucleosidase reveals similarity to the purine nucleoside phosphorylases. Structure. 2001;9(10):941-53.

319. Lee JE, Cornell KA, Riscoe MK, Howell PL. Structure of Escherichia coli5′-Methylthioadenosine/S-Adenosylhomocysteine Nucleosidase Inhibitor Complexes Provide Insight into the Conformational Changes Required for Substrate Binding and Catalysis. Journal of Biological Chemistry. 2003;278(10):8761-70.

320. Siu KK, Lee JE, Smith GD, Horvatin-Mrakovcic C, Howell PL. Structure of Staphylococcus aureus 5′-methylthioadenosine/S-adenosylhomocysteine nucleosidase. Acta Crystallographica Section F: Structural Biology and Crystallization Communications. 2008;64(5):343-50.

321. Lee JE, Singh V, Evans GB, Tyler PC, Furneaux RH, Cornell KA, et al. Structural rationale for the affinity of pico-and femtomolar transition state analogues of Escherichia coli 5′-methylthioadenosine/S-adenosylhomocysteine nucleosidase. Journal of Biological Chemistry. 2005;280(18):18274-82.

322. Cornell KA, Swarts WE, Barry RD, Riscoe MK. Characterization of RecombinantEschericha coli5′-Methylthioadenosine/S-Adenosylhomocysteine Nucleosidase: Analysis of Enzymatic Activity and Substrate Specificity. Biochemical and biophysical research communications. 1996;228(3):724-32.

323. Haapalainen AM, Thomas K, Tyler PC, Evans GB, Almo SC, Schramm VL. Salmonella enterica MTAN at 1.36 Å resolution: A structure-based design of tailored transition state analogs. Structure. 2013;21(6):963-74.

324. Singh V, Lee JE, Núñez S, Howell PL, Schramm VL. Transition state structure of 5 '-methylthioadenosine/S-adenosylhomocysteine nucleosidase from Escherichia coli and its similarity to transition state analogues. Biochemistry. 2005;44(35):11647-59.

325. Singh V, Schramm VL. Transition-State Analysis of S. pneumoniae 5 '-Methylthioadenosine Nucleosidase. Journal of the American Chemical Society. 2007;129(10):2783-95.

326. Singh V, Luo M, Brown RL, Norris GE, Schramm VL. Transition-State Structure of Neisseria meningitides 5 '-Methylthioadenosine/S-Adenosylhomocysteine Nucleosidase. Journal of the American Chemical Society. 2007;129(45):13831-3.

327. Gutierrez JA, Crowder T, Rinaldo-Matthis A, Ho M-C, Almo SC, Schramm VL. Transition state analogs of 5′-methylthioadenosine nucleosidase disrupt quorum sensing. Nature chemical biology. 2009;5(4):251-7.

328. Schramm VL, Gutierrez JA, Cordovano G, Basu I, Guha C, Belbin TJ, et al., editors. Transition state analogues in quorum sensing and SAM recycling. Nucleic acids symposium series (2004); 2008: NIH Public Access.

329. Cornell KA, Primus S, Martinez JA, Parveen N. Assessment of methylthioadenosine/S-adenosylhomocysteine nucleosidases of Borrelia burgdorferi as targets for novel antimicrobials using a novel high-throughput method. Journal of antimicrobial chemotherapy. 2009:dkp129.

330. Miller CH, Duerre JA. S-ribosylhomocysteine cleavage enzyme from Escherichia coli. Journal of Biological Chemistry. 1968;243(1):92-7.

331. Schauder S, Bassler BL. The languages of bacteria. Genes & Development. 2001;15(12):1468-80.

332. Xavier KB, Bassler BL. Regulation of uptake and processing of the quorum-sensing autoinducer AI-2 in Escherichia coli. Journal of bacteriology. 2005;187(1):238-48.

333. Sperandio V, Torres AG, Girón JA, Kaper JB. Quorum sensing is a global regulatory mechanism in enterohemorrhagic Escherichia coli O157: H7. Journal of bacteriology. 2001;183(17):5187-97.

334. Taga ME, Miller ST, Bassler BL. Lsr-mediated transport and processing of AI-2 in Salmonella typhimurium. Molecular microbiology. 2003;50(4):1411-27.

335. Sircili MP, Walters M, Trabulsi LR, Sperandio V. Modulation of enteropathogenic Escherichia coli virulence by quorum sensing. Infection and immunity. 2004;72(4):2329-37.

336. Choi J, Shin D, Ryu S. Implication of quorum sensing in Salmonella enterica serovar typhimurium virulence: the luxS gene is necessary for expression of genes in pathogenicity island 1. Infection and immunity. 2007;75(10):4885-90.

337. Perrett CA, Karavolos MH, Humphrey S, Mastroeni P, Martinez-Argudo I, Spencer H, et al. LuxS-based quorum sensing does not affect the ability of Salmonella to express the SPI-1 Type 3 secretion system, induce membrane ruffles or invade epithelial cells. Journal of bacteriology. 2009.

338. Bao Y, Li Y, Jiang Q, Zhao L, Xue T, Hu B, et al. Methylthioadenosine/S-adenosylhomocysteine nucleosidase (Pfs) of Staphylococcus aureus is essential for the virulence independent of LuxS/AI-2 system. International Journal of Medical Microbiology. 2013;303(4):190-200.

339. Miller MB, Bassler BL. Quorum sensing in bacteria. Annual Reviews in Microbiology. 2001;55(1):165-99.

340. Surette MG, Bassler BL. Quorum sensing in Escherichia coli and Salmonella typhimurium. Proceedings of the National Academy of Sciences. 1998;95(12):7046-50.

341. Surette MG, Miller MB, Bassler BL. Quorum sensing in Escherichia coli, Salmonella typhimurium, and Vibrio harveyi: a new family of genes responsible for autoinducer production. Proceedings of the National Academy of Sciences. 1999;96(4):1639-44.

342. Eberhard A, Widrig CA, McBath P, Schineller JB. Analogs of the autoinducer of bioluminescence inVibrio fischer. Archives of microbiology. 1986;146(1):35-40.

343. Eberhard A, Burlingame A, Eberhard C, Kenyon G, Nealson K, Oppenheimer N. Structural identification of autoinducer of Photobacterium fischeri luciferase. Biochemistry. 1981;20(9):2444-9.

344. Cao J-G, Meighen EA. Purification and structural identification of an autoinducer for the luminescence system of Vibrio harveyi. Journal of Biological Chemistry. 1989;264(36):21670-6.

345. Swift S, Downie JA, Whitehead NA, Barnard AM, Salmond GP, Williams P. Quorum sensing as a population-density-dependent determinant of bacterial physiology. Advances in microbial physiology. 2001;45:199-270.

346. Whitehead NA, Barnard AM, Slater H, Simpson NJ, Salmond GP. Quorum-sensing in Gram-negative bacteria. FEMS microbiology reviews. 2001;25(4):365-404.

347. Beeston AL, Surette MG. pfs-dependent regulation of autoinducer 2 production in Salmonella enterica serovar Typhimurium. Journal of bacteriology. 2002;184(13):3450-6.

348. Struck AW, Thompson ML, Wong LS, Micklefield J. S-Adenosyl-Methionine-Dependent Methyltransferases: Highly Versatile Enzymes in Biocatalysis, Biosynthesis and Other Biotechnological Applications. ChemBioChem. 2012;13(18):2642-55.

349. Bowman WH, Tabor CW, Tabor H. Spermidine Biosynthesis PURIFICATION AND PROPERTIES OF PROPYLAMINE TRANSFERASE FROM ESCHERICHIA COLI. Journal of Biological Chemistry. 1973;248(7):2480-6.

350. Hibasami H, Borchardt RT, Chen SY, Coward JK, Pegg AE. Studies of inhibition of rat spermidine synthase and spermine synthase. Biochemical Journal. 1980;187(2):419-28.

351. Sofia H, Chen G, Hetzler B, Reyes-Spindola J, Miller N. Radical SAM, a novel protein superfamily linking unresolved steps in familiar biosynthetic pathways with radical mechanisms: functional characterization using new analysis and information visualization methods

Nucleic Acid Research. 2001:1097-106.

352. Geier GE, Modrich P. Recognition sequence of the dam methylase of Escherichia coli K12 and mode of cleavage of Dpn I endonuclease. Journal of Biological Chemistry. 1979;254(4):1408-13.

353. Gomez-Eichelmann M, Levy-Mustri A, Ramirez-Santos J. Presence of 5-methylcytosine in CC (A/T) GG sequences (Dcm methylation) in DNAs from different bacteria. Journal of bacteriology. 1991;173(23):7692-4.

354. Laengle-Rouault F, Maenhaut-Michel G, Radman M. GATC sequence and mismatch repair in Escherichia coli. The EMBO journal. 1986;5(8):2009.

355. Campbell JL, Kleckner N. E. coli oriC and the dnaA gene promoter are sequestered from dam methyltransferase following the passage of the chromosomal replication fork. Cell. 1990;62(5):967-79.

356. Bickle TA, Krüger D. Biology of DNA restriction. Microbiological reviews. 1993;57(2):434-50.

357. Pingoud A, Fuxreiter M, Pingoud V, Wende W. Type II restriction endonucleases: structure and mechanism. Cellular and molecular life sciences. 2005;62(6):685-707.

358. El Yacoubi B, Bailly M, de Crécy-Lagard V. Biosynthesis and function of posttranscriptional modifications of transfer RNAs. Annual review of genetics. 2012;46:69-95.

359. Bjork GR, Ericson JU, Gustafsson CE, Hagervall TG, Jonsson YH, Wikstrom PM. Transfer RNA modification. Annual review of biochemistry. 1987;56(1):263-85.

360. Björk GR, Hagervall TG. Transfer RNA modification: presence, synthesis, and function. EcoSal Plus. 2014;6(1).

361. Doi Y, Arakawa Y. 16S ribosomal RNA methylation: emerging resistance mechanism against aminoglycosides. Clinical Infectious Diseases. 2007;45(1):88-94.

362. Hagervall TG, Tuohy TM, Atkins JF, Björk GR. Deficiency of 1-methylguanosine in tRNA from Salmonella typhimurium induces frameshifting by quadruplet translocation. Journal of molecular biology. 1993;232(3):756-65.

363. Benítez-Páez A, Villarroya M, Armengod M-E. The Escherichia coli RlmN methyltransferase is a dual-specificity enzyme that modifies both rRNA and tRNA and controls translational accuracy. Rna. 2012;18(10):1783-95.

364. Urbonavičius J, Qian Q, Durand JM, Hagervall TG, Björk GR. Improvement of reading frame maintenance is a common function for several tRNA modifications. The EMBO journal. 2001;20(17):4863-73.

365. Xu Z, O'farrell HC, Rife JP, Culver GM. A conserved rRNA methyltransferase regulates ribosome biogenesis. Nature structural & molecular biology. 2008;15(5):534.

366. O'Dwyer K, Watts JM, Biswas S, Ambrad J, Barber M, Brulé H, et al. Characterization of Streptococcus pneumoniae TrmD, a tRNA methyltransferase essential for growth. Journal of bacteriology. 2004;186(8):2346-54.

367. Anantharaman V, Koonin EV, Aravind L. SPOUT: a class of methyltransferases that includes spoU and trmD RNA methylase superfamilies, and novel superfamilies of predicted prokaryotic RNA methylases. Journal of molecular microbiology and biotechnology. 2002;4(1):71-6.

368. Cavaillé J, Chetouani F, Bachellerie J-P. The yeast Saccharomyces cerevisiae YDL112w ORF encodes the putative 2'-O-ribose methyltransferase catalyzing the formation of Gm18 in tRNAs. Rna. 1999;5(1):66-81.

369. Koonin EV. Pseudouridine synthases: four families of enzymes containing a putative uridine-binding motif also conserved in dUTPases and dCTP deaminases. Nucleic acids research. 1996;24(12):2411-5.

370. Persson BC, Jäger G, Gustafsson C. The spoU gene of Escherichia coli, the fourth gene of the spoT operon, is essential for tRNA (Gm18) 2′-O-methyltransferase activity. Nucleic acids research. 1997;25(20):4093-7.

371. Bjork GR, Wikstrom PM, Bystrom AS. Prevention of translational frameshifting by the modified nucleoside 1-methylguanosine. Science. 1989;244(4907):986-90.

372. Vester B, Long KS. Antibiotic resistance in bacteria caused by modified nucleosides in 23S ribosomal RNA. DNA and RNA modification enzymes: Structure, mechanism, function and evolution. 2009:537-49.

373. Douthwaite S, Fourmy D, Yoshizawa S. Nucleotide methylations in rRNA that confer resistance to ribosome-targeting antibiotics. Fine-tuning of RNA Functions by Modification and Editing: Springer; 2005. p. 285-307.

374. Chen R, Brosius J, Wittmann-Liebold B, Schäfer W. Occurrence of methylated amino acids as N-termini of proteins from Escherichia coli ribosomes. Journal of molecular biology. 1977;111(2):173-81.

375. Nesterchuk M, Sergiev P, Dontsova O. Posttranslational modifications of ribosomal proteins in Escherichia coli. Acta Naturae (англоязычная версия). 2011;3(2 (9)).

376. Djordjevic S, Stock AM. Chemotaxis receptor recognition by protein methyltransferase CheR. Nature Structural & Molecular Biology. 1998;5(6):446-50.

377. Djordjevic S, Stock AM. Crystal structure of the chemotaxis receptor methyltransferase CheR suggests a conserved structural motif for binding S-adenosylmethionine. Structure. 1997;5(4):545-58.

378. Lee PT, Hsu AY, Ha HT, Clarke CF. A C-methyltransferase involved in both ubiquinone and menaquinone biosynthesis: isolation and identification of the Escherichia coli ubiE gene. Journal of bacteriology. 1997;179(5):1748-54.

379. Law JH. Biosynthesis of cyclopropane rings. Accounts of Chemical Research. 1971;4(6):199-203.

380. Grogan DW, Cronan JE. Cyclopropane ring formation in membrane lipids of bacteria. Microbiology and Molecular Biology Reviews. 1997;61(4):429-41.

381. Courtois F, Guérard C, Thomas X, Ploux O. Escherichia coli cyclopropane fatty acid synthase. European Journal of Biochemistry. 2004;271(23-24):4769-78.

382. Roth J, Lawrence J, Bobik T. Cobalamin (coenzyme B12): synthesis and biological significance. Annual Reviews in Microbiology. 1996;50(1):137-81.

383. Jeter RM, Olivera BM, Roth JR. Salmonella typhimurium synthesizes cobalamin (vitamin B12) de novo under anaerobic growth conditions. Journal of bacteriology. 1984;159(1):206-13.

384. Moore SJ, Warren MJ. The anaerobic biosynthesis of vitamin B12. Portland Press Limited; 2012.

385. Roth JR, Lawrence J, Bobik T. Cobalamin (coenzyme B12): synthesis and biological significance. Annual Reviews in Microbiology. 1996;50(1):137-81.

386. Warren MJ, Raux E, Schubert HL, Escalante-Semerena JC. The biosynthesis of adenosylcobalamin (vitamin B12). Natural product reports. 2002;19(4):390-412.

387. Blethen SL, Boeker EA, Snell EE. Arginine decarboxylase from Escherichia coli I. Purification and specificity for substrates and coenzyme. Journal of Biological Chemistry. 1968;243(8):1671-7.

388. Boeker EA, Snell EE. Arginine decarboxylase from Escherichia coli II. Dissociation and reassociation of subunits. Journal of Biological Chemistry. 1968;243(8):1678-84.

389. Møller V. Simplified tests for some amino acid decarboxylases and for the arginine dihydrolase system. Acta Pathologica Microbiologica Scandinavica. 1955;36(2):158-72.

390. Morris DR, Pardee AB. Multiple pathways of putrescine biosynthesis in Escherichia coli. Journal of Biological Chemistry. 1966;241(13):3129-35.

391. Tabor CW, Tabor H. Polyamines in microorganisms. Microbiological reviews. 1985;49(1):81.

392. Kyriakidis DA, Heller JS, Canellakis E. Modulation of ornithine decarboxylase activity in Escherichia coli by positive and negative effectors. Proceedings of the National Academy of Sciences. 1978;75(10):4699-703.

393. Kyriakidis DA, Heller JS, Canellakis ES. Purification of ornithine decarboxylase antizymes (Escherichia coli). Methods in enzymology. 1982;94:193-9.

394. Morris DR, Pardee AB. A biosynthetic ornithine decarboxylase in Escherichia, coli. Biochemical and biophysical research communications. 1965;20(6):697-702.

395. Gale EF. The bacterial amino acid decarboxylases. Advances in Enzymology and Related Areas of Molecular Biology, Volume 6. 2006:1-32.

396. Morris DR, Fillingame RH. Regulation of amino acid decarboxylation. Annual review of biochemistry. 1974;43(1):303-21.

397. Applebaum DM, Dunlap JC, Morris DR. Comparison of the biosynthetic and biodegradative ornithine decarboxylases of Escherichia coli. Biochemistry. 1977;16(8):1580-4.

398. IGARASHI K, SUGAWARA K, IZUMI I, NAGAYAMA C, HIROSE S. Effect of Polyamines on Polyphenylalanine Synthesis by Escherichia coli and Rat-Liver Ribosomes. European Journal of Biochemistry. 1974;48(2):495-502.

399. ITO K, IGARASHI K. The increase by spermidine of fidelity of protamine synthesis in a wheat-germ cell-free system. The FEBS Journal. 1986;156(3):505-10.

400. Basu H, Marton LJ. The interaction of spermine and pentamines with DNA. Biochemical Journal. 1987;244(1):243-6.

401. Terui Y, Higashi K, Taniguchi S, Shigemasa A, Nishimura K, Yamamoto K, et al. Enhancement of the synthesis of RpoN, Cra, and H-NS by polyamines at the level of translation in Escherichia coli cultured with glucose and glutamate. Journal of bacteriology. 2007;189(6):2359-68.

402. Higashi K, Kashiwagi K, Taniguchi S, Terui Y, Yamamoto K, Ishihama A, et al. Enhancement of+ 1 frameshift by polyamines during translation of polypeptide release factor 2 in Escherichia coli. Journal of Biological Chemistry. 2006;281(14):9527-37.

403. Terui Y, Higashi K, Tabei Y, Tomitori H, Yamamoto K, Ishihama A, et al. Enhancement of the synthesis of RpoE and StpA by polyamines at the level of translation in Escherichia coli under heat shock conditions. Journal of bacteriology. 2009;191(17):5348-57.

404. Khan AU, Di Mascio P, Medeiros M, Wilson T. Spermine and spermidine protection of plasmid DNA against single-strand breaks induced by singlet oxygen. Proceedings of the National Academy of Sciences. 1992;89(23):11428-30.

405. Khan AU, Mei Y-H, Wilson T. A proposed function for spermine and spermidine: protection of replicating DNA against damage by singlet oxygen. Proceedings of the National Academy of Sciences. 1992;89(23):11426-7.

406. Chattopadhyay MK, Tabor CW, Tabor H. Polyamines protect Escherichia coli cells from the toxic effect of oxygen. Proceedings of the National Academy of Sciences. 2003;100(5):2261-5.

407. Tabor CW, Tabor H, Xie Q-W. Spermidine synthase of Escherichia coli: localization of the speE gene. Proceedings of the National Academy of Sciences. 1986;83(16):6040-4.

408. Gutnick D, Calvo JM, Klopotowski T, Ames BN. Compounds which serve as the sole source of carbon or nitrogen for Salmonella typhimurium LT-2. Journal of bacteriology. 1969;100(1):215.

409. Tabor CW, Tabor H, Hafner EH. [12] Mass screening for mutants in the biosynthetic pathway for polyamines in Escherichia coli: A general methods for mutants in enzymatic reactions producing CO 2. Methods in enzymology. 1983;94:83-91.

410. Jelsbak L, Thomsen LE, Wallrodt I, Jensen PR, Olsen JE. Polyamines are required for virulence in Salmonella enterica serovar Typhimurium. PloS one. 2012;7(4):e36149.

411. Durand J, Björk GR. Putrescine or a combination of methionine and arginine restores virulence gene expression in a tRNA modification-deficient mutant of Shigella flexneri: a possible role in adaptation of virulence. Molecular microbiology. 2003;47(2):519-27.

412. Barbagallo M, Di Martino ML, Marcocci L, Pietrangeli P, De Carolis E, Casalino M, et al. A new piece of the shigella pathogenicity puzzle: spermidine accumulationby silencing of the speG gene. PloS one. 2011;6(11):e27226.

413. Russo BC, Horzempa J, O'Dee DM, Schmitt DM, Brown MJ, Carlson PE, et al. A Francisella tularensis locus required for spermine responsiveness is necessary for virulence. Infection and immunity. 2011;79(9):3665-76.

414. Carlson PE, Horzempa J, O'Dee DM, Robinson CM, Neophytou P, Labrinidis A, et al. Global transcriptional response to spermine, a component of the intramacrophage environment, reveals regulation of Francisella gene expression through insertion sequence elements. Journal of bacteriology. 2009;191(22):6855-64.

415. Schroll C, Christensen JP, Christensen H, Pors SE, Thorndahl L, Jensen PR, et al. Polyamines are essential for virulence in Salmonella enterica serovar Gallinarum despite evolutionary decay of polyamine biosynthesis genes. Veterinary microbiology. 2014;170(1):144-50.

416. Di Martino ML, Campilongo R, Casalino M, Micheli G, Colonna B, Prosseda G. Polyamines: emerging players in bacteria–host interactions. International Journal of Medical Microbiology. 2013;303(8):484-91.

417. Cadieux N, Bradbeer C, Reeger-Schneider E, Köster W, Mohanty AK, Wiener MC, et al. Identification of the periplasmic cobalamin-binding protein BtuF of Escherichia coli. Journal of bacteriology. 2002;184(3):706-17.

418. Challand MR, Ziegert T, Douglas P, Wood RJ, Kriek M, Shaw NM, et al. Product inhibition in the radical S-adenosylmethionine family. FEBS letters. 2009;583(8):1358-62.

419. Devine JH, Shadel GS, Baldwin TO. Identification of the operator of the lux regulon from the Vibrio fischeri strain ATCC7744. Proceedings of the National Academy of Sciences. 1989;86(15):5688-92.

420. Galletti P, Oliva A, Manna C, Della Ragione F, Cartenì-Farina M. Effect of 5'-methylthioadenosine on in vivo methyl esterification of human erythrocyte membrane proteins. FEBS letters. 1981;126(2):236-40.

421. Avila MA, Garcıa-Trevijano ER, Lu SC, Corrales FJ, Mato JM. Methylthioadenosine. The international journal of biochemistry & cell biology. 2004;36(11):2125-30.

422. Pajula R-L, Raina A. Methylthioadenosine, a potent inhibitor of spermine synthase from bovine brain. FEBS letters. 1979;99(2):343-5.

423. Parveen N, Cornell KA. Methylthioadenosine/S-adenosylhomocysteine nucleosidase, a critical enzyme for bacterial metabolism. Molecular microbiology. 2011;79(1):7-20.

424. Yao Y, Martinez-Yamout MA, Dickerson TJ, Brogan AP, Wright PE, Dyson HJ. Structure of the Escherichia coli quorum sensing protein SdiA: activation of the folding switch by acyl homoserine lactones. Journal of molecular biology. 2006;355(2):262-73.

425. Parker CT, Sperandio V. Cell-to-cell signalling during pathogenesis. Cellular microbiology. 2009;11(3):363-9.

426. Kanamaru K, Kanamaru K, Tatsuno I, Tobe T, Sasakawa C. SdiA, an Escherichia coli homologue of quorum-sensing regulators, controls the expression of virulence factors in enterohaemorrhagic Escherichia coli O157: H7. Molecular microbiology. 2000;38(4):805-16.

427. Dai Y, Pochapsky TC, Abeles RH. Mechanistic Studies of Two Dioxygenases in the Methionine Salvage Pathway of Klebsiella pneumoniae†. Biochemistry. 2001;40(21):6379-87.

428. Sekowska A, Danchin A. The methionine salvage pathway in Bacillus subtilis. BMC microbiology. 2002;2(1):8.

429. Furfine ES, Abeles RH. Intermediates in the conversion of 5'-S-methylthioadenosine to methionine in Klebsiella pneumoniae. Journal of Biological Chemistry. 1988;263(20):9598-606.

430. Gianotti AJ, Tower PA, Sheley JH, Conte PA, Spiro C, Ferro AJ, et al. Selective killing of Klebsiella pneumoniae by 5-trifluoromethylthioribose. Chemotherapeutic exploitation of the enzyme 5-methylthioribose kinase. Journal of Biological Chemistry. 1990;265(2):831-7.

431. Schroeder HR, Barnes C, Bohinski R, Mallette M. Biological production of 5-methylthioribose. Canadian journal of microbiology. 1973;19(11):1347-54.

432. Hughes JA. In vivo hydrolysis of S-adenosyl-L-methionine in Escherichia coli increases export of 5-methylthioribose. Canadian journal of microbiology. 2006;52(6):599-602.

433. Mackie A, Keseler IM, Nolan L, Karp PD, Paulsen IT. Dead end metabolites-Defining the known unknowns of the E. coli metabolic network. PloS one. 2013;8(9):e75210.

434. Sekowska A, Kung H-F, Danchin A. Sulfur metabolism in Escherichia coli and related bacteria: facts and fiction. Journal of molecular microbiology and biotechnology. 2000;2(2):145-77.

435. Davis BD, Mingioli ES. Mutants of Escherichia coli requiring methionine or vitamin B12. Journal of bacteriology. 1950;60(1):17.

436. Strugnell R, Dougan G, Chatfield S, Charles I, Fairweather N, Tite J, et al. Characterization of a Salmonella typhimurium aro vaccine strain expressing the P. 69 antigen of Bordetella pertussis. Infection and immunity. 1992;60(10):3994-4002.

437. Turner S, Carbone F, Strugnell R. Salmonella typhimurium delta aroA delta aroD mutants expressing a foreign recombinant protein induce specific major histocompatibility complex class I-restricted cytotoxic T lymphocytes in mice. Infection and immunity. 1993;61(12):5374-80.

438. Grant SG, Jessee J, Bloom FR, Hanahan D. Differential plasmid rescue from transgenic mouse DNAs into Escherichia coli methylation-restriction mutants. Proceedings of the National Academy of Sciences. 1990;87(12):4645-9.

439. Casadaban MJ. Transposition and fusion of the lac genes to selected promoters in Escherichia coli using bacteriophage lambda and Mu. Journal of molecular biology. 1976;104(3):541-55.

440. Herring CD, Glasner JD, Blattner FR. Gene replacement without selection: regulated suppression of amber mutations in Escherichia coli. Gene. 2003;311:153-63.

441. Chang AC, Cohen SN. Construction and characterization of amplifiable multicopy DNA cloning vehicles derived from the P15A cryptic miniplasmid. Journal of bacteriology. 1978;134(3):1141-56.

442. Cherepanov PP, Wackernagel W. Gene disruption in Escherichia coli: Tc R and Km R cassettes with the option of Flp-catalyzed excision of the antibiotic-resistance determinant. Gene. 1995;158(1):9-14.

443. Datsenko KA, Wanner BL. One-step inactivation of chromosomal genes in Escherichia coli K-12 using PCR products. Proceedings of the National Academy of Sciences of the United States of America. 2000;97(12):6640-5.

444. Sambrook J. russell DW (2001) Molecular cloning: a laboratory manual. Cold Spring laboratory Press, new York.

445. Chung C, Niemela SL, Miller RH. One-step preparation of competent Escherichia coli: transformation and storage of bacterial cells in the same solution. Proceedings of the National Academy of Sciences. 1989;86(7):2172-5.

446. Herring CD, Glasner JD, Blattner FR. Gene replacement without selection: regulated suppression of amber mutations in Escherichia coli. Gene. 2003;311:153-63.

447. Bochner B. Curing bacterial cells of lysogenic viruses by using UCB indicator plates. Biotechniques. 1984;2(4):234-40.

448. Davis RW, Botstein D, Roth JR. Advanced bacterial genetics: Cold Spring Harbor Laboratory; 1980.

449. Dunstan SJ, Simmons CP, Strugnell RA. In vitro and in vivo stability of recombinant plasmids in a vaccine strain of Salmonella enterica var. Typhimurium. FEMS Immunology & Medical Microbiology. 2003;37(2-3):111-9.

450. Bennett-Wood V, Carapetis J, Robins-Browne R. Ability of clinical isolates of group A streptococci to adhere to and invade HEp-2 epithelial cells. Journal of medical microbiology. 1998;47(10):899-906.

451. Johnson P, Oppedisano F, Bennett-Wood V, Gilbert GL, Robins-Browne RM. Sporadic invasion of cultured epithelial cells by Haemophilus influenzae type b. Infection and immunity. 1996;64(3):1051-3.

452. Cobbold SA, Chua HH, Nijagal B, Creek DJ, Ralph SA, McConville MJ. Metabolic dysregulation induced in Plasmodium falciparum by dihydroartemisinin and other front-line antimalarial drugs. Journal of Infectious Diseases. 2016;213(2):276-86.

453. Tautenhahn R, Böttcher C, Neumann S. Highly sensitive feature detection for high resolution LC/MS. BMC bioinformatics. 2008;9(1):504.

454. Smith CA, Want EJ, O'Maille G, Abagyan R, Siuzdak G. XCMS: processing mass spectrometry data for metabolite profiling using nonlinear peak alignment, matching, and identification. Analytical chemistry. 2006;78(3):779-87.

455. Xia J, Sinelnikov IV, Han B, Wishart DS. MetaboAnalyst 3.0—making metabolomics more meaningful. Nucleic acids research. 2015;43(W1):W251-W7.

456. Clasquin MF, Melamud E, Rabinowitz JD. LC-MS data processing with MAVEN: a metabolomic analysis and visualization engine. Current protocols in bioinformatics. 2012:14.1. 1-.1. 23.

457. Berg JM, Tymoczko JL, Stryer L. Amino Acids Are Made from Intermediates of the Citric Acid Cycle and Other Major Pathways. 2002.

458. Gomes J, Kumar D. Production of L-methionine by submerged fermentation: A review. Enzyme and microbial technology. 2005;37(1):3-18.

459. Ingraham JL, Maaløe O, Neidhardt FC. Growth of the bacterial cell: Sinauer Associates; 1983.

460. Milner L, Whitfield C, Weissbach H. Effect of L-methionine and vitamin B 12 on methionine biosynthesis in Escherichia coli. Archives of biochemistry and biophysics. 1969;133(2):413-9.

461. Graham RM, Deery E, Warren MJ. Vitamin B12: Biosynthesis of the corrin ring. Tetrapyrroles: Springer; 2009. p. 286-99.

462. Heithoff DM, Sinsheimer RL, Low DA, Mahan MJ. An essential role for DNA adenine methylation in bacterial virulence. Science. 1999;284(5416):967-70.

463. Blyn LB, Braaten BA, Low DA. Regulation of pap pilin phase variation by a mechanism involving differential dam methylation states. The EMBO journal. 1990;9(12):4045.

464. Belfaiza J, Parsot C, Martel A, De La Tour CB, Margarita D, Cohen GN, et al. Evolution in biosynthetic pathways: two enzymes catalyzing consecutive steps in methionine biosynthesis originate from a common ancestor and possess a similar regulatory region. Proceedings of the National Academy of Sciences. 1986;83(4):867-71.

465. Old IG, Phillips SE, Stockley PG, Saint Girons I. Regulation of methionine biosynthesis in the Enterobacteriaceae. Progress in biophysics and molecular biology. 1991;56(3):145-85.

466. Saint-Girons I, Parsot C, Zakin MM, Baˇrzu O, Cohen GN, Weissbach H. Methionine Biosynthesis in Enterobacteriaceae: Biochemical, Regulatory, and Evolutionary Aspect. Critical Reviews in Biochemistry. 1988;23(sup1):S1-S42.

467. Kung H-F, Spears C, Greene RC, Weissbach H. Regulation of the terminal reactions in methionine biosynthesis by vitamin B12 and methionine. Archives of biochemistry and biophysics. 1972;150(1):23-31.

468. Phillips SE, Manfield I, Parsons I, Davidson BE, Rafferty JB, Somers WS, et al. Cooperative tandem binding of met repressor of Escherichia coli. 1989.

469. Figge RM. Methionine biosynthesis in Escherichia coli and Corynebacterium glutamicum. Amino Acid Biosynthesis~ Pathways, Regulation and Metabolic Engineering: Springer; 2006. p. 163-93.

470. Augustus AM, Spicer LD. The MetJ regulon in gammaproteobacteria determined by comparative genomics methods. BMC genomics. 2011;12(1):1.

471. Maxon ME, Redfield B, Cai X-Y, Shoeman R, FuJITA K, Fisher W, et al. Regulation of methionine synthesis in Escherichia coli: effect of the MetR protein on the expression of the metE and metR genes. Proceedings of the National Academy of Sciences. 1989;86(1):85-9.

472. Gonzalez JC, Banerjee RV, Huang S, Sumner JS, Matthews RG. Comparison of cobalamin-independent and cobalamin-dependent methionine synthases from Escherichia coli: two solutions to the same chemical problem. Biochemistry. 1992;31(26):6045-56.

473. González JC, Peariso K, Penner-Hahn JE, Matthews RG. Cobalamin-independent methionine synthase from Escherichia coli: a zinc metalloenzyme. Biochemistry. 1996;35(38):12228-34.

474. Born TL, Blanchard JS. Enzyme-catalyzed acylation of homoserine: mechanistic characterization of the Escherichia coli metA-encoded homoserine transsuccinylase. Biochemistry. 1999;38(43):14416-23.

475. Michaeli S, Ron EZ. Expression of the metA gene of Escherichia coli K-12 in recombinant plasmids. FEMS microbiology letters. 1984;23(2-3):125-9.

476. Kaplan MM, Flavin M. Cystathionine gamma-synthetase of Salmonella. Structural properties of a new enzyme in bacterial methionine biosynthesis. The Journal of biological chemistry. 1966;241(24):5781-9.

477. Kaplan MM, Flavin M. Cystathionine gamma-synthetase of Salmonella. Catalytic properties of a new enzyme in bacterial methionine biosynthesis. The Journal of biological chemistry. 1966;241(19):4463-71.

478. Holbrook EL, Greene RC, Krueger JH. Purification and properties of cystathionine. gamma.-synthase from overproducing strains of Escherichia coli. Biochemistry. 1990;29(2):435-42.

479. Dwivedi CM, Ragin RC, Uren JR. Cloning, purification, and characterization of. beta.-cystathionase from E. coli. Biochemistry. 1982;21(13):3064-9.

480. Clausen T, Huber R, Laber B, Pohlenz H-D, Messerschmidt A. Crystal Structure of the Pyridoxal-5′-phosphate Dependent Cystathionine β-lyase fromEscherichia coliat 1.83 Å. Journal of molecular biology. 1996;262(2):202-24.

481. Hatch FT, Larrabee AR, Cathou RE, Buchanan JM. Enzymatic Synthesis of the Methyl Group of Methionine I. IDENTIFICATION OF THE ENZYMES AND COFACTORS INVOLVED IN THE SYSTEM ISOLATED FROM ESCHERICHIA COLI. Journal of Biological Chemistry. 1961;236(4):1095-101.

482. Sheppard CA, Trimmer EE, Matthews RG. Purification and Properties of NADH-Dependent 5, 10-Methylenetetrahydrofolate Reductase (MetF) fromEscherichia coli. Journal of bacteriology. 1999;181(3):718-25.

483. Foster M, Tejerina G, Guest J, Woods D. Two enzymic mechanisms for the methylation of homocysteine by extracts of Escherichia coli. Biochemical Journal. 1964;92(3):476.

484. Drummond JT, Loo RRO, Matthews RG. Electrospray mass spectrometric analysis of the domains of a large enzyme: observation of the occupied cobalamin-binding domain and redefinition of the carboxyl terminus of methionine synthase. Biochemistry. 1993;32(36):9282-9.

485. Kadner RJ, Watson WJ. Methionine transport in Escherichia coli: physiological and genetic evidence for two uptake systems. Journal of bacteriology. 1974;119(2):401-9.

486. Hondorp ER, Matthews RG, Cohen G. Methionine. 2006.

487. Wong VK, Baker S, Pickard DJ, Parkhill J, Page AJ, Feasey NA, et al. Phylogeographical analysis of the dominant multidrug-resistant H58 clade of Salmonella Typhi identifies inter-and intracontinental transmission events. Nature genetics. 2015;47(6):632-9.

488. Okoro CK, Kingsley RA, Connor TR, Harris SR, Parry CM, Al-Mashhadani MN, et al. Intracontinental spread of human invasive Salmonella Typhimurium pathovariants in sub-Saharan Africa. Nature genetics. 2012;44(11):1215-21.

489. Lissner C, Swanson R, O'brien A. Genetic control of the innate resistance of mice to Salmonella typhimurium: expression of the Ity gene in peritoneal and splenic macrophages isolated in vitro. The Journal of Immunology. 1983;131(6):3006-13.

490. Gophna U, Bapteste E, Doolittle WF, Biran D, Ron EZ. Evolutionary plasticity of methionine biosynthesis. Gene. 2005;355:48-57.

491. Ferla MP, Patrick WM. Bacterial methionine biosynthesis. Microbiology. 2014;160(8):1571-84.

492. Jelsbak L, Mortensen MI, Kilstrup M, Olsen JE. The in vitro redundant enzymes PurN and PurT are both essential for systemic infection of mice in Salmonella enterica serovar Typhimurium. Infection and immunity. 2016:IAI. 00182-16.

493. Malo D, Vidal S, Lieman JH, Ward DC, Gros P. Physical delineation of the minimal chromosomal segment encompassing the murine host resistance locus Bcg. Genomics. 1993;17(3):667-75.

494. Malo D, Vidal SM, Hu J, Skamene E, Gros P. High-resolution linkage map in the vicinity of the host resistance locus Bcg. Genomics. 1993;16(3):655-63.

495. Skamene M, PhD, Emil, Schurr P, Erwin, Gros P, Philippe. Infection genomics: Nramp1 as a major determinant of natural resistance to intracellular infections. Annual review of medicine. 1998;49(1):275-87.

496. Plant J, Glynn A. Genetics of resistance to infection with Salmonella typhimurium in mice. Journal of Infectious Diseases. 1976;133(1):72-8.

497. Raman SB, Nguyen MH, Cheng S, Badrane H, Iczkowski KA, Wegener M, et al. A competitive infection model of hematogenously disseminated candidiasis in mice redefines the role of Candida albicans IRS4 in pathogenesis. Infection and immunity. 2013;81(5):1430-8.

498. Beuzón CR, Holden DW. Use of mixed infections with Salmonella strains to study virulence genes and their interactions in vivo. Microbes and infection. 2001;3(14):1345-52.

499. Dawes J, Foster M. Vitamin B12 and methionine synthesis in Escherichia coli. Biochimica et Biophysica Acta (BBA)-General Subjects. 1971;237(3):455-64.

500. Wu W, Urbanowski ML, Stauffer GV. Role of the MetR regulatory system in vitamin B12-mediated repression of the Salmonella typhimurium metE gene. Journal of bacteriology. 1992;174(14):4833-7.

501. Brown L, Wolf JM, Prados-Rosales R, Casadevall A. Through the wall: extracellular vesicles in Gram-positive bacteria, mycobacteria and fungi. Nature Reviews Microbiology. 2015;13(10):620-30.

502. Cohen G. The common pathway to lysine, methionine, and threonine. Biotechnology Series[BIOTECHNOL SER] 1983. 1983.

503. Fondi M, Brilli M, Fani R. On the origin and evolution of biosynthetic pathways: integrating microarray data with structure and organization of the common pathway genes. BMC bioinformatics. 2007;8(1):S12.

504. Berg JM, Tymoczko J. Stryer: Biochemistry. WH Freeman and Company. 2002;5:306-7.

505. Sikora M, Jakubowski H. Homocysteine editing and growth inhibition in Escherichia coli. Microbiology. 2009;155(6):1858-65.

506. Tuite NL, Fraser KR, O'byrne CP. Homocysteine toxicity in Escherichia coli is caused by a perturbation of branched-chain amino acid biosynthesis. Journal of bacteriology. 2005;187(13):4362-71.

507. Bertrand EM, Moran DM, McIlvin MR, Hoffman JM, Allen AE, Saito MA. Methionine synthase interreplacement in diatom cultures and communities: Implications for the persistence of B12 use by eukaryotic phytoplankton. 2013.

508. Bumann D. Has nature already identified all useful antibacterial targets? Current opinion in microbiology. 2008;11(5):387-92.

509. Levy SB. The challenge of antibiotic resistance. Scientific American. 1998;278(3):32-9.

510. Piddock LJ. The crisis of no new antibiotics--what is the way forward? The Lancet infectious diseases. 2012;12(3):249-53.

511. Coates A, Hu Y. Novel approaches to developing new antibiotics for bacterial infections. British journal of pharmacology. 2007;152(8):1147-54.

512. Markham GD, Hafner E, Tabor CW, Tabor H. S-Adenosylmethionine synthetase from Escherichia coli. Journal of Biological Chemistry. 1980;255(19):9082-92.

513. Cornell KA, Riscoe MK. Cloning and expression of Escherichia coli 5′-methylthioadenosine/S-adenosylhomocysteine nucleosidase: identification of the pfs gene product. Biochimica et Biophysica Acta (BBA)-Gene Structure and Expression. 1998;1396(1):8-14.

514. Ollagnier-de-Choudens S, Mulliez E, Fontecave M. The PLP-dependent biotin synthase from Escherichia coli: mechanistic studies. FEBS letters. 2002;532(3):465-8.

515. Niedergang F, Sirard J-C, Blanc CT, Kraehenbuhl J-P. Entry and survival of Salmonella typhimurium in dendritic cells and presentation of recombinant antigens do not require macrophage-specific virulence factors. Proceedings of the National Academy of Sciences. 2000;97(26):14650-5.

516. Arigony ALV, de Oliveira IM, Machado M, Bordin DL, Bergter L, Prá D, et al. The influence of micronutrients in cell culture: a reflection on viability and genomic stability. BioMed research international. 2013;2013.

517. Einhauer A, Jungbauer A. The FLAG™ peptide, a versatile fusion tag for the purification of recombinant proteins. Journal of biochemical and biophysical methods. 2001;49(1):455-65.

518. Kupz A, Bedoui S, Strugnell RA. Cellular requirements for systemic control of Salmonella enterica serovar Typhimurium infections in mice. Infection and immunity. 2014;82(12):4997-5004.

519. Kupz A, Curtiss III R, Bedoui S, Strugnell RA. In vivo IFN-γ secretion by NK cells in response to Salmonella typhimurium requires NLRC4 inflammasomes. PloS one. 2014;9(5):e97418.

520. Kashiwagi K, Kobayashi H, Igarashi K. Apparently unidirectional polyamine transport by proton motive force in polyamine-deficient Escherichia coli. Journal of bacteriology. 1986;165(3):972-7.

521. Elder JR, Chiok KL, Paul NC, Haldorson G, Guard J, Shah DH. The Salmonella pathogenicity island 13 contributes to pathogenesis in streptomycin pre-treated mice but not in day-old chickens. Gut pathogens. 2016;8(1):16.

522. Espinel IC, Guerra PR, Jelsbak L. Multiple roles of putrescine and spermidine in stress resistance and virulence of Salmonella enterica serovar Typhimurium. Microbial pathogenesis. 2016;95:117-23.

523. Shah P, Swiatlo E. A multifaceted role for polyamines in bacterial pathogens. Molecular microbiology. 2008;68(1):4-16.

524. DeLisa MP, Wu C-F, Wang L, Valdes JJ, Bentley WE. DNA Microarray-Based Identification of Genes Controlled by Autoinducer 2-Stimulated Quorum Sensing inEscherichia coli. Journal of bacteriology. 2001;183(18):5239-47.

525. Zhu J, Miller MB, Vance RE, Dziejman M, Bassler BL, Mekalanos JJ. Quorum-sensing regulators control virulence gene expression in Vibrio cholerae. Proceedings of the National Academy of Sciences. 2002;99(5):3129-34.

526. Siller M, Janapatla RP, Pirzada ZA, Hassler C, Zinkl D, Charpentier E. Functional analysis of the group A streptococcal luxS/AI-2 system in metabolism, adaptation to stress and interaction with host cells. BMC microbiology. 2008;8(1):1.

527. Fernandez MI, Sansonetti PJ. Shigella interaction with intestinal epithelial cells determines the innate immune response in shigellosis. International journal of medical microbiology. 2003;293(1):55-67.

528. Ohtani K, Hayashi H, Shimizu T. The luxS gene is involved in cell–cell signalling for toxin production in Clostridium perfringens. Molecular microbiology. 2002;44(1):171-9.

529. Heurlier K, Vendeville A, Halliday N, Green A, Winzer K, Tang CM, et al. Growth deficiencies of Neisseria meningitidis pfs and luxS mutants are not due to inactivation of quorum sensing. Journal of bacteriology. 2009;191(4):1293-302.

530. Pajula R-L. Kinetic properties of spermine synthase from bovine brain. Biochemical Journal. 1983;215(3):669-76.

531. Gulig PA, Doyle TJ, Clare-Salzler MJ, Maiese RL, Matsui H. Systemic infection of mice by wild-type but not Spv-Salmonella typhimurium is enhanced by neutralization of gamma interferon and tumor necrosis factor alpha. Infection and immunity. 1997;65(12):5191-7.

532. Eckmann L, Fierer J, Kagnoff MF. Genetically resistant (Ityr) and susceptible (Itys) congenic mouse strains show similar cytokine responses following infection with Salmonella dublin. The Journal of Immunology. 1996;156(8):2894-900.

533. Matsumura H, Onozuka K, Terada Y, Nakano Y, Nakano M. Effect of murine recombinant interferon-γ in the protection of mice against Salmonella. International journal of immunopharmacology. 1990;12(1):49-56.

534. Nairz M, Fritsche G, Brunner P, Talasz H, Hantke K, Weiss G. Interferon-γ limits the availability of iron for intramacrophage Salmonella typhimurium. European journal of immunology. 2008;38(7):1923-36.

535. Muotiala A, Mäkelä P. Role of gamma interferon in late stages of murine salmonellosis. Infection and immunity. 1993;61(10):4248-53.

536. Muotiala A, Mäkelä PH. The role of IFN-γ in murine Salmonella typhimurium infection. Microbial pathogenesis. 1990;8(2):135-41.

537. Mweu E, English M. Typhoid fever in children in Africa. Tropical Medicine & International Health. 2008;13(4):532-40.

538. Buckle GC, Walker CL, Black RE. Typhoid fever and paratyphoid fever: Systematic review to estimate global morbidity and mortality for 2010. Journal of global health. 2012;2(1):010401.

539. Medalla F. Ciprofloxacin-Resistant Salmonella enterica Serotype Typhi, United States, 1999–2008-Volume 17, Number 6—June 2011-Emerging Infectious Disease journal-CDC. 2011.

540. Butt T. Ciprofloxacin Treatment Failure in Typhoid Fever Case, Pakistan-Volume 9, Number 12—December 2003-Emerging Infectious Disease journal-CDC. 2003.

541. Galán JE. Typhoid toxin provides a window into typhoid fever and the biology of Salmonella Typhi. Proceedings of the National Academy of Sciences. 2016:201606335.

542. Fidock DA, Rosenthal PJ, Croft SL, Brun R, Nwaka S. Antimalarial drug discovery: efficacy models for compound screening. Nature Reviews Drug Discovery. 2004;3(6):509-20.

543. Xie Q-W, Tabor CW, Tabor H. Spermidine biosynthesis in Escherichia coli: promoter and termination regions of the speED operon. Journal of bacteriology. 1989;171(8):4457-65.

544. Lee JE, Cornell KA, Riscoe MK, Howell PL. Expression, purification, crystallization and preliminary X-ray analysis of Escherichia coli 5′-methylthioadenosine/S-adenosylhomocysteine nucleosidase. Acta Crystallographica Section D: Biological Crystallography. 2001;57(1):150-2.

545. Li X, Chu S, Feher VA, Khalili M, Nie Z, Margosiak S, et al. Structure-based design, synthesis, and antimicrobial activity of indazole-derived SAH/MTA nucleosidase inhibitors. Journal of medicinal chemistry. 2003;46(26):5663-73.

546. Tedder ME, Nie Z, Margosiak S, Chu S, Feher VA, Almassy R, et al. Structure-based design, synthesis, and antimicrobial activity of purine derived SAH/MTA nucleosidase inhibitors. Bioorganic & medicinal chemistry letters. 2004;14(12):3165-8.

547. Ankomah P, Levin BR. Exploring the collaboration between antibiotics and the immune response in the treatment of acute, self-limiting infections. Proceedings of the National Academy of Sciences. 2014;111(23):8331-8.

Appendix

Schematic representation of the deleted region of the mutants from the whole genome sequencing

1. *S.* Typhimurium Δ*metA*:

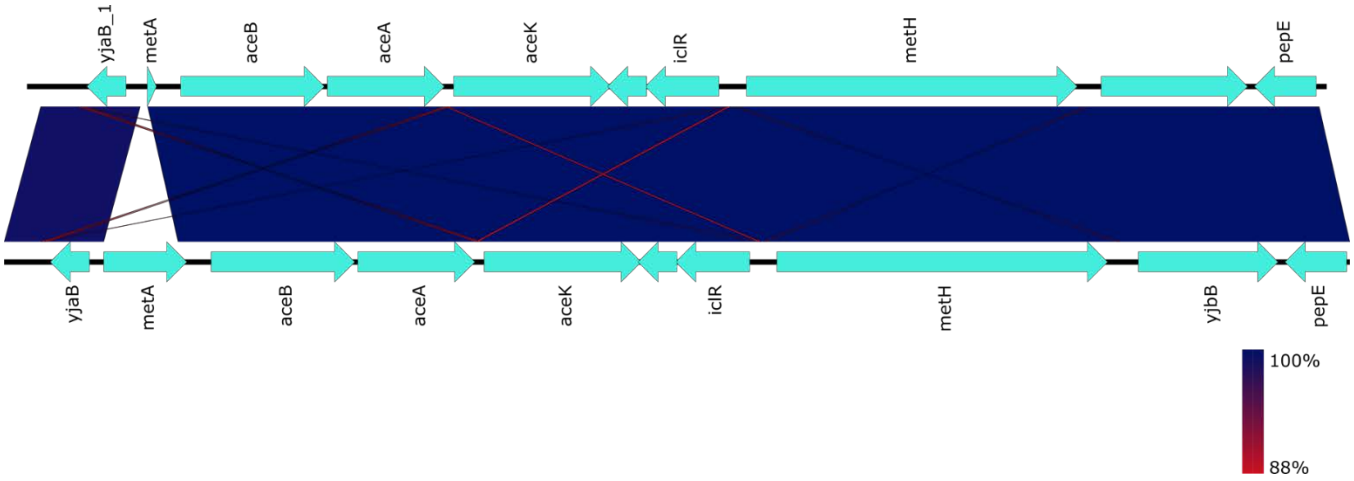

2. *S.* Typhimurium Δ*metB*:

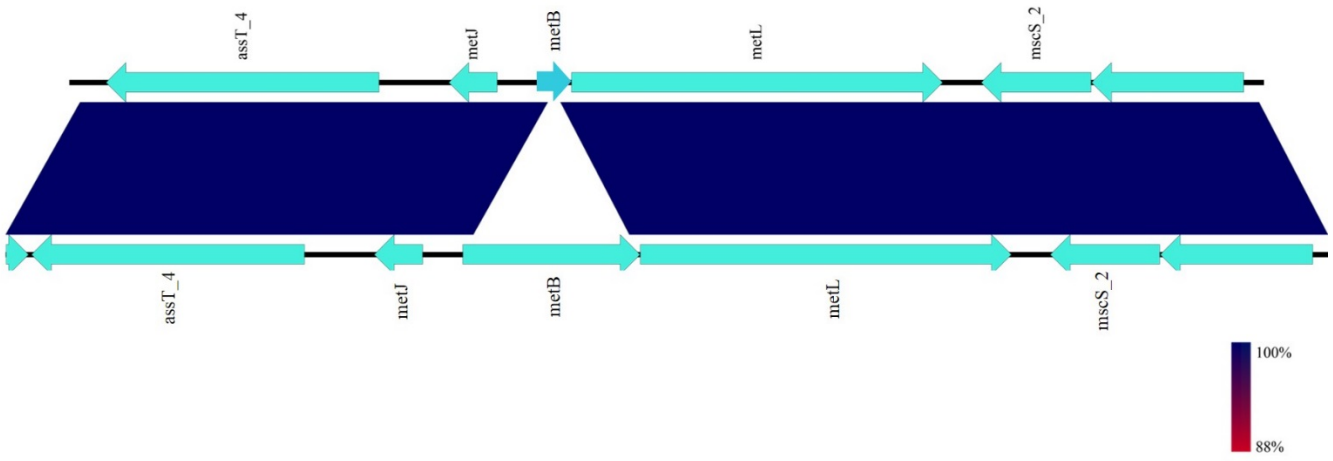

3. *S.* Typhimurium Δ*metC*:

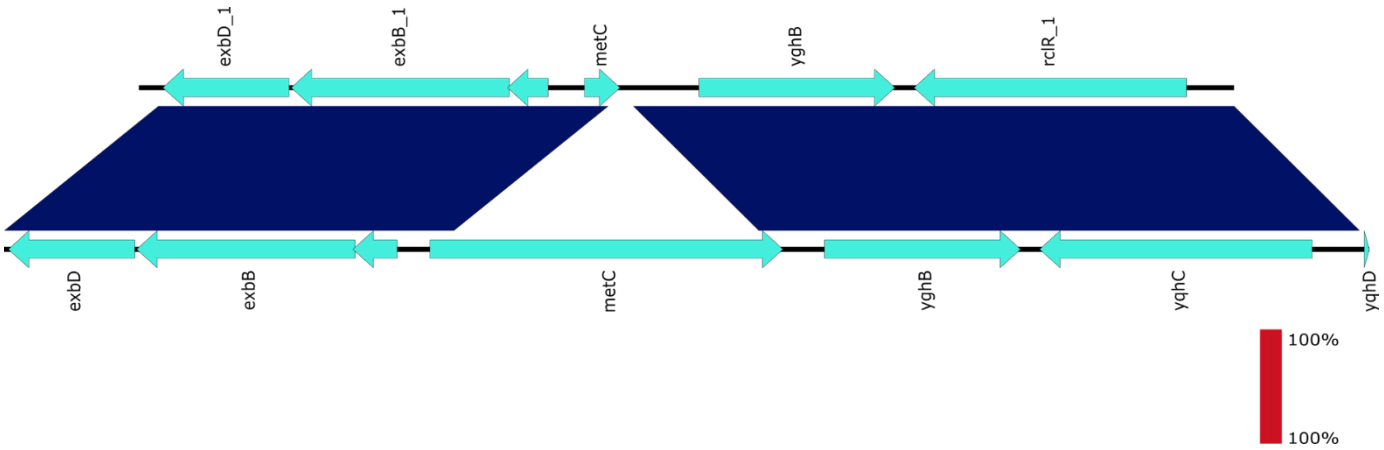

4. *S.* Typhimurium Δ*metE*:

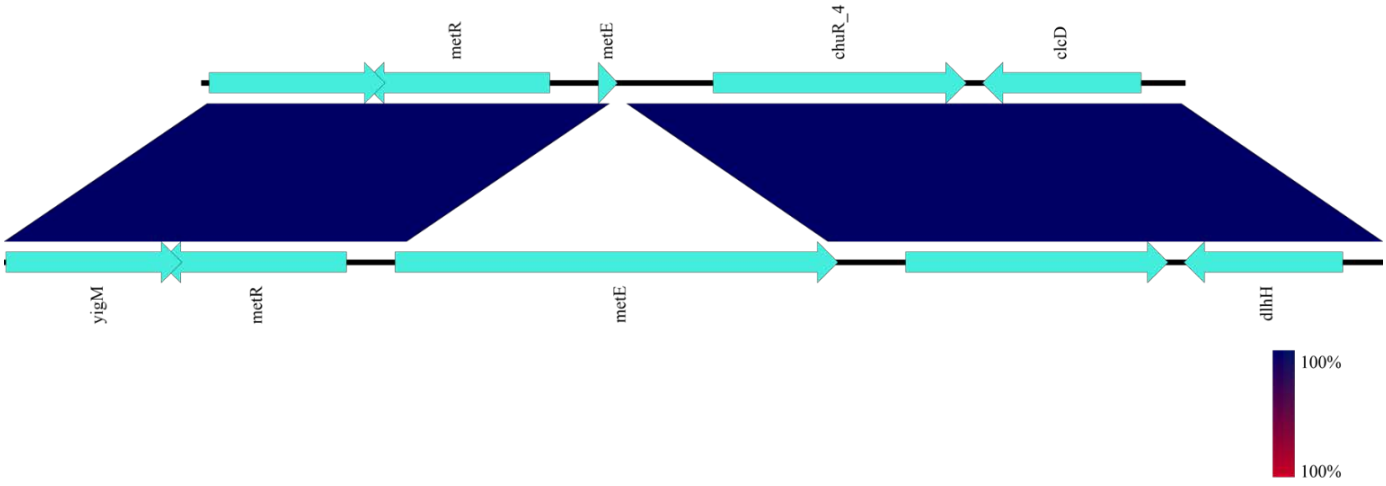

5. *S.* Typhimurium Δ*metF*:

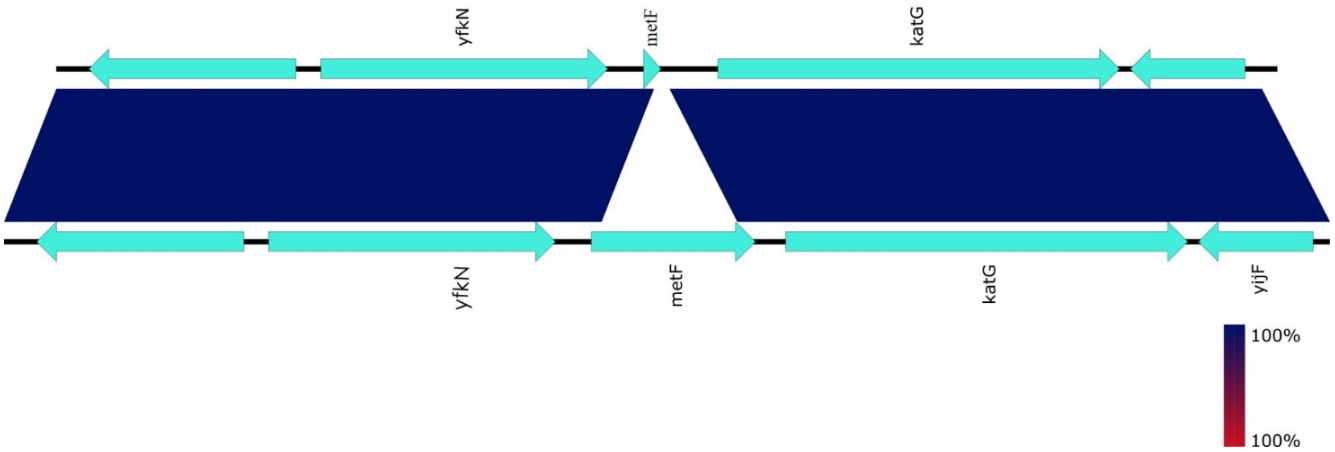

6. *S.* Typhimurium Δ*metH*:

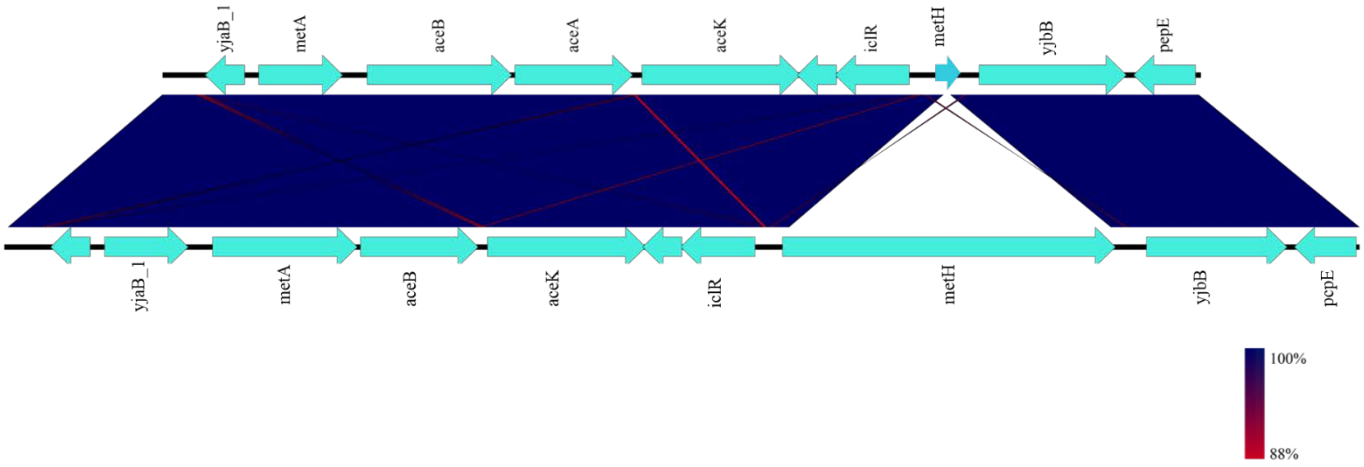

7. *S.* Typhimurium Δ*metNIQ*: